Pharmaceutical formulations of bionanoparticles for siRNA delivery

Metwally, Abdelkader

Award date:
2012

Awarding institution:
University of Bath

Pharmaceutical formulations of bionanoparticles for siRNA delivery

Abdelkader Ali Metwally BSc (Alexandria), MSc (Ain Shams)

A thesis submitted for the degree of Doctor of Philosophy

University of Bath

Department of Pharmacy and Pharmacology
Bath BA2 7AY, UK

November 2011

Signed: …….

Table of Contents

Contents listed		**page number**
Title	Pharmaceutical formulations of bionanoparticles for siRNA delivery	1
Table of Contents		2
Acknowledgements		3
Abstract		4
Aims		5
Chapter One	Introduction and review of siRNA formulation	6
Chapter Two	Efficient gene silencing by self-assembled complexes of siRNA and symmetrical fatty acid amides of spermine	32
Chapter Three	Self-assembled lipoplexes of siRNA using fatty acid amide guanidines, based on spermine, effect efficient gene silencing	61
Chapter Four	Efficient silencing of EGFP reporter gene with siRNA delivered by asymmetrical N^4,N^9-diacyl spermines	81
Chapter Five	Quantitative silencing of EGFP reporter gene by self-assembled siRNA lipoplexes of mixtures of LinOS or DOS with either cholesterol or DOPE	112
Chapter Six	On consideration of mechanisms	132
Conclusions		154
References		158
Output arising from this research		181

Acknowledgements

I thank Dr Ian S. Blagbrough for his supervision and dedicated support throughout this work.

I thank the Egyptian Government for a fully funded studentship for my project.

I thank Dr C. Pourzand (University of Bath) and Dr O. Reelfs (University of Bath) for helpful discussions about stably expressing EGFP cell lines and cell biology assays.

I also acknowledge CRUK Cell Service (Clare Hall Laboratories, South Mimms, Herts, U.K.) for providing the HeLa-EGFP-Centrin cell line and Dr Y. Liu for the details of the construct.

I thank S. Crocket (University of Bristol) for assistance with particle size and ζ-potential measurements, and J. Mantell (University of Bristol) for running the cryo-TEM study. The expert help of Dr A. Rogers (Microscopy and Analysis Suite), C. Rehbein (Mass Spectrometry), and Dr T. Woodman (NMR Spectroscopy), all at the University of Bath, is also gratefully acknowledged.

I thank my lab colleagues and the technical staff in the Department of Pharmacy and Pharmacology: Kevin Smith, Jo Carter, and Don Perry.

I am grateful to the endless enthusiastic support that I have received from my parents and my wife Amira.

Abstract

The aims of this thesis are to design and synthesize non-viral cationic lipid vectors based on spermine, for the intracellular delivery of siRNA (short interfering RNA) and the subsequent siRNA mediated gene silencing. Two parameters were varied: the type of fatty acid and the cationic head-group. Among the symmetrical spermine conjugates, N^4,N^9-dierucoyl spermine (DES) resulted in higher siRNA delivery compared to N^4,N^9-dioleoyl spermine (DOS), while enhanced green fluorescent protein (EGFP) silencing in HeLa cells showed that the unsaturated fatty acid conjugates are more efficient than the saturated fatty acid ones, and cell viability was 75%-85% for conjugates with chain length ≥ 18. Two cationic lipids with guanidine head-groups, N^1,N^{12}-diamidino-N^4,N^9-dioleoylspermine and N^1,N^{12}-diamidino-N^4-linoleoyl-N^9-oleoylspermine, were more efficient in EGFP gene silencing compared to cationic lipids with shorter C12 (lauroyl) and very long C22 (erucoyl) chains, with cell viability (64%-83% for chain length ≥ 18). Changing the cationic head-group to guanidine did not offer a significant advantage in gene silencing over the conjugates with terminal primary amine groups. The asymmetrical N^4-linoleoyl-N^9-oleoyl-1,12-diamino-4,9-diazadodecane (LinOS) resulted in the best gene silencing, while LigOS (with one lignoceroyl 24:0 chain) resulted in the best siRNA delivery. Conjugates with two unsaturated fatty chains generally resulted in better EGFP gene silencing, while conjugates with one saturated chain and one unsaturated chain resulted in better siRNA delivery. Increasing the chain length also resulted in increased siRNA delivery (cell viabilities of asymmetrical > 74%, LinOS 88%). siRNA lipoplexes prepared using mixtures of LinOS with either cholesterol or DOPE (1,2-dioleoyl-*sn*-glycero-3-phosphoethanolamine) resulted in increased siRNA delivery, and enhanced EGFP silencing, with LinOS/Chol mixture (1:2 molar ratio) resulting in the highest siRNA delivery and the best gene silencing (EGFP reduced to 20%). Temperature studies of intracellular entry showed that the majority of lipoplexes are internalized by endocytosis, however the majority of gene-silencing occurs due to lipoplexes internalized via another mechanism.

Aims

The aims of this thesis are to design, synthesize, and evaluate non-viral cationic lipid vectors, based on spermine, for the intracellular delivery of siRNA and the subsequent siRNA mediated gene silencing. The synthesized vectors should optimally be efficient (approaching 100% silencing) and non-toxic. Two parameters related to the design of the non-viral vector will be varied: the type of fatty acid (chain length and saturation) and the cationic head group type. A structure-activity relationship (SAR) study is therefore to be carried out to find the best combination of these parameters. This SAR study will encompass the design, synthesis, and characterization of a series of symmetrical spermine conjugates, a series of guanidinylated spermine conjugates, and a series of asymmetrical spermine conjugates. Evaluating the ability of the synthesized spermine conjugates to bind siRNA and form lipoplexes, and evaluating the lipoplex diameter and zeta potential will then follow. The efficiency of in vitro siRNA delivery and gene silencing by these siRNA lipoplexes prepared with spermine conjugates, as well as quantifying their safety will enable the best vector design parameters to be evaluated. A formulation based approach introducing neutral helper lipids (cholesterol and DOPE) in the lipoplex formulation will also be investigated. Finally, aspects of the mechanisms involved in siRNA delivery and gene silencing will be considered.

These aims will be met through six objectives, divided into Chapters:

1. A focussed and critical review of gene silencing mediated by siRNA, siRNA in clinical trials, and factors affecting siRNA delivery.
2. Synthesis and characterization of five symmetrical diacyl spermine conjugates, investigating their SAR with respect to siRNA delivery, gene silencing, and effects on cell viability in vitro in HeLa cells stably expressing enhanced green fluorescent protein, EGFP.
3. Synthesis, characterization, and SAR of four guanidinylated diacyl spermine conjugates.
4. Synthesis, characterization, and SAR of seven asymmetrical diacyl spermine conjugates.
5. Coformulation of selected spermine conjugates with the neutral helper lipids cholesterol and DOPE to investigate their siRNA delivery, gene silencing, and effect on cell viability in vitro.
6. Further coformulation of selected spermine conjugates with reagents which enhance siRNA escape from lipoplexes or from endosomes and investigations of the mechanism of intracellular delivery of selected lipoplex preparations by decreasing the temperature and thus inhibiting endocytosis.

Chapter One Introduction and review of siRNA formulation

RNA interference

History and mechanism of RNA interference

Small interfering RNA (siRNA, also known as short interfering RNA) is a double-stranded RNA (dsRNA), typically of 21-25 nucleotides per strand. Sequence specific post-transcriptional gene silencing by siRNA has many potential therapeutic applications[1] as well as being an important tool in the study of functional genomics. siRNA operates as a part of the cellular mechanism called RNA interference (RNAi), which was first noticed in petunia flowers (*Petunia hybrida*) which showed reduced pigmentation on the introduction of exogenous genes that were meant to increase pigmentation.[2, 3] These experiments aimed at increasing the pigmentation of the petunia flowers by means of introducing additional gene constructs expressing either chalcone synthase[2, 3] or dihydroflavonol-4-reductase.[2] However, the resultant plants produced completely white flowers and/or flowers with white or pale sectors on a pigmented background. The exact mechanism was not identified at the time and was simply termed co-suppression. The transcription level of the suppressed chalcone synthase genes in Petunia flowers was found to be similar to that of the non-suppressed genes, and thus the co-suppression must have been in the post-transcriptional level.[4] Later in 1997, the suppression of chalcone synthase endogene in Petunia flowers was suggested to be related to formation of RNA duplexes by intermolecular pairing of complementary sequences between the coding sequence and the 3′ UTR sequence of the transgene mRNA.[5] In 1998, Fire, Mello and co-workers reported the reduction or inhibition (hence genetic 'interference') of the expression of the *unc-22* gene *in Caenorhabditis elegans* by means of dsRNA that is homologous to 742 nucleotides in the targeted gene,[6] a discovery that was awarded the Nobel Prize in medicine or physiology in 2006. The target gene expresses an abundant although nonessential myofilament protein. Decreasing *unc-22* activity resulted in an increasingly severe twitching phenotype, while complete inhibition resulted in impaired motility and muscle structural defects. The target gene inhibition was best achieved with dsRNA, while using the individual sense or anti-sense RNA strands resulted only in modest silencing. The authors also noticed that only few copies of the dsRNA are required per cell to initiate a potent and specific response, rejecting the hypothesis that the mechanism of interaction with target gene mRNA is stoichiometric in nature, and thus the role of the dsRNA in the interference machinery must be catalytic or amplifying.

Elbashir et al. found in 2001 that sequence-specific gene silencing of endogenous and heterologous genes with 21 nucleotide siRNA occurs in mammalian cell cultures.[7] The reporter genes coding for sea pansy (*Renilla reniformis*) and firefly (*Photinus pyralis*)

luciferases were silenced successfully in different cell lines including human embryonic kidney cells (293) and the cervix cancer cells (HeLa), as well as the endogenous gene coding for the nuclear envelope proteins lamin A and lamin C in HeLa cells. The authors used dsRNA of length 21 or 22 nucleotides with symmetrical 3' 2-nucleotide overhangs on each strand, since dsRNA having length >30 nucleotides initiate an immune response (induce interferon synthesis) that leads to non-specific mRNA degradation, which was evident from non-specific silencing of luciferase with 50 and 500 nucleotides dsRNA in HeLa S3 cells, COS-7 cells (kidney cells of the African green monkey), and NIH/3T3 cells (mouse fibroblasts).[7]

Since then, RNAi mechanism has been, and still is, investigated and reviewed thoroughly.[8-13] RNAi mechanism involves the incorporation of dsRNA segments (e.g. siRNA) that have a complementary sequence to the targeted mRNA in a protein complex. This core complex which carries-out mRNA degradation is the RNA induced silencing complex (RISC).[14-16] The key protein in the degradation process belongs to the argonaute family of proteins, which contain a domain with RNase H (endonuclease) type of activity that catalyse cleavage of the phosphodiester bonds of the targeted mRNA . The assembly of RISC and subsequently its function to mediate sequence specific mRNA degradation occur in the cytoplasm of the cell.[12] The source of the dsRNA segments incorporated in RISC can be endogenously processed microRNA (miRNA), short hairpin RNA (shRNA), or synthetic siRNA. miRNA is produced from endogenous DNA through the action of RNA polymerase II resulting in the formation of non-coding RNA called primary miRNA (pri-miRNA), which is processed in the nucleus by a protein complex containing an enzyme known as Drosha and a dsRNA binding protein cofactor called Pasha (DGCR8). Drosha cleaves pri-miRNA to produce (pre-miRNA), a dsRNA of 70–90 nucleotides and having a hairpin loop, which binds to Exportin 5 protein and is transferred from the nucleus into the cytoplasm. Pre-miRNA is processed by Dicer (RNase III enzyme) in the cytoplasm to give miRNA, typically of 22 nucleotides in length and having two nucleotide overhangs at the 3' position.[12, 17] shRNA is produced by transcription from an exogenous DNA that is delivered to the nucleus, and codes for a hair pin shaped RNA with segments of length 19-29 nucleotides and loop of 9 nucleotides[18, 19] which can then be processed by Dicer and incorporated in the RNAi machinery.

Once in the cytoplasm, the processed dsRNA (miRNA, processed shRNA, or siRNA) is then incorporated into a protein complex (in some literature sources referred to as RISC-loading complex, RLC). In *Drosophila* the RLC is composed of the dsRNA, heterodimer protein DCR2 (Dicer variant)/R2D2. Some literature resources suggested the presence of the catalytic argonaute proteins as well in this complex. The active RISC is formed when one of

the RNA strands in the complex is cleaved (the passenger strand) and the strand with the less thermodynamic stable 5' end (guide/anti-sense strand) remains in the complex. The mRNA with complementary sequence to the guide strand binds to the active RISC and is cleaved by the endoribonuclease activity of the argonaute component of the complex (Figure 1).

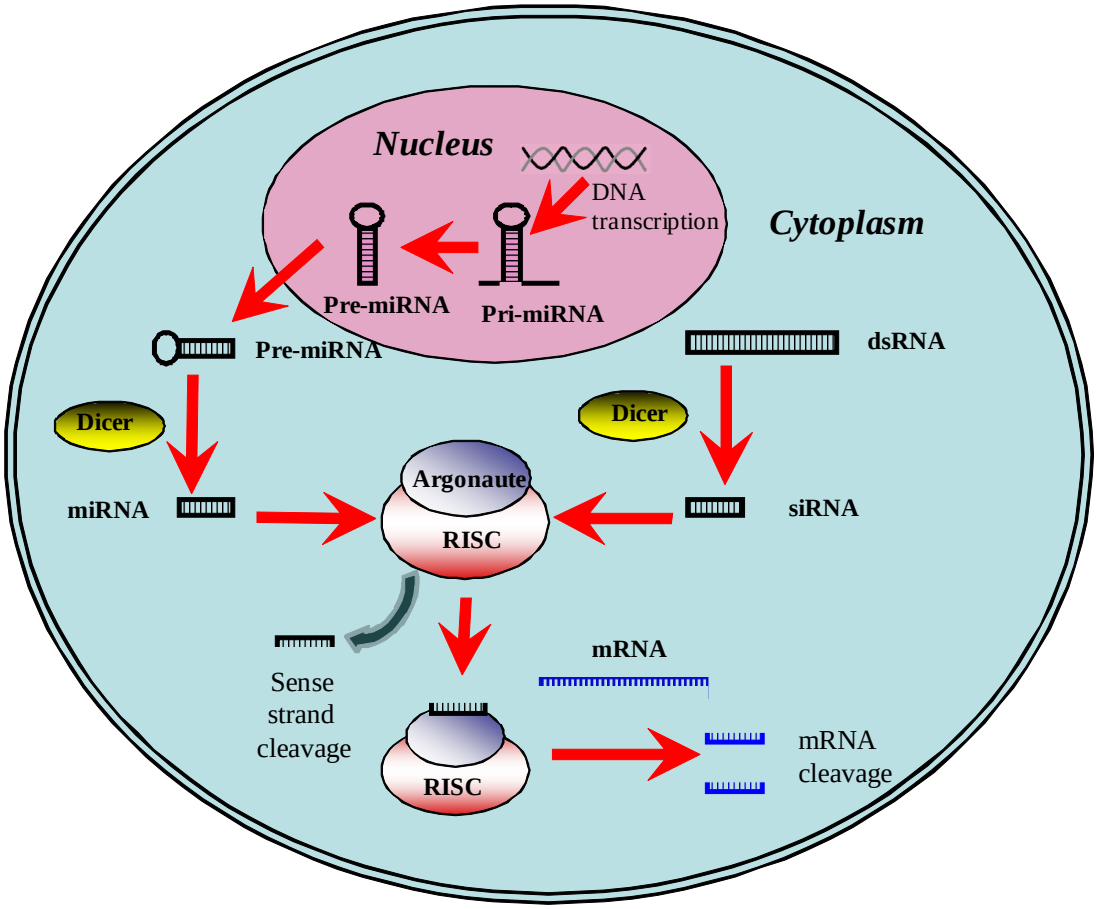

Figure 1. RNAi mechanism in an eukaryotic cell. The source of antisense strand incorporated in RISC can be miRNA, processed exogenous long dsRNA, or synthetic siRNA delivered to the cell.

RNA duplex structure

RNA is a polymer of ribonucleotides. Each RNA nucleotide is composed of one nucleobase, the monosaccharide pentose ribose, and one phosphate group. The nucleobases in RNA are adenine (purine base), guanine (purine base), uracil (pyrimidine base), and cytosine (pyrimidine base) (Figure 2). A nucleoside is formed when each base is connected via a glycosidic bond to the anomeric carbon 1' of ribose, thus when glycosylated, adenine, guanine, uracil, and cytosine nucleobases give adenosine, guanosine, uridine, and cytidine nucleosides. Each two nucleosides are connected via a phosphate diester bond between the 3'

of one nucleoside and 5' of the next nucleoside to form the RNA polynucleotide strand. The main differences in the primary structure of RNA and DNA are that RNA pentose is ribose while DNA pentose is 2'-deoxyribose, and the RNA incorporates the nucleobase uracil instead of thymine.

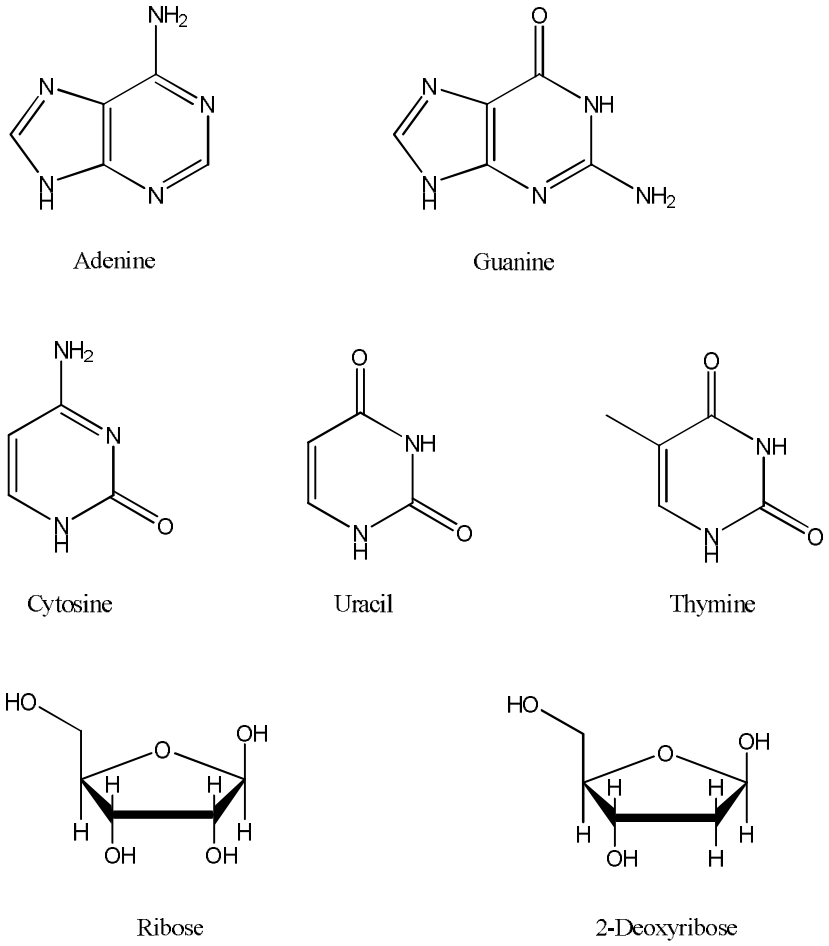

Figure 2. Nucleobases and pentoses of RNA and DNA.

In order to form an RNA duplex (Figure 3), the strands with complementary nucleotide sequence bind together by hydrogen bonds. Adenine is bound to uracil with two hydrogen bonds while guanine is bound to cytosine with three hydrogen bonds, thus forming what is known as Watson-Crick base pairs. RNA duplexes under normal physiological conditions are in the form of A-helix. This type of duplex is a right-handed helix.[20-22]

The presence of the 2'-hydroxyl group of the ribose and the lack of the methyl group on the nucleotide uridine (in contrast to the methylated thymidine) results in structural differences between RNA and DNA, with the 2'-hydroxyl group of RNA being the major cause of the differences. The sugar phosphate backbone of RNA duplexes is stabilized by the 2' hydroxyl in the C3'-endo position, while DNA is in the C2'-endo position (Figure 4).

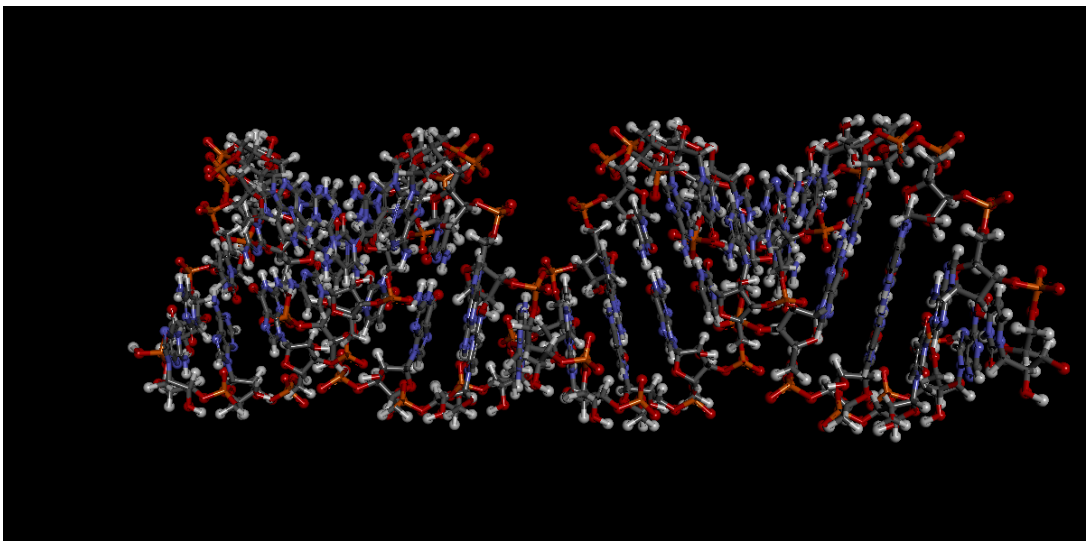

Figure 3. siRNA duplex typically 21-25 nucleotides per strand.

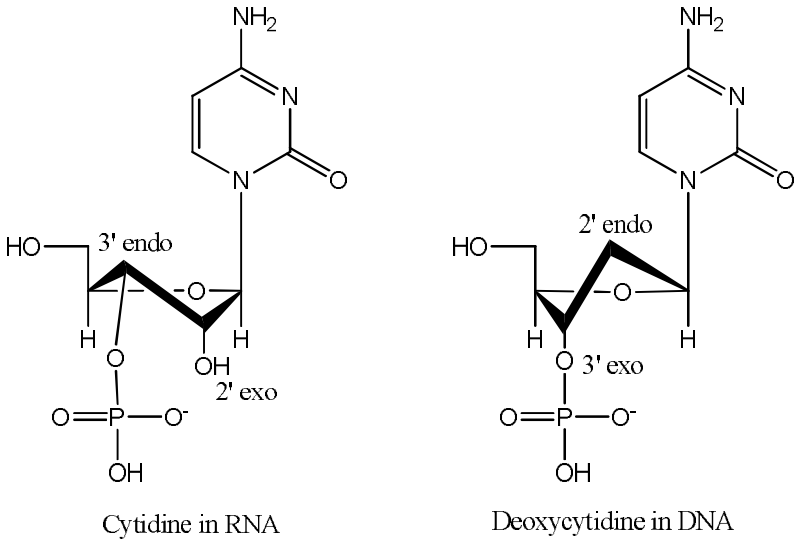

Figure 4. 3'-endo ribose configuration of RNA (left) vs. 2'-endo (right) of 2'-deoxyribose in DNA. Shown is cytidine (RNA) and deoxycytidine (DNA) with the 3' hydroxyl phosphorylated. The hydrogen atoms at C2' and C3' were not displayed for clarity.

Thus RNA duplex takes the A helix form while the DNA helix takes the B form. The A-helix form is suggested to have a greater hydration shell, giving RNA duplexes more thermodynamic stability and more rigidity compared to DNA duplexes.[20-22] RNA A-helix completes one complete rotation in 11–12 base pair (bp) compared to 10 bp for DNA, with a rise of 2.7 Å per bp of RNA.[23] The A- helix geometry has been suggested to be the major factor explaining why dsRNA and not dsDNA is involved in the RNAi machinery,[24] where the A-helix geometry between the guide strand and the complementary target mRNA is essential for the catalytic activity of the argonaute 2 protein in the RISC.

As a result of the presence of a hydroxyl group in the 2' position of the ribose in the RNA backbone, the RNA phosphodiester backbone is more susceptible to hydrolysis by nucleases compared to the DNA which lacks the 2' hydroxyl in its 2'-deoxyribose.[25] Incubation of siRNA in fetal bovine or human serum at 37 °C resulted in the degradation and partial or complete loss of activity.[26] When incubated in human plasma at 37 °C, more than 50% of the unmodified siRNA was degraded within one minute, and practically all siRNA was completely degraded within 4 hours.[27] Although Ribonuclease A (RNase A, an endoribonuclease) cleaves single stranded RNA, siRNA degradation in serum was reported to be mainly due to RNase-like activity,[28] which is suggested to occur during transient breaking of the hydrogen bonds joining the two siRNA strands. In addition to RNase A family of enzymes, blood serum contains also phosphatases and exoribonucleases which can also affect degradation of siRNA at nuclease sensitive sites on both strands.[29]

Therapeutic potential of RNAi based therapies

RNAi based therapies emerged in the period following its discovery in 1998, and are promising therapeutic candidates to treat various types of diseases, ranging from age related macular oedema to respiratory tract infections to various types of cancer.[30-32] In addition to siRNA based therapies, shRNA[33, 34] and miRNA[35] are potential therapeutic tools. siRNA based therapeutics are already in phase I and phase II of clinical trials. Representative examples of clinical trials involving siRNA are shown in Table 1. The basic concept is the reduction or inhibition of the expression of a protein that is involved in the pathophysiological pathway of the target disease (silencing/knocking-down the target gene). This concept is evident from using Cand5 siRNA targeting the mRNA translating the vascular endothelial growth factor (VEGF), thus reducing/inhibiting angiogenesis and preventing progression of wet age related macular oedema (Table 1).[36] Atu027 siRNA targets the protein kinase N3, the latter plays a role in cancer metastasis.[37]

The therapeutic application of siRNA requires overcoming several barriers (Figure 5) for its intracellular delivery and the subsequent functional gene silencing activity.[38-40] Those barriers are mainly due to siRNA specific characteristics, most important are having a highly negative charge due to their phosphate backbone (on average 40-50 negative charges per siRNA), being susceptible to degradation by nucleases, and having relatively large molecular weight (13-15 kDa) compared to conventional small drug molecules. First, local delivery (such as intravitreal) is different from intravenous delivery, where the latter will subject the siRNA to the serum ribonucleases, which results in degrading non-modified siRNA within time periods that varies from minutes to hours.[27] siRNA injected intravenously in rats was reported to be cleared rapidly from circulation and accumulates in kidneys within minutes of

injection,[41] making it useful only if the target organ is the kidney. In order to gain access into the cytoplasm where siRNA can exert its biological activity, the polyribonucleotide must pass first through the interstitial space then through cell membrane. This will be a difficult task, since both the extracellular matrix in many tissue types and the cell membrane incorporate negatively charged glycosaminoglycans (e.g. heparan sulfate).[42] In addition, cell membrane has negatively charged phospholipids (e.g. phosphatidyl serine phospholipids) and the membrane is negatively charged.[42, 43] The net result is unfavourable repulsive interaction with the naked siRNA.

As a result, different strategies were developed to overcome the barriers to reproducible and functional siRNA delivery. These strategies fall into two general categories. One category is modifying the siRNA. The other category is deploying a vector to protect the siRNA and increase its efficiency of delivery.

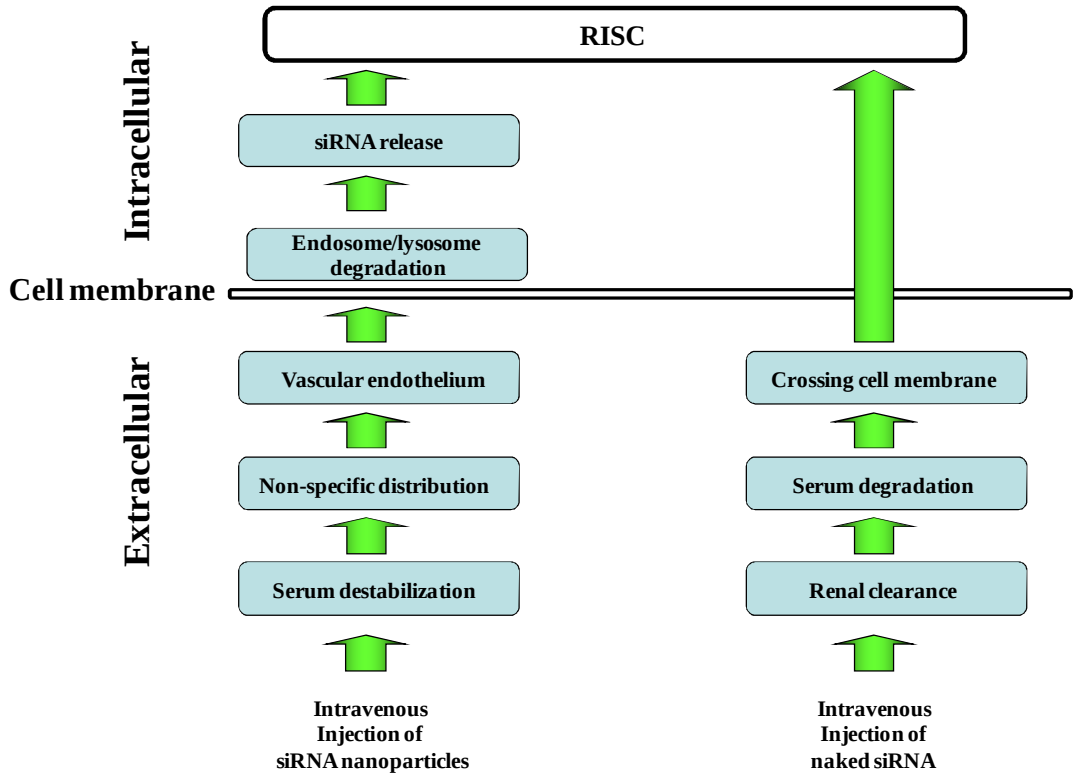

Figure 5. Summary of barriers to successful gene-silencing mediated by siRNA after intravenous injection, whether delivered naked or incorporated in nanoparticles.

Strategies to achieve efficient siRNA delivery and gene silencing

siRNA modifications

siRNA modifications include those carried out at the ribose residue, at the phosphate backbone, at the RNA nucleotides, the siRNA termini, and/or by conjugation of other molecules to the siRNA molecule. Modifications to the ribose at the 2' position are common,[44] and include 2'-*O*-alkylation (e.g. 2'-*O*-Methyl and 2'-*O*-Methylethoxy) modifications. 2'-Fluoro RNA is another common modification. Locked nucleic acids (LNAs) have a methylene bridge connecting the 2'-*O* to the 4'-C of the ribose unit, locking the sugar in the 3'-endo conformation. These modifications lead to an increased ribonuclease resistance[44, 45] Modifications at the phosphate backbone include phosphorthioate, boranophosphate, and methylphosphonate linkages[44, 45] and is reported to increase siRNA stability against various ribonucleases and phophodiesterases.[46] siRNA nucleotides can be substituted with DNA nucleotides aiming at increasing stability and/or decreasing unwanted siRNA off-target effects.[47] Modifications of the 3' overhangs (usually two nucleotides in length), include incorporating deoxyribonucleotides aiming to reduce costs and increasing stability towards 3' exoribonucleases. The 5'-termini chemical phosphorylation of the antisense strands results in higher gene silencing efficiency, while blunt ended duplexes were reported to be more resistant to exonucleases. The advantages of each of the aforementioned techniques, other modification strategies, as well as the considerations related to the degree of modification and its effect on gene silencing efficiency and associated cytotoxic effects were reviewed thoroughly.[44, 48-50]

The conjugation of drug molecules, aptamers, lipids, polymers, and peptides/ proteins to siRNA could enhance in vivo delivery characteristics.[51] The main aims of such conjugations are to enhance siRNA stability, increase in vivo half-life, control biodistribution, increase efficiency of intracellular delivery, while maintaining the gene silencing activity.

One strategy is to increase the hydrophobicity of the siRNA. Cholesterol was conjugated to the 5' termini of siRNA, the cholesterol−siRNA conjugate (chol-siRNA) resulted in better intracellular delivery compared to unmodified siRNA and retained gene silencing activity in vitro in β-galactosidase expressing liver cells.[52] When cholesterol was conjugated to the 3' terminus of the sense (passenger) strand of siRNA, the conjugate had improved in vivo pharmacokinetics as the intravenous administration of chol-siRNA in mice resulted in its distribution and detection in the fat tissues, heart, kidneys, liver, and lungs, even 24 h after intravenous injection.[53] No significant amounts of unmodified siRNA were detected in the tissues 24 h after the intravenous injection. Conjugation of siRNA to bile acids and long-chain fatty acids, in addition to cholesterol, mediates siRNA uptake into cells and gene silencing in vivo.[54] The shorter chain fatty-acid conjugates, namely lauroyl (C12), myristoyl

(C14) and palmitoyl (C16) did not silence the target apolipoprotein B mRNA levels in mouse livers after intravenous injection. siRNA fatty-acid conjugates having the long saturated chains stearoyl (C18) and docosanoyl (C22), significantly reduced apolipoprotein B mRNA levels.

Cell penetrating peptides (CPP) are used to facilitate cellular membrane crossing of many molecules of various properties such as antisense oligonucleotides, peptides, and proteins and are used already in vivo.[55] siRNA was conjugated to penetratin and transportin, to silence luciferase and the green fluorescent protein (GFP) in different types of mammalian cells.[56] However, in vivo lung delivery in mouse of siRNA conjugated to penetratin and TAT(48-60), targeting p38 MAP kinase mRNA showed that the reduction in gene expression was peptide induced and the penetratin conjugated siRNA resulted in innate immunity response.[57]

siRNA functioning against the vascular endothelial growth factor (VEGF) mRNA was conjugated to poly(ethylene glycol) (PEG, 25 kDa) via a disulfide linkage at the 3' terminus of the sense strand.[58] The siRNA-PEG conjugate formed polyelectrolyte complex micelles (PEC) by electrostatic interaction with the cationic polymer polyethyleneimine (PEI). The formed VEGF siRNA-PEG/PEI PEC micelles showed enhanced stability against nuclease degradation compared to the unmodified siRNA. These micelles efficiently silenced VEGF gene expression in prostate carcinoma cells (PC-3) and showed superior VEGF gene silencing compared to VEGF siRNA/PEI complexes in the presence of serum. PEG conjugation on its own enhanced the stability of the siRNA in serum containing medium. The prolonged stability of the PEC micelles was suggested to be due to the presence of PEG chains in the outer micellar shell layer, thus sterically hindering nuclease access into the siRNA in the micelle core.[58]

Targeting molecules such as antibodies[59] and aptamers (peptides or single stranded DNA or RNA that have selective affinities toward target proteins)[60] have also been conjugated to siRNA, with the aim of increasing the efficiency of siRNA delivery to the targeted tissues.

Conjugating molecules to siRNA requires specific considerations. First, the site of conjugation (3' and/or 5' terminus, on sense and/or antisense strand) should be chosen such that it does not affect the activity of the siRNA and its ability to be incorporated in the RISC, or its ability to bind the target mRNA in the correct helix conformation. Second, the conjugated siRNA might have new properties that were not present in the unmodified parent siRNA. An example is the in vivo immune response resulting from the penetratin-siRNA conjugate.[57] Third, the conjugation process is multi-step, and the chemical reaction intermediates and products require efficient purification in order to meet the specifications of in vivo applications. These steps need to be repeated for each siRNA under investigation, which can be costly and time consuming. Thus, although there are clear advantages to

synthesize siRNA conjugates, there are also disadvantages, and conjugation is therefore one of two valuable approaches in the toolbox for preparing siRNA based therapies. The other valuable tool is complexing or incorporating the siRNA in a vector.

Table 1. Representative clinical trials using siRNA (http://clinicaltrials.gov/ct2/home, accessed on 20/8/2011).

siRNA	**Disease**	**Vector/ *Route***	**Phase**	**Sponsor**
Cand5/ Bevasiranib	Diabetic macular oedema	None/ *Intravitreal*	Phase II	Opko Health (Miami, USA)
Cand5/ Bevasiranib	Age-related macular degeneration	None/ *Intravitreal*	Phase II (Phase III halted)	Opko Health (Miami, USA)
ALN-RSV01	Respiratory syncytial virus infection	None/ *Intranasal*	Phase II	Alnylam Pharmaceuticals (Cambridge, USA)
CALAA-01	Solid tumour/ melanoma	Cyclodextrin nanoparticles/ *Intravenous*	Phase I	Calando (Pasadena, CA, USA)
Atu027	Colorectal cancer metastasizing to the liver	AtuPlex-Liposome/ *Intravenous*	Phase I	Silence Therapeutics (London, UK)
Two siRNA against TGFBI and COX-2 STP705	Wound healing	Nanoparticles/ *Intravenous*	Phase I	Sirnaomics (Gaithersburg, MD, USA)
I5NP	Protection from acute kidney injury after cardiac bypass surgery	None/ *Intravenous*	Phase I	Quark Pharmaceuticals (Fremont, USA)

Viral vectors for shRNA delivery

Vectors for RNAi based therapies are either viral or non viral vectors. Viral vectors (Table 2) are used to deliver genes encoding hairpin RNA structures such as shRNA and miRNA, which are then processed by the cellular RNAi machinery to the functional silencing dsRNA.[61, 62] Viral vectors offer two main advantages, the first is the very high efficiency

compared to non-viral vectors,[63] which can reach few orders of magnitude more than that achieved with non-viral vectors, and the second is the potential of long term expression of the delivered RNAi therapeutic, which is very useful in the treatment of chronic diseases such as HIV infection and viral hepatitis.[64, 65] Retroviruses are enveloped, single stranded RNA viruses and have a genome capacity of 7-10 kilobases (kb). They preferentially target dividing cells which limits their use to mitotic tissues (thus for example excluding brain and neurons). Retroviruses integrate their DNA in the host genome using an integrase enzyme, which provides the advantage of stable long term expression of the delivered transgene in the host cell and its descendents. However, integrating new DNA sequences into host genome carries the risk of insertional mutagenesis.[63, 66] shRNA expression cassette delivered by a retroviral vector was used in rats to silence a RAS oncogene in order to suppress tumour growth.[67] Herpes virus was used successfully to deliver shRNA targeting exogenous β-galactosidase or endogenous trpv1 gene mRNA in the peripheral neurons in mice by injecting once directly into the sciatic nerve of the animals.[68]

Unlike other retroviruses, lentiviruses can infect dividing as well as differentiated and non-dividing cells. The lentiviral genome can accommodate 7.5 kb,[62] and their genome is integrated in the host cell genome, lentiviral vectors are generally preferred for long-term expression of transgenes, and efficient delivery in vivo to the brain, eye, and liver to induce long-term transgene expression as reported.[69] A lentiviral vector was used to deliver shRNA targeting Smad3 gene mRNA, and enhanced myogenesis of old and injured muscles.[70]

Adenoviruses are non-enveloped viruses, with linear double stranded DNA. They preferably infect the upper respiratory tract and the ocular tissue. Their genome can accommodate up to 8 kb which can be extended to $\geq$25 kb in modified viruses that have their viral genes deleted.[63] These viruses can infect post mitotic cells and thus are good candidates for neurological diseases. Unless delivering genes that can exist as episomes in host cells, adenoviruses result only in transient expression of their cargo. However, although the host cells with the episome can express the delivered genes for the cell life time, these cells will eventually be removed by the host immune system.[63] shRNA targeting VEGF that was delivered by an adenoviral vector resulted in potent inhibition of angiogenesis and tumour growth in mice.[71]

Adeno-associated virus is a single stranded DNA non-pathogenic virus that can accommodate a 4.7 kb genome. They can infect dividing or non-dividing cells. The replication of adeno-associated virus requires co-infection with adenovirus. The viral genome integrates into the host cell genome at a specific location on chromosome 19.[63] Direct intracerebellar injection in a mouse model of spinocerebellar ataxia of an adeno-associated viral vector delivering a cargo expressing shRNA targeting polyglutamine induced

neurodegeneration, significantly restored cerebellar morphology and improved motor coordination in the mice.[72]

Table 2. Summary of properties of viral vectors that are commonly used in gene therapy (adapted from http://www.genetherapynet.com/viral-vectors.html, accessed on 21/8/2011).

		Retrovirus/ Lentivirus	Adenovirus	Adeno-associated virus	Herpes virus
Viral vector properties	**Genome**	ssRNA	dsDNA	ssDNA	dsDNA
	Capsid	Icosahedral	Icosahedral	Icosahedral	Icosahedral
	Envelope	Enveloped	None	None	Enveloped
	Viral Polymerase	Positive	Negative	Negative	Negative
	Diameter (nm)	80-130	70-90	18-26	150-200
	Genome size (kb)	7-10	38	5	120-200
Gene therapy related	**Infection tropism**	Dividing*	Dividing/ Non-dividing	Dividing/ Non-dividing	Dividing/ Non-dividing
	Virus genome integration	Integrating	Non-integrating	Integrating	Non-integrating
	Transgene expression	Lasting	Transient	Lasting	Transient
	Packaging capacity (kb)	7-8	8	4.5	>30

* Lentiviral vectors can infect non-dividing cells as their pre-integration complex can traverse the nuclear membrane pores (NMP), in contrast to retrovirus pre-integration complex which does not traverse NMP, requiring the host cell division to integrate the retroviral genome.[73]

Although highly efficient in delivering their cargo, viral vectors have their disadvantages. Adenoviral vectors have the disadvantage of triggering a strong immune (adaptive and innate) response by repeated administration, in addition to target organ immunotoxicity, specially hepatotoxicity,[74-76] which resulted in 1999 in the death of one 18-year-old male who received high dose of adenovirus that was delivered directly in the hepatic artery in a clinical gene therapy safety study.[77] Clonal T-cell acute lymphoblastic leukemia caused by insertional mutagenesis in a gene therapy completed clinical trial involving patients suffering X-linked severe combined immunodeficiency (SCID-X1) was reported in one out of the 10 patients

using a retroviral vector.[78] Integration of the vector genome material in the antisense orientation 35 kb upstream of the protooncogene (LMO2) caused over expression of the gene in the leukemic cells. In a similar study, 4 out of 9 patients developed leukemia within 3-6 years post-treatment mainly due to vector-mediated upregulation of host cellular oncogenes.[79, 80] In addition, immune responses (whether adaptive or innate) of varying degrees depending on the type of vector, dose, and target organs were reported for lentiviral, adenoviral, adeno-associated viral vectors.[76]

Current research on viral vectors for gene therapy is focussed on approaches such as vector engineering e.g. modifying the viral capsid or pseudotyping the envelope, different delivery strategies, and administration to immune-privileged sites that can tolerate the delivered viral vectors without responding with an inflammatory response.[76, 81] Other research focuses on the essential scaling-up process of vector production and increasing the packaging efficiency of the vectors,[81] the processes without which, the wide spread and successful therapeutic use of the viral vectors will be very difficult to achieve.

Non viral vectors

Non-viral vectors for gene and siRNA delivery are an alternative to the viral vectors, as they do not suffer many of the disadvantages of the viral vectors, especially immunogenicity and tumourigenicity. The non-viral vectors can be classified generally as peptides, polymeric based vectors, carbohydrate based, and lipid based.[82] Cell penetrating peptides (CPPs), also known as peptide transduction domains (PTDs), have shown the ability to cross the cellular membrane despite their relatively high molecular weight and size (Table 3). PTDs generally are short amphipathic and/or cationic peptides that can transport many hydrophilic molecules across the cell membrane. A wide range of molecules including liposomes,[83, 84] peptides, proteins,[85] peptide nucleic acids [86] and polynucleotides[87] are delivered intracellularly using PTDs and they have also been applied in vivo.[55, 88, 89]

The TAT protein, which is derived from HIV-1, was found in 1988 that it could be taken up by cells growing in tissue culture,[90] and it was reported that a small basic region of TAT (48–60) was essential for uptake by the cells.[91] PTDs include antennapedia homeodomain protein (Antp, penetratin), mitogen-activated protein (MAP), poly-arginine, transportan, VP22 [55, 88]. Two major pathways are involved in the uptake of PTDs and PTD-cargos: direct translocation at 4 °C and 37 °C and endocytosis-translocation at 37 °C. These mechanisms depend on many factors: cargo size, cell line, PTD concentration, and the type of PTD.[55, 92, 93] siRNA can be conjugated covalently to the CPP or can be complexed with the cationic groups of basic amino acids that are present in the backbone of the CPP. As a representative example of non-covalent complexation, CADY,[94] which is basic due to its five arginine

residues can complex with the negatively charged siRNA. Another example of non-covalent complexation is the poly-arginine CPP.[95]

Table 3. Selected CPPs used for siRNA delivery.[55]

CPP	Sequence of CPP	Type of association with siRNA	Target mRNA
CADY	GLWRALWRLLRSLWRLLWRA	Non-covalent	GAPDH, p53[94]
EB1	LIRLWSHLIHIWFQNRRLKWKKK	Non-covalent	Luc[96]
MPG	GALFLGFLGAAGSTMGAWSQPKKKRKV	Non-covalent	Luc, GAPDH[97] Oct-3/4[98]
Poly-arginine	RRRRRRRRR	Non-covalent	VEGF[95]
Penetratin	RQIKIWFQNRRMKWKK	Covalent Covalent Covalent	Luciferase (Luc), EGFP[56] SOD1, caspase-3[99] Luc, p38 MAP kinase[57, 100]
Transportan	LIKKALAALAKLNIKLLYGASNLTWG	Covalent	Luc, EGFP[100]
TAT	GRKKRRQRRRPPQ	Covalent	EGFP, CDK9[101]

PEI (Figure 6) is known as a very efficient plasmid DNA (pDNA) delivery vector. However, PEI as a siRNA delivery vector is reported to be much less efficient.[102, 103] This decreased efficiency is due to the dissociation of the siRNA/PEI complex upon interaction with the negatively charged cell membrane, which is suggested to be because of the short length of siRNA and the associated weak electrostatic interaction with PEI.[104, 105] Another drawback of PEI is its relatively high toxicity.[106] Thus, in addition to linear PEI, PEI polymers with a wide range of molecular weights were developed to increase PEI efficiency and/or decrease toxicity, although not all PEI are suitable for siRNA delivery.[107] The main advantage of PEI is the ability of its variety of amino-groups to be protonated at lower pH (inside endosomes) leading to what is known as the “proton sponge effect”,[108] and efficient escape from endosomes.

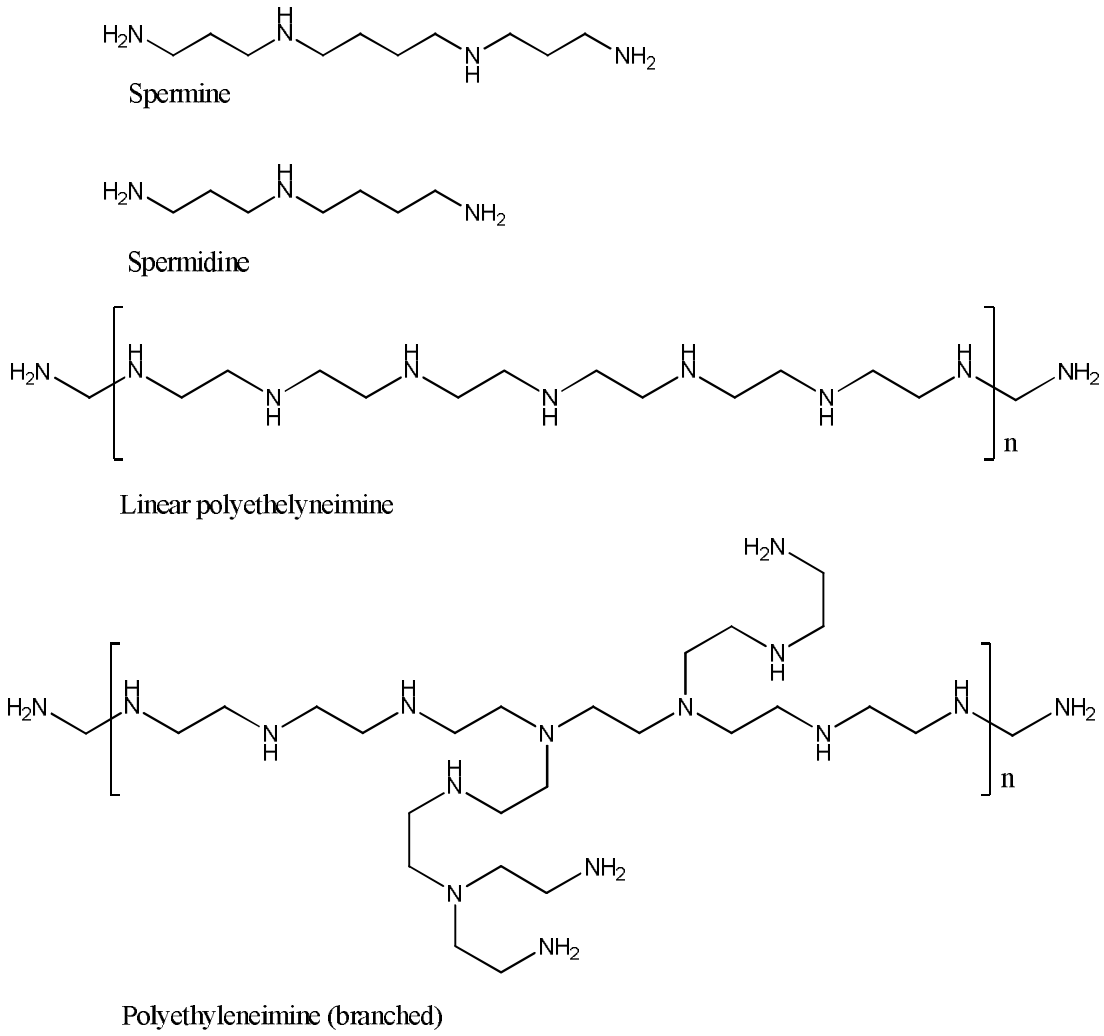

Figure 6. Representative examples of polyamines used in siRNA delivery either as is (PEI) or as a part of cationic polymers and/or lipids (e.g. spermine).

One approach to enhance siRNA delivery with PEI is increasing the hydrophobicity of PEI by covalently conjugating alkyl chains,[109] where increasing the hydrophobic alkyl chain length generally improved the stability of the PEI/siRNA complex. In a similar strategy, cholesterol was conjugated to PEI[110] with decreased toxicity of the conjugates. Low molecular weight PEI (MW < 5 kDa) is less toxic than the higher molecular weight PEI (≈25 kDa), but less efficient in polynucleotide delivery, thus, cross linking of the low molecular weight PEI with disulfide bonds which are cleaved in the reducing environment of the cytoplasm increased the efficiency of siRNA delivery through the enhanced release of siRNA in the cytoplasm.[111]

Chitosan is a biocompatible and biodegradable polysaccharide that is a copolymer of N-acetyl-D-glucosamine and D-glucosamine. Chitosan has weakly basic properties due to the presence of the D-glucosamine residue with a p*K*a value 6.2-7.0. The molecular weight of chitosan affects the complex stability, size, zeta-potential and in vitro gene knock-down of siRNA/chitosan nanoparticles.[112] Chitosan with high molecular weight (64.8-170 kDa), formed stable complexes with siRNA and resulted in high gene knock-down efficiency in H1299 (human lung carcinoma) cells, while chitosan with low molecular weight (10 kDa) could not complex the siRNA into stable nanoparticles and showed almost no knockdown.[113] The method of association affects gene silencing efficiency, where chitosan-TPP/siRNA nanoparticles (siRNA entrapped inside the nanoparticles, and TPP is sodium tripolyphosphate and used as a polyanion to cross-link with the cationic chitosan groups by electrostatic interactions) showed high siRNA binding and better gene silencing in vitro compared to siRNA/chitosan particles prepared by simple complexation and adsorption of siRNA onto chitosan.[114]

Although chitosan has good potential as a non-viral gene delivery vector, its wide use is largely limited due to its poor solubility (because of their p*K*a, chitosan amino groups are only partially protonated at the physiological pH 7.4), poor stability of its siRNA complexes at the physiological pH, and low transfection efficiency. Various strategies are adopted to overcome these drawbacks, such as covalently conjugating PEG polymers to chitosan and binding targeting ligands to enhance cell specificity.[112]

Cyclodextrins (CD) are cyclic oligosaccharides composed of 6, 7, or 8 D(+)-glucose units, known as α-CD, β-CD, or γ-CD respectively, that are linked by α-1,4-linkages. Polymers conjugated to β-CD lack immunogenicity and hence are attractive vectors for polynucleotide delivery. β-CD have a hydrophilic outer surface and a hydrophobic inner cavity which enable them to form inclusion complexes. Efficient cellular transfection of siRNA labelled with a fluorescent tag into human embryonic lung fibroblasts (MRC-5 cells) was observed by siRNA complexes with the β-CD guanidine derivatized bis-(guanidinium)-tetrakis-(β-cyclodextrin) tetrapod (having four β-CD units).[115] The ability of β-CD to form inclusion complexes was used to develop a siRNA delivery vector. β-CD was covalently bound to a polycationic segment (to electrostatically bind siRNA), while adamantane-PEG-transferrin (adamantane can fit in the β-CD cavity) formed an inclusion complex which can enhance the stability of siRNA nanoparticles in vivo.[116] This system was used to deliver siRNA silencing the *EWS-FLI1* gene thus inhibiting tumour growth in a murine model of metastatic Ewing's sarcoma.

Dendrimers have a central core to which are connected several branched arms in a manner that can be symmetrical or asymmetrical. During the synthesis of dendrimers, arms

(branches) are added to the core structure. Each addition is called a generation and increases the previous generation number by one. Due to their unique structure, dendrimers can have a planar, elliptical, or spherical shape depending on generation number. Among the most widely used dendrimers are polyamidoamine (PAMAM) and polypropylenimine (PPI) dendrimers.[117] Dendrimers which have positively charged cationic groups on their outer surface are commonly used for polynucleotide delivery. The transfection efficiency of dendrimers increases with increasing the charge density or generation number.[118] However, dendrimers with high generation number are generally more cytotoxic compared to dendrimers with low generation number.[119] Usually the inner space near the core is larger compared to outer space near the surface due to the lower density of molecules (less number of arms) near the core, which allow small molecules to be incorporated in the inner space. Owing to the relatively large molecular weight of polynucleotides, they are usually bound to the surface of cationic dendrimers and not in the inner space of the dendrimer. Generally, the toxicity of dendrimers is lower than that of PEI or poly-L-lysine (PLL).[120] One advantage of dendrimers is that they have pH buffering capacity (proton-sponge effect), an important feature for endosomal escape and enhancing the release of polynucleotides.[118, 121]

PPI dendrimers with high generation numbers (4 and 5) were more efficient in forming discrete nanoparticles with siRNA and in gene silencing in A549 (human lung cancer) cells than lower generation dendrimers (2 and 3). The PPI dendrimers with generation number 5 were more toxic, probably due to the increased positive charge density per dendrimers, than generation 4 dendrimers.[122] Complex formation between PAMAM dendrimers having an ethylenediamine core with siRNA as a function of three variables was reported.[123] The ionic strength of the medium (without or with 150 mM NaCl), the generation number (4, 5, 6 and 7) and the *N/P* ratio (ratio of positively charged amine groups per negative phosphate) were varied. The size of the complexes depended on the ionic strength of the media, with the strong electrostatic interactions in medium without NaCl making siRNA/dendrimer complexes smaller than those obtained in 150 mM NaCl. Both the intracellular delivery and silencing of EGFP expression in cell culture was dependent on complex size, with smaller complexes being massively delivered, and resulting in the highest silencing of EGFP expression. siRNA complexed with generation 7 dendrimers resulted in the highest silencing of EGFP expression both in human brain tumour cell line T98G-EGFP (35%) and mouse macrophage cell line J-774-EGFP (45%) cells, in spite of having lower protection of siRNA against degradation with RNase A, showing the importance of formulation procedures on the efficiency of transfection.[123]

Cationic lipids as non-viral vectors for siRNA and DNA delivery

Gene delivery by cationic lipids

Gene delivery (DNA transfection) with cationic lipids (Figure 7) dates back to 1987 when it was reported by Felgner et al.,[124] and the term 'lipofection' was coined. Small unilamellar liposomes containing the cationic lipid *N*-[1-(2,3-dioleyloxy)propyl]-*N,N,N*-trimethyl ammonium chloride (DOTMA) was reported to spontaneously complex DNA completely entrapping the DNA, and enhanced fusion with the cell membrane in vitro in cell cultures, resulting in efficient delivery and expression of the delivered DNA. The lipofection was 5-100-fold more effective than the commonly used transfection techniques at the time by either calcium phosphate or DEAE-dextran (diethylaminoethyl-dextran), depending on the cell line used.[124] Cationic lipids have polar and non polar domains and thus are amphiphilic in nature, with three general structural domains: (a) a cationic hydrophilic head-group (positively charged). The head group can carry a permanent positive charge as in quaternary ammonium groups, or can be protonated at the physiological pH 7.4, such as primary and secondary amine groups. There can be one cationic group per lipid molecule (monovalent cationic lipids) or more than one cationic group per lipid molecule (multivalent cationic lipids); (b) a hydrophobic domain coavalently attached by a linker to the cationic head-group. This domain can be in the form of either alkyl chains (commonly 2 chains) of various chain lengths (with various oxidation states) or can be a steroid such as cholesterol; (c) the linker between the head group and the hydrophobic domain.[125, 126] This linker controls the biodegradation of the cationic lipid and its stability under different conditions according to the type of chemical bonds (e.g. ester, ether, or amide). Each domain can be controlled to change a specific character of the cationic lipid, e.g. using a bioresponsive linker (disulfide)[127] which is reduced in the intracellular environment by glutathione/glutathione reductase and enhance biodegradation characters of the lipid and decrease its cytotoxicity.

The cationic head-group

The cationic head-group's main function is to electrostatically bind the negatively charged phosphates of the polynucleotides. The complexes of cationic lipids with polynucleotides such as DNA and siRNA are called lipoplexes. This requires the presence of a positive charge on the head group at the physiological pH 7.4, i.e. the p*K*a of the head group is ideally at least one unit higher than the physiological pH. The most commonly used head groups contain nitrogen (e.g. amines or guanidines). However other head groups, e.g. arsonium and phosphonium have been reported.[128] Arsonium is less toxic than arsenic (III), and in vitro cytotoxicity evaluation showed that arsonium and phosphonium are less toxic than the ammonium group.[128, 129]

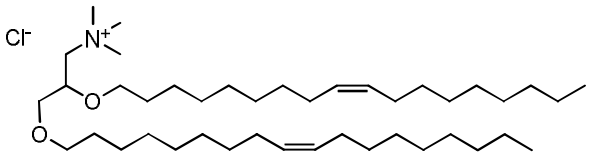

N-[1-(2,3-dioleyloxy)propyl]-*N*,*N*,*N*-trimethyl ammonium chloride (DOTMA)

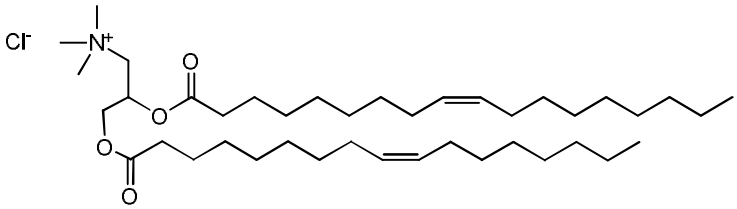

1,2-dioleoyloxy-3-[trimethylammonio]-propane chloride (DOTAP)

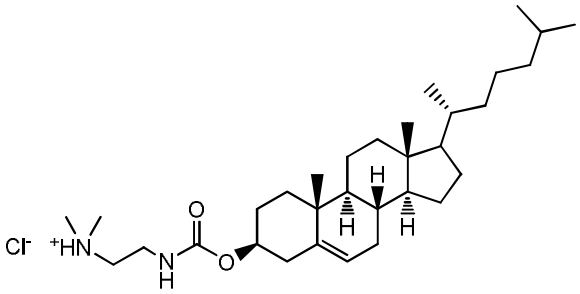

3β(*N*-(*N*',*N*'-dimethylaminoethane)carbamoyl)-cholesterol (DC-Chol)

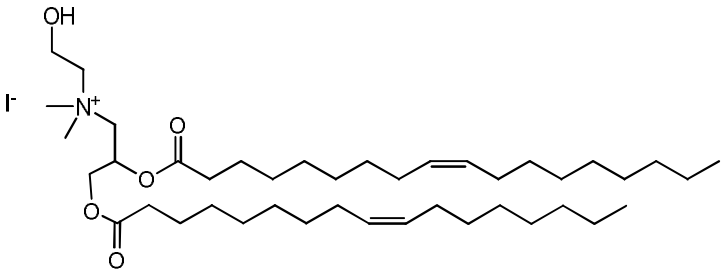

N-[1-(2,3-dioleoyloxy)propyl-*N*-[1-(2-hydroxy)ethyl]-*N*,*N*-dimethyl ammonium iodide (DORI)

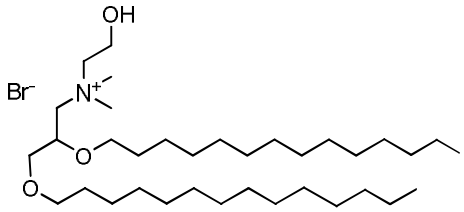

1,2-dimyristyloxypropyl-3-dimethyl-hydroxyethylammonium bromide (DMRIE)

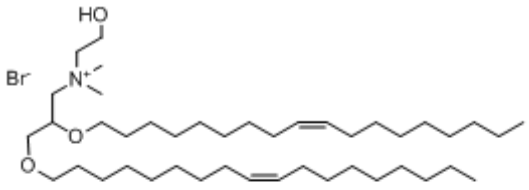

1,2-dioleyloxypropyl-3-dimethyl-hydroxyethylammonium bromide (DORIE)

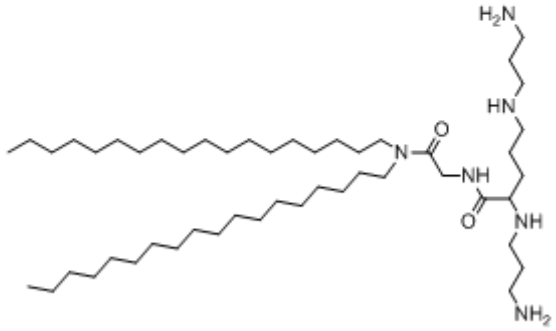

dioctadecylamidoglycylspermine (DOGS)

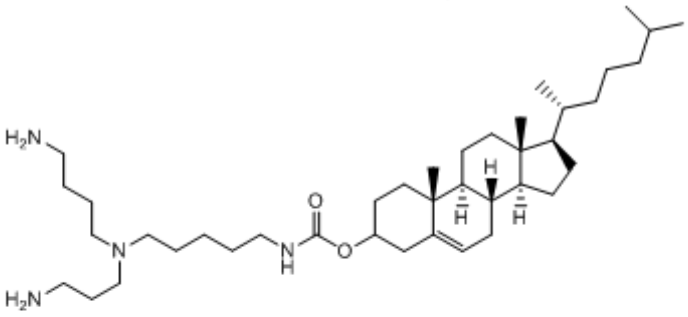

cholesteryl-spermidine

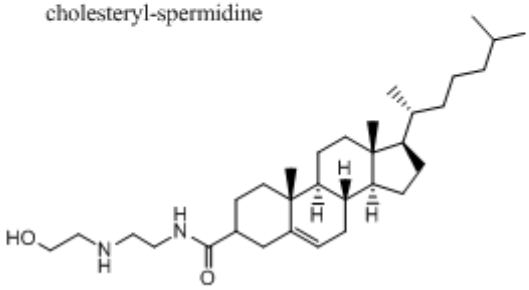

cholesteryl-3β-carboxyamidoethylene-*N*-hydroxyethylamine

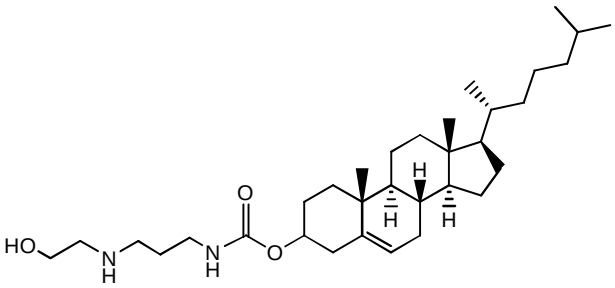

N-hydroxyethyl aminopropane carbamoyl cholesterol

Figure 7. Representative examples of cationic lipids used in DNA and siRNA delivery.

One property that can be changed by controlling the type of the head group is the head group cross-sectional area. The greater the difference between the cross-sectional area of the polar head-group and that of the hydrophobic domain, with the former is designed to be smaller than the latter, the greater is the ability of the cationic lipid to fuse with the cell membrane and endosomal membrane and the greater is the release of polynucleotides from their complex with the cationic lipid due to the decreased structural stability of the lipid assembly.[126, 130] The hydration of the head group affects its cross-sectional area, thus, the conjugation of groups which decrease the hydration state (such as hydroxyalkyl groups that form intermolecular H-bonds) decreases the head group cross-sectional area.

Thus, gene delivery by DOTMA and DOTAP (1,2-dioleoyloxy-3-[trimethylammonio]-propane) was enhanced by incorporation of a hydroxyethyl group to yield the lipids DORIE (1,2-dioleyloxypropyl-3-dimethyl-hydroxyethyl ammonium bromide) and DORI (*N*-[1-(2,3-dioleoyloxy)propyl-*N*-[1-(2-hydroxy)ethyl]-*N*,*N*-dimethyl ammonium iodide) respectively.[131, 132] The head group cross-sectional area can be also controlled by subtle changes to the head group structure. The DC-Chol (3β(*N*-(*N*',*N*'-dimethylaminoethane)carbamoyl)cholesterol) with dimethylamino head-group resulted in more efficient transfection compared to DC-Chol with diethylamino or diisopropylamino head-groups, probably due to increased steric repulsion of the head groups.

The in vitro gene transfer with six non-cholesterol-based cationic lipids (each having two alkyl chains) with a single guanidinium head-group in CHO, COS-1, MCF-7, A549, and HepG2 cells was reported.[133] These lipids were able to form lipoplexes with size range 200−600 nm and ζ-potential +3.4 to -34 mV. The efficiencies of the lipids which had an extra quaternized cationic centre were 2-4-fold more than that of the commercially available reagent Lipofectamine in transfecting COS-1, CHO, A-549, and MCF-7 cells. MTT viability assay in CHO cells showed high (>75%) cell viabilities at the lipid/DNA charge ratios used. DNase I protection assays showed that the lipids having the extra quaternized centre protected DNA better. These results shed light on the importance of choosing the type of head group and number of cationic centres in designing cationic lipids.[133]

A series of cationic cholesterol derivatives were synthesized by covalently attaching the heterocycles imidazole, piperazine, pyridine, and morpholine groups (the head groups) to the parent cholesterol via a biodegradable carbamoyl linker.[134] These lipids were compared with the parent DC-Chol with the linear amine head-group, and they generally showed better or comparable transfection efficiency of pCMV-luciferase into human HepG2 cells (human liver cancer cell line) in the presence or absence of FCS. The most efficient two of these lipids were with morpholine and piperazine head-groups, and they gave higher levels of gene expression in HepG2 and KZ2 (human melanoma cell line) which are generally very hard to

transfect with the commonly used reagents such as DC-chol, Lipofectamine, and PEI. In vivo studies with lipids having morpholine and piperazine head-groups resulted in successful delivery of the reporter gene to the target cells through intrasplenic injection.[134] Cationic lipids which have more than one cationic head-group (multivalent cationic lipids) have more surface charge density than their monovalent (with one head group) analogues, and they are generally expected to better bind and complex polynucleotides. Many multivalent cationic lipids contain a natural occurring polyamine such as spermidine and spermine, which are well known to interact with the minor groove of B-DNA.[135] The triamine spermidine and the tetramine spermine, and their diamine precursor putrescine, are organic polycations that are widely but unevenly distributed in both mammalian and non-mammalian cells and tissues. They have an essential role in controlling DNA, RNA and protein synthesis during normal and neoplastic growth, in cell differentiation, and in tissue regeneration.[136] These polyamines exhibit many metabolic and neurophysiological effects in the nervous system, and are important for the developing and mature nervous system and affect modulation of ionic channels and calcium-dependent transmitter release.[136-142]

Spermine (Figure 6) is incorporated in DOGS[143] (dioctadecylamidoglycylspermine); spermidine bound in cholesteryl-spermidine.[144] The free amine groups of spermine in cholesteryl-spermine conjugates have different p*K*a values and provide a buffering effect in the endosomes facilitating the escape of lipoplex from the endosomes.[145] The length of the linear polyamine attached to the hydrophobic domain and the charge distribution on it affects the transfection efficiency of the cationic lipid.[146] Addition of amine groups separated by methylene groups to the linear polyamine attached to a cholesterol residue did not automatically increase transfection efficiency regardless of the increased charge density. Molecular modelling simulations suggested that increasing chain length led to an increased number of folded conformations due to greater flexibility of the conjugates, which is unfavourable for interaction with DNA.[125, 146]

The central tetramethylene motif of spermine was reported to be essential in conferring high transfection efficiency in a series of cholesterol-polyamine conjugates.[145] It was suggested that the tetramethylene segment of spermine can bridge between the DNA complementary strands, while the polyamine with a central trimethylene segment would only bind with the adjacent phosphates on the same DNA strand. These results point to the importance of the structure of the polyamine head-group and the relation between its amine groups, and also points to the fact that increasing efficiency of transfection is not only a matter of increasing number of positive charges per head group.

The hydrophobic domain

The length, saturation state and type of the hydrophobic chains conjugated to cationic lipids affect their transfection efficiency.[147-149] Although these factors were studied extensively for the effect on transfection, and although the majority of studies accepted that the type of alkyl chains influence the outcome of transfection, it is difficult to set a definitive set of rules to describe the best type of alkyl chains to be conjugated to the polar head-groups. The contribution of the alkyl chains (and the hydrophobic domain) to the cationic lipid properties as a whole is what determines the transfection efficiency of the lipid.

Results obtained with DMRIE[150] (1,2-dimyristyloxypropyl-3-dimethyl-hydroxyethyl-ammonium bromide), glycine betaine conjugates[131] with two alkyl chains, alkyl acyl carnitine esters having chains of length C12 to C18,[151] lactic acid conjugates of *N*,*N*-dialkyl amine group,[152] lipids related to DOTAP with two alkyl chains (C12-C18) linked to the head group through ether bonds,[153] and cationic lipids with different hydroxyethyl or dihydroxypropyl ammonium backbones and esterified hydrocarbon chains and hydroxy substituents[154] showed that a comparison of the cationic lipids based only on the lengths of the two saturated aliphatic chains led to the observation of the superior transfection efficiency of C14 chains over the longer C16 and C18 chains.[125, 126] It was proposed that a shorter chain length facilitates mixing with cellular membranes[131] which is important for endosomal escape.[155]

In another set of experiments, the longer chain C18 oleoyl (with one *cis*-double bond) was found to be more efficient than cationic lipids with shorter chain lengths. Varying the chain length in N^4,N^9-diacyl spermines plasmid DNA delivery from C10 to C18 resulted in the conjugate with the C18 oleoyl chains to be the most efficient and less toxic than the shorter chain conjugates.[156] A series of multivalent gemini surfactants with the hydrophobic chains systematically varied resulted in the conjugates with C18 oleoyl chains to be better in transfection than the C16 and C14 alkyl chains.[157] Chain saturation also was shown to affect the efficiency of transfection. The results of studies on a set of cationic triester phosphatidyl choline derivatives (each having two alkyl chains) show a strong dependence of their transfection efficiency on the lipid hydrocarbon chain characteristics, where transfection activity increases with increasing chain unsaturation from fully saturated to having two double bonds. Transfection efficiency decreased with increasing chain length (increasing the total number of carbons per lipid molecule ~30-50). Maximum transfection was with monounsaturated myristoleoyl 14:1 chains.[149] The data obtained from transfection experiments with 20 cationic phosphatidylcholine (PC) derivatives show that hydrocarbon chain variations results in transfection efficiencies that varies by more than 2 orders of magnitude. The most important variables were chain saturation state and total number of carbon atoms in the lipid chains. Transfection increased with decreasing chain length and

increasing chain unsaturation. Best transfection efficiency was found for cationic lipids with monounsaturated (myristoleoyl) 14:1 chains.[147] Higher levels of transfection were also reported with lipids having oleoyl chains in comparison with stearoyl chains.[150, 151] Unsaturated chains promote lipid fusion between the lipoplexes and the various cellular membranes, which is essential for delivery and endosomal escape.[126, 147, 158]

Cholesterol derivatives with various cationic head-groups were synthesized to investigate their efficiency as siRNA delivery vectors. The transfection efficiencies of siRNA lipoplexes prepared with the cationic cholesterol derivatives DC-Chol, cholesteryl-3β-carboxyamido-ethylene-*N*-hydroxyethylamine (OH-Chol), and *N*-hydroxyethylaminopropane carbamoyl cholesterol (HAPC) was investigated in human prostate tumour cells that stably express the luciferase gene (PC-3-Luc). When lipoplexes were prepared in water, HAPC was more effective in knocking-down luciferase activity than OH-Chol and DC-Chol.[159] The presence of NaCl while preparing the lipoplexes increased the gene silencing efficiency of luciferase, while it did not affect efficiency of HAPC. The commercially available transfection reagent, Lipofectamine 2000 (a cationic lipid liposomal preparation) resulted in strong gene silencing by siRNA, but exhibited increased toxicity (~40% cell viability), in contrast to OH-Chol, DC-Chol, and HAPC lipoplexes (~80–100% cell viability). These results indicated that siRNA lipoplexes prepared with OH-Chol, and HAPC can efficiently suppress gene expression without increased cytotoxicity.[159]

The linker

The linker is represented by the type (hence properties) of the functional group and the length (number of carbons) of the linker. The linker has two main functions: (a) to covalently conjugate the polar head-group to the hydrophobic domain; (b) to control the biodegradability of the cationic lipid and/or introduce a new property to the cationic lipid, e.g. responding to the intracellular reducing environment.[126, 160] The most commonly used linkers are amide, carbamate, ester, ether, orthoesters, and disulfide linkers.

Both amides and ester bonds are biodegradable and hence are hypothesized to be less toxic than other non-biodegradable bonds (e.g. ethers).[161] Lipids with a pyridinium head-group (with palmitoyl 16:0 hydrophobic domains and with ester and amide linkers) were used to prepare liposomes with either DOPE or cholesterol at the cationic lipid/helper-lipid molar ratio of 1:1. Following transfection of Chinese hamster ovary (CHO) cells with lipoplexes delivering plasmids expressing EGFP, the cationic lipids having amide linkers significantly increased transfection efficiency in all liposomal formulations compared to their counterparts having the ester linker.[162] The high transfection efficiency of lipids with amide linker was suggested to be due to their lower phase transition temperature which makes the liposome's

bilayer structure more stable in aqueous media during the transfection process as well as liposome storage. The phase transition temperature of a lipid is the temperature at which there is a change in the lipid's physical state from the ordered gel phase (where the hydrocarbon chains are closely packed and fully extended) to the disordered liquid crystalline phase (where the hydrocarbon chains are fluid and randomly oriented).[162]

Depending on the structure of the cationic lipid, the linker influence on transfection efficiency can be more than on cytotoxicity. Cholesterol-based cationic lipids that have different nitrogenous heterocyclic head-groups (*N*-methylimidazole, *N*-methylmorpholine, and pyridine) and acid-labile linkers (carbamate, ester, and *N*,*O*-acetal ether) were used to transfect human embryonic kidney 293 (HEK 293) cells with EGFP plasmid.[163] Choosing those linkers was based on the concept that incorporation of acid-labile bonds in the cationic lipid structure enhances the release of polynucleotides from the endosomes, therefore increasing the transfection efficiency.[164] *N*,*O*-Acetals are known to undergo hydrolysis in acidic environment.[163, 164] The results showed that the structure of these lipids only slightly affected their cytotoxicity but largely changes the efficiency of intracellular accumulation of the polynucleotides. The lipids having the cationic head-groups pyridine and/or methylimidazole head-groups with either an ester or a carbamate linker resulted in better transfection efficiency as compared with the cationic lipids with either the *N*-methylmorpholine head-groups and/or an ether linker. The lipid that has a pyridine head-group and a carbamate linker to deliver EGFP plasmid resulted in comparable transfection efficiency with that of the commercially available Lipofectamine 2000.

Two cleavable cationic lipids having a linear or a cyclic ortho ester linker between the cationic head-group and the unsaturated hydrophobic domain (two oleoyl chains) were previously reported.[165] It is hypothesized that the acidic pH in the endosomes catalyzes the hydrolysis of the linker group to result in fragmentation products that destabilize the endosomal membranes. At pH 7.4, the lipids (with DOPE) formed stable lipoplexes with plasmid DNA. Decreasing the pH enhanced the hydrolysis of the ortho ester linkers which removed the cationic head-groups and caused lipoplex aggregation. At pH 5.5, the cationic lipid *N*-[2-methyl-2-(1',2'-dioleylglyceroxy)dioxolan-4-yl]methyl-*N*,*N*,*N*-trimethylammonium iodide that have a cyclic ortho ester linker showed increased pH-sensitivity and caused the permeation of its lipoplexes to model biomembranes within the time span of endosomal processing before the lysosomal degradation. This lipid markedly increased gene transfection (~3-50-fold) of the luciferase reporter protein in monkey kidney fibroblast (CV-1) and human breast cancer (HTB-129) cells in culture compared to the pH-insensitive control lipid DOTAP lipoplexes.[165]

Transfection with DNA lipoplexes of three thiocholesterol-derived gemini cationic lipids possessing disulfide linkages incorporated between the cationic head-group and the thiocholesterol backbone in order to render the lipids biodegradable was reported.[166] Comparing transfection in prostate cancer line (PC3AR) and a human keratinocyte cell line (HaCat) with two commercially available reagents showed comparable or better expression of GFP in the transfected cells. Cytotoxic studies showed the nontoxic property of these lipid−DNA complexes at different *N/P* ratios used for transfection studies. The rationale behind this design was to ensure the destabilization of the lipid-polynucleotide lipoplexes in the cytoplasm after reduction of the disulfide linker by the intracellular glutathione (GSH), which is the most abundant low molecular weight thiol present in cells and is involved in controlling cellular redox environment. GSH is found at high intracellular concentrations and very low extracellular concentrations e.g. blood plasma concentrations (2 µM) are 1000-fold less than concentration in erythrocytes (2 mM). This large difference between intra- and extracellular environments provides a potential mechanism for release of polynucleotides from lipoplexes of lipids that have a disulfide linker.[166]

In Chapter 2, five symmetrical acyl spermine derivatives (fatty acid amides of spermine) are synthesized, characterized, and evaluated as non-viral vectors for siRNA. The intracellular delivery of siRNA and the subsequent sequence specific gene silencing will be quantified by flow cytometry techniques (FACS analysis). The ability of the spermine conjugates to bind siRNA and form nanoparticles is investigated. The effect of the complexes of siRNA lipoplexes on the cell viability 48 h post transfection is measured. The SAR study in Chapter 2 aims to indentify the most efficient fatty acid(s) in terms of high gene-silencing efficiency and high cell viability.

Chapter Two Efficient gene silencing by self-assembled complexes of siRNA and symmetrical fatty acid amides of spermine

1. Introduction

Cationic lipids are widely used as non-viral vectors for the intracellular delivery of DNA and later oligonucleotides such as siRNA.[160, 167, 168] The cationic head-group of a cationic lipid should contain one or more functional groups that can acquire a positive charge at a physiological pH of 7.4 such as amines (primary, secondary, tertiary, and quaternary),[169, 170] guanidines, imidazoles, or pyridinium salts.[169] The positive charge on the cationic head-group interacts electrostatically with the negative charge of the phosphate backbone of the siRNA while the hydrophobic part of the cationic lipids promotes the formation of vesicles or siRNA/cationic lipid aggregates called lipoplexes. The hydrophobic moiety of cationic lipids can affect the siRNA delivery and the biological activity (gene knock-down) according to its physical and chemical properties such as chain length and saturation state.[147] Therefore in this Chapter, a series of symmetrical diacyl lipopolyamines are designed in order to prepare lipoplex formulations (without any pre-preparation of liposomes) of an Alexa Fluor 647-tagged siRNA to investigate if they are suitable for efficient gene silencing in target cells, by forming nanoparticles which will efficiently enter cells either by endocytosis only (a major pathway) or possibly by endocytosis in combination with fusion between siRNA lipoplexes and the plasma membrane (a minor pathway).[171]

In this Chapter, five symmetrical diacylated spermine conjugates are designed and synthesized, with variation in the length (from short C12 lauroyl to very long C22 erucoyl) and/or oxidation state from stearoyl (18:0) to oleoyl (18:1) to linoleoyl (18:2). The two acyl fatty chains are regiospecifically covalently bound to spermine at the N^4- and N^9-positions. Detailed evidence for the characterisation of the nanoparticles, the delivery of Alexa Fluor 647-tagged siRNA, the subsequent silencing of EGFP in HeLa cells stably expressing the fluorescent protein, and cell viability evaluation after transfection are provided. These results are compared with those obtained with the commercially available transfection reagents Lipofectamine 2000 (liposomal) and TransIT-TKO (non-liposomal). Gene silencing studies in comparable systems on human embryonic kidney 293T cells stably expressing GFP,[172] HeLa705 cells expressing luciferase,[173] human embryonic retinoblast cells (911 cells) stably expressing luciferase,[174] HeLa cells expressing GFP,[171, 175, 176] and glioma cells (C6) expressing GFP[177] have been reported.

2. Materials and methods

2.1. Materials and general methods

Glassware used when anhydrous conditions were required was heated for 18 h at 80 °C, assembled while hot, filled with anhydrous nitrogen then allowed to cool to 20 °C before being used. Thin layer chromatography (TLC) was performed using aluminium-backed plates coated with Kieselgel 60 F_{254} (Merck). Ninhydrin (0.2 g) in ethanol (100 mL) was used for detecting polyamines on TLC plates. $KMnO_4$ solution was used as universal indicator for lipopolyamines and other compounds/impurities on TLC plates (prepared by dissolving 1.5 g of $KMnO_4$, 10 g K_2CO_3, and 1.2 mL 10% NaOH in 200 mL water). Column chromatography was performed over flash silica gel 60 (35-75 μm; Prolabo-Merck). Dicyclohexyl carbodiimide (DCC), 4-dimethylaminopyridine (DMAP), fatty acids, fatty acid chlorides, G418, hydrazine monohydrate, *N*-carbethoxyphthalimide, spermine, and triethylamine (TEA), were purchased from Sigma-Aldrich (Gillingham, UK). All solvents were purchased from Fisher Scientific UK (Loughborough, UK). Anhydrous dichloromethane (DCM) was distilled over calcium hydride. Anhydrous tetrahydrofuran (THF) was distilled from sodium benzophenone ketyl. Cell culture media were purchased from Gibco (Invitrogen Ltd, Paisley, UK). NMR spectra were recorded in chloroform-D using a Varian Mercury 400 (operating at 400 MHz for ^{1}H and 100.8 MHz for ^{13}C) spectrometer. The high resolution (HR) time-of-flight mass spectra were obtained on a Bruker Daltonics micrOTOF mass spectrometer using electrospray ionisation (ESI). Transfection reagents Lipofectamine 2000 (liposomal) and TransIT-TKO (proprietary non-liposomal cationic polymer/lipid formulation) were purchased from Invitrogen and Mirus Bio (Cambridge, UK). AllStars negative controls siRNA (siNC) tagged with Alexa Fluor® 647 (AF647) at the 3'-position (siNC-AF) were purchased from Qiagen (Crawley, UK) as was siRNA against EGFP labelled with Alexa Fluor® 647 (siEGFP-AF) at the 3'-position of the sense strand, sequences:

Sense strand: 5'-GCAAGCUGACCCUGAAGUUCAUTT-3',
Anti-sense strand: 5'-AUGAACUUCAGGGUCAGCUUGCCG-3',
Target DNA sequence: 5'-CGGCAAGCTGACCCTGAAGTTCAT-3'.

2.2. Synthesis of fatty acid amides of spermine

N-Carbethoxyphthalimide (0.44 g, 2 mmol) was added to a solution of 1,12-diamino-4,9-diazadodecane (spermine) (0.20 g, 1 mmol) in DCM (10 mL). The solution was stirred 20 °C for 3 h then evaporated to dryness in vacuo and the residue was either purified over silica gel (DCM/MeOH 10:1 then 2:1 v/v) or alternatively used directly in the following step. To a solution of 1,12-diphthalimido-4,9-diazadodecane in DCM (10 mL) and TEA (0.28 mL, 2

mmol) fatty acid chloride (2 mmol), or alternatively fatty acid (2 mmol), DMAP (0.24 g, 2 mmol), and DCC (0.4 g, 2 mmol) were added and stirred for 18 h under nitrogen atmosphere. The solvent was then evaporated to dryness in vacuo and the residue was treated with hydrazine monohydrate (2 mL) in a mixture of DCM (15 mL) and THF (15 mL) and heated under reflux for 4 h then the solvent was evaporated in vacuo to dryness and the residue purified over silica gel (DCM/MeOH 10:1 v/v then DCM/MeOH/NH_4OH 20:10:1 v/v/v) to afford the title compounds as the free bases which were then fully characterised by both high-field ^{1}H and ^{13}C NMR spectroscopy and HR-ESI-MS.

N^4,N^9-Dierucoyl-1,12-diamino-4,9-diazadodecane (DEruS).

To a solution of 1,12-diphthalimido-4,9-diazadodecane (0.46 g, 1 mmol) in DCM (30 mL) erucic acid (0.68 g, 2 mmol), DMAP (0.24 g, 2 mmol), and DCC (0.4 g, 2 mmol) were added. The solution was stirred at 20 °C for 18 h under an atmosphere of nitrogen, then filtered and the filtrate was evaporated to dryness in vacuo. The residue was reacted with hydrazine monohydrate (2 mL) in a mixture of DCM (15 mL) and THF (15 mL) and heated under reflux for 4 h, cooled to 20 °C, and then the solvent was evaporated in vacuo. The residue was purified over silica gel (DCM/MeOH 10:1 v/v then DCM/MeOH/NH_4OH 20:10:1 v/v/v) to afford the title compound (0.34 g, 40% over two steps). ^{1}H NMR, 0.8 (t, J = 7 Hz, 6H, H22'), 1.1-1.3 (m, 60H, H4'-H11', H16'-H21', 2 x NH_2), 1.4-1.6 (m, 12H, H2, H6, H7, H11, H3'), 1.9 (m, 8H, H12'-H15'), 2.2-2.4 (m, 4H, H2'), 2.5-2.7 (m, 4H, H1, H12), 3.2-3.6 (m, 8H, H3, H5, H8, H10), 5.2 (m, 4H, H13', H14'). ^{13}C NMR, 14.0 (C22'), 22.6 (C21'), 25.1-32.8 (C2, C6, C7, C11, C12, C3'-C12', C15'-C20'), 33.1 (C2'), 39.2-39.4 (C1, C12), 42.6-47.4 (C3, C5, C8, C10), 129.8 (C13', C14'), 172.8-173.0 (C1'). HRMS, found $(M+H)^+$ 843.8364, $C_{54}H_{107}N_4O_2$ requires $(M+H)^+$ 843.8389; found $(M+Na)^+$ 865.8194, $C_{54}H_{106}N_4O_2Na$ requires $(M+Na)^+$ 865.8208.

N^4,N^9-Dilauroyl-1,12-diamino-4,9-diazadodecane (DLauS).

To a solution of 1,12-diphthalimido-4,9-diazadodecane (2.31 g, 5 mmol) in DCM (30 mL) and TEA (1.4 mL, 10 mmol) lauroyl chloride (2.4 mL, 10 mmol) was added. The solution was stirred for 18 h at 20 °C, and then the solvent was evaporated to dryness in vacuo. The residue was reacted with hydrazine monohydrate (2 mL) in a mixture of DCM (15 mL) and THF (15 mL) and heated under reflux for 4 h, cooled to 20 °C, and then the solvent was evaporated in vacuo. The residue was purified over silica gel (DCM/MeOH 10:1 v/v then DCM/MeOH/NH_4OH 10:5:1 v/v/v) to afford the title compound (1.46 g, 40% over two steps). ^{1}H NMR, 0.9 (t, J = 7 Hz, 6H, H12'), 1.2-1.3 (m, 32H, H4'-H11'), 1.4-1.7 (m, 12H, H2, H6, H7, H11, H3'), 1.9 (m, 2 x NH_2), 2.1-2.3 (m, 4H, H2'), 2.5-2.7 (m, 4H, H1, H12), 3.2-3.5 (m, 8H, H3,

H5, H8, H10). ^{13}C NMR, 14.0 (C12'), 22.6 (C11'), 25.1-32.7 (C2, C6, C7, C11, C4'-C10'), 33.1-36.8 (C2'), 38.1-39.4 (C1, C12), 42.5-47.7 (C3, C5, C8, C10), 172.9-173.3 (C1'). HRMS, found $(M+H)^+$ 567.5553, $C_{34}H_{71}N_4O_2$ requires $(M+H)^+$ 567.5572 $C_{34}H_{71}N_4O_2$ 567.5572.

***N*^{4},*N*^{9}-Dilinoleoyl-1,12-diamino-4,9-diazadodecane (DLinS)**.

To a solution of 1,12-diphthalimido-4,9-diazadodecane (0.46 g, 1 mmol) in DCM (30 mL) linoleic acid (0.56 g, 2 mmol), DMAP (0.24 g, 2 mmol), and DCC (0.4 g, 2 mmol) were added. The solution was stirred at 20 °C for 18 h under an atmosphere of nitrogen, then filtered and the filtrate was evaporated to dryness in vacuo. The residue was reacted with hydrazine monohydrate (2 mL) in a mixture of DCM (15 mL) and THF (15 mL) and heated under reflux for 4 h, cooled to 20 °C, and then the solvent was evaporated in vacuo and the residue purified over silica gel (DCM/MeOH 10:1 v/v then DCM/MeOH/NH_4OH 20:10:1 v/v/v) to afford the title compound (0.29 g, 40% over two steps). ^{1}H NMR, 0.8 (t, *J* = 7 Hz, 6H, H18'), 1.2-1.3 (m, 28H, H4'-H7', H15'-H17'), 1.4-1.8 (m, 16H, H2, H6, H7, H11, H3', 2 x NH_2), 1.9-2.0 (m, 8H, H8', H14'), 2.0-2.3 (m, 4H, H2'), 2.5-2.7 (m, 8H, H1, H12, H11'), 3.2-3.4 (m, 8H, H3, H5, H8, H10), 5.2-5.3 (m, 8H, H9', H10', H12', H13'). ^{13}C NMR, 14.0 (C18'), 22.4 (C17'), 25.0-33.0 (C2, C6, C7, C11, C2'-C8', C11', C14'-C16'), 39.0-39.3 (C1, C12), 42.4-47.6 (C3, C5, C8, C10), 127.8-130.0 (C9', C10', C12', C13'), 172.7-173.0 (C1'). HRMS, found $(M+H)^+$ 727.6851, $C_{46}H_{87}N_4O_2$ requires $(M+H)^+$ 727.6824.

***N*^{4},*N*^{9}-Dioleoyl-1,12-diamino-4,9-diazadodecane (DOS)**.

To a solution of 1,12-diphthalimido-4,9-diazadodecane (2.31 g, 5 mmol) in DCM (30 mL) and TEA (1.4 mL, 10 mmol) oleoyl chloride (3.3 mL, 10 mmol) was added. The solution was heated under reflux for 18 h, cooled to 20 °C, and then the solvent was evaporated to dryness in vacuo. The residue was reacted with hydrazine monohydrate (2 mL) in a mixture of DCM (15 mL) and THF (15 mL) and heated under reflux for 4 h, cooled to 20 °C, and then the solvent was evaporated in vacuo. The residue was purified over silica gel (DCM/MeOH 10:1 v/v then DCM/MeOH/NH_4OH 10:5:1 v/v/v) to afford the title compound (1.46 g, 40% over two steps). ^{1}H NMR, 0.8 (t, *J* = 7 Hz, 6H, H18'), 1.2-1.3 (m, 40H, H4'-H7', H12'-H17'), 1.4-1.8 (m, 12H, H2, H6, H7, H11, H3'), 1.9-2.1 (m, 8H, H8', H11'), 2.1-2.3 (m, 4H, H2'), 2.6-2.8 (m, 8H, H1, H12, 2 x NH_2), 3.2-3.5 (m, 8H, H3, H5, H8, H10), 5.3-5.4 (m, 4H, H9', H10'). ^{13}C NMR, 14.1 (C18'), 22.6-29.7 (C2, C6, C7, C11, C4'-C8', C11'-C17'), 31.9 (C3'), 33.1 (C2'), 38.9-39.2 (C1, C12), 42.5-47.4 (C3, C5, C8, C10), 129.8 (C9', C10'), 172.9 (C1'). HRMS, found $(M+H)^+$ 731.7162, $C_{46}H_{91}N_4O_2$ requires $(M+H)^+$ 731.7137.

N^4,N^9-Distearoyl-1,12-diamino-4,9-diazadodecane (DSS).

To a solution of 1,12-diphthalimido-4,9-diazadodecane (2.31 g, 5 mmol) in DCM (30 mL) and TEA (1.4 mL, 10 mmol) stearoyl chloride (3.3 mL, 10 mmol) was added. The solution was stirred for 18 h at 20 °C, and then the solvent was evaporated to dryness in vacuo. The residue was reacted with hydrazine monohydrate (2 mL) in a mixture of DCM (15 mL) and THF (15 mL) and heated under reflux for 4 h, cooled to 20 °C, and then the solvent was evaporated in vacuo. The residue was purified over silica gel (DCM/MeOH 10:1 v/v then DCM/MeOH/NH_4OH 10:5:1 v/v/v) to afford the title compound (1.46 g, 40% over two steps). ^1H NMR, 0.9 (t, J = 7 Hz, 6H, H18'), 1.2-1.4 (m, 56H, H4'-H17'), 1.4-1.7 (m, 12H, H2, H6, H7, H11, H3'), 1.9-2.0 (m, 4H, 2 x NH_2), 2.1-2.3 (m, 4H, H2'), 2.6-2.8 (m, 4H, H1, H12), 3.2-3.4 (m, 8H, H3, H5, H8, H10). ^{13}C NMR, 14.0 (C18'), 22.6 (C17'), 25.0-32.7 (C2, C6, C7, C11, C3'-C16'), 33.1 (C2'), 38.9-39.4 (C1, C12), 42.4-47.43(C3, C5, C8, C10), 12), 172.9-173.1 (C1'). HRMS, found $(M+H)^+$ 735.7428, $C_{46}H_{95}N_4O_2$ requires $(M+H)^+$ 735.7450.

2.3. HeLa cell line stably expressing EGFP (HeLa-EGFP)

The HeLa cell line stably expressing the red-shifted enhanced variant of wild-type GFP (EGFP) used here as a reporter protein was obtained from the Cell Service at Cancer Research UK (CRUK, London Research Institute, Clare Hall Laboratories, South Mimms, London, UK) and was constructed by Dr Yilun Liu. Briefly, the centrin protein (CEN) was subcloned into the expression vector pEGFP-C1 (Clontech, Cowley, UK), downstream of EGFP, under the control of the human CMV promoter. The plasmid was linearized and transfected into HeLa cells. Stably transfected cells were selected with G418 and maintained as a polyclonal cell line, cultivated in DMEM medium supplemented with 10% FCS, penicillin base (50 units/mL), streptomycin (50 μg/mL), and G418 (1 mg/mL). The cells were passaged every 3 or 4 days and cultures were routinely checked under inverted light microscope for any signs of microbial contamination. The FCS used in culture media preparations and other experiments is heat inactivated at 56 °C for 45 min. The percentage of EGFP positive cells was >80% as measured by flow cytometry (FACS) (data not shown) and regularly was verified prior to siRNA transfection experiments.

2.4. Transfection studies of HeLa cells stably expressing EGFP

Cells were trypsinized (0.25% trypsin in PBS, 3-4 min incubation at 37 °C, 5% CO_2) at confluency 80-90% and counted under an inverted light microscope by means of a haemocytometer using trypan blue dye (0.4% dye in 0.81% sodium chloride and 0.06% dibasic potassium phosphate) to exclude dead cells. The cells were then seeded at a density of

65,000 cells/well in 24-well plates and were incubated for 24 h at 37 °C, 5% CO_2, prior to transfection. On the day of transfection, the lipoplexes were prepared by mixing two solutions A and B. Solution A was prepared by adding the specified volume of an ethanol solution containing the required amount of the cationic lipid to Opti-MEM serum-free medium (total volume is 50 μL), followed by mixing with a vortex mixer for 2-3 s. Solution B was prepared by adding the required volume of siRNA stock solution to Opti-MEM serum-free medium to make a final volume of 15 μL of 1 μM siRNA, then mixing briefly by pipetting gently up and down by means of a micropipette . Solution B was then added to solution A (in Eppendorf microtubes, 1.5 mL) followed by mixing for 4 s by means of a vortex mixer. The lipoplexes were then allowed to form for 20 min at 20 °C. The 24-well plates containing the HeLa cells were then removed from the incubator, and the lipoplex solutions (65 μL) were added to each well containing 935 μL DMEM (10% FCS) to make the final volume 1 mL. The plates were then incubated for 48 h at 37 °C, 5% CO_2. siRNA against EGFP used in these experiments has 24 base-pairs, thus each molecule of siRNA contains 46 negative charges corresponding to 46 negatively charged phosphate groups in the siRNA backbone. The synthesized spermine fatty acid amides each contain two terminal primary amine groups which will be positively charged at physiological pH 7.4, therefore, each cationic lipid molecule carries two positive charges. *N/P* ratio was calculated using the following equation:

$$N/P = \frac{number\ of\ moles\ of\ cationic\ lipid \times 2.0}{number\ of\ moles\ of\ siRNA \times total\ number\ of\ phosphates\ in\ ds\ siRNA}$$

Transfection with the commercial non-viral vectors Lipofectamine 2000 and TransIT-TKO was carried out according to the protocol supplied by the manufacturers.

2.5. Flow Cytometry (FACS)

For analysis of delivery and then reduction of expression of EGFP by flow cytometry (fluorescence-activated cell sorting, FACS), cells were washed twice with PBS and then were trypsinized (0.25% trypsin in PBS, 5-7 min incubation at 37 °C, 5% CO_2) and resuspended in DMEM medium containing 10% FCS and without phenol red. Cells were centrifuged (1,000 rpm Falcon 6/300 MSE, London, UK, for 5 min) then washed twice by resuspending in PBS containing 0.1% BSA, and then re-centrifuged (1,000 rpm for 5 min). The collected cells were then resuspended in PBS and transferred to a flow cytometer tube (Becton Dickinson, UK), and kept on ice at 1 °C and protected from light until starting FACS analysis. Cells were then analyzed (10,000 or 20,000 events) using a FACSCanto flow cytometer (Becton Dickinson, UK), equipped with an argon ion laser at 488 nm for excitation, a Long Pass (LP)

filter at 502 nm and a detector at 530 nm (range +/-15 nm) for green fluorescence emission, and a helium/neon laser at 633 nm for excitation of Alexa Fluor 647 and a detector at 660 nm (range +/- 10 nm). EGFP expression was calculated as:

$$\%EGFP = \frac{EGFP\ fluorescence\ of\ transfected\ cells}{EGFP\ fluorescence\ of\ control\ cells} \times 100$$

siRNA delivery was evaluated (48 h post-transfection) by means of normalizing the geometric mean fluorescence (calculated using BD FACSDiva™ software) of the Alexa Fluor 647 of each sample relative to the geometric mean fluorescence of Alexa Fluor 647-siRNA delivered by either of two standards (DOS or TransIT-TKO).

2.6. Confocal microscopy cell imaging

Cells were trypsinized (0.25% trypsin in PBS, 3-4 min incubation at 37 °C, 5% CO_2) at confluency 80-90% and counted under an inverted light microscope by means of a haemocytometer using trypan blue dye (0.4% dye in 0.81% sodium chloride and 0.06% dibasic potassium phosphate) to exclude dead cells. Cells were then seeded at a density of 65,000 cells/well in 24-well plates that have a round-glass cover slip (12 mm in diameter, sterilized) already placed in each well and were incubated for 24 h prior to transfection. The lipoplexes preparation and the transfection protocol were carried out as described above (section 2.4). After 48 h, the cell culture media, in each well, was aspirated and the cells were washed with PBS (3 x 0.5 mL). The cell membrane was then stained with wheat germ agglutinin (WGA) conjugated to Alexa Fluor® 555 (WGA is a cationic probe that can bind to glycoconjugates in cell membrane such as *N*-acetylglucosamine and *N*-acetylneuraminic acid (sialic acid) residues). The concentration of WGA-Alexa Fluor 555 working solution was adjusted to a concentration of 5 µg/mL in Hank's balanced salt solution without phenol red. The cells were then incubated for 10 min in the dye working solution at 37 °C, 5% CO_2 in the dark. The cells were then washed with PBS (3 x 0.5 mL) and then fixed with 4% paraformaldehyde in PBS solution for 20 min at 20 °C in the dark. The cover slips were then removed from each well, washed gently with PBS (2 x 0.5 mL), left to dry briefly in air, and then mounted on glass slides using Mowiol (polyvinyl alcohol) solution as the mounting media and left in the dark at 20 °C (18 h) to allow hardening of the mounting media. The cells were examined using a Carl Zeiss laser scanning microscope LSM 510 meta, with EGFP excitation 488 nm, emission 509 nm (505-550 nm band pass filter), Alexa Fluor 555 excitation 543 nm, emission 565 nm (560-615 nm band pass filter), and Alexa Fluor 647 excitation 633 nm, emission 668 nm (657-753 nm meta detector).

2.7. Cell viability assay

Cells were trypsinized (0.25% trypsin in PBS, 3-4 min incubation at 37 °C, 5% CO_2) at confluency 80-90% and counted under an inverted light microscope by means of a haemocytometer using trypan blue dye (0.4% dye in 0.81% sodium chloride and 0.06% dibasic potassium phosphate) to exclude the dead cells. Cells were then seeded at a density of 6,500 cells per well of 96-well plates that have flat bottom wells, and incubated for 24 h at 37 °C, 5% CO_2**.** The lipoplexes were prepared using the same protocol in section 2.4. The transfection was carried out using the same protocol as transfecting the 24-well plates (Section 2.4) with the exception of reducing the amount of lipoplexes such that each well of the 96-well plates contains 1.5 pmol siRNA in a final volume of 100 μL/well of DMEM that contains 10% FCS. After 44 h, alamarBlue® [178] (10 μL) was added to each well. After incubation (3.5 h), the absorbance of each well was measured at 570 nm and 600 nm using a microplate-reader (VERSAmax), using the cell culture media in 3 wells without alamarBlue as blank. The amount of reduced alamarBlue at 570 nm was calculated as:

$$amountreduced = A_{570} - (A_{600} \times R)$$

$$R = \frac{AOx_{570}}{AOx_{600}}$$

R is correction factor for cell culture medium (without cells). AOx_{570} and AOx_{600} are the absorbance of oxidized alamarBlue at 570 and 600 nm respectively, and are measured by adding 10 μL of alamarBlue to 3 wells of each 96-well plate that contain 100 μL cell culture media without cells directly prior to measuring the absorbance. Percentage viability was calculated as:

$$\%viability = \frac{amount\ reduced\ of\ alamarBlue\ of\ sample cells}{amount\ reduced\ of\ alamarBlue\ of\ control cells} \times 100$$

2.8. Particle size and zeta potential measurements

Lipoplexes were prepared by mixing two solutions A and B. Solution A was prepared by adding the specified volume of an ethanolic solution containing the required amount of the cationic lipid to HEPES (final volume 250 μL, 10 mM buffer, pH 7.4) and mixing for 2-3 s by means of a vortex mixer. Solution B was prepared by adding the specified volume of stock siRNA solution to a HEPES buffer solution (10 mM, pH 7.4) to make a final volume of 75 μL (1 μM siRNA solution), and mixing gently by pipetting up and down using a micropipette. Solution B was then added to solution A (in an Eppendorf microtube, 1.5 mL), followed by mixing for 3-4 s by means of a vortex mixer. The lipoplexes were then allowed to form for 20 min at 20 °C. Before carrying out the measurements, samples were diluted to a

final volume of 3 mL with HEPES buffer and mixed gently. Dynamic light scattering (DLS) and ζ-potential measurements were carried out using a Malvern Zetasizer Nano S90 with refractive index 1.59, viscosity 0.89 cP, dielectric constant 79, at 25 °C with equilibrium time 3 min. DLS measures the hydrodynamic diameter which is expressed as the mean Z-Average diameter in nm. This diameter was calculated from the translational diffusion coefficient by using the Stokes-Einstein equation:

$$d(H) = \frac{kT}{3\pi\eta \mathrm{D}}$$

where:-

d(H) = hydrodynamic diameter

D = translational diffusion coefficient

k = Boltzmann's constant

T = absolute temperature

η = viscosity

The ζ-potential (in mV) was measured by determining the electrophoretic mobility of the lipoplexes in buffer medium and was calculated according to Henry equation:

$$U_E = \frac{2\varepsilon\zeta\ f(\kappa a)}{3\eta}$$

where U_E = electrophoretic mobility, ε = dielectric constant, ζ = zeta potential, η = viscosity and f(κa) = Henry's function, κa measures the ratio of the particle radius to electrical double layer thickness. Electrophoretic determinations of ζ-potential were commonly made in aqueous media having moderate concentration of electrolyte, and f(κa) in this case = 1.5, which is referred to as the Smoluchowski approximation.

Both lipoplex diameter and ζ-potential were recorded as averages of three and six measurements respectively ± SD.

2.9. siRNA Binding (RiboGreen Intercalation Assay)

RiboGreen working solution was prepared by diluting RiboGreen stock solution 1 to 400 in TE buffer (10 mM Tris-HCl, 1 mM EDTA, pH 7.5 diluted 1 to 20 in RNase free water). The lipoplexes were prepared by mixing two solutions A and B. Solution A was prepared by adding the specified volume of an ethanol solution containing the required amount of the cationic lipid to TE buffer (total volume is 50 μL), followed by mixing with a vortex mixer for 2-3 s. Solution B was prepared by adding the required volume of siRNA stock solution to TE buffer to make a final volume of 15 μL of 1 μM siRNA, then mixing briefly by pipetting gently up and down by means of a micropipette . Solution B was then added to solution A (in Eppendorf microtubes, 1.5 mL) followed by mixing for 4 s by means of a vortex mixer. The

lipoplexes were then allowed to form for 20 min at 20 °C. The lipoplexes were prepared at the lipid/siRNA ratios that showed the best reduction in EGFP expression. RiboGreen working solution (40 μL) was added to each well of a 96-well plate (flat, black bottom) containing free siRNA (1 pmol) or siRNA lipoplexes (1 pmol siRNA/well). Each well contained a final volume of 120 μL. The fluorescence was measured (n = 4) using FLUOstar Optima Microplate Reader (BMG-LABTECH), λ_{ex} = 480 nm and λ_{em} = 520 nm. The amount of siRNA available to interact with the dye was calculated by subtracting the values of RiboGreen background fluorescence (RiboGreen without siRNA) from each measurement, and expressed as a percentage of the control that contained naked siRNA only, calculated as:

$$\%\ free\ siRNA = \frac{RiboGreen\ fluorescence\ of\ complexes}{RiboGreen\ fluorescence\ of\ naked\ siRNA} \times 100$$

2.10. Statistical analysis

All data are presented as mean + SD (n = 3 as triplicate of triplicate experiments unless otherwise stated where n = 2 as triplicate samples of duplicate experiments). The mean values and SD were determined using MS Office Excel 2003. Statistical significance of differences between data was evaluated by Student's unpaired two tailed *t*-test. A value of $p < 0.05$ was considered significant and *p* values were determined using GraphPad online software (http://www.graphpad.com/quickcalcs/index.cfm).

3. Results and discussion

3.1. Synthesis of fatty acid amides of spermine

Spermine (*N*,*N*′-bis(3-aminopropyl)-1,4-diaminobutane or 4,9-diazadodecane-1,12-diamine) was used as the starting material to synthesize the five desired fatty acid amide conjugates: N^4,N^9-dierucoyl spermine **1**, N^4,N^9-dilauroyl spermine **2**, N^4,N^9-dilinoleoyl spermine **3**, N^4,N^9-dioleoylspermine **4**, and N^4,N^9-distearoyl spermine **5** (Figure 1 and Table 1). Spermine has two terminal primary amine groups (N^1 and N^{12}) and two secondary amine groups (N^4 and N^9). In order to conjugate the fatty acids to the N^4 and N^9 amine groups, the two terminal primary amine groups of spermine were chemo-selectively protected with the phthalimido protecting group using Nefkens' reagent (*N*-carbethoxyphthalimide, 2 eq. in DCM).

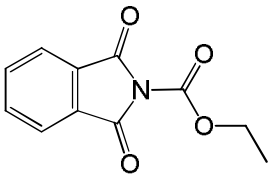

Nefkens' reagent (*N*-carbethoxyphthalimide)

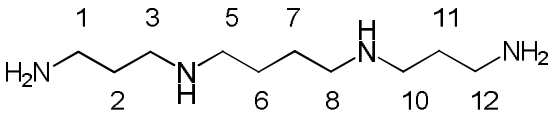

Spermine

(4,9-diazadodecane-1,12-diamine)

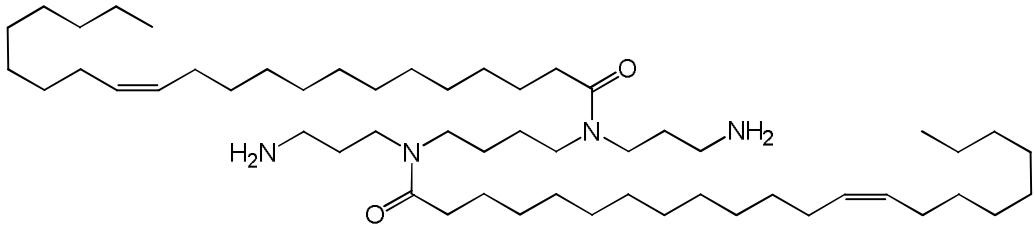

DEruS, **1**

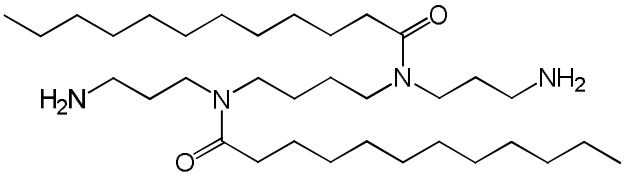

DLauS, **2**

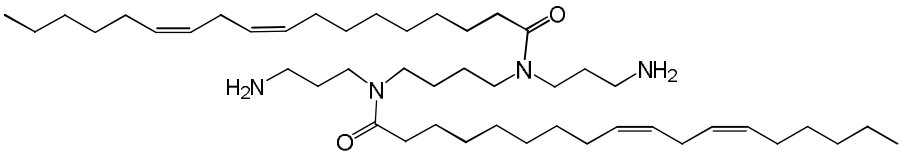

DLinS, **3**

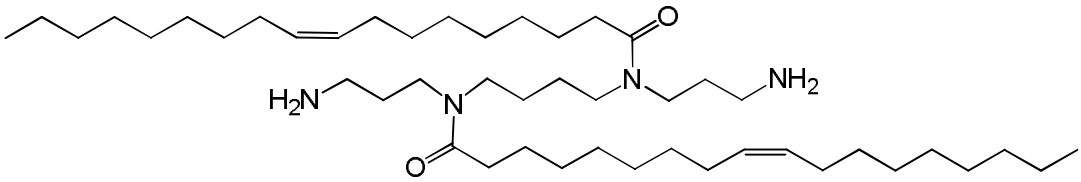

DOS, **4**

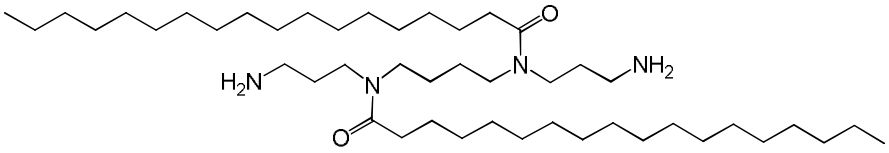

DSS, **5**

Figure 1. N^4,N^9-Difatty acid amides of spermine.

Nefkens' reagent (Figure 1) was introduced by G. H. L. Nefkens[179] as a mild phthaloylating reagent for amino acids. Sosnovsky et al.[180] were the first to report the use of Nefkens' reagent for the selective protection of primary amine groups in the presence of secondary amine groups in polyamines. Several research groups reported the use of Nefkens' reagent to protect primary amine groups of polyamines since Sosnovsky et al. published their work.[181, 182]

Table 1. N^4,N^9-Difatty acid amides of spermine. The fatty acids are described by two numbers separated by a colon, first the chain length and then the number of double bonds. Particle size, ζ-potential, and siRNA binding of fatty acid amides of spermine measured at the cationic lipid/siRNA ratios that showed best knock-down.

Name of compound	Fatty acid	Particle size (nm) ± SD	ζ-potential (mV) ± SD	% fluorescence of RiboGreen
N^4,N^9-Dierucoylspermine DEruS **1**	Erucic (22:1)	192 ± 1	63 ± 4	2 ± 1
N^4,N^9-Dilauroylspermine DLauS **2**	Lauric (12:0)	283 ± 41	25 ± 4	5 ± 1
N^4,N^9-Dilinoleoylspermine DLinS **3**	Linoleic (18:2)	353 ± 8	54 ± 1	6 ± 2
N^4,N^9-Dioleoylspermine DOS **4**	Oleic (18:1)	247 ± 4	54 ± 1	2 ± 1
N^4,N^9-Distearoylspermine DSS **5**	Stearic (18:0)	145 ± 24	41 ± 7	4 ± 1

The ^{1}H-NMR and ^{1}H-^{1}H-NMR-COSY (Figure 2) is of 1,12-diphthalimido-4,9-diazadodecane (Figure 4, top right). The integration of the peaks at δ = 1.5-1.8 shows that there are 2 protons attached to the amine groups, in addition to the 4 protons of carbons number 2 and 11. There are 4 protons (H1, H12) next to the phthalimido groups, deshielded, at δ = 3.6, as well as the 8 protons (deshielded, H3, H5, H8, and H10) next to the free secondary amine groups at δ = 2.4-2.5. The presence of the two phthalimide protecting groups can be verified by the aromatic protons integrating for 8 protons at δ = 7.5-7.7. Taken altogether with the HRMS shown in Figure 3, it is evident that the phthalimido groups were at positions 1 and 12 of the spermine; i.e. the terminal primary amines are the protected ones, while the secondary amine groups at 4 and 9 positions are free, which are essential features for the successful synthesis of the target N^4,N^9-spermine conjugates.

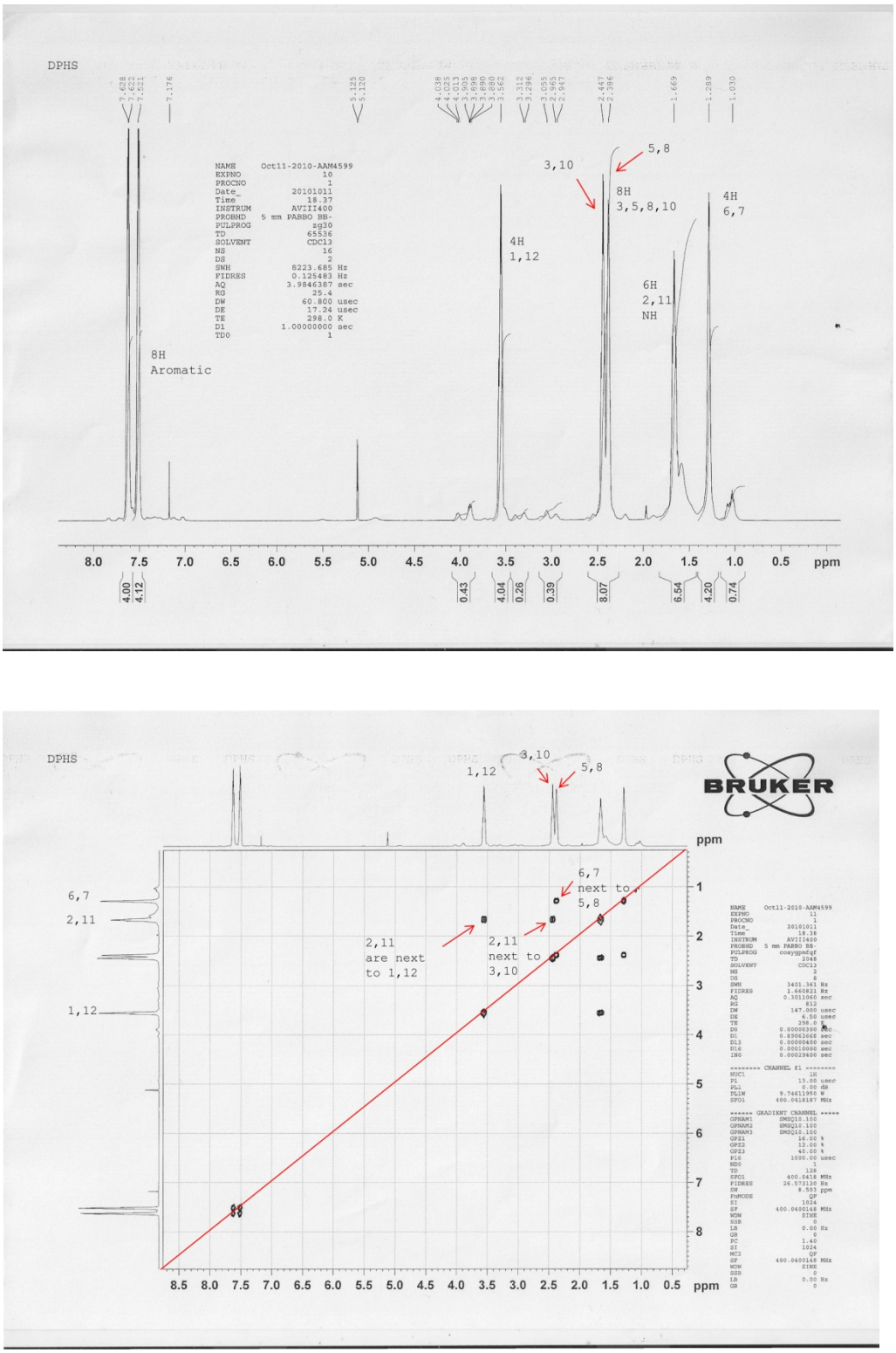

Figure 2. ^{1}H-NMR (upper) and ^{1}H-^{1}H-COSY (lower) of 1,12-diphthalimido-4,9-diazadodecane.

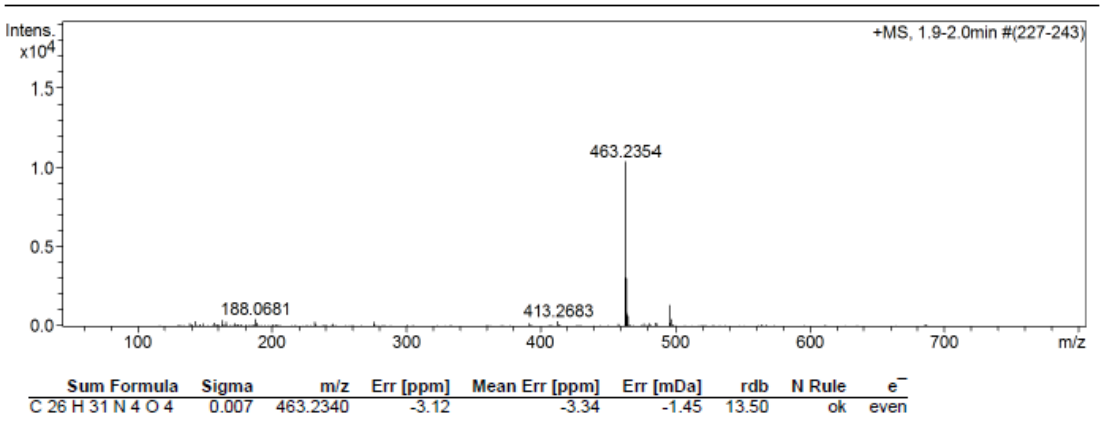

Sum Formula	Sigma	m/z	Err [ppm]	Mean Err [ppm]	Err [mDa]	rdb	N Rule	e⁻
C 26 H 31 N 4 O 4	0.007	463.2340	-3.12	-3.34	-1.45	13.50	ok	even

Figure 3. HRMS of 1,12-diphthalimido-4,9-diazadodecane.

The fatty acids were conjugated to the N^4- and N^9-position of the diphthalimido protected spermine by one of two methods as shown in the scheme in Figure 4, either fatty acyl chloride (lauroyl, oleoyl, or stearoyl) (2 eq.) and triethylamine (2 eq.) or alternatively fatty acid (erucic or linoleic) (2 eq.), DCC (2 eq.), DMAP (2 eq.) were added to the diphthalimido protected spermine solution in anhydrous DCM. After the completion of conjugation reaction, as evident by the complete disappearance of 1,12-diphthalimido-4,9-diazadodecane spot using TLC, the solution was filtered and then the filtrate was evaporated in vacuo and the residue was dissolved in 1:1 mixture of DCM/THF. Refluxing then with hydrazine (2 mL) resulted in deprotection of the primary amine groups and the precipitation of phthalhydrazide (2,3-dihydro-1,4-phthalazinedione) which was removed by filtration. The required fatty acid conjugates of spermine were purified by flash silica column chromatography to homogeneity by TLC.

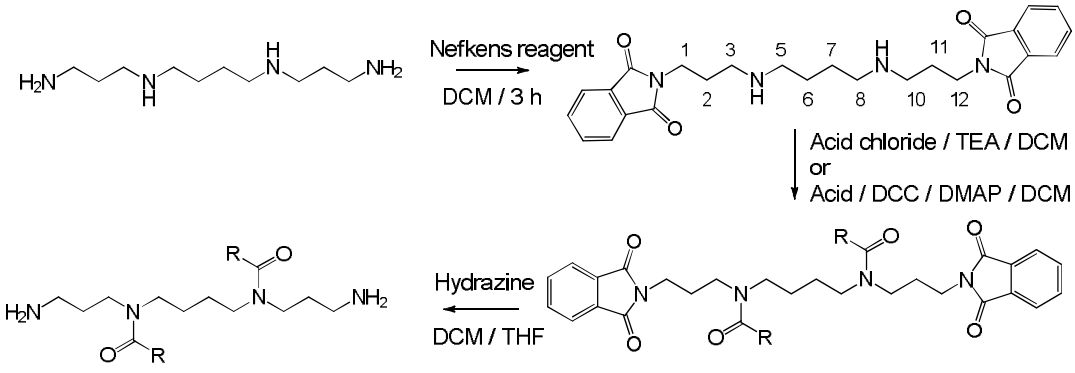

Figure 4. Synthesis of N^4,N^9-diacyl spermine conjugates.

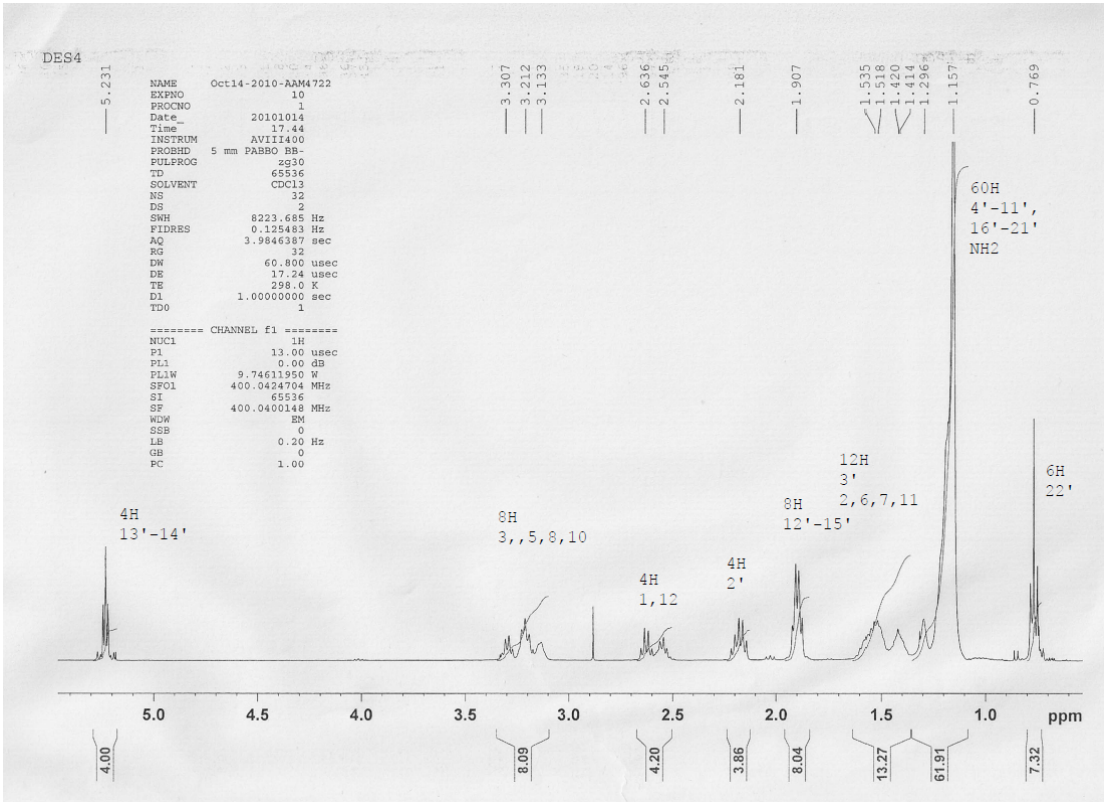

Figure 5. ^{1}H-NMR of DES.

Figure 5 shows the 1H-NMR of DES, $C_{54}H_{106}N_4O_2$, which is the spermine fatty acid conjugate with the highest molecular weight (having the largest number of carbon atoms in the fatty acyl chains). The most important features necessary for the identification of the target product, include: (a) the presence of the double bond protons (4 protons at δ = 5.3); (b) the presence of 8 protons at δ = 3.2-3.3, which are deshielded because they are next to the nitrogen atoms of the amide groups, indicating the successful conjugation of the fatty acids to the N^4 and N^9; (c) 6 protons at δ = 0.9 representing the two terminal methyl groups of the two conjugated fatty acids; (d) 4 protons at δ = 2.5-2.7 representing two CH_2 groups deshielded because they are next to an amine group, which means that the amine groups are successfully deprotected; (e) The total proton integration which fits the formulae of DES, including the four protons of the amine groups at δ = 1.3. Taken altogether, in addition to the found HRMS results reported, it can be concluded that the target compound has been synthesised successfully.

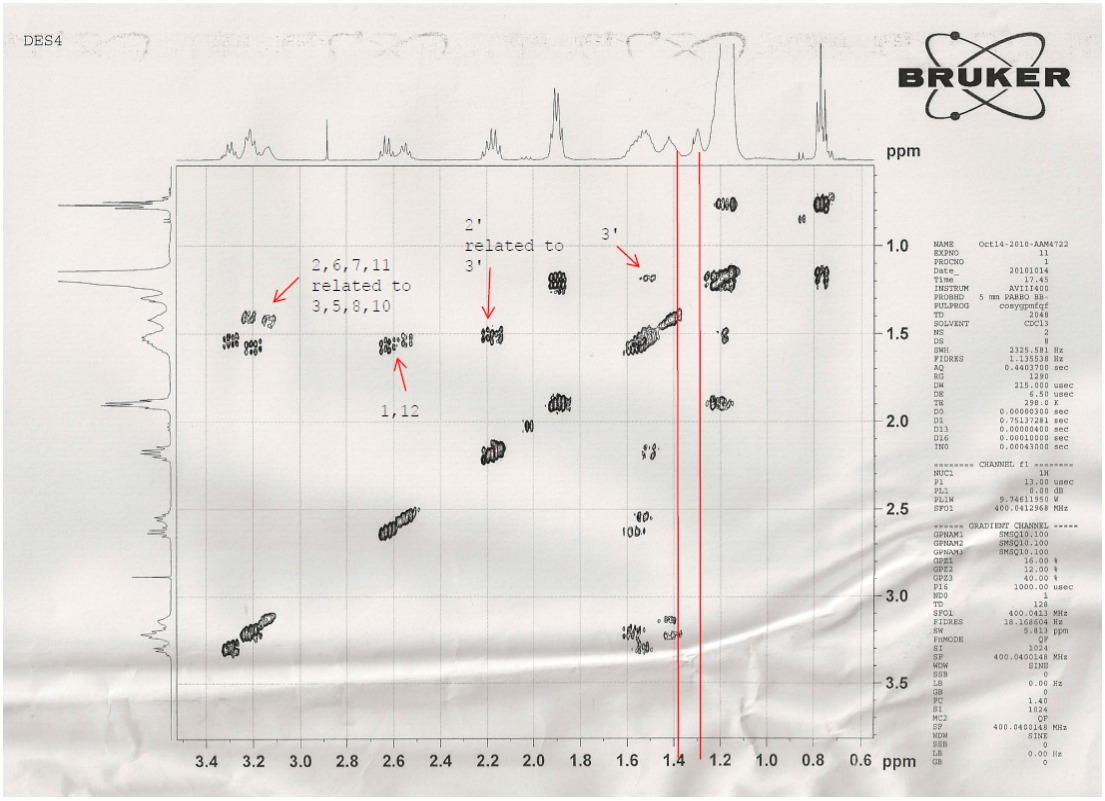

Figure 6. ^{1}H-^{1}H-NMR COSY of DES.

Figure 6 shows the ^{1}H-NMR COSY of DES. The assignments of ^{1}H-NMR of DES can be verified, as seen from the cross peaks representing protons of 1 and 12 in relation to protons 2, 6, 7, and 11. The cross peaks of protons of 3, 5, 8, and 10 to protons 2, 6, 7, and 11 can also be seen as shown in Figure 6. Cross peaks relating protons of the terminal methyl groups to the fatty acyl chains CH_2 groups can also be seen. The absence of any cross peaks of the NH_2, verifying the presence of the terminal NH_2 protons, can be noticed.

3.2. Lipoplex particle size, ζ-potential, and siRNA binding

The particle size and ζ-potential (Table 1) measurements were carried out on the lipoplexes at the cationic lipid/siNC (AllStars siRNA negative control) ratio which gave the best knock-down for the specified fatty acid amide of spermine. Particle size characterization by dynamic light scattering showed that the particle size of the formed lipoplexes varied from 145 to 353 nm which is within the size range for lipoplexes required for siRNA and/or DNA delivery, probably via endocytosis. The largest lipoplex diameter (353 nm) was obtained with **3** while the smallest (145 nm) was obtained with **5**. There was no obvious direct relationship between the lipoplex particle size and the characteristics (chain length and/or number of double bonds) of the fatty acid used. The ζ-potentials of the lipoplexes were all positive (+25-63 mV), playing a role in the stabilization of the lipoplexes by imparting repulsion between

the formed lipoplexes and preventing their aggregation. The positive charge of the lipoplexes also facilitates interaction with the negatively charged cell membrane. The RiboGreen binding assay depends on the increased fluorescence (approx. 1000-fold) of bound RiboGreen dye compared to the free (unbound) dye which is practically non-fluorescent.[183] The RiboGreen siRNA binding assay results (Table 1) show that the spermine conjugates were able to bind the siNC efficiently as shown by the reduction of RiboGreen fluorescence to 2-6% relative to the RiboGreen fluorescence of the free siNC control. Thus, the lipospermines successfully bound siNC, formed lipoplexes having positive ζ-potential and had diameter in the nanometre range, which are favourable characteristics for transfection with lipoplexes.

3.3. Transfection with siRNA and evaluating delivery and knock-down

The human cervical epithelial adenocarcinoma HeLa cell line[184] is a well-described model of cancer cells and is commonly used as a target for proof of principle of transfection efficiency[185, 186] and hence is a relevant tool for studies on siRNA- or shRNA-mediated silencing. In this Chapter, as a first step towards assessing the efficiency of the compounds at delivering siRNA into cells, HeLa cells stably expressing a reporter gene coding for the fluorescent protein EGFP, under the control of a constitutive promoter, were chosen, a strategy used in a number of other studies.[175, 176] The advantages of using a stably transfected cell line are that this simple experimental system allows expression of the protein, translated from the reporter gene at a steady-state level, and a fast assessment on the effect of EGFP-directed siRNA delivery by flow cytometry (FACS) and fluorescence microscopy. Stable transfection of the target gene of interest (with expression vector pEGFP-C1 pDNA in this study) only requires the cells to be kept under selective pressure with an antibiotic (G418 in the current system) to prevent loss of pDNA at each cell division. Furthermore, as in this experimental system, cell populations studied are asynchronous, any potential effects of the cell cycle on the reporter gene are averaged and the related protein levels will vary with the efficiency in silencing of the delivered siRNA.

GFP (and EGFP) is an 11-stranded β-barrel threaded by an α-helix along the axis of the cylinder (Figure 7). The chromophore is attached to the α-helix and is located perfectly in the centre of the cylinder.[187] The GFP chromophore is intrinsic to the protein primary structure, and no other substrates or co-factors are required for the fluorescence. The chromophore responsible for light absorption is located within a hexapeptide at positions 64–69 of GFP (and EGFP). This region contains a Ser_{65}-dehydroTyr_{66}-Gly_{67} tripeptide which acts as the minimal fluorophore in GFP.[188]

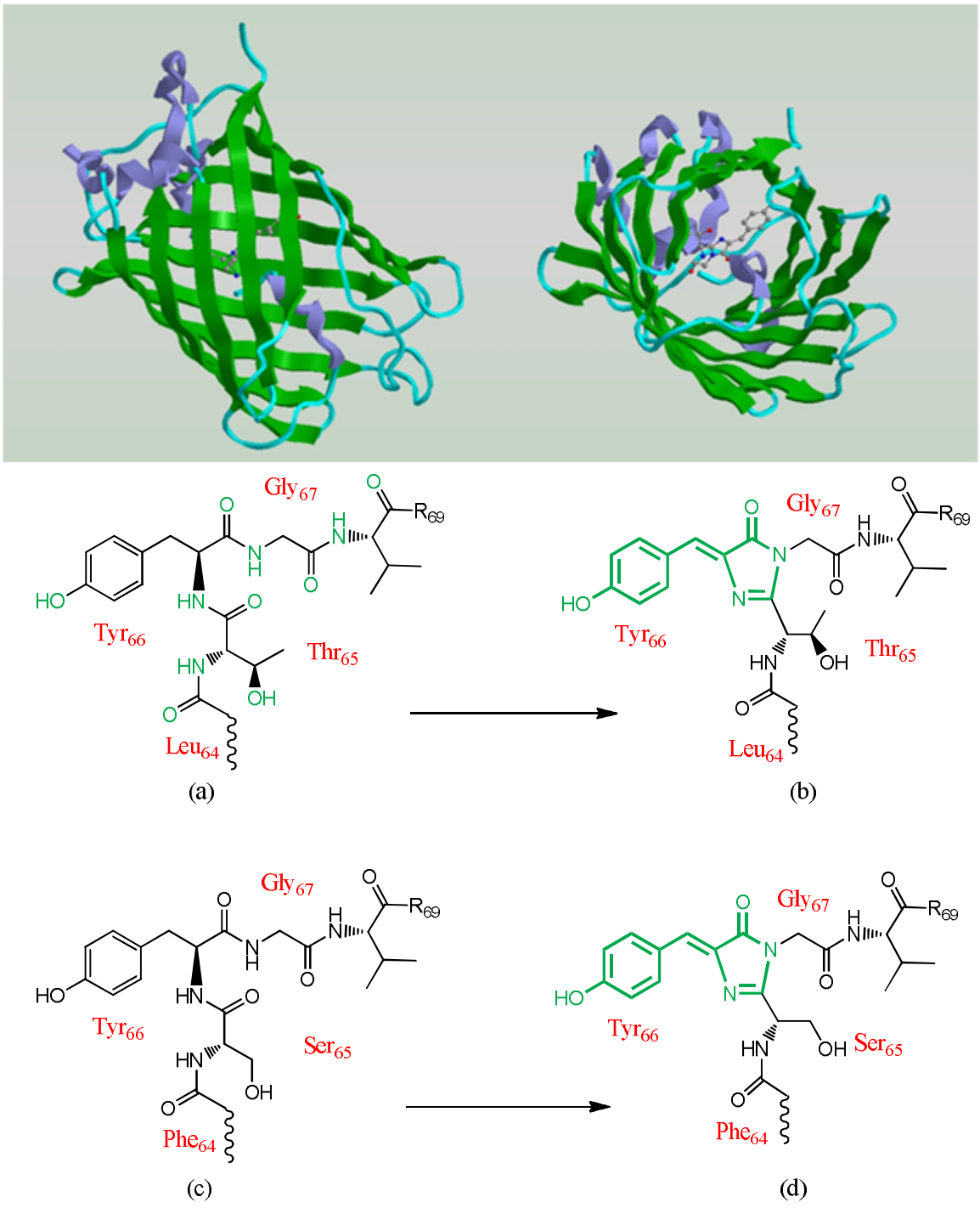

Figure 7. Upper left: EGFP protein structure showing the barrel shaped structure, with β-sheets in green, α-helix in violet, and random coils in light blue. Upper right: EGFP from different viewer perspective showing the fluorophore located in the centre in the ball-and-stick models (EGFP protein data bank entry 2Y0G).[189] Middle: (a) Thr_{65}, Tyr_{66}, and Gly_{67} residues constitute the fluorophore (b) the structure of the EGFP mature fluorophore (imidazolidinone) shown in green.[187] Lower: (c) the GFP fluorophore incorporates Phe_{64} (not Leu_{64}) and Ser_{65} (not Thr_{65}) (d) GFP mature fluorophore.

The Clontech pEGFP used to transfect the HeLa cells in this thesis express an EGFP variant which has Ser_{65} to Thr mutation and Phe_{64} to Leu mutation, and exhibits ~35-fold brighter fluorescence compared to wild type GFP, and enhanced folding. This EGFP has a single peak of excitation at 490 nm making it more suitable than wild type GFP for detection using the commonly used fluorescein filters and argon ion lasers of flow cytometers. EGFP also contains more than 190 silent base mutations which allow mammalian cells to translate the EGFP mRNA more efficiently, thus increasing EGFP expression. EGFP contains the Kozak consensus sequence which increases the efficiency of translation in eukaryotic cells, a neomycin resistance DNA sequence to allow for selection, and the cytomegalovirus promoter (CMV), for constitutive expression in mammalian cells.[187, 188]

The three amino acids ($Thr_{65,}$ Tyr_{66}, and Gly_{67}) present in the central α-helix of the barrel shaped EGFP are shown in Figure 7, Lower (a). These amino acids undergo cyclization to form the imidazolidinone ring, followed by dehydration then oxidation to form the mature chromophore, which is shown in green, Figure 7 Lower (b).

Lipoplexes prepared with the synthetic fatty acid spermine conjugates **1**-**5** and siRNA tagged with the fluorescent dye Alexa Fluor 647 (siEGFP-AF) were delivered to modified HeLa cells that stably express EGFP in order to evaluate both the delivery of siRNA and the knock-down of EGFP expression. Both the delivery of siRNA and EGFP knock-down were evaluated by calculating the geometric mean fluorescence of Alexa Fluor 647 and EGFP by means of flow cytometry (FACS analysis) after gating the population of healthy cells (Figure 8a). The gates AF647 and GFP are set for the calculation of the geometric mean fluorescence. The increase in Alexa Fluor 647 fluorescence within the gated population (i.e. delivery of fluorescent siEGFP-AF) and the decrease in EGFP fluorescence (i.e. knock-down) are shown in Figures 8d-8i. The amount of Alexa Fluor 647 fluorescence 48 h post-transfection was used to evaluate the relative efficiency of siEGFP-AF delivery by the lipospermine conjugates. Lipoplexes of **1** showed the highest Alexa Fluor 647 fluorescence (159 units) at 6 µg of **1** (Figure 9 Upper). Lipoplexes of **4** were second (17 units) at 6 µg of **4** (Figure 9 Lower). Typically, there is a relationship between the amount of each fatty acid spermine conjugate and the intensity of the Alexa Fluor 647 fluorescence measured, except for **2** at 0.75-3 µg and for **3** at 1.5 and 3 µg. Thus, increasing the amount of cationic lipid, from 0.75 to 6 µg, gave an increase in Alexa Fluor 647 fluorescence (Figure 9 Upper and Lower).

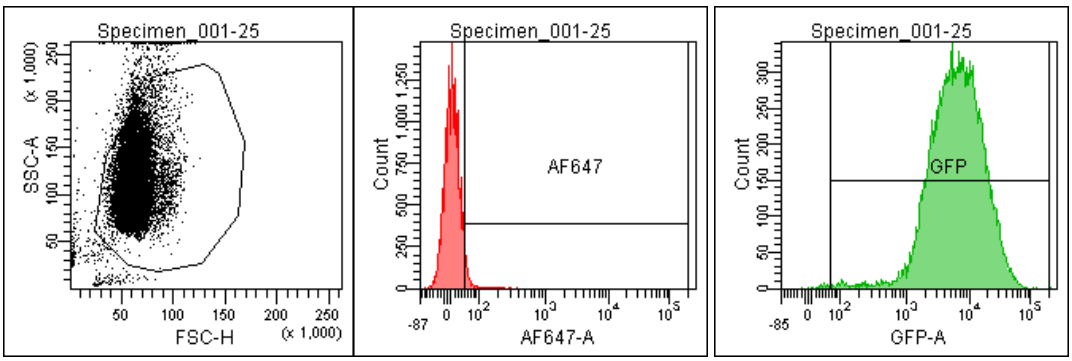

(8a) (8b) (8c)

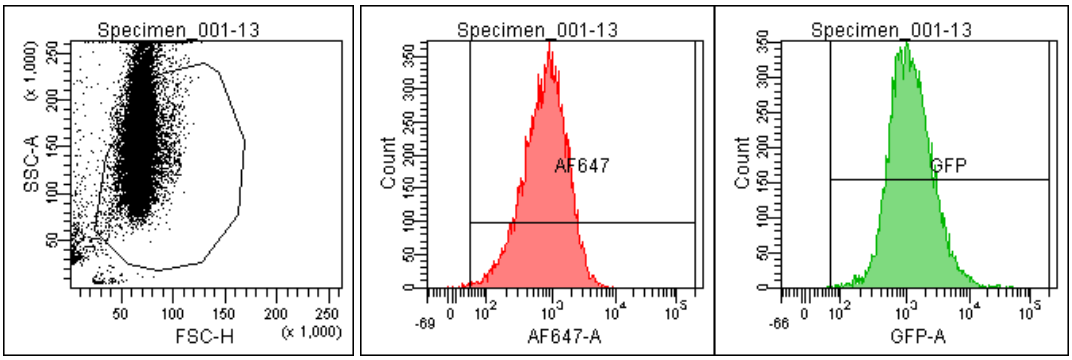

(8d) (8e) (8f)

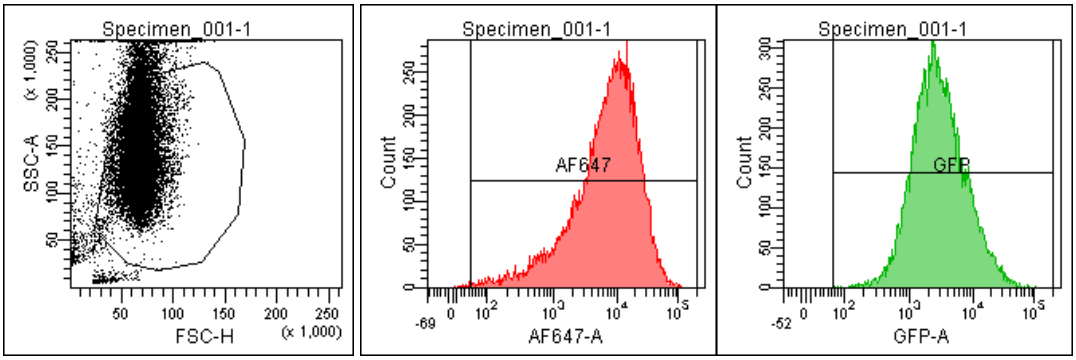

(8g) (8h) (8i)

Figure 8. (a), (d), and (g) The gating of a population of healthy cells (b) Alexa Fluor 647 channel autofluorescence of control cells (c) EGFP expression of control cells (e) Alexa Fluor 647 fluorescence after transfection with **4** at 6 µg/well (f) EGFP expression after transfection with **4** at 6 µg/well (e) Alexa Fluor 647 fluorescence after transfection with **1** at 6 µg/well (f) EGFP expression after transfection with **1** at 6 µg/well.

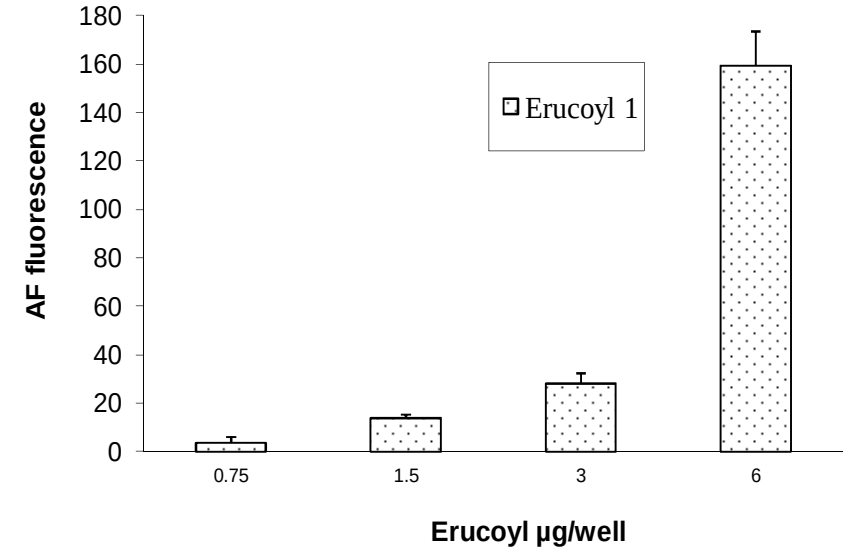

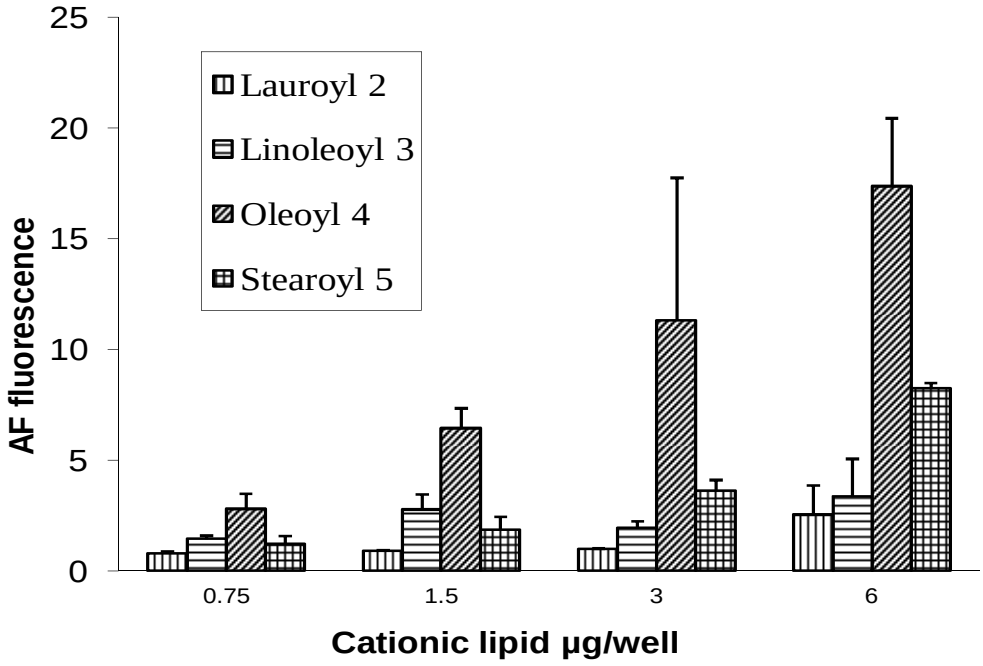

Figure 9. Upper: siEGFP-AF delivery using **1**. Values are presented as mean of normalized geometric mean fluorescence (AF fluorescence) ± SD (n = 2, triplicate samples of duplicate experiments). Lower: siEGFP-AF delivery measured as the normalized values of Alexa Fluor 647 (AF) geometric mean fluorescence using **2-5**.

Fatty acids with longer chain lengths and one C=C (erucoyl 22:1 and oleoyl 18:1) resulted generally in higher fluorescence at the same amount of lipid used. The least fluorescence was obtained with **2** (lauroyl 12:0) (Figure 9 Lower) which is saturated and has a relatively shorter chain length.

The *N/P* ratio is defined as the ratio of cationic lipid ammonium ions to RNA phosphate anions. In this case, the numerator is calculated as the number of moles of cationic lipid multiplied by the positive charge carried, 2.0. The value 2.0 reflects the p*K*a of each primary amine (~10.5) and the pH at which the experiments are performed (7.4) using the Henderson-Hasselbalch equation.[190] The denominator is the total number of phosphate anions which here is calculated from the total number of moles of siEGFP-AF multiplied by the total number of phosphates in the double stranded siEGFP-AF, where a synthetic 24-mer carries 23 phosphates in each strand following phosphoramidite synthesis. Though the terminal sugars of uncomplexed siRNA will be phosphorylated in cells, the lipoplexes are prepared before this reaction. Thus, at a fixed amount of siEGFP-AF (15 pmol), DOS at 6 μg/well will have *N/P* = 23.8.

Reduction in EGFP expression (Figures 10 and 11) was best achieved by lipoplexes of **4** (19% at 6 μg cationic lipid, *N/P* = 23.8, and 22% at 3 μg) followed by **3** (28% at 1.5 μg). These values are comparable with the commercial agents Lipofectamine 2000 and TransIT-TKO (both 24%). Lipoplexes of **4** (19% EGFP at 6 μg cationic lipid were statistically significantly different from Lipofectamine 2000 and TransIT TKO, with $p < 0.05$). Lipoplexes of **1** resulted in modest reduction of EGFP (43% at 6 μg). Lipoplexes of the saturated fatty acid conjugates **2** and **5** resulted in the lowest knock-down (highest EGFP expression) with values of 80% and 69% respectively. The overall better efficiency of unsaturated fatty acid spermine amides in reducing EGFP expression is attributed to the effects of double bonds restricting chain flexibility, allowing better interaction with the cell membrane lipids. The effect of saturation state of spermine fatty acid conjugates on their ability to transfect primary skin cell lines (FEK4, FCP4, FCP5, FCP7, and FCP8) and the cancer cell line HtTA transfected with pEGFP using the C18 derivatives of spermine linoleoyl (18:2), oleoyl (18:1), and stearoyl (18:0) was reported.[191] The unsaturated oleoyl **4** and linoleoyl **3** spermine conjugates were found to be much more efficient (3-5-fold) than the stearoyl **5** spermine conjugate. Higher fusogenic ability of unsaturated fatty acids (in the *cis*-configuration) probably favours (L_α to H_{II}) transition. A similar conclusion was reported[192] where unsaturated fluorinated lipospermines were more efficient than their saturated analogues due to the ability of unsaturated derivatives to promote membrane fusion and endosomal escape.

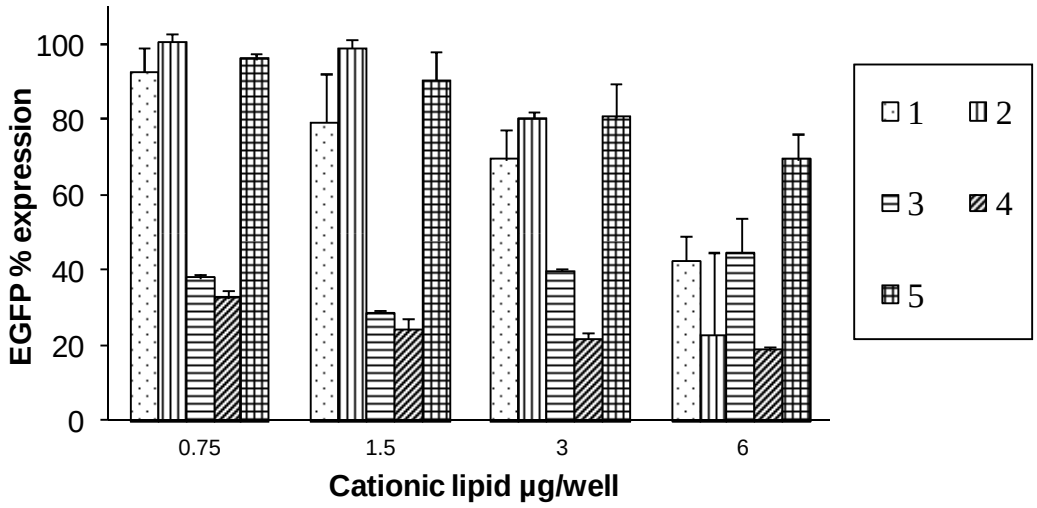

Figure 10. Reduction in EGFP expression in HeLa cells after transfection with lipoplexes of fatty acid amides of spermine at different cationic lipid/siEGFP-AF ratios. siEGFP-AF concentration is kept constant at 15 pmol/well. Values are presented as mean ± SD (n = 2).

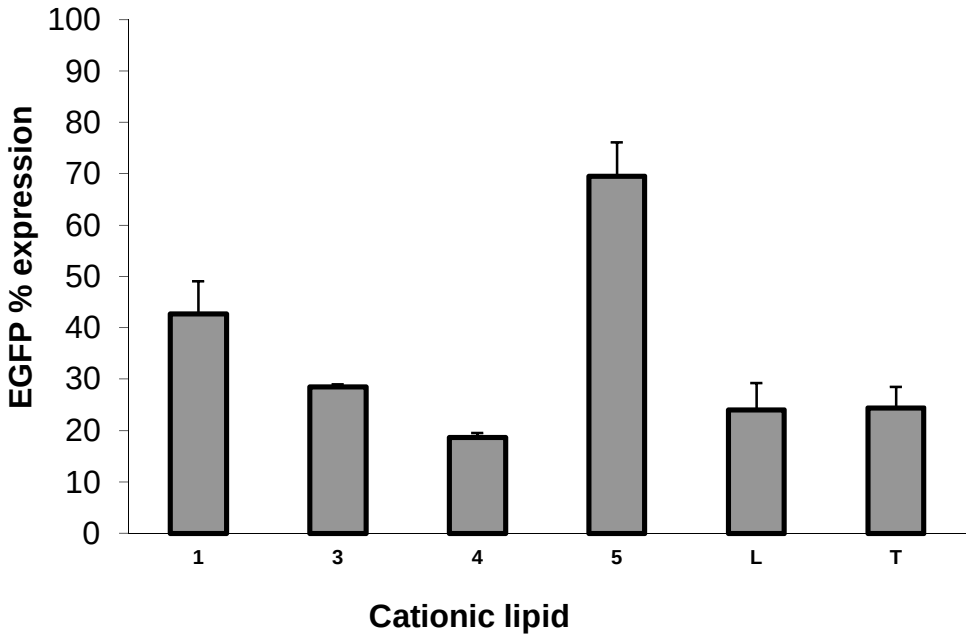

Figure 11. Comparison of reduction in EGFP expression in HeLa cells (knock-down) at their optimal cationic lipid/siEGFP-AF ratios and compared with the commercially available transfection agents Lipofectamine 2000 (L, 2 μL/well) and TransIT-TKO (T, 4 μL/well). Values are presented as mean ± SD (n = 2) using erucoyl (**1**, 6 μg/well), linoleoyl (**3**, 1.5 μg/well), oleoyl (**4**, 6 μg/well), and stearoyl (**5**, 6 μg/well).

There was no obvious direct relationship between the particle size and the efficiency of delivery or knock-down. The particle size of lipoplexes formed with vectors **2** and **4** were 283 and 247 nm respectively, but **2** resulted in less delivery (3 units compared to 17 units of **4**) and lower reduction in EGFP expression. Lipoplexes of **3** had larger particle size than **4** (353 and 247 nm respectively) and **3** showed less EGFP reduction compared to **4**. On the other hand, though lipoplexes of **5** had the lowest diameter (145 nm), they showed less reduction in EGFP (to 69%) compared to **3** and **4** (to 28% and to 19% respectively). These results show that, while keeping particle size within the normal lipoplex transfection range, particle size is not the only significant factor. Vectors **3**, **4**, and **5** have the same chain length while they differ in oxidation (saturation) state (18:2, 18:1, and 18:0 respectively).

The amount of siEGFP-AF delivered was evaluated by the fluorescence of Alexa Fluor 647 remaining after 48 h post-transfection. There was no direct relationship between the amount of siEGFP-AF delivered and the knock-down efficiency. Lipoplexes of **1** resulted in the highest delivery (159 units at 6 µg) and EGFP reduction (43%) while lipoplexes of **4** resulted in less siEGFP-AF delivery (17 units at 6 µg) and EGFP reduction (19%) at the same amount of cationic lipid. The same can be said with respect to **3** (EGFP reduction to 28% at 1.5 µg and delivery 3 units only) compared to **1**. However, with respect to vectors **1**, **4**, and **5**, the increase of Alexa Fluor 647 fluorescence is accompanied by better reduction in EGFP. These observations can be related to the different barriers to successful knock-down. Lipoplexes must first be internalized inside the cells (probably by endocytosis) followed by release from the endosomes before turning into lysosomes, then the release of siEGFP-AF in the cytoplasm to integrate with the RNAi machinery and promote the sequence specific gene silencing. Thus, it is not a necessity that higher number of lipoplexes (i.e. more siEGFP-AF get into the cells) corresponds to an increase in gene knock-down, because successful knock-down will require the success of all the aforementioned steps.

Figure 12 shows the effect of transfecting HeLa cells with AllStars negative control siNC-AF at the optimum cationic lipid/ siNC-AF ratios that resulted in the best EGFP knock-down with respect to each of the spermine conjugate vectors. Although there was an increase in the levels of fluorescence of Alexa Fluor 647, there was no corresponding significant decrease in the EGFP expression levels, except for compound **2** which is relatively toxic (as discussed below in section 3.5). This indicates that the reduction of EGFP fluorescence levels when transfecting with siEGFP-AF directed against EGFP is due to the sequence-specific gene silencing mediated by the siRNA and not due to any cytotoxic or non-specified effects of the vector. The scrambled siNC-AF is reported by the manufacturer to lack homology to any mammalian genes and it also did not result in significant changes in EGFP expression due to off-target effects. siRNA against EGFP with sequence 5'-

GCAAGCUGACCCUGAAGUUCAUTT-3' sense strand and 5'-AUGAACUUCAGGGUCAGCUUGCCG-3' anti-sense strand has one report of off-target effects that might affect gene-expression in HeLa and HEK cell lines.[186] The target DNA homology for silencing EGFP is 5'-CGGCAAGCTGACCCTGAAGTTCAT-3'.

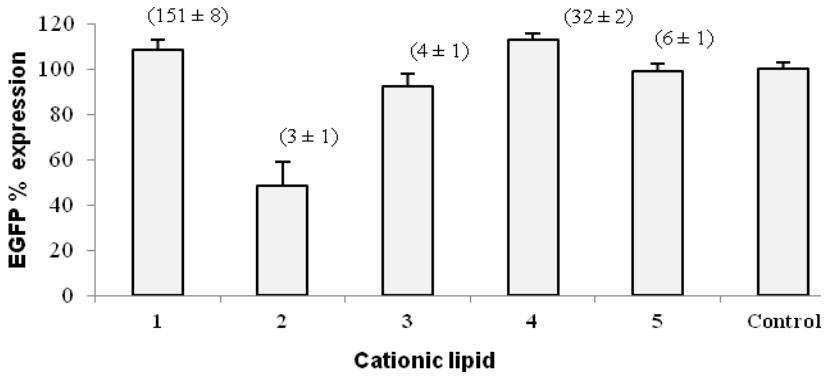

Figure 12. EGFP percentage expression 48 h post-transfection with scrambled negative control siNC-AF. Numbers in brackets are siNC-AF delivery expressed as Alexa Fluor 647 normalized geometric mean fluorescence ± SD.

3.4. Confocal microscopy cell imaging

Vector **4** was used to prepare lipoplexes with Alexa Fluor 647 labelled AllStars negative control siNC-AF and siRNA against EGFP (siEGFP-AF) at *N/P* = 23.8, the optimum ratio for the best EGFP knock-down (6 µg/15 pmol siEGFP-AF). Figure 13a shows the control HeLa cells (non-transfected) showing the bright green fluorescence of EGFP and the cell membrane stained with WGA-Alexa Fluor 555 (in blue). Figure 13b shows the HeLa cells 48 h post-transfection where the fluorescence of EGFP is significantly reduced and bright red spots indicate the fluorescence of Alexa Fluor 647 tagged siEGFP-AF, showing the uptake of the tagged siRNA. Figure 13d shows a magnified image of one cell (from Figure 13b) where many red spots show the uptake of the Alexa Fluor 647 and the absence of any green colour, the obvious reduction in EGFP expression. Figure 13c shows HeLa cells 48 h post-transfection with AllStars negative control siNC-AF, the red spots indicate cellular uptake of the tagged siRNA with no noticeable difference in EGFP fluorescence relative to the control HeLa cells (Figure 13a). Figure 13c provide evidence that the reduction in EGFP (seen in Figures 13b and 13d) is due to the sequence specific gene silencing by siEGFP-AF and not due to non-specific effects of N^4,N^9-dioleoylspermine **4**.

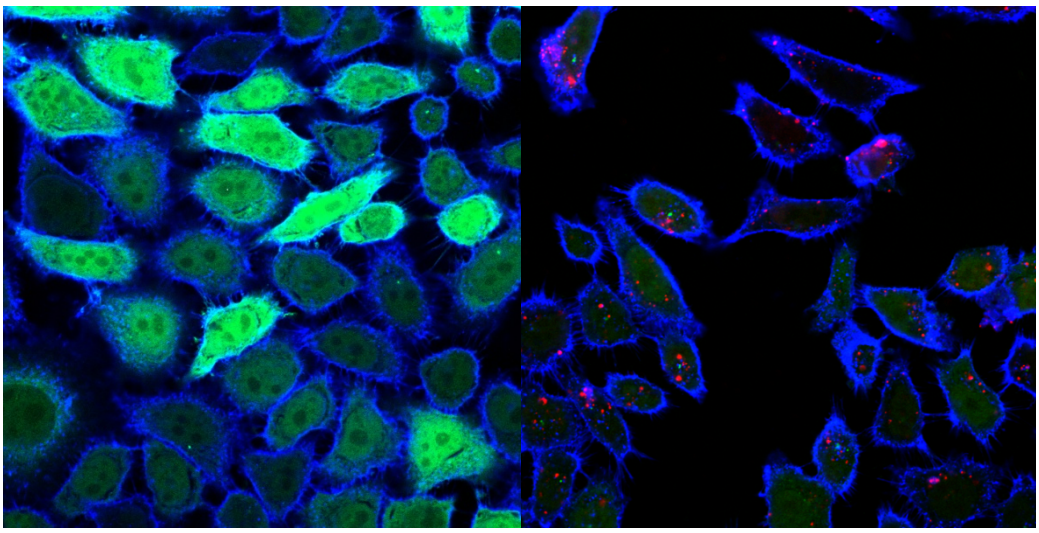

13a 13b

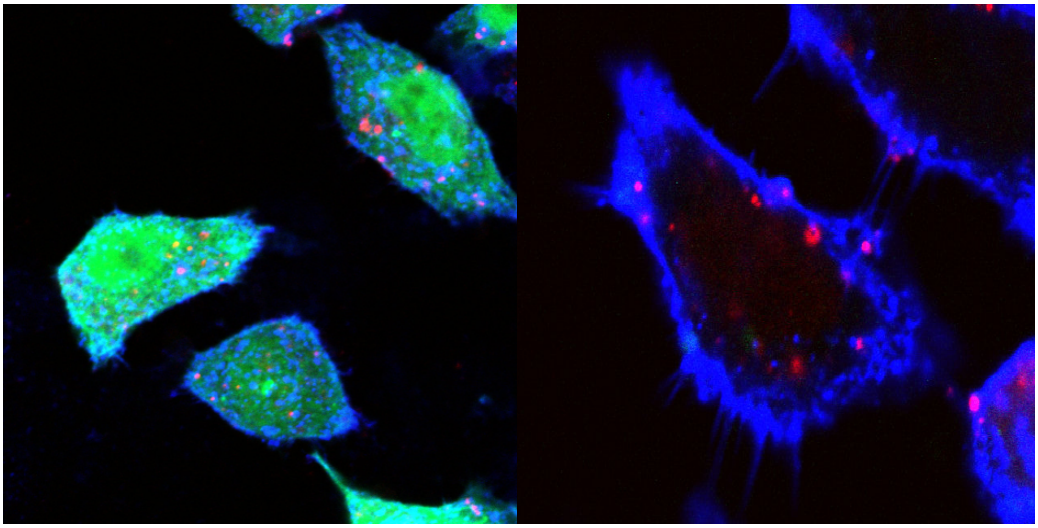

13c 13d

Figure 13. Confocal microscopy cell imaging. EGFP fluorescence (green), cell membrane stained with WGA-Alexa Fluor 555 (blue), and Alexa Fluor 647 (red) represents tagged siRNA delivered with N^4,N^9-dioleoylspermine **4**. 13a: non-transfected HeLa cells (control); 13b and 13d: HeLa cells 48 h post-transfection with siEGFP-AF; 13c: HeLa cells transfected with AllStars negative control siNC-AF.

3.5. Cell viability assay

The alamarBlue assay was used to measure cell viability. The active component of the commercial alamarBlue was reported to be resazurin (Figure 14).[193] It was reported that mitochondrial, cytosolic and microsomal enzymes reduce alamarBlue. The enzymes catalyzing alamarBlue reduction were suggested to be the various reductases present in both cytosol and microsomes, including alcohol and aldehyde oxidoreductases, cytochromes ,

flavin reductase, NADH dehydrogenase and NAD(P)H:quinone oxidoreductase.[194] As shown in Figure 15, there is spectral overlap of the oxidized and reduced form of alamarBlue. A simple and accurate method for calculating the amount of reduced alamarBlue was derived[195] and recommended by the alamarBlue supplier (equation shown in section 2.7 above).

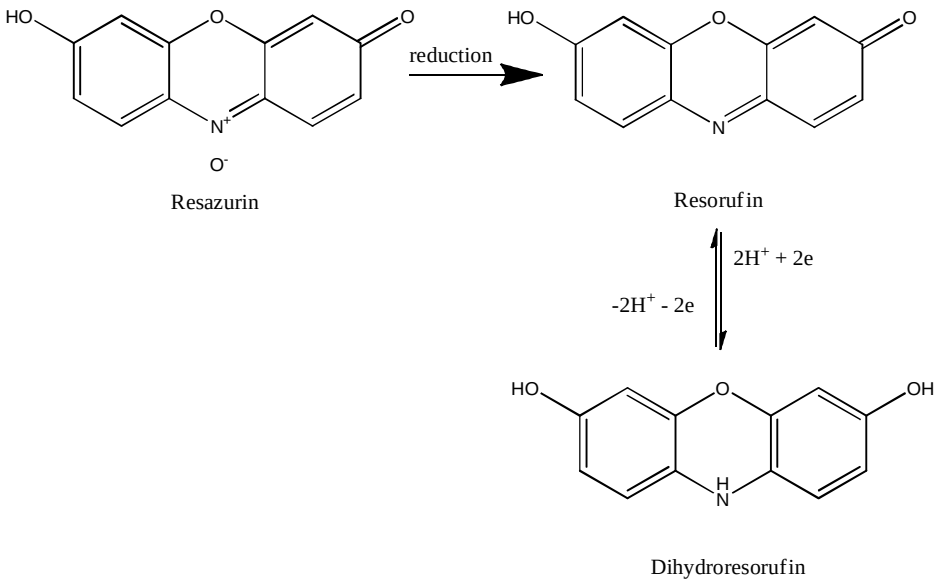

Figure 14. The active component of alamarBlue is resazurin (oxidized, non-fluorescent, and blue in color) which is reduced by viable cells to resorufin (reduced form, fluorescent, red coloured). Resorufin can be further reduced in a reversible manner to colourless dihydroresorufin.[193]

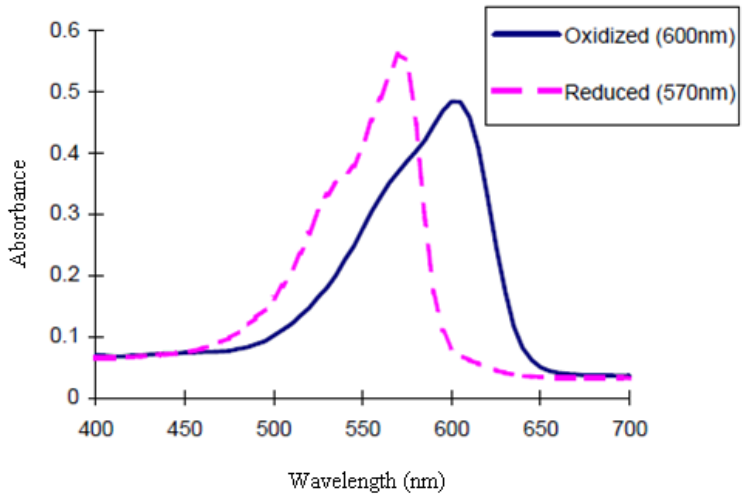

Figure 15. AlamarBlue absorbance of the oxidized (600 nm) and reduced (570 nm) forms. Taken from the manual supplied by the manufacturer (http://tools. invitrogen.com/content/sfs/manuals/PI-DAL1025-1100_TI%20alamarBlue%20Rev%201.1.pdf, accessed on 5/9/2011).

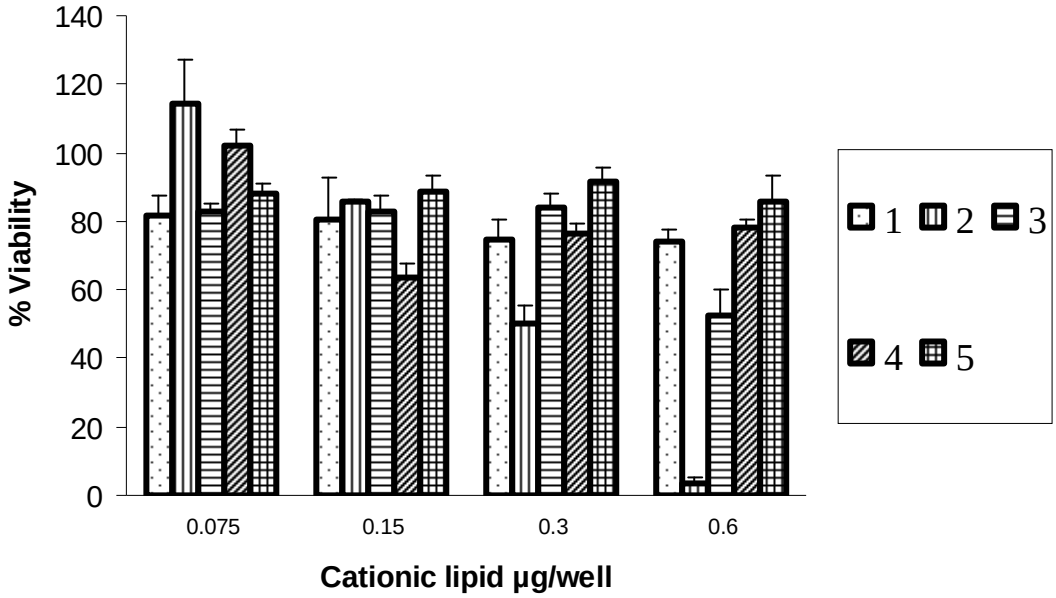

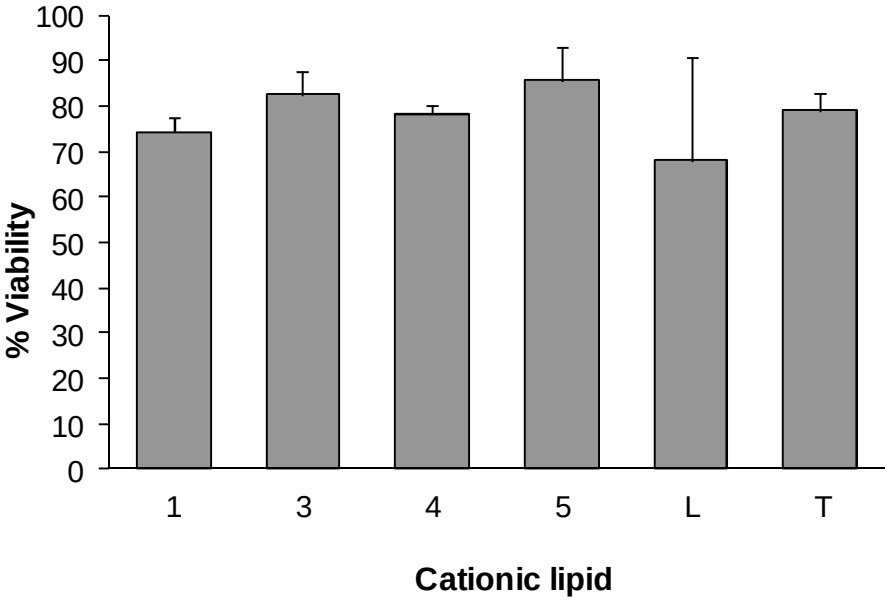

Figure 16. Upper: Cell viability alamarBlue assay of fatty acid amides of spermine at different cationic lipid/siNC ratios. siNC concentration is kept constant at 1.5 pmol/well (n = 2). Lower: Comparison of cell viability of HeLa cells after transfection with fatty acid amides of spermine at their optimal cationic lipid/siNC ratios and compared with the commercially available transfection agents Lipofectamine 2000 (L) and TransIT-TKO (T) Values are presented as mean ± SD (n = 2) using erucoyl (**1**, 0.6 µg/well), linoleoyl (**3**, 0.15 µg/well), oleoyl (**4**, 0.6 µg/well), and stearoyl (**5**, 0.6 µg/well).

The cell viability assay was carried out in 96-well plates. In order to keep the viability assay conditions as close as possible to the conditions used in the knock down experiments which were carried out in 24-well plates, the amounts of siRNA and cationic lipid, and the number of cells/well were multiplied by the same factor (one tenth), thus maintaining the *N/P* ratio and the amount of siRNA per total number of cells constant while downscaling from the 24-well format to the 96-well format. Thus, the 24-well format used 15 pmol siRNA/well, 6 µg cationic lipid/well, and 65,000 cells/well, and the 96-well format used 1.5 pmol siRNA/well, 0.6 µg cationic lipid/well, and 6,500 cells/well.

Cell viability evaluation after transfection was carried out with the alamarBlue assay. It can be seen from Figure 16 Upper that increasing the amount of lipid vector (from 0.075 µg to 0.6 µg) was accompanied by a decrease in cell viability. Short chain **2** (lauroyl, 12:0) was much more toxic than the other four spermine conjugates, at 0.6 µg of **2** there was only 3% cell viability. The cell viability with **2** was reported to be lower than that of N^4,N^9-dioleoyl **4** or distearoyl **5** spermine used to transfect HtTA cell line with a scrambled (negative control) fluorescein-labelled siRNA.[182] Indeed, while using the MTT cell viability assay, the fatty acid conjugates of spermine with shorter chain length (C12-C16) were reported to result in lower cell viability than the C18 fatty acid spermine conjugates.[182] Figure 16 Lower shows that, with the exception of **2**, all fatty acid spermine amides were at least as well tolerated as the commercially available reagents Lipofectamine 2000 and TransIT-TKO in HeLa cells.

4. Conclusions

Saturated shorter chain (C12:0) **2** showed concentration dependent toxicity when compared with the longer chain (C18-C22) spermine fatty acid amides. Transfection with lipoplexes of siEGFP-AF and N^4,N^9-difatty acid amides of spermine resulted in successful delivery and gene silencing of EGFP in HeLa cells. Varying the chain length or oxidation state of the fatty acids affected both the siEGFP-AF delivery and gene silencing efficiency with non-saturated fatty acids (C18:1), (C18:2), and (C22:1) being more efficient compared to saturated fatty acids (C12:0) and (C18:0). There was no evidence of a direct relationship between the amount of siEGFP-AF delivered and the efficiency of gene silencing. N^4,N^9-Dilinoleoyl spermine **3** and N^4,N^9-dioleoyl spermine **4** were at least as efficient and as well tolerated as the commercially available market leaders Lipofectamine 2000 and TransIT-TKO in HeLa cells. In Chapter 3, the effect of changing the two terminal cationic head-groups from primary amine to guanidine groups will be investigated.

Chapter Three Self-assembled lipoplexes of siRNA using fatty acid amide guanidines, based on spermine, effect efficient gene silencing

1. Introduction

In order to achieve gene silencing mediated by siRNA, the siRNA should be delivered intact to the cytoplasm of the cell. Due to the negative charge of the siRNA phosphate backbone, and its susceptibility to degradation by various nucleases, a vector is needed to achieve efficient intracellular delivery of siRNA. Cationic lipids are currently under investigation for the non-viral delivery of lipoplexes of DNA and siRNA.[196-198] The polar (cationic) head-group can be an amine (primary, secondary, tertiary, and even quaternary e.g. imidazolium[199]), or guanidine functional group. Guanidines, the most basic functional group in biological chemistry, are positively charged at physiological pH 7.4 as they have p*K*a = 12.5.[190] Guanidines have the extra advantage, being bidentate, of being able to form two hydrogen bonds with negatively charged groups e.g. carboxylates, phosphates, sulfates present on the carbohydrates associated with the cell membrane, and this advantage has been used in other vectors (e.g. R8, Arg_8[200, 201]) to transport cargoes across cell membranes. These characteristics led to the design of many non-viral vectors for DNA and siRNA, varying from cationic lipids incorporating guanidine head-groups[202-204] e.g. AtuFECT,[204] to cationic polymers[205, 206] and dendrimers,[115, 207] to carbohydrate derivatives,[115, 208] and hydrogels of guanidinylated hyaluronic acid.[209] The use of guanidinium-containing lipid based carriers for gene delivery dates back to 1996 where Lehn et al. synthesized two guanidinium cholesterol lipids; bis-guanidiniumspermidine-cholesterol (BGSC) and bis-guanidinium-trencholesterol (BGTC), each containing two guanidine groups, which were synthesized and evaluated for their DNA transfection efficiencies in eukaryotic cells[210] (Figure 1) where they were found to be efficient DNA transfecting agents. Furthermore, BGTC was found to mediate transfection in an aqueous solution without the need to prepare it first in a liposomal form.

In this Chapter, spermine is acylated with different fatty acids on its secondary amine groups, and then is guanidinylated at the terminal primary amine groups. The guanidinylated non-viral cationic lipid vectors are characterized and evaluated for their ability to deliver siRNA that targets EGFP in HeLa cells that stably express EGFP.

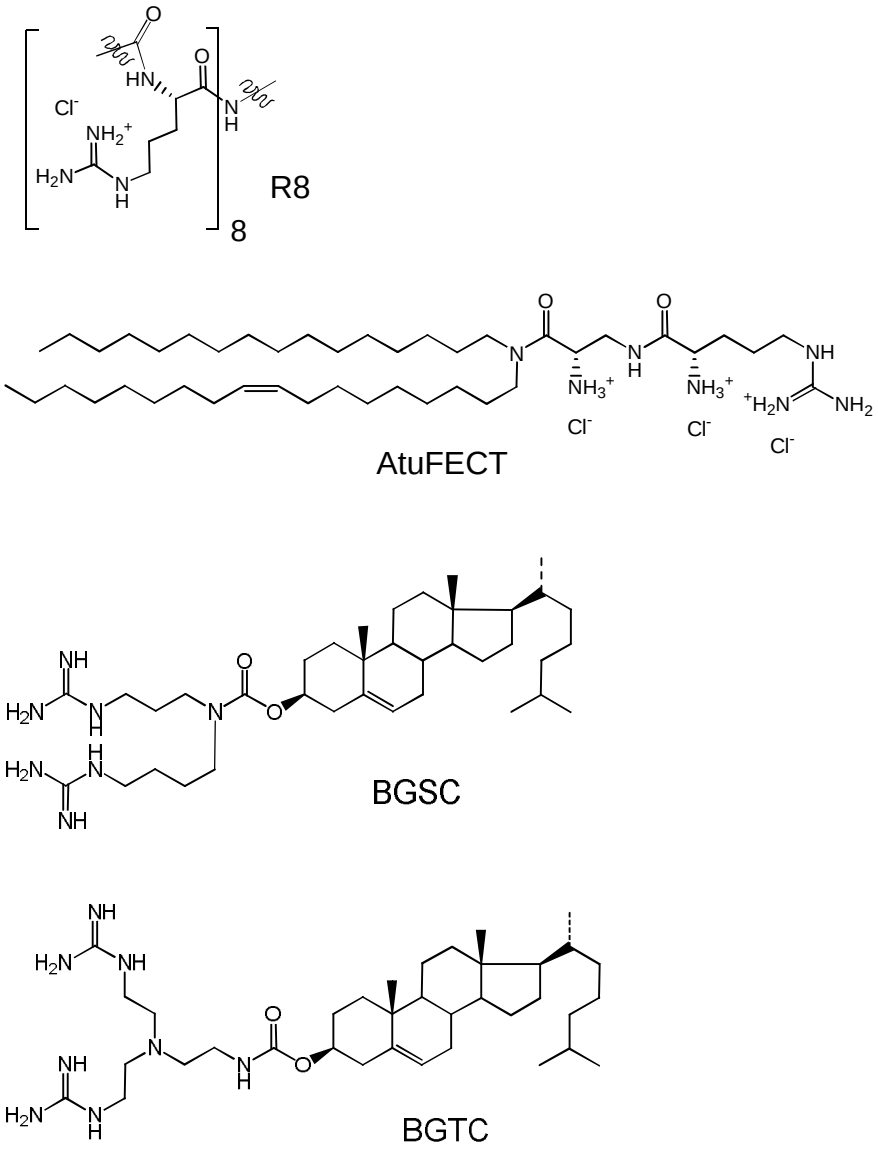

Figure 1. Some guanidines used in delivery of genes and other cargoes.

2. Materials and methods

2.1. Materials and general methods

1,3-Di-Boc-2-(trifluoromethylsulfonyl)guanidine was purchased from Sigma-Aldrich (Gillingham, UK). All solvents and other chemicals were purchased as described in Chapter 2 (Section 2.1), and all general procedures for preparing anhydrous solvents, and purification and characterization of the target compounds were carried out as described in Chapter 2 (Section 2.1).

2.2. Synthesis of N^1,N^{12}-diamidino-N^4,N^9-diacylated spermines

N-Carbethoxyphthalimide (0.44 g, 2 mmol) was added to a solution of 1,12-diamino-4,9-diazadodecane (spermine) (0.20 g, 1 mmol) in DCM (10 mL). The solution was stirred 20 °C for 3 h then evaporated to dryness in vacuo and the residue was used directly in the following step. To a solution of 1,12-diphthalimido-4,9-diazadodecane in DCM (10 mL) and TEA (0.28 mL, 2 mmol) fatty acid chloride (2 mmol), or alternatively fatty acid (2 mmol), DMAP (0.24 g, 2 mmol), and DCC (0.4 g, 2 mmol) were added and stirred for 18 h under nitrogen atmosphere. To prepare, 1,12-diphthalimido-N^4-linoleoyl-N^9-oleoylspermine, first, 1,12-diphthalimido-4-oleoylspermine was prepared by reacting 1,12-diphthalimido-4,9-diazadodecane (1 mmol) with 1 (mmol) oleic acid using DCC as described in Chapter 2. After purifying the product over silica gel (DCM/MeOH 20:1 v/v then 10:1 v/v), it was further conjugated to linoleic acid (1 mmol) using DCC as the coupling agent. The solvent was then evaporated (for all of the prepared compounds) to dryness in vacuo and the residue was treated with hydrazine monohydrate (2 mL) in a mixture of DCM (15 mL) and THF (15 mL) and heated under reflux for 4 h then the solvent was evaporated in vacuo to dryness and the residue purified over silica gel (DCM/MeOH 10:1 v/v then DCM/MeOH/NH_4OH 20:10:1 v/v/v) to afford the N^4,N^9 fatty acid amides of spermine. HRMS of N^4,N^9-dierucoylspermine, N^4,N^9-dilauroylspermine, and N^4,N^9-dioleoylspermine were found as previously described in Chapter 2 (Section 2.2). N^4-Linoleoyl-N^9-oleoyl-1,12-diamino-4,9-diazadodecane HRMS m/z, found $(M+H)^+$ 729.6980, $C_{46}H_{89}N_4O_2$ requires $(M+H)^+$ 729.6986.

The N^1,N^{12}-diamidino-N^4,N^9-diacylated spermines were prepared by reacting each of the prepared N^4,N^9-diacylated spermine (1 mmol) with 1,3-di-Boc-2-(trifluoromethylsulfonyl)guanidine (2 mmol) and TEA (2 mmol) in DCM (10 mL) at 20 °C for 24 h. The reaction mixture was then evaporated to dryness in vacuo and the residue was purified over silica gel (DCM/MeOH 100:1 v/v then 100:2 v/v) and the required fractions were concentrated. The residue was then added to DCM (6 mL), TFA (2 mL) was added, and the mixture stirred at 20 °C for 4 h. The reaction mixture was then evaporated to dryness in vacuo to afford the title compounds as the trifluoroacetate salts.

N^1,N^{12}-Di(*N*,*N'*-Bis(*tert*-butoxycarbonyl)amidino)-N^4,N^9-dierucoylspermine (DESdiBocG)

^{1}H NMR, 0.8 (m, 6H, H22'), 1.2-1.3 (m, 56H, H4'-H11', H16'-H21'), 1.3-1.4 (m, 40H, methyl groups of Boc, H6, H7), 1.4-1.8 (m, 10H, H2, H11, H3', 2 x NH attached to Boc), 1.9 (m, 8H, H12', H15'), 2.3 (m, 4H, H2'), 3.1-3.3 (m, 12H, H1, H3, H5, H8, H10, H12), 5.2 (4H, H13', H14'), 8.2-8.4 (m, 2H, NH attached to C1 and C12).

N^1,N^{12}-Di(*N*,*N'*-Bis(*tert*-butoxycarbonyl)amidino)-N^4,N^9-dilauroylspermine (DLauSdiBocG)

^{1}H NMR, 0.8 (m, 6H, H12'), 1.2-1.3 (m, 32H, H4'-H11'), 1.4-1.5 (m, 40H, methyl groups of Boc, H6, H7), 1.4-1.8 (m, 10H, H2, H11, H3', 2 x NH attached to Boc), 2.3 (m, 4H, H2'), 3.2-3.5 (m, 12H, H1, H3, H5, H8, H10, H12), 5.2 (4H, H13', H14'), 8.3-8.6 (m, 2H, NH attached to C1 and C12).

N^1,N^{12}-Di(*N*,*N'*-Bis(*tert*-butoxycarbonyl)amidino)-N^4,N^9-dioleoylspermine (DOSdiBocG)

^{1}H NMR, 0.8 (m, 6H, H18'), 1.2-1.3 (m, 40H, H4'-H7', H12'-H17'), 1.3-1.4 (m, 40H, methyl groups of Boc, H6, H7), 1.4-1.9 (m, 10H, H2, H11, H3', 2 x NH attached to Boc), 2.0 (m, 8H, H8', H11'), 2.4 (m, 4H, H2'), 3.0-3.3 (m, 12H, H1, H3, H5, H8, H10, H12), 5.3 (4H, H9', H10'), 8.1-8.4 (m, 2H, NH attached to C1 and C12).

N^1,N^{12}-Di(*N*,*N'*-Bis(*tert*-butoxycarbonyl)amidino)-N^4-linoleoyl-N^9-oleoylspermine (DLinOSdiBocG)

^{1}H NMR, 0.9 (m, 6H, H18', H18''), 1.3-1.4 (m, 34H, H4'-H7', H15'-H17', H4''-H7'', H12''-H17''), 1.3-1.4 (m, 42H Methyl groups of Boc, H6, H7, 2 x NH attached to Boc), 1.4-1.8 (m, 8H, H2, H11, H3', H3''), 2.0 (m, 8H, H8', H14', H8'', H11''), 2.3 (m, 4H, H2', H2''), 2.8 (m, 2H, H11'), 3.2-3.5 (m, 12H, H1, H3, H5, H8, H10, H12), 5.3 (6H, H9', H10', H12', H13', H9'', H10''), 8.3-8.5 (m, 2H, NH attached to C1 and C12).

N^1,N^{12}-Diamidino-N^4,N^9-dierucoylspermine (DESdiG, 1)

^{1}H NMR, 0.9 (m, 6H, H22'), 1.2-1.4 (m, 56H, H4'-H11', H16'-H21'), 1.5-1.9 (m, 12H, H2, H6, H7, H11, H3'), 2.0 (m, 8H, H12', H15'), 2.4 (m, 4H, H2'), 3.0-3.4 (m, 12H, H1, H3, H5, H8, H10, H12), 5.3 (4H, H13', H14'), 6.7-7.2 and 12.6-13.1 (broad, 10H, protonated guanidine groups protons). ^{13}C NMR, 14.0 (C22'), 22.6 (C21'), 25.6-32.8 (C2'-C12', C15'-C21', C2, C6, C7, C11), 38.7 (C1,C12), 43.6-48.1 (C3, C5, C8, C10), 114.0-116.9 (CF_3), 129.7-129.9 (C13', C14'), 157.1-161.2 (C of guanidine, C=O of TFA), 175.9 (C1', C1''). HRMS m/z, ESI found $(M+H)^+$ 927.8795, $C_{56}H_{111}N_8O_2$ requires $(M+H)^+$ 927.8825.

N^1,N^{12}-Diamidino-N^4,N^9-dilauroylspermine (DLauSdiG, 2)

^{1}H NMR, 0.9 (m, 6H, H12'), 1.2-1.4 (m, 32H, H4'-H11'), 1.5-1.9 (m, 12H, H2, H6, H7, H11, H3'), 2.4 (m, 4H, H2'), 3.0-3.5 (m, 12H, H1, H3, H5, H8, H10, H12), 6.4-6.9, 7.2, 11.8-12.6 (broad, 10H, protonated guanidines). ^{13}C NMR, 14.0 (C12'), 22.5 (C11'), 25.6-32.8 (C2'-C11', C2, C6, C7, C11), 38.7 (C1,C12), 43.0-48.0 (C3, C5, C8, C10), 113.9-116.8 (CF_3),

157.1-161.0 (C of guanidine, C=O of TFA), 176.0 (C1', C1''). HRMS m/z, ESI found $(M+H)^+$ 651.5996, $C_{36}H_{75}N_8O_2$ requires $(M+H)^+$ 651.6008.

N^1,N^{12}-Diamidino-N^4,N^9-dioleoylspermine (DOSdiG, 3)

^{1}H NMR, 0.9 (m, 6H, H18'), 1.2-1.4 (m, 40H, H4'-H7', H12'-H17'), 1.5-1.9 (m, 12H, H2, H6, H7, H11, H3'), 2.0 (m, 8H, H8', H11'), 2.4 (m, 4H, H2'), 3.0-3.4 (m, 12H, H1, H3, H5, H8, H10, H12), 5.3 (8H, H9', H10'), 6.4-6.7, 7.0, 13.4-13.6 (broad, 10H, protonated guanidine groups protons). ^{13}C NMR, 13.9 (C18'), 22.6 (C17'), 25.6-32.7 (C2'-C8', C11'-C17', C2, C6, C7, C11), 38.4 (C1, C12), 43.3-48.1 (C3, C5, C8, C10), 110.0-119.0 (CF_3), 129.4-130.1 (C9', C10'), 156.8-161.3 (C of guanidine, C=O of TFA), 176.8 (C1', C1''). HRMS m/z, ESI found $(M+H)^+$ 815.7549, $C_{48}H_{95}N_8O_2$ requires $(M+H)^+$ 815.7573.

N^1,N^{12}-Diamidino-N^4-linoleoyl-N^9-oleoylspermine (DLinOSdiG, 4)

^{1}H NMR, 0.9 (m, 6H, H18',H18''), 1.2-1.4 (m, 34H, H4'-H7', H15'-H17', H4''-H7'', H12''-H17''), 1.5-1.6 (m, 8H, H6, H7, H3', H3''), 1.7-1.9 (m, 4H, H2, H11), 2.0 (m, 8H, H8', H14', H8'', H11''), 2.4 (m, 4H, H2', H2''), 2.8 (m, 2H, H11'), 3.1-3.4 (m, 12H, H1, H3, H5, H8, H10, H12), 5.3-5.4 (6H, H9', H10', H12', H13', H9'', H10''), 6.6-7.2 and 7.5-7.7 (broad, 10H, protonated guanidines). ^{13}C NMR, 14.0 (C18',C18''), 22.5 (C17',C17''), 25.6-32.9 (C2'-C8', C14'-C17', C2''-C8'', C11''-C17'', C2, C6, C7, C11), 39.0 (C1,C12), 43.5-48.1 (C3, C5, C8, C10), 114.0-116.9 (CF_3), 127.7-130.1 (C9', C10', C12', C13', C9'', C10''), 157.4-161.2 (C of guanidine, C=O of TFA), 174.7 (C1',C1''). HRMS m/z, ESI found $(M+H)^+$ 813.7384, $C_{48}H_{93}N_8O_2$ requires $(M+H)^+$ 813.7416.

2.3. Experimental Protocols

Transfection experiments were carried out on HeLa cells stably expressing EGFP using the protocol described in Chapter 2 (Section 2.4). FACS analysis was carried out as described in Chapter 2 (Section 2.5). Confocal microscopy cell imaging was carried out as described in Chapter 2 (Section 2.6). Cell viability assay was carried out as described in Chapter 2 (Section 2.7). Particle size and ζ-potential measurements were carried out as described in Chapter 2 (Section 2.8). siRNA binding assay (RiboGreen intercalation assay) was carried out as described in Chapter 2 (Section 2.9). Statistical analysis was carried out as described in Chapter 2 (Section 2.10).

3. Results and discussion

3.1. Synthesis of N^1,N^{12}-diamidine derivatives of spermine

A series of novel lipoguanidines were designed in order to investigate the SAR of replacing primary amines with guanidine functional groups (Figures 2 and 3). These are formally called di-imidamides of alkanes and the nomenclature also permits *N*-aminoiminomethyl. Where these compounds were referred to as guanidines, they are more correctly *N*-amidines of spermine.

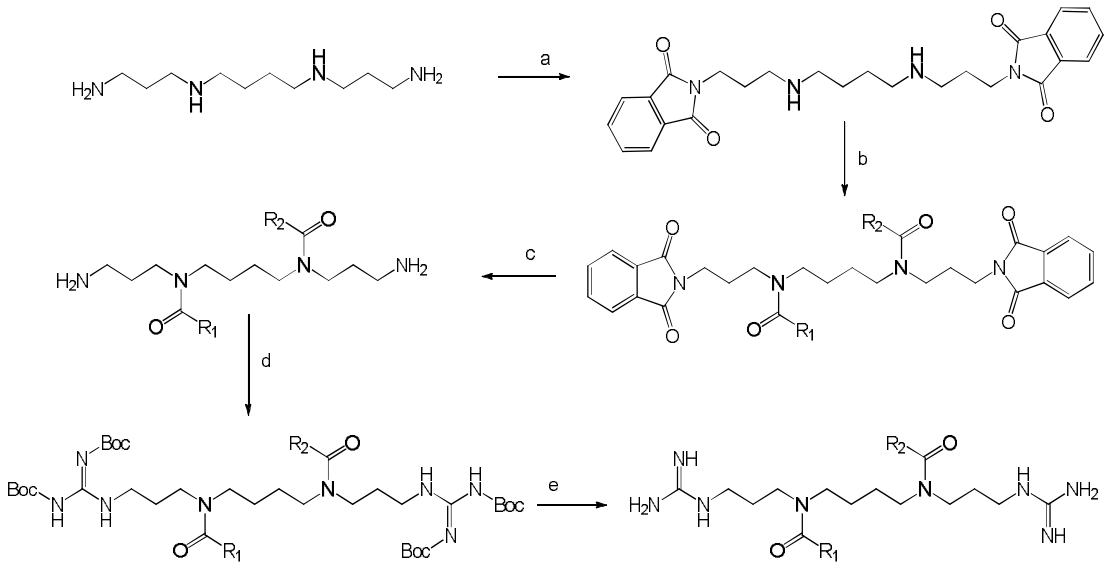

Figure 2. Schematic representation of the synthesis of N^1,N^{12}-diamidino-N^4,N^9-diacylated spermines. a: *N*-carbethoxyphthalimide, DCM; b: fatty acid, DCC, TEA; c: hydrazine monohydrate, DCM/THF 1:1; d: 1,3-di-Boc-2-(trifluoromethylsulfonyl)guanidine, TEA, DCM; e: TFA, DCM.

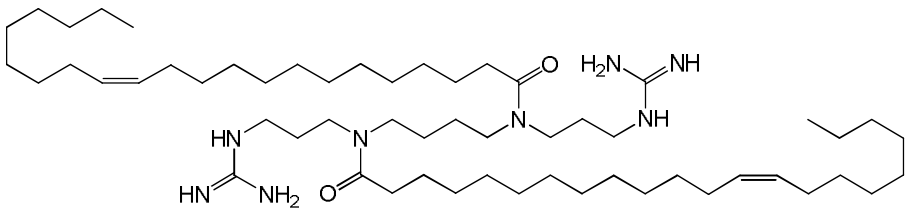

DESdiG, 1

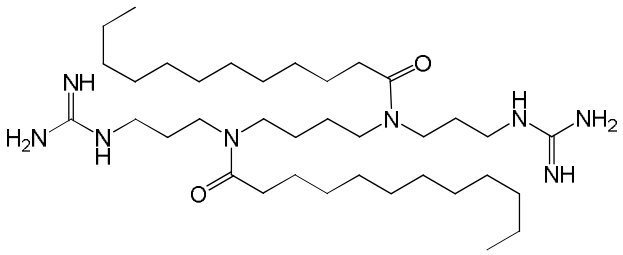

DLauSdiG, 2

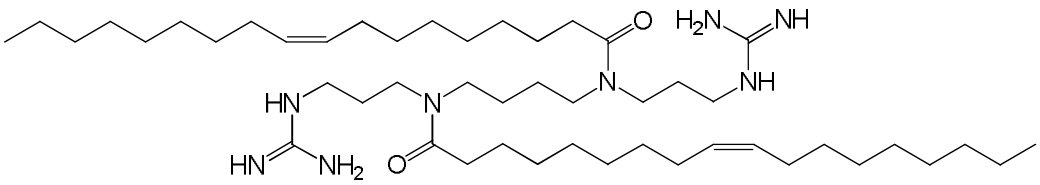

DOSdiG, 3

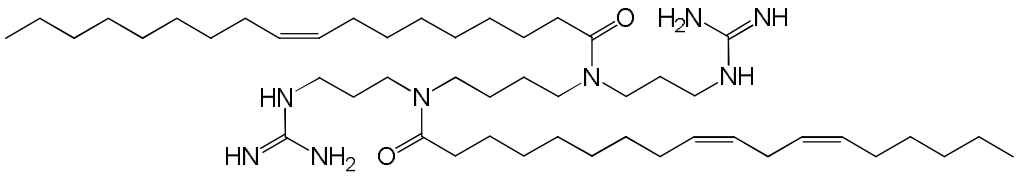

LinOSdiG, 4

Figure 3. N^1,N^{12}-Diamidine derivatives of different lipospermines

Table 1. N^1,N^{12}-Diamidine derivatives of different lipospermines. The fatty acids are described by two numbers separated by a colon, first the chain length and then the number of double bonds. Particle size, ζ-potential, and RiboGreen binding of guanidinylated lipospermines were measured at the cationic lipid/siRNA ratios that showed best reduction in EGFP expression.

Name of compound	**Fatty acid**	**Diameter (nm) ± SD**	**ζ-potential (mV) ± SD**	**% fluorescence of RiboGreen**
N^1,N^{12}-Diamidino-N^4,N^9-dierucoylspermine DESdiG, **1**	Erucic 22:1	132 ± 4	50 ± 1	5 ± 2
N^1,N^{12}-Diamidino-N^4,N^9-dilauroylspermine DLauSdiG, **2**	Lauric 12:0	575 ± 61	28 ± 3	12 ± 3
N^1,N^{12}-Diamidino-N^4,N^9-dioleoylspermine DOSdiG, **3**	Oleic 18:1	303 ± 6	45 ± 3	0 ± 1
N^1,N^{12}-Diamidino-N^4-linoleoyl-N^9-oleoylspermine LinOSdiG, **4**	Linoleic 18:2 Oleic 18:1	158 ± 24	45 ± 3	8 ± 2

Figure 4 shows the ^{1}H NMR assignments of LinOSdiBocG. The most important features necessary to identify the target compound include: (a) the presence of the double bonds protons (6 protons at δ = 5.3, H9', H10', H12', H13', H9", H10") which correspond to the two double bonds of the linoleoyl chain and the one double bond of the oleoyl chain; (b) the presence of 12 protons at δ = 3.2-3.5 (m, 12H, H1, H3, H5, H8, H10, H12), which are deshielded because they are next to the nitrogen atoms of the amide groups (protons 3, 5, 8, and 10), and next to the two terminal nitrogens of the guanidine groups (protons 1 and 12), indicating the successful conjugation of the fatty acids to the spermine N^4 and N^9 as well to the successful guanidinylation of the terminal primary amines; (c) 6 protons at δ = 0.9 (6H, H18', H18") representing the two terminal methyl groups of the two conjugated fatty acids; (d) 36 protons at δ = 1.3-1.4 (protons of the methyl groups of Boc); (e) The two protons at 8.3-8.5 (NH attached to C1 and C12); (f) The total proton integration which fits the formulae of LinOSdiBocG, $C_{68}H_{124}N_8O_{10}$. Thus, the ^{1}H NMR proves that the target compound was synthesized successfully.

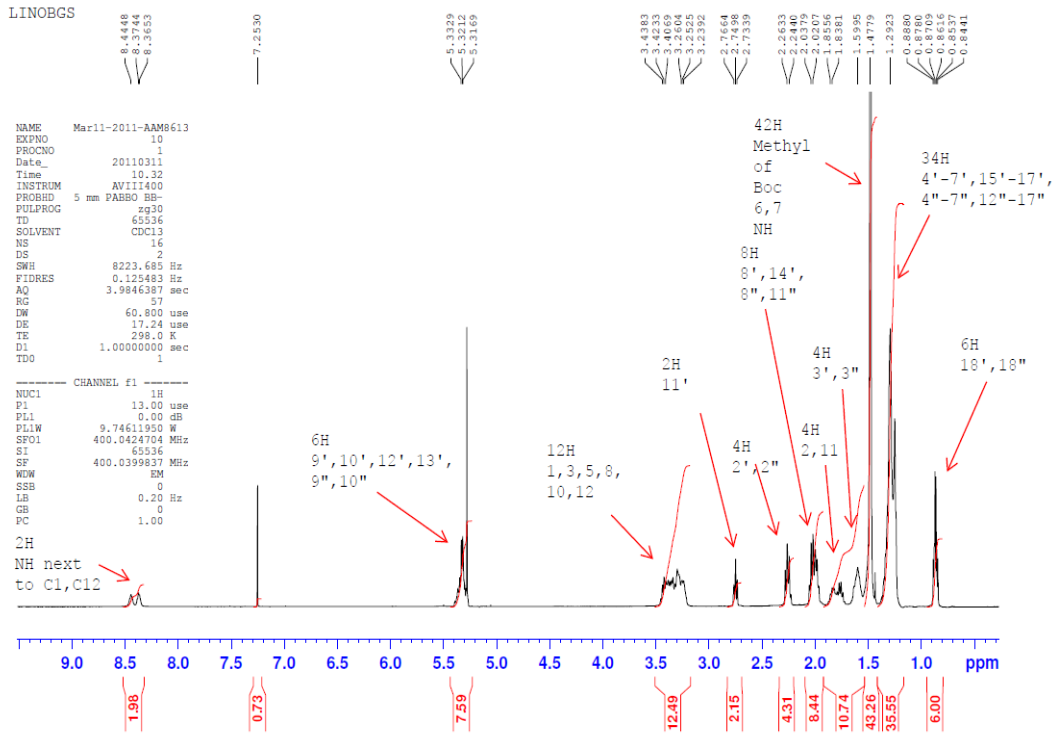

Figure 4. ^{1}H-NMR of LinOSdiBocG.

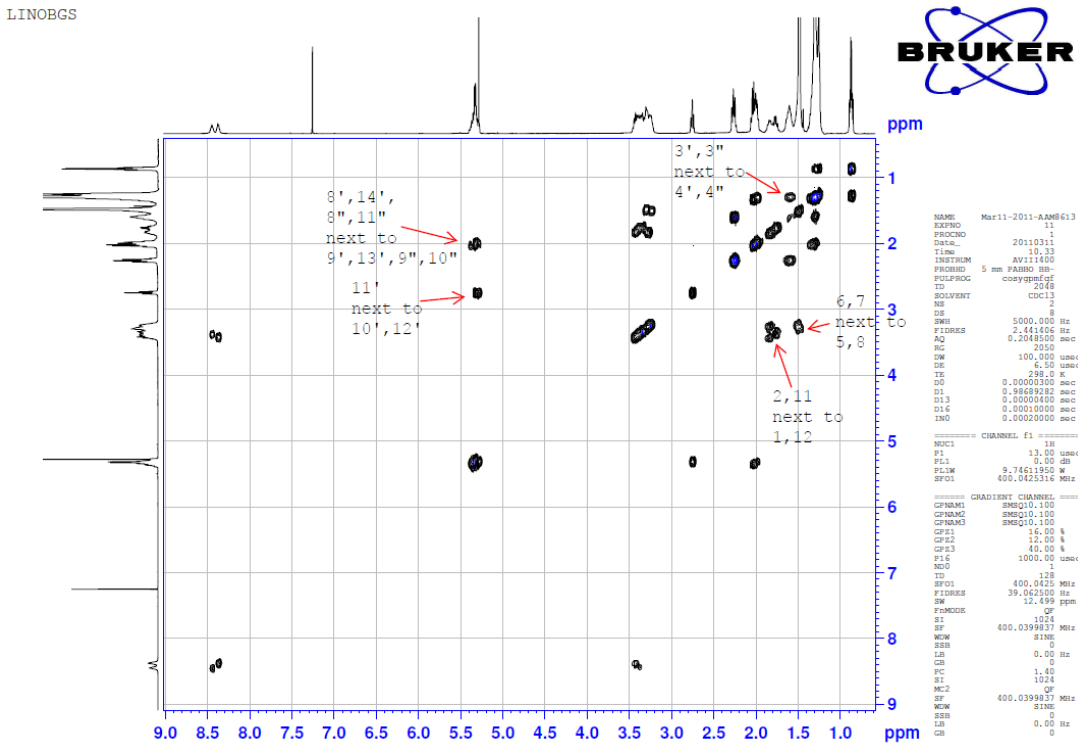

Figure 5. ^{1}H-^{1}H-NMR COSY of LinOSdiBocG.

Figure 5 shows the ^{1}H-^{1}H-NMR COSY of LinOSdiBocG. Among the most characteristic cross-peaks are those showing protons 6 and 7 (at δ = 1.3-1.4) cross-peak with protons 5 and 8 (at δ = 3.2-3.5) while no other cross-peaks are observed at δ = 1.3-1.4, which fits with the methyl groups of Boc and the NH next to Boc groups, which will lack cross-peaks. Also of interest are the four protons at position 1 and 12 (δ = 3.2-3.5) which are next to the guanidine group, as they have one cross-peak with the NH of the guanidine groups next to C1 and C12, and another cross-peak with the protons at position 2 and 11 (δ = 1.4-1.8). These results further verify the successful synthesis of the target compound.

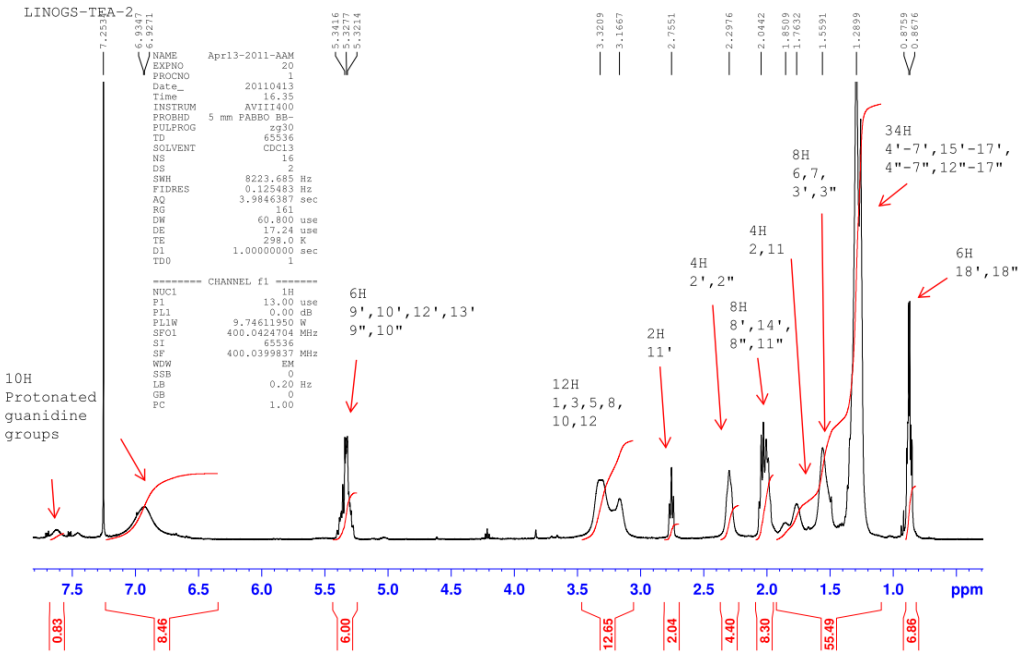

Figure 6. LinOSdiG ^{1}H-NMR.

Figure 6 shows the ^{1}H NMR assignments of LinOSdiG **4**. The most characteristic features essential to identify the target compound include: (a) the presence of the double bonds protons (6 protons at δ = 5.3, H9', H10', H12', H13', H9", H10") which correspond to the two double bonds of the linoleoyl chain and the one double bond of the oleoyl chain, as well to the 6 protons at δ = 0.9 (6H, H18', H18") representing the two terminal methyl groups of the two conjugated fatty acids, indicating the successful conjugation of the fatty acids; (b) the presence of 10 protons at δ = 6.6-7.7 which are the protonated guanidine groups protons; (c) The disappearance of the large peak at δ = 1.5 which was the peak due to methyl groups of Boc, thus indicating the successful deprotection of the guanidine; (d) 12 protons at δ = 3.1-3.4 (protons 12H, H1, H3, H5, H8, H10, and H12) which are CH_2 protons deshielded because they are next to either amide group nitrogen or guanidine group nitrogen.

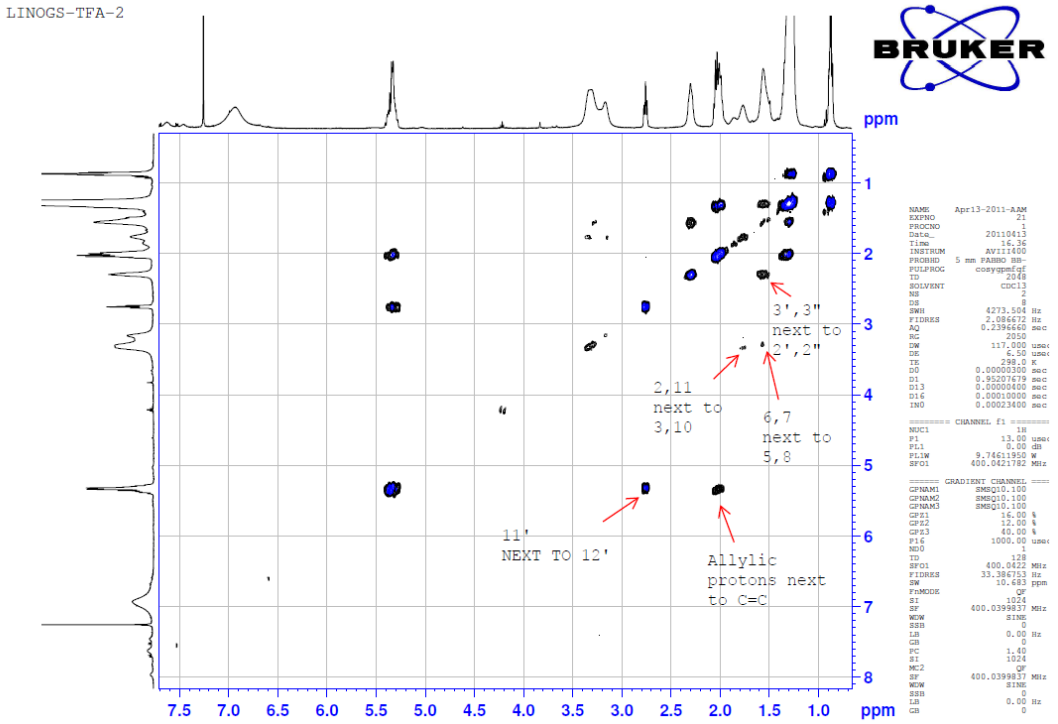

Figure 7. ^{1}H-^{1}H-NMR COSY of LinOSdiG.

Figure 7 shows the ^{1}H-^{1}H-NMR COSY of LinOSdiG. The most characteristic cross-peaks are: (a) The cross-peaks of protons H2 and H11 (δ = 1.7-1.9) with protons H3 and H10 (δ = 3.1-3.4), as well as protons H6 and H7 (δ = 1.5-1.6) with H5 and H8 (δ = 3.1-3.4). The guanidine protons (δ = 6.6-7.7) do not have any cross-peaks which is expected. The results of ^{1}H-NMR and ^{1}H-^{1}H-NMR COSY as well to the accurate HRMS obtained (m/z of $(M+H)^{+}$ = 813.7384, $C_{48}H_{93}N_8O_2$ requires $(M+H)^{+}$ 813.7416) prove LinOSdiG successful synthesis.

The four lipoguanidines will be used to investigate their efficiency and their effect on cell viability as non-viral vectors for siRNA delivery. An amidine group was attached to each of the two terminal primary amines of spermine to result in the di-guanidines (N^1,N^{12}-diamidino-amines). Three fatty acids of different chain length and saturation were used to synthesise the lipoguanidines **1**, **2**, and **3** by acylation at N^4 and N^9 of spermine. The fourth lipoguanidine LinOSdiG **4** was synthesized by acylating sequentially using two different long-chain fatty acids (linoleic and oleic) to N^4 and N^9.

The synthesis of the guanidinylated N^4,N^9-diacylated spermine conjugates started with the synthesis of the N^4,N^9-difatty acids spermine derivatives (Figure 2). The symmetrical lipospermines synthesis; i.e. those with the same fatty acid chains conjugated to positions N^4 and N^9 of the spermine chain, was carried out as described in Chapter 2. For the synthesis of the unsymmetrical N^4-linoleoyl-N^9-oleoylspermine, the primary amine groups of spermine were selectively protected with the phthalimide protecting group (2 eq. of *N*-

carbethoxyphthalimide in DCM). Then one oleoyl chain was conjugated to one of the free secondary amine groups of spermine (1 eq. oleic acid, 1 eq. DCC, and 1 eq. DMAP). Purification of the mono-acylated spermine then followed by flash chromatography. The second linoleoyl chain was added using DCC coupling of linoleic acid to the 1,12-diphthalimido-N^9-oleoyl-4,9-diazadodecane (1 eq. linoleic acid, 1 eq. DCC, and 1 eq. DMAP). Deprotection of the phthalimide protecting groups then followed by refluxing in hydrazine monohydrate in DCM/THF 1:1 mixture to obtain N^4-linoleoyl-N^9-oleoylspermine, which was purified by flash chromatography. The guanidinylation of amines typically involves an electrophilic amidine group as part of the guanidinylating reagent.[211] 1,3-Di-Boc-2-(trifluoromethylsulfonyl)guanidine was used as it can carry out the guanidinylation of primary and secondary amines under mild conditions.[211, 212] The guanidinylation was carried out on the di-acylated spermine derivatives and deprotection of the Boc protected guanidine group was carried out using TFA to obtain the trifluoroacetate salts of the synthesized compounds (Figure 3).

3.2. Lipoplex particle size and ζ-potential

The lipoplexes prepared at the cationic lipid/siNC ratios for each guanidinylated lipid which resulted in the best reduction in EGFP expression were chosen to be characterized for their particle size and **ζ**-potential (Table 1). Particle size measurement using dynamic light scattering showed that the particle size varied from 132-575 nm. The two cationic lipids **3** and **4** which are acylated with unsaturated C18 fatty acids (dioleoyl and linoleoyl/oleoyl respectively) and which showed the best reduction in EGFP expression had the particle size of 303 and 158 nm for **3** and **4** respectively. The particle size of the C22 (dierucoyl) conjugate **1** was the smallest (132 nm) while the short chain C12 (dilauroyl) conjugate **2** had the largest particle size of 575 nm. Lipoplex size has been pointed to be an important factor in transfection efficiency though not being the only determinant factor.[213] Lipoplexes within size range 200-300 nm have been previously reported.[214] Although size of lipoplexes will determine the main route of entry with smaller lipoplexes (<300 nm) likely to enter via clathrin mediated endocytosis, and larger particles (>500 nm) entering cells via caveoli mediated endocytosis,[214, 215] one recent report suggests that the actual entry route for functional siRNA mediated gene silencing is fusion with the plasma membrane rather than the endocytosis pathway.[171] The ζ-potentials measurements showed that all the lipoplexes had positive values within the range 28-50 mV. Cationic lipids **3** and **4** had the similar ζ-potential of 45 mV. Positive ζ-potential is important in promoting stability of the prepared lipoplexes by enhancing repulsion between the nanoparticles. Although having positive ζ-potential will promote interaction between the positively charged lipoplexes and the negatively charged

groups present on the cell membrane surface, it was reported that in the presence of serum, the lipoplexes actually acquire a negative ζ-potential[214] while still maintaining efficient transfection efficiency.

3.3. siRNA binding (RiboGreen intercalation assay)

An siRNA binding assay was used to evaluate the ability of the synthesized guanidinylated lipids **1**, **2**, **3**, and **4** to complex and bind siRNA. The loss of fluorescence compared to control free siNC indicates its binding to the cationic lipids and hence prevention of RiboGreen binding with siNC which leads to reduction of fluorescence compared to the control (free) siNC.[170, 216] The four cationic lipids **1**-**4** efficiently bound siNC (Table 1) and the normalised fluorescence, relative to free siNC (100%), was reduced to: 5 ± 2 (**1**), 12 ± 3 (**2**), 0 ± 1 (**3**), and 8 ± 2 (**4**). These results prove that the guanidinylated lipids are able to efficiently bind siNC.

3.4. Transfection with siRNA and evaluating delivery and knock-down

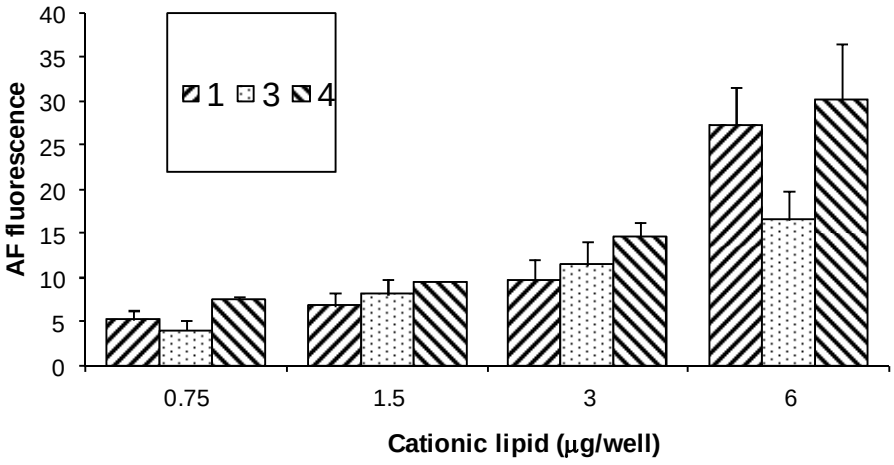

Figure 8. Delivery of siEGFP-AF (15 nM, 15 pmol/well) against EGFP (labelled with Alexa Fluor 647 at the 3'-position of the sense strand) using **1**, **3**, and **4**. Values are presented as means of normalized geometric mean fluorescence of AF647 ± SD (n = 2).

HeLa cells that stably express EGFP were used to evaluate the siEGFP-AF delivery and sequence specific knock-down of EGFP expression. The siRNA against EGFP used (siEGFP-AF) was labelled with Alexa Fluor 647 (AF647) in the 3'-position of the sense strand to enable simultaneous tracking of the siRNA delivery and reduction of EGFP expression by measuring the fluorescence of the AF647 and the EGFP during the FACS analysis. Healthy population of sample cells were gated before recording the fluorescence during FACS.

The normalized fluorescence of AF647 measured 48 h post-transfection was measured as an estimate for the delivered amount of siRNA. Figure 8 shows that, for each cationic lipid, there is a general trend of increasing fluorescence by increasing the amount of the lipid. Cationic lipid **2** data are not shown due to the very low siEGFP-AF delivery**.** With respect to **1**, **3**, and **4**, there was a significant statistical difference between the geometric mean AF647 fluorescence measured at 3 and 6 µg/well for each lipid (lipid **4** *N/P* = 10.7 and 21.4 respectively) with $p < 0.05$. There was also a significant statistical difference between the amounts of siEGFP-AF delivered (geometric mean fluorescence of AF647) by **3** and **4** ($p < 0.05$) with lipoplexes formulated at 6 µg/well (*N/P* = 21.4). There was no significant statistical difference between **1** and **4** at 6 µg/well ($p = 0.33$). These results show that given that **1**, **3**, and **4** have in common two guanidine head-groups in the form of trifluoroacetate salts, the C18 (18:1 and 18:2) unsaturated fatty acids conjugated at positions N^4 and N^9 of the parent spermine provided the optimum chain length for siEGFP-AF delivery compared to the C12 (12:0) and C22 (22:1) chains.

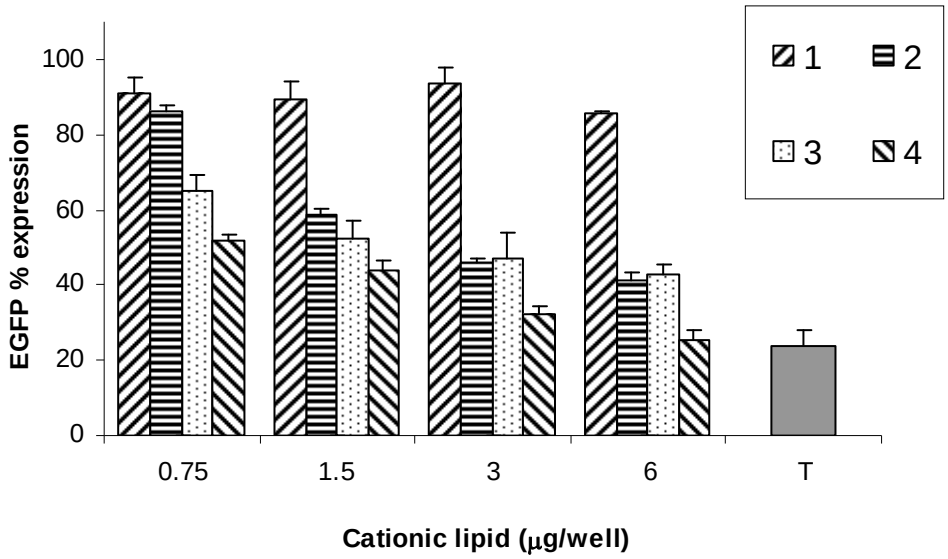

Figure 9. Reduction in EGFP expression in HeLa cells after transfection with lipoplexes of **1**, **2**, **3**, and **4** at different cationic lipid/siEGFP-AF ratios. siEGFP-AF concentration is kept constant (15 nM, 15 pmol/well). Values are presented as mean ± SD (n = 2). Commercial TransIT-TKO (T) is shown for comparison.

Figure 9 shows that the best reduction of EGFP expression was achieved by **4** followed by **3**. At 6 µg/well, EGFP expression was reduced to 26% and 43% for **4** and **3** respectively ($p < 0.05$). Lipid **1** did not show any practically significant reduction in EGFP (reduced to 85%) at 6 µg/well (*N/P* = 18.8). Lipid **2** resulted in EGFP reduction to 46% at 6 µg/well (*N/P* = 26.8), however, this reduction cannot be evaluated without considering the high toxicity of **2** which

will affect the expression of EGFP as will be discussed in this Chapter (Section 3.6). Lipids **3** and **4** with C18 (18:1 and 18:2) resulted in the best knock-down of EGFP expression which might be attributed to the fusogenic ability of unsaturated fatty acids (in *cis*-configuration) which favours (L_α to H_{II}) transition as they can promote both membrane fusion and endosomal escape.[191, 192] The chain length is an important factor that affects the efficiency of EGFP knock-down because although the C22 (22:1) has one centre of unsaturation, lipid **1** resulted in less reduction in EGFP (85%) compared to **3** (43%) and **4** (26%) with significant statistical difference between the compared means ($p < 0.05$) at 6 µg/well. The chain length affected siEGFP-AF delivery and knock-down differently, as evident from comparing the delivery of **1**, **3**, and **4** and their EGFP reduction at a concentration of 6 µg/well. Although **1** and **4** resulted in similar siEGFP-AF delivery efficiencies, lipid **4** was much better than **1** in terms of EGFP reduction (to 26% and 85% respectively). These differences in gene silencing efficiency compared with lipoplex cellular uptake reflect the multi-step processes of gene silencing and/or more than one mechanism of cell entry.[171] Also, cationic lipid **3** resulted in better EGFP reduction when compared to **1** (to 43% and 85% respectively) despite the fact that **1** resulted in higher siEGFP-AF delivery compared to **3** ($p < 0.05$). The importance of chain length and chain unsaturation of cationic lipids has been previously reported to be among the most significant factors that affect transfection efficiency because of the effect on the hydrophobic volume of lipid and its hydrophilic/lipophilic ratio which will in turn affect the properties of the formed lipoplexes.[147] When compared to the commercial transfecting agent TransIT-TKO, the reduction in EGFP expression obtained with lipoplexes of **4** (26%) was the same as that obtained with TransIT-TKO (24%), i.e. there was no significant statistical difference ($p = 0.30$).

The increases in fluorescence shown in Figure 8 reflect increase in siEGFP-AF delivery with increasing concentrations of cationic lipids in the lipoplexes up to a *N/P* ratio of 18-26 (6 µg/well). Figure 9 shows the corresponding reduction in EGFP expression. These data were obtained from gated FACS analyses of the healthy populations of HeLa cells (parent gate), representative examples of which are shown in Figure 10 together with the percentage of cells transfected. In order to evaluate siEGFP-AF delivery, the AF647 gate was set-up to include cells that have fluorescence signals higher than the auto-fluorescence of control cells detected at $\lambda_{em} = 660$ nm. The EGFP gate was set to calculate the geometric mean fluorescence of EGFP.

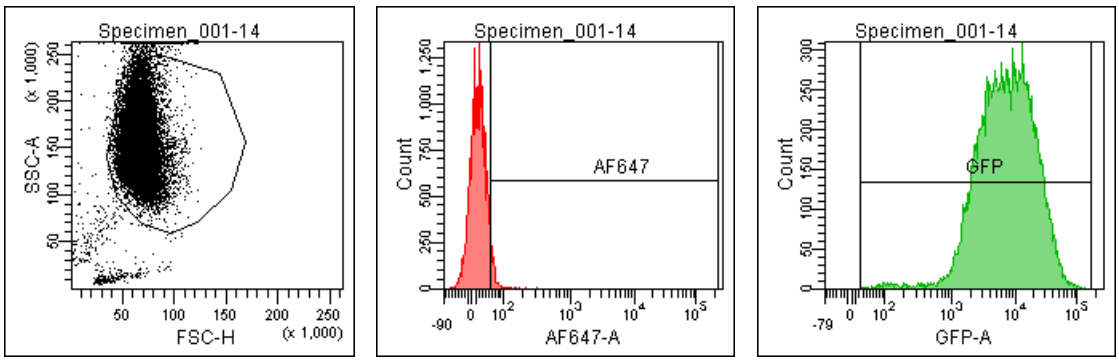

Control non-transfected HeLa cells

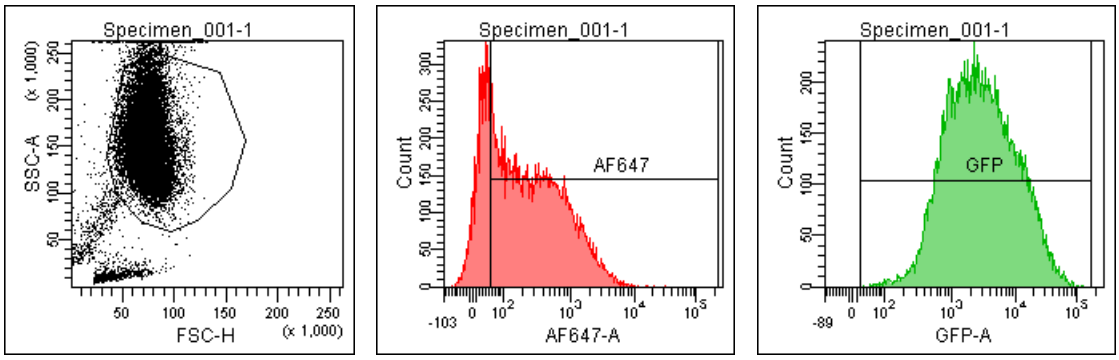

Cells transfected with siEGFP-AF lipoplexes prepared with **3**

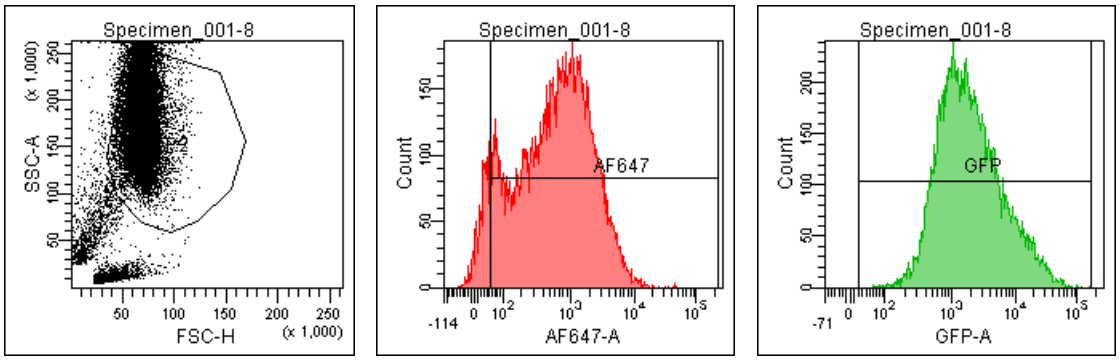

Cells transfected with siEGFP-AF lipoplexes prepared with **4**

Figure 10. Gated FACS analysis of delivery of siEGFP-AF (15 nM, 15 pmol/well) against EGFP and EGFP expression in HeLa cells 48 h post-transfection with lipoplexes of **3** and **4** (6 µg/well) at an siEGFP-AF concentration of 15 pmol/well. The AF647 gate (red) shows 75% of parent-gated cells with **3**, and 92% of parent-gated cells with **4**. The EGFP gate (green) shows silencing to ~40% and ~25% respectively measured by geometric mean fluorescence relative to control (top line).

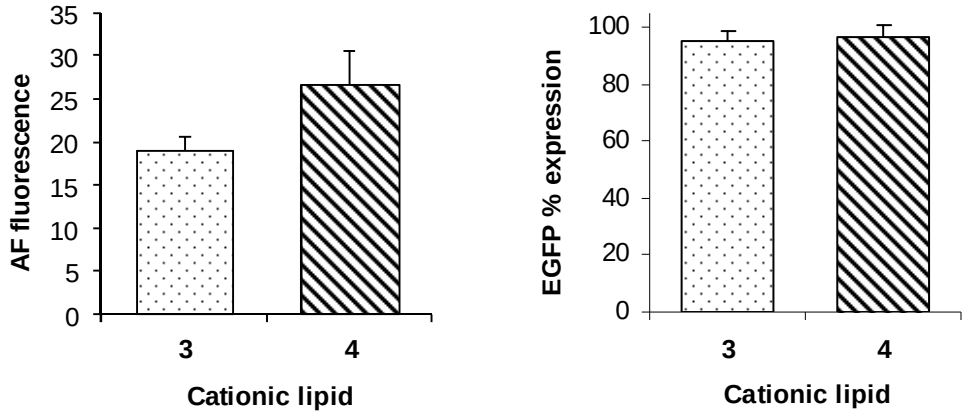

Figure 11. Scrambled AllStars siRNA (siNC-AF, 15 nM, 15 pmol/well) was delivered with cationic lipids **3** and **4** (at 6 μg/well). Delivery of tagged siNC-AF (left) is expressed as Alexa Fluor 647 normalized geometric mean fluorescence ± SD (n = 2). EGFP percentage expression (right, showing absence of silencing as a negative control) 48 h post-transfection.

The effects of transfecting HeLa cells using **3** and **4** with the scrambled siNC-AF on lipoplex delivery and EGFP expression are shown in Figure 11. Qiagen report that their scrambled siRNA lacks any homology to mammalian genes. Figure 11 shows that the EGFP expression was practically not affected by the transfection process while the scrambled siNC-AF was delivered in comparable amounts (i.e. comparable normalized fluorescence) to delivery with siEGFP-AF. Thus, cationic lipids **3** and **4** deliver two different siRNAs with similar efficiency. These results prove that EGFP reduction after transfection with siEGFP-AF (shown as averaged data in Figure 9 and as representative examples in Figure 10) is due to sequence specific gene silencing and not due to any non-specific effects of the cationic lipid vectors.

3.5. Confocal microscopy cell imaging

Figure 12 shows confocal microscope images of HeLa cells after transfection with **3** and **4** using siEGFP-AF or scrambled siRNA (siNC-AF) at 6 μg/well of cationic lipid which is the amount of lipid that resulted in the best reduction of EGFP expression with respect to each of the cationic lipids.

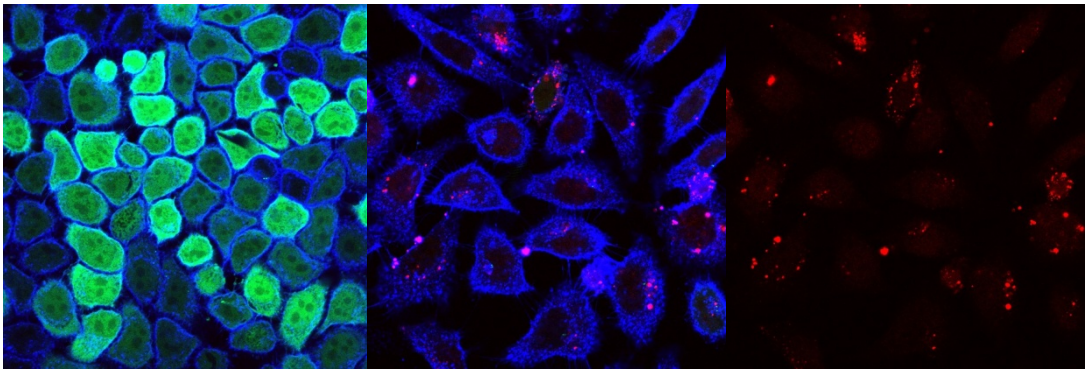

12a 12b 12c

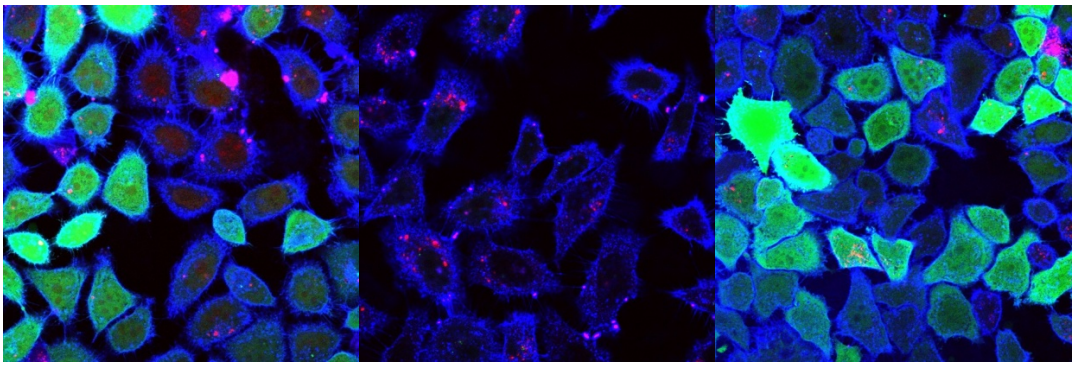

12d 12e 12f

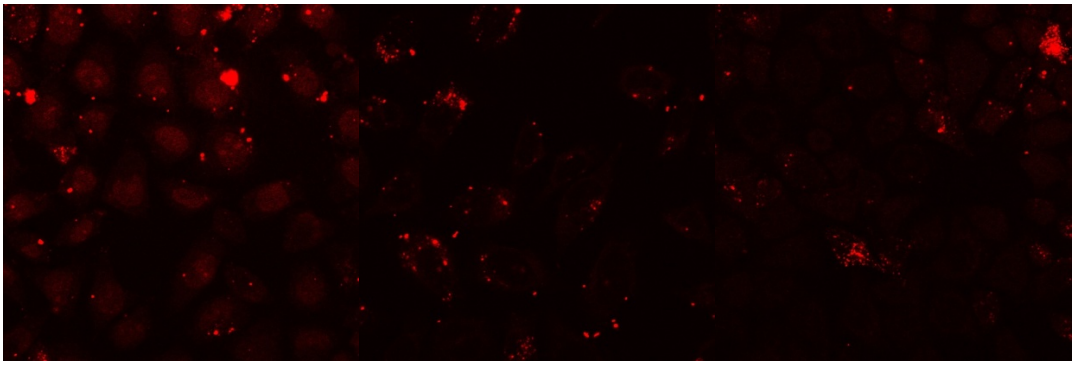

12g 12h 12i

Figure 12. Confocal microscopy cell imaging. EGFP fluorescence (green), cell membrane stained with WGA-Alexa Fluor 555 (blue), and Alexa Fluor 647 (red) represents tagged siRNA delivery. 12a: non-transfected HeLa cells (control); 12b: reduction in EGFP expression after transfection with siEGFP-AF delivered with **3** (6 µg/well); 12c: as 12b, but only the red channel; 12d: as 12b, but using the scrambled siNC-AF; 12e: reduction in EGFP expression after transfection with siEGFP-AF delivered with **4** (6 µg/well); 12f: as 12e, but using siNC-AF; 12g: as 12d, but only the red channel; 12h: as 12e, but only the red channel; 12i: as 12f, but only the red channel.

Figure 12a shows negative control HeLa cells. Figures 12b shows the reduction of EGFP expression after transfection with siEGFP-AF using **3** at 6μg/well. Figure 12c is the same as 12b, but only the red channel is turned on to track better the delivery of the AF647 labelled siEGFP-AF. It can be seen that the AF647 fluorescence (red) is distributed throughout the cell and concentrated in some cell areas. Figure 12d shows that lipoplexes of **3** did not cause reduction in EGFP expression when using siNC-AF, which was delivered to HeLa cells successfully as shown in Figure 12g. These results prove that the siEGFP-AF was delivered successfully to the HeLa cells and that the reduction in EGFP expression is due to sequence specific knock-down of EGFP and not due to any non-specified effects of the cationic lipid vectors. The same conclusion is drawn when examining the transfection of HeLa cells with **4** as shown in Figures 12e with 12h, and 12f with 12i.

3.6. Cell viability assay

Following transfection with cells seeded at a density of 65,000 cells/well in 24-well plates, i.e. 65,000 cells/1 mL (Section 3.4), cell viability was assayed in 96-well plates with 6,500 cells/0.1 mL. The ratio of number of cells to the amount of cationic lipid used (0.6 μg lipid/0.1 mL), and to siNC (15 nM, 1.5 pmol/well) was exactly the same as the ratio used in the transfection experiments in 24-well formats. Figure 13 shows that **1**, **3**, and **4** resulted in more than 64% cell viability. There were no statistical significant difference between the cell viability of **3** and **4** ($p = 0.32$) with cell viabilities of 70% and 64% respectively. The best cell viability obtained by **1** (83%) was significantly different ($p < 0.05$) from the cell viability of **3** and **4**. Whilst diacylated C12 (12:0) **2** is a new compound, the very high toxicity of its parent diamine, N^4,N^9-dilauroylspermine, has been previously reported in both HtTA cells[182] and HeLa cells (Chapter 2) with scrambled siRNA. There were no significant differences between cell viability of TransIT-TKO (76%) and **3** (64%), $p = 0.12$, or between TransIT-TKO and **4** (70%), $p = 0.41$. There is a probability that the counter ion, trifluoroacetate in this case, has a contributing negative effect on cell viability as been reported before[217] where the presence of residual TFA in the concentration range 10^{-8} to 10^{-7} M resulted in reduction of cell proliferation of osteoblasts , chondrocytes (mature cells found in cartilage), and neonatal mice calvariae (bone organ culture).

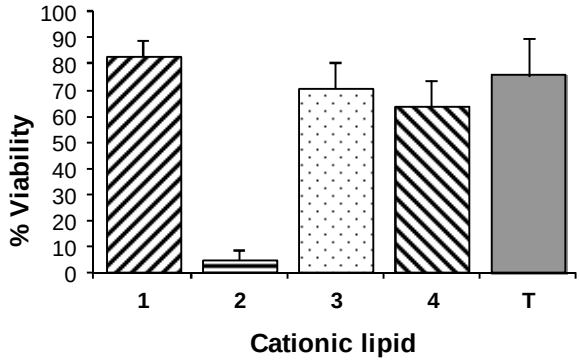

Figure 13. Comparison of cell viability of HeLa cells after transfection with lipoplexes at their optimal cationic lipid/siNC ratios and compared with the commercially available transfection agent TransIT-TKO (T). Values are presented as mean ± SD (n = 2). Experiments were carried out at: 0.6 μg/well synthesized cationic lipids, 1.5 pmol siRNA/well (15 nM), and 6,500 cells/well.

4. Conclusions

The four synthesized diguanidinylated diacylated spermine-based cationic lipids were able to bind siRNA efficiently and to form particles with sizes in the nanometre range (132-575 nm). Saturated shorter chain (C12:0) **2** showed relatively high toxicity when compared with the longer chain (C18-C22) N^1,N^{12}-diamidino-N^4,N^9-diacylated spermine derivatives. Transfection with self-assembled siRNA lipoplexes of **3** and **4** resulted in the sequence specific knock-down of EGFP in HeLa cells, exhibiting comparable (low) toxicity to the commercial transfecting agent TransIT-TKO. Lipid **4** with one linoleoyl and one oleoyl chains acylated on positions N^4 and N^9 respectively of the N^1,N^{12}-diamidinospermine was the best transfecting agent. Lipoplexes of lipid **4** showed the same efficiency, in HeLa cells, in terms of reduction of EGFP expression as TransIT-TKO.

In this Chapter, the synthesis of four novel spermine-derived fatty acid amide guanidines applied to the self-assembly of siRNA lipoplexes which were then tested in EGFP expressing HeLa cells was described. The major endpoints include detection of siRNA complexation in the lipoplexes, cellular uptake, toxicity, and gene silencing efficiency even in the presence of serum. This is a structure-activity relationship (SAR) study of the cationic head-groups, the two primary amine groups of spermine were transformed to guanidine groups. To investigate further the SAR regarding the two acylated fatty acids of lipospermines, a series of asymmetrical N^4,N^9-diacylated spermine conjugates will be synthesized and evaluated in Chapter 4.

Chapter Four Efficient silencing of EGFP reporter gene with siRNA delivered by asymmetrical N^4,N^9-diacyl spermines

1. Introduction

Since being introduced as non-viral gene delivery vectors in 1987 by Felgner and co-workers,[124] cationic lipids have been widely studied as non-viral gene and siRNA vectors.[160, 196, 218] The majority of phospholipids in mammalian cell membranes are acylated with two different fatty acids at the *sn*-1 and *sn*-2 positions of the glycerol 3-phosphate.[219-223] In this Chapter, the design and synthesis of seven new N^4,N^9-diacylated asymmetrical spermine derivatives is reported. The asymmetry is in that they contain two different fatty acid chains per spermine residue. The fatty acids are different either in chain length (from C18 to C24) and/or in their oxidation state. All seven target compounds have one chain (oleoyl) held constant while the other fatty acid chain is varied. This is based on the efficiency of the symmetrical DOS in gene silencing which has been established in Chapter 2. The cationic group is chosen to be the primary amine. These novel asymmetrical polyamine amides are structurally similar to the naturally occurring diacyl lipids that form lipid cellular membranes, as the majority of the latter lipids are asymmetrical.[219-223] Using the two positive charges from the terminal primary amino groups (at the physiological pH 7.4), they are rationally designed to form nanoparticles with polynucleotides (e.g. siRNA) by electrostatically binding the negatively charged siRNA in aqueous buffered media, and without any pre-formulation steps to form liposomes prior to lipoplex formation. This process occurs by the simple mixing of the cationic lipids with the polyanionic siRNA enabling the self-assembly of the lipoplexes. The asymmetry of the fatty acid chains in these spermine conjugates is hypothesized to enhance the efficiency of interaction with the cell membrane phospholipids, leading to better mixing or fusion with the membrane lipids, and hence enhancing the siRNA delivery and/or gene silencing. Such enhancement was reported previously for DNA lipoplexes with asymmetrical lipid components.[153]

The synthesized compounds will be used in SAR studies of siRNA delivery and EGFP silencing in HeLa cells. Investigating the siRNA delivery and EGFP silencing with selected mixtures of symmetrical spermine conjugates is carried out, and compared to the delivery and silencing efficiency resulting from using the asymmetrical conjugates which has the same type of fatty acids as that in the mixture spermine conjugates, i.e. investigating whether the transfection properties of asymmetrical vectors are due to merely using two different types of fatty acids regardless of the molecular structure, or the asymmetry itself affects transfection.

2. Materials and methods

2.1. Materials and general methods

All solvents and chemicals were purchased as described in Chapter 2 (Section 2.1). All general procedures for preparing anhydrous solvents and purification and characterization of the target compounds were carried out as described in Chapter 2 (Section 2.1).

2.2. Synthesis of N^4,N^9-diacylated spermines

1,12-Diphthalimido-4,9-diazadodecane.

To a solution of 1,12-diamino-4,9-diazadodecane (spermine) (2.02 g, 10 mmol) in DCM (30 mL) *N*-carbethoxyphthalimide (4.38 g, 20 mmol) was added. The solution was stirred at 20 °C for 3 h then evaporated to dryness in vacuo. The residue was purified over silica gel (DCM/MeOH 10:1 then 2:1 v/v) to afford the title compound (2.13 g, 46%). ^{1}H NMR, 1.2-1.4 (m, 4H, H6, H7), 1.4-1.7 (m, 6H, H2, H11, 2 x NH), 2.4-2.5 (m, 8H, H3, H5, H8, H10), 3.6 (m, 4H, H1, H12), 7.5-7.7 (m, 8H, aromatic protons). ^{13}C NMR, 27.1 (C6, C7), 28.2 (C2, C11), 35.5 (C1, C12), 46.3 (C3, C5, C8, C10), 122.7 and 133.6 (aromatic carbons), 168.1 (C=O). HRMS, found $(M+H)^+$ 463.2354, $C_{26}H_{31}N_4O_4$ requires $(M+H)^+$ 463.2340. Often, for the synthesis of the following target molecules, the purification of 1,12-diphthalimido-4,9-diazadodecane can be skipped and the crude product taken on directly into the acylation.

N^4,N^9-Dioleoyl-1,12-diamino-4,9-diazadodecane (DOS).

To a solution of 1,12-diphthalimido-4,9-diazadodecane (2.31 g, 5 mmol) in DCM (30 mL) and TEA (1.4 mL, 10 mmol) oleoyl chloride (3.3 mL, 10 mmol) was added. The solution was stirred for 18 h at 20 °C and then the solvent was evaporated to dryness in vacuo. The residue was reacted with hydrazine monohydrate (2 mL) in a mixture of DCM (15 mL) and THF (15 mL) and heated under reflux for 4 h, cooled to 20 °C, and then the solvent was evaporated in vacuo. The residue was purified over silica gel (DCM/MeOH 10:1 v/v then DCM/MeOH/NH_4OH 10:5:1 v/v/v) to afford the title compound (1.46 g, 40% over two steps). ^{1}H NMR, 0.8 (t, *J* = 7, 6H, H18'), 1.2-1.3 (m, 40H, H4'-H7', H12'-H17'), 1.4-1.8 (m, 12H, H2, H6, H7, H11, H3'), 1.9-2.1 (m, 8H, H8', H11'), 2.1-2.3 (m, 4H, H2'), 2.6-2.8 (m, 8H, H1, H12, 2 x NH_2), 3.2-3.5 (m, 8H, H3, H5, H8, H10), 5.3-5.4 (m, 4H, H9', H10'). ^{13}C NMR, 14.1 (C18'), 22.6-29.7 (C2, C6, C7, C11, C4'-C8', C11'-C17'), 31.9 (C3'), 33.1 (C2'), 38.9-39.2 (C1, C12), 42.5-47.4 (C3, C5, C8, C10), 129.8 (C9', C10'), 172.9 (C1'). HRMS, found $(M+H)^+$ 731.7162, $C_{46}H_{91}N_4O_2$ requires $(M+H)^+$ 731.7137.

N^4,N^9-Dierucoyl-1,12-diamino-4,9-diazadodecane (DEruS).

To a solution of 1,12-diphthalimido-4,9-diazadodecane (0.46 g, 1 mmol) in DCM (30 mL) erucic acid (0.68 g, 2 mmol), DMAP (0.24 g, 2 mmol), and DCC (0.40 g, 2 mmol) were added. The solution was stirred at 20 °C for 18 h under an atmosphere of nitrogen, then filtered and the filtrate was evaporated to dryness in vacuo. The residue was reacted with hydrazine monohydrate (2 mL) in a mixture of DCM (15 mL) and THF (15 mL) and heated under reflux for 4 h, cooled to 20 °C, and then the solvent was evaporated in vacuo. The residue was purified over silica gel (DCM/MeOH 10:1 v/v then DCM/MeOH/NH_4OH 20:10:1 v/v/v) to afford the title compound (0.34 g, 40% over two steps). ^{1}H NMR, 0.8 (t, J = 7, 6H, H22'), 1.1-1.3 (m, 60H, H4'-H11', H16'-H21', 2 x NH_2), 1.4-1.6 (m, 12H, H2, H6, H7, H11, H3'), 1.9 (m, 8H, H12'-H15'), 2.2-2.4 (m, 4H, H2'), 2.5-2.7 (m, 4H, H1, H12), 3.2-3.6 (m, 8H, H3, H5, H8, H10), 5.2 (m, 4H, H13', H14'). ^{13}C NMR, 14.0 (C22'), 22.6 (C21'), 25.1-32.8 (C2, C6, C7, C11, C3'-C12', C15'-C20'), 33.1 (C2'), 39.2-39.4 (C1, C12), 42.6-47.4 (C3, C5, C8, C10), 129.8 (C13', C14'), 172.8-173.0 (C1'). HRMS, found $(M+H)^+$ 843.8364, $C_{54}H_{107}N_4O_2$ requires $(M+H)^+$ 843.8389; found $(M+Na)^+$ 865.8194, $C_{54}H_{106}N_4O_2Na$ requires $(M+Na)^+$ 865.8208.

N^4,N^9-Dilinoleoyl-1,12-diamino-4,9-diazadodecane (DLinS).

To a solution of 1,12-diphthalimido-4,9-diazadodecane (0.46 g, 1 mmol) in DCM (30 mL) linoleic acid (0.56 g, 2 mmol), DMAP (0.24 g, 2 mmol), and DCC (0.40 g, 2 mmol) were added. The solution was stirred at 20 °C for 18 h under an atmosphere of nitrogen, then filtered and the filtrate was evaporated to dryness in vacuo. The residue was reacted with hydrazine monohydrate (2 mL) in a mixture of DCM (15 mL) and THF (15 mL) and heated under reflux for 4 h, cooled to 20 °C, and then the solvent was evaporated in vacuo and the residue purified over silica gel (DCM/MeOH 10:1 v/v then DCM/MeOH/NH_4OH 20:10:1 v/v/v) to afford the title compound (0.29 g, 40% over two steps). ^{1}H NMR, 0.8 (t, J = 7, 6H, H18'), 1.2-1.3 (m, 28H, H4'-H7', H15'-H17'), 1.4-1.8 (m, 16H, H2, H6, H7, H11, H3', 2 x NH_2), 1.9-2.0 (m, 8H, H8', H14'), 2.0-2.3 (m, 4H, H2'), 2.5-2.7 (m, 8H, H1, H12, H11'), 3.2-3.4 (m, 8H, H3, H5, H8, H10), 5.2-5.3 (m, 8H, H9', H10', H12', H13'). ^{13}C NMR, 14.0 (C18'), 22.4 (C17'), 25.0-33.0 (C2, C6, C7, C11, C2'-C8', C11', C14'-C16'), 39.0-39.3 (C1, C12), 42.4-47.6 (C3, C5, C8, C10), 127.8-130.0 (C9', C10', C12', C13'), 172.7-173.0 (C1'). HRMS, found $(M+H)^+$ 727.6851, $C_{46}H_{87}N_4O_2$ requires $(M+H)^+$ 727.6824.

1,12-Diphthalimido-N^4-oleoyl-4,9-diazadodecane.

To a solution of 1,12-diphthalimido-4,9-diazadodecane (2.31 g, 5 mmol) in DCM (30 mL) oleic acid (1.6 mL, 5 mmol), DMAP (610 mg, 5 mmol), and DCC (1.03 g, 5 mmol) were

added. The solution was stirred at 20 °C for 20 h then filtered and the filtrate was evaporated to dryness in vacuo. The residue was purified over silica gel (DCM/MeOH 20:1 v/v) to afford the title compound (1.34 g, 37%). ^{1}H NMR, 0.9 (t, *J* = 7, 3H, H18'), 1.3 (m, 20H, H4'-H7', H12'-H17'), 1.5-1.6 (m, 8H, H6, H7, H11, H3'), 1.9-2.0 (m, 7H, H2, H8', H11', 1 x NH), 2.1-2.3 (m, 2H, H2'), 2.7-2.8 (m, 4H, H8, H10), 3.2-3.5 (m, 4H, H3, H5), 3.6-3.8 (m, 4H, H1, H12), 5.3 (m, 2H, H9', H10'), 7.7-7.8 (m, 8H, aromatic). ^{13}C NMR, 14.1 (C18'), 22.6 (C17'), 25.1-31.8 (C2, C6, C7, C11, C3'-C8', C11'-C16'), 33.1 (C2'), 35.3-35.9 (C1, C12), 45.2-50.6 (C3, C5, C8, C10), 123.1-123.3 and 131.8-134.1 (aromatic carbons), 129.7-129.9 (C9', C10'), 168.2-168.4 (C=O phthalimide), 173.0 (C1'). HRMS, found $(M+H)^+$ 727.4774, $C_{44}H_{63}N_4O_5$ requires $(M+H)^+$ 727.4793.

N^4-Linoleoyl-N^9-oleoyl-1,12-diamino-4,9-diazadodecane (LinOS).

To a solution of 1,12-diphthalimido-N^4-oleoyl-4,9-diazadodecane (0.72 g, 1 mmol) and TEA (0.14 mL, 1 mmol) in DCM (30 mL) linoleoyl chloride (0.33 mL, 1 mmol) was added. The solution was stirred at 20 °C for 18 h then the solvent was evaporated to dryness in vacuo. The residue was reacted with hydrazine monohydrate (2 mL) in a mixture of DCM (15 mL) and THF (15 mL) and heated under reflux for 4 h, cooled to 20 °C, and then the solvent was evaporated in vacuo. The residue was purified over silica gel (DCM/MeOH 10:1 v/v then DCM/MeOH/NH_4OH 10:5:1 v/v/v) to afford the title compound (0.27 g, 37% over two steps). ^{1}H NMR, 0.9 (t, *J* = 7, 6H, H18', H18''), 1.2-1.4 (m, 34H, H4'-H7', H15'-H17', H4''-H7'', H12''-H17''), 1.4-1.7 (m, 12H, H2, H6, H7, H11, H3', H3''), 1.8-2.0 (m, 12H, H8', H14', H8'', H11'', 2 x NH_2), 2.0-2.3 (m, 4H, 2', 2''), 2.6-2.8 (m, 6H, H1, H12, H11'), 3.2-3.4 (m, 8H, H3, H5, H8, H10), 5.3 (m, 6H, H9', H10', H12', H13', H9'', H10''). ^{13}C NMR, 14.0 (C18', C18''), 22.4 (C17', C17''), 25.0-26.8 (C2, C6, C7, C11, C11') , 27.1-27.2 (8', 14', 8'', 11'') , 29.1-29.6 (4'-7', 15'-17', 4''-7'', 12''-17''), 30.9-32.9 (C3', C16', C3'', C16''), 33.0-36.7 (C2', C2''), 38.9-39.3 (C1, C12), 42.4-47.6 (C3, C5, C8, C10), 127.8-130.0 (C9', C10', C12', C13', C9'', C10''), 172.7-173.0 (C1', C1''). HRMS, found $(M+H)^+$ 729.6980, $C_{46}H_{89}N_4O_2$ requires $(M+H)^+$ 729.6986.

N^4-Oleoyl-N^9-stearoyl-1,12-diamino-4,9-diazadodecane (OSS).

To a solution of 1,12-diphthalimido-N^4-oleoyl-4,9-diazadodecane (0.72 g, 1 mmol) and TEA (0.14 mL, 1 mmol) in DCM (30 mL) stearoyl chloride (0.34 mL, 1 mmol) was added. The solution was stirred at 20 °C for 18 h then the solvent evaporated to dryness in vacuo. The residue was reacted with hydrazine monohydrate (2 mL) in a mixture of DCM (15 mL) and THF (15 mL) and heated under reflux for 4 h, cooled to 20 °C, and then the solvent was evaporated in vacuo. The residue was purified over silica gel (DCM/MeOH 10:1 v/v then

DCM/MeOH/NH_4OH 10:5:1 v/v/v) to afford the title compound (0.31 g, 43% over two steps). ^{1}H NMR, 0.8 (t, *J* = 7, 6H, H18', H18''), 1.2-1.4 (m, 48H, H4'-H7', H12'-H17', H4''-H17''), 1.4-1.8 (m, 16H, H2, H6, H7, H11, H3', H3'', 2 x NH_2), 1.9-2.0 (m, 4H, H8', H11'), 2.1-2.3 (m, 4H, H2', H2''), 2.6-2.8 (m, 4H, H1, H12), 3.2–3.4 (m, 8H, H3, H5, H8, H10), 5.3 (m, 2H, H9', H10'). ^{13}C NMR, 14.3 (C18', C18''), 22.9 (C17', C17''), 25.4-29.6 (C2, C6, C7, C11, C4'-C8', C11'-C15', C4''-C15''), 31.4, 32.9 (C3', C3''), 32.1 (C16', C16''), 33.3 (C2', C2''), 39.4 (C1, C12), 42.7-47.6 (C3, C5, C8, C10), 130.0 (C9', C10'), 173.1 (C1', C1''). HRMS, found $(M+Na)^+$ 755.7112, $C_{46}H_{92}N_4O_2Na$ requires $(M+Na)^+$ 755.7118.

General Procedure for the synthesis of asymmetrical acyl spermine derivatives using DCC coupling. The required carboxylic acid (1 mmol), DMAP (122 mg, 1 mmol), and DCC (206 mg, 1 mmol) were added to a solution of 1,12-diphthalimido-N^4-oleoyl-4,9-diazadodecane (726 mg, 1 mmol) in DCM (15 mL). The solution was stirred at 20 °C for 20 h then filtered and the filtrate was evaporated to dryness in vacuo. The residue was reacted with hydrazine monohydrate (2 mL) in a mixture of DCM (10 mL) and THF (10 mL) and heated under reflux for 4 h, cooled to 20 °C, and then the solvent was evaporated in vacuo. The residue was purified over silica gel (DCM/MeOH 10:1 v/v then DCM/MeOH/NH_4OH 100:10:1 v/v/v) to afford the title compound.

N^4-Arachidonoyl-N^9-oleoyl-1,12-diamino-4,9-diazadodecane (AOS).

According to the General Procedure, arachidonic acid (304 mg, 1 mmol) was reacted to afford the title compound (301 mg, 40% over two steps). ^{1}H NMR, 0.9 (m, 6H, *J* = 7, H20', H18''), 1.2-1.8 (m, 42H, H2, H6, H7, H11, H3', H17'-H19', H3''-H7'', H12''-H17'', 2 x NH_2), 2.0-2.2 (m, 8H, H4', H16', H8'', H11''), 2.2-2.4 (m, 4H, 2', 2''), 2.6-2.8 (m, 10H, H1, H12, H7', H10', H13'), 3.2-3.4 (m, 8H, H3, H5, H8, H10), 5.3-5.4 (m, 10H, H5', H6', H8', H9', H11', H12', H14', H15', H9'', H10''). ^{13}C NMR, 14.1 (C20', C18''), 22.5-22.6 (C19', C17''), 25.3-27.2 (C4', C7', C10', C13', C16', C8'', C11''), 29.2-32.7 (C2, C6, C7, C11, C3', C17', C18', C3''-C7'', C12''-C16''), 33.1 (C2', C2''), 39.0-39.4 (C1, C12); 42.5-47.3 (C3, C5, C8, C10), 127.5-130.5 (C5', C6', C8', C9', C11', C12', C14', C15', C9'', C10''), 172.6-172.8 (C1', C1''). HRMS, found $(M+H)^+$ 753.6982, $C_{48}H_{89}N_4O_2$ requires $(M+H)^+$ 753.6980.

N^4-Eicosenoyl-N^9-oleoyl-1,12-diamino-4,9-diazadodecane (EicOS).

According to the General Procedure, eicosenoic acid (310 mg, 1 mmol) was reacted to afford the title compound (273 mg, 36% over two steps). ^{1}H NMR, 0.9 (t, *J* = 7, 6H, H20', H18''), 1.2-1.3 (m, 44H, H4'-H9', H14'-H19', H4''-H7'', H12''-H17''), 1.4-1.8 (m, 12H, H2, H6, H7, H11, H3', H3''), 2.0 (m, 8H, H10', H13', H8'', H11''), 2.2-2.4 (m, 8H, H2', H2'', 2 x

NH_2), 2.6-2.8 (m, 4H, H1, H12), 3.2-3.45 (m, 8H, H3, H5, H8, H10), 5.3-5.4 (m, 4H, H11', H12', H9'', H10''). ^{13}C NMR, 14.1 (C20', C18''), 22.7 (C19', C17''), 25.1-32.6 (C2, C6, C7, C11, C3'-C10', C13'-C18', C3''-C8'', C11''-C16''), 33.1 (C2', C2''), 38.8-39.4 (C1, C12), 42.5-47.5 (C3, C5, C8, C10), 129.8 (C11', C12', C9'', C10''), 172.9-173.4 (C1', C1''). HRMS, found $(M+H)^+$ 759.7450, $C_{48}H_{95}N_4O_2$ requires $(M+H)^+$ 759.7455.

N^4-Erucoyl-N^9-oleoyl-1,12-diamino-4,9-diazadodecane (EruOS).

According to the General Procedure, erucic acid (339 mg, 1 mmol) was reacted to afford the title compound (268 mg, 34% over two steps). ^{1}H NMR, 0.9 (t, *J* = 7, 6H, H22', H18''), 1.2-1.4 (m, 48H, H4'-H11', H16'-H21', H4''-H7'', H12''-H17''), 1.4-1.7 (m, 16H, H2, H6, H7, H11, H3', H3'', 2 x NH_2), 2.0 (m, 8H, H12', H15', H8'', H11''), 2.3 (m, 4H, H2', H2''), 2.8 (m, 4H, H1, H12), 3.2-3.4 (m, 8H, H3, H5, H8, H10), 5.3 (m, 4H, H13', H14', H9'', H10''). ^{13}C NMR, 14.1 (C22', C18''), 22.6 (C21', C17''), 25.1-27.2 (C2, C6, C7, C11, C12', C15', C8'', C11''), 29.1-32.7 (C3'-C11', C16'-C20', C3''-C7'', C12''-C16''), 33.1 (C2', C2''), 39.1-39.4 (C1, C12), 42.4-47.3 (C3, C5, C8, C10), 129.7-129.9 (C13', C14', C9'', C10''), 172.8-173.0 (C1', C1''). HRMS, found $(M+H)^+$ 787.7763, $C_{50}H_{99}N_4O_2$ requires $(M+H)^+$ 787.7768.

N^4-Lignoceroyl-N^9-oleoyl-1,12-diamino-4,9-diazadodecane (LigOS).

According to the General Procedure, lignoceric acid (369 mg, 1 mmol) was reacted to afford the title compound (310 mg, 38% over two steps). ^{1}H NMR, 0.9 (t, *J* = 7, 6H, H24', H18''), 1.2-1.4 (m, 64H H4'-H23', H4''-H7'', H12''-H17'', 2 x NH_2), 1.4-1.7 (m, 12H, H2, H6, H7, H11, H3', H3''), 2.0 (m, 4H, H8'', H11''), 2.2-2.3 (m, 4H, 4H, H2', H2''), 2.6-2.8 (m, 4H, H1, H12), 3.2-3.4 (m, 8H, H3, H5, H8, H10), 5.3 (m, 2H, H9'', H10''). ^{13}C NMR, 14.1 (C24', C18''), 22.6 (C23', C17''), 25.1-27.2 (C2, C6, C7, C11, C8'', C11''), 29.2-32.7 (3'-22', 3''-7'', 12''-16''), 33.1 (C2', C2''), 39.2-39.4 (C1, C12), 42.5-47.3 (C3, C5, C8, C10), 129.7-129.9 (C9'', C10''), 172.8-173.0 (C1', C1''). HRMS, found $(M+H)^+$ 817.8232, $C_{52}H_{105}N_4O_2$ requires $(M+H)^+$ 817.8238.

N^4-Nervonoyl-N^9-oleoyl-1,12-diamino-4,9-diazadodecane (NOS).

According to the General Procedure, nervonic acid (367 mg, 1 mmol) was reacted to afford the title compound (302 mg, 37% over two steps). ^{1}H NMR, 0.9 (t, *J* = 7, 6H, H24', H18''), 1.2-1.4 (m, 52H, H4'-H13', H18'-H23', H4''-H7'', H12''-H17''), 1.4-1.8 (m, 12H, H2, H6, H7, H11, H3', H3''), 2.0 (m, 8H, H14', H17', H8'', H11''), 2.2-2.4 (m, 4H, H2', H2''), 2.6-2.8 (m, 4H, H1, H12), 3.2-3.4 (m, 12H, H3, H5, H8, H11, 2 x NH_2), 5.3 (m, 4H, H15', H16', H9'', H10''). ^{13}C NMR, 14.1 (C24', C18''), 22.6 (C23', C17''), 25.5-27.2 (C2, C6, C7, C11, C14', C17', C8'', C11''), 29.1-32.8 (C3'-C13', C18'-C22', C3''-C7'', C12''-C16''), 33.1 (C2', C2''),

39.0-39.5 (C1, C12), 42.5-47.6 (C3, C5, C8, C10), 129.8 (C15', C16', C9'', C10''), 172.7-172.8 (C1', C1''). HRMS, found $(M+H)^+$ 815.8076, $C_{52}H_{103}N_4O_2$ requires $(M+H)^+$ 815.8081.

2.3. Transfection studies of HeLa cells stably expressing EGFP

On the day of transfection, cells were trypsinized (0.25% trypsin, 3-4 min) at a confluency of 80-90% and were counted under inverted light microscope by means of haemocytometer using trypan blue (0.4%) to exclude the dead cells, then seeded at a density of 100,000 cells/well in 24-well plates. The lipoplexes were prepared by mixing the specified amounts of the transfection reagent in Opti-MEM serum-free medium (50 μL) with siRNA (15 μL, 1 μM working solution) in Opti-MEM serum-free medium. Lipofectamine 2000 (2 μL/well) and TransIT-TKO (4 μL/well) were used in accordance with the manufacturers' instructions, both were used in the presence of 10% FCS. The solutions were vortex-mixed for 2-3 s, and added to wells containing DMEM (10% FCS, and without G418), within 0.5 h of seeding, to make the final volume in each well 1 mL (siRNA final concentration 15 nM). The plates were then incubated for 48 h at 37 °C in 5% CO_2. *N/P* ratios (defined as the ratio of cationic lipid ammonium ions to RNA phosphate anions) were calculated as:

$$N/P = \frac{number\ of\ moles\ of\ cationic lipid \times 2.0}{number\ of\ \ moles\ of\ \ siRNA \times total\, number\ of\ \ phosphates\ in\ ds\, siRNA}$$

2.4. Cell viability assay

HeLa cells were trypsinized (0.25% trypsin, 3-4 min) at a confluency of 80-90% and counted under inverted light microscope by means of haemocytometer using trypan blue (0.4%) to exclude the dead cells, then seeded at a density of either 6,500 (transfection after 24 h) or 4,000 (transfection after 0.5 h) cells per well of 96-well plates. The transfection was carried out using the same protocol as transfecting the 24-well plates with the exception of reducing the amount of lipoplexes such that each well contains 1.5 pmol siRNA in a final volume of 100 μL/well of DMEM containing 10% FCS. After incubation for 44 h at 37 °C in 5% CO_2, alamarBlue (10 μL) was added to each well. After incubation for 3.5 h at 37 °C in 5% CO_2, the absorbance of each well was measured at 570 nm and 600 nm using a microplate-reader (VERSAmax), and the calculation of the amount of alamarBlue reduced measured at 570 nm was carried out according to the standard protocol provided by the alamarBlue supplier (Invitrogen). Percentage viability was calculated as:

$$\%\, viability = \frac{amount\ \ reduced\ \ of\ \ alamarBlue\ of\ \ sample cells}{amount\ \ reduced\ \ of\ \ alamarBlue\ of\ \ control\, cells} \times 100$$

2.5. Experimental Protocols

Flow cytometry *(*FACS analysis) was carried out as described above in Chapter 2 (Section 2.5). Confocal microscopy cell imaging was carried out as described in Chapter 2 (Section 2.6). Particle size and ζ-potential measurements were carried out as described in Chapter 2 (Section 2.8). siRNA binding *(RiboGreen intercalation assay)* was carried out as described in Chapter 2 (Section 2.9). Statistical analysis was carried out as described in Chapter 2 (Section 2.10).

3. Results and discussion

Spermine (1,12-diamino-4,9-diazadodecane or *N,N′*-bis(3-aminopropyl)-1,4-diaminobutane) has two terminal primary amine groups at carbons 1 and 12, and two secondary amine groups with their nitrogen atoms numbered 4 and 9. In order to conjugate two different fatty acids at the N^4 and N^9 positions, first, the two terminal primary amines were protected with phthalimide, then one fatty acid (oleic, 18:1) was acylated on position N^4 using oleic acid/DCC/DMAP to conjugate in a 1:1 stoichiometry with an oleoyl chain (Figure 1). The purified mono-acylated product, 1,12-diphthalimido-N^4-oleoyl-4,9-diazadodecane, was then conjugated with the second long-chain fatty acid using DCC/DMAP or acid chloride/TEA. This method avoids using orthogonal protection of the primary and secondary amino groups with different protecting groups (e.g. phthalimide for the primary amines and then Boc for the secondary amines) and hence the target products were obtained in fewer reactions. Keeping one fatty acid chain constant as oleic acid (18:1), the free secondary amine group of 1,12-diphthalimido-N^4-oleoyl-4,9-diazadodecane was acylated with: arachidonic (20:4), eicosenoic (20:1), erucic (22:1), lignoceric (24:0), linoleic (18:2), nervonic (24:1), and stearic (18:0) acids. Whilst all the other molecules are named with the oleoyl group at N^9, N^4-oleoyl-N^9-stearoyl-1,12-diamino-4,9-diazadodecane (OSS) is named as such to reflect the alphabetical order of oleoyl-stearoyl (IUPAC nomenclature), but this does not alter the relative structures within the diacylated-spermine series. Thus, seven asymmetrical spermine derivatives were synthesised (Figure 2), purified to homogeneity, and then characterized by NMR and HRMS. All of the spermine fatty acid conjugates in this Chapter were obtained as the free bases.

Spermine requires orthogonal protection to synthesize unsymmetrical N^4,N^9-diacylated lipospermines. One approach is to protect the primary amine functional groups as phthalimides, followed by Boc protection of only one secondary amine (by using 1.0 eq). HRMS, found $(M+H)^+$ 563.2853, $C_{31}H_{39}N_4O_6$ requires $(M+H)^+$ 563.2864. The first fatty acid could be introduced by DCC/DMAP coupling to the free secondary amine (Figure 1).

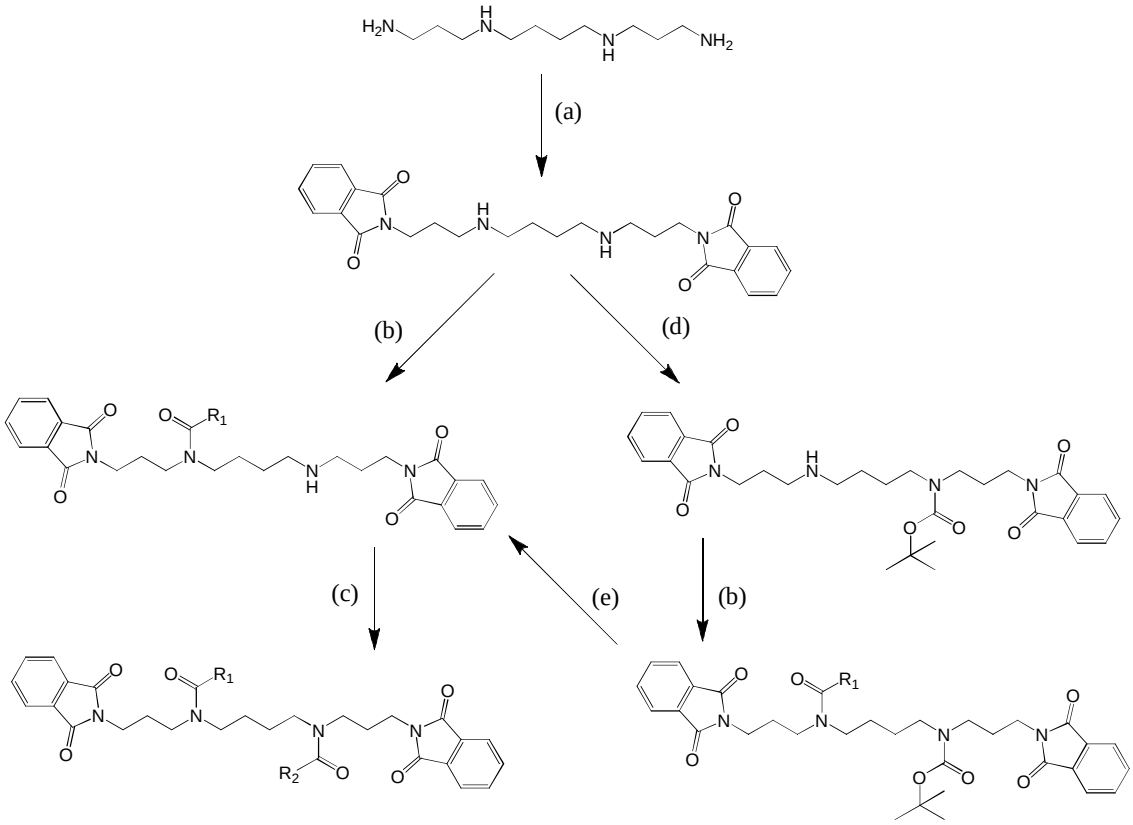

Figure 1. Synthesis of the asymmetrical spermine fatty acid conjugates by two possible routes. (a) Nefkens' reagent, DCM (Chapter 2, Section 2.2); (b) DCC/DMAP, R_1COOH (oleic acid), DCM; (c) DCC/DMAP, R_2COOH, DCM; (d) Boc-O-Boc, MeOH; (e) TFA, DCM, DCM/ aqueous $NaHCO_3$.

Boc deprotection and obtaining the free base after extraction with DCM from aq. $NaHCO_3$ solution then conjugation of the secondary amine functional group with the second long-chain fatty acid (e.g. arachidonic, eicosenoic, erucic, linoleic, lignoceric, nervonic, and stearic acids). Another practical approach uses DCC/DMAP to conjugate stoichiometrically only one fatty acid to the diphthalimido protected spermine then after purification conjugating the second fatty acid, thus avoiding Boc introduction and TFA-mediated Boc deprotection. In the current work, the synthetic scheme of sequential stoichiometric conjugation of fatty acids to diphthalimido protected spermine (reaction steps a, b, and c) was used to synthesize the asymmetrical lipospermines as it resulted in a higher yield of the mono oleoyl diphthalimido spermine in fewer reaction steps compared to the synthetic route involving a Boc-protected intermediate (Figure 1).

1,12-Diphthalimido-4,9-diazadodecane

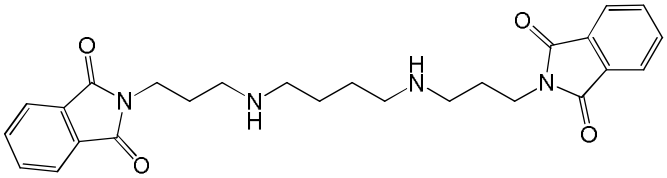

N^4,N^9-Dioleoyl-1,12-diamino-4,9-diazadodecane (DOS) C18:1 Δ^9 and C18:1 Δ^9

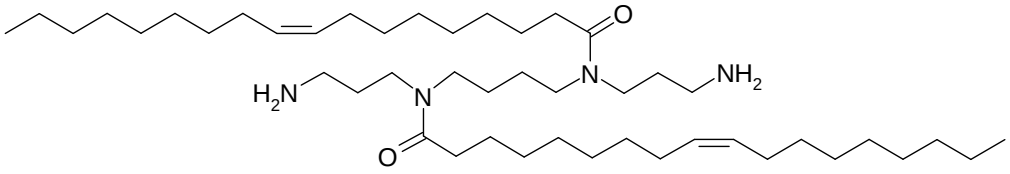

N^4,N^9-Dierucoyl-1,12-diamino-4,9-diazadodecane (DEruS) C22:1 Δ^{13} and C22:1 Δ^{13}

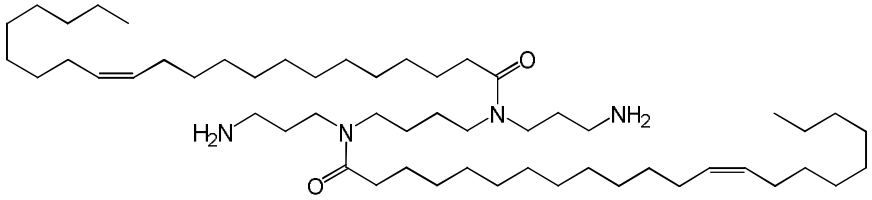

N^4,N^9-Dilinoleoyl-1,12-diamino-4,9-diazadodecane (DLinS) C18:2 $\Delta^{9,12}$ and C18:2 $\Delta^{9,12}$

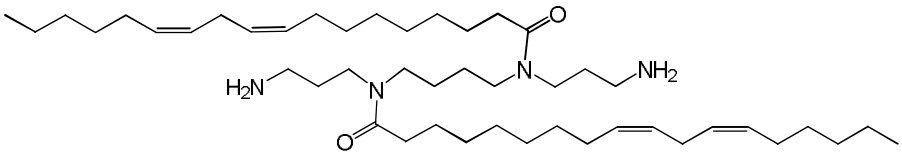

1,12-Diphthalimido-N^4-oleoyl-4,9-diazadodecane

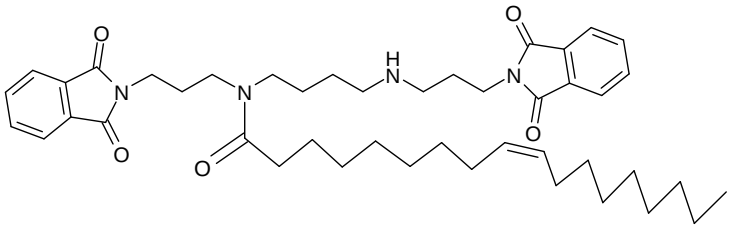

N^4-Arachidonoyl-N^9-oleoyl-1,12-diamino-4,9-diazadodecane (AOS) C20:4 $\Delta^{5,8,11,14}$ and C18:1 Δ^9

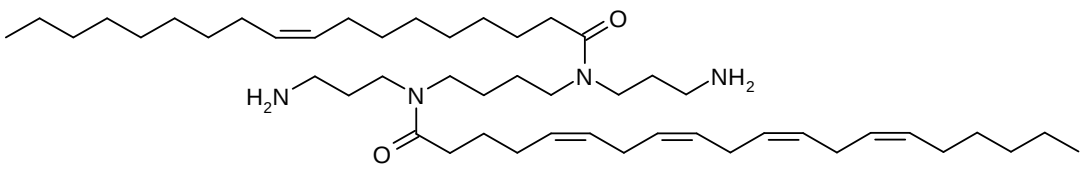

N^4-Eicosenoyl-N^9-oleoyl-1,12-diamino-4,9-diazadodecane (EicOS) C20:1 Δ^{11} and C18:1 Δ^9

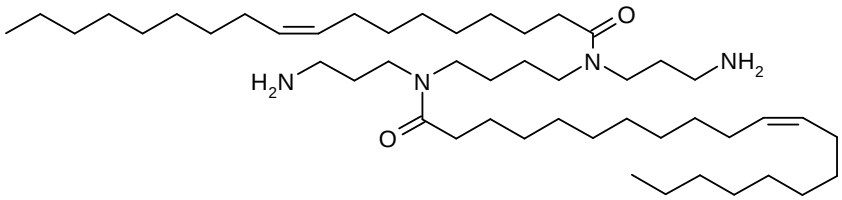

N^4-Erucoyl-N^9-oleoyl-1,12-diamino-4,9-diazadodecane (EruOS) C22:1 Δ^{13} and C18:1 Δ^9

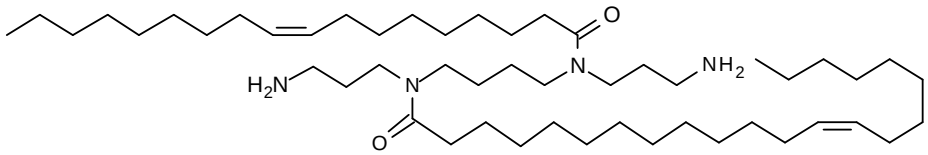

N^4-Lignoceroyl-N^9-oleoyl-1,12-diamino-4,9-diazadodecane (LigOS) C24:0 and C18:1 Δ^9

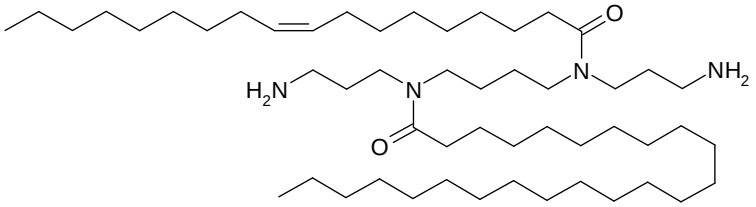

N^4-Linoleoyl-N^9-oleoyl-1,12-diamino-4,9-diazadodecane (LinOS) C18:2 $\Delta^{9,12}$ and C18:1 Δ^9

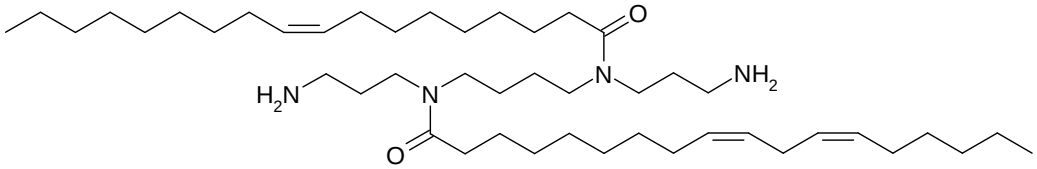

N^4-Nervonoyl-N^9-oleoyl-1,12-diamino-4,9-diazadodecane (NOS) C24:1 Δ^{15} and C18:1 Δ^9

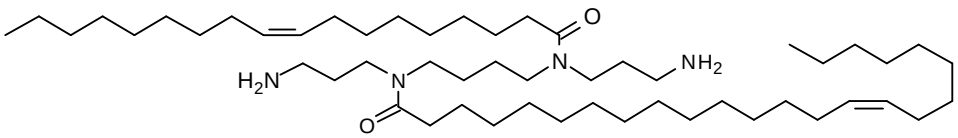

N^4-Oleoyl-N^9-stearoyl-1,12-diamino-4,9-diazadodecane (OSS) C18:1 Δ^9 and C18:0

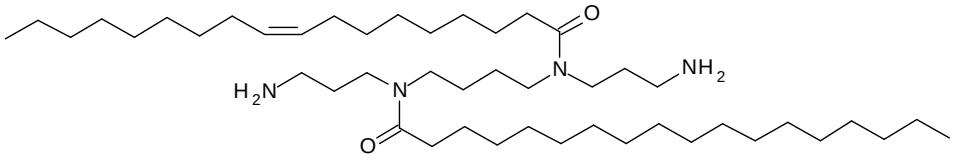

Figure 2. Target asymmetrical and symmetrical N^4,N^9-diamides of spermine.

The HRMS shown in Figure 3 is of 1,12-diphthalimido-N^4-oleoyl-4,9-diazadodecane. Figure 4 shows the ^{1}H NMR (upper) and HMQC (lower) assignments of 1,12-diphthalimido-N^4-oleoyl-4,9-diazadodecane. The numbering convention is that the spermine residue is the parent residue, and the oleoyl carbon numbers are primed. The most important features essential to identify the target compound include: (a) the presence of the double bonds protons of the oleoyl chain (2 protons at δ = 5.3, H9', H10'); (b) 3 protons at δ = 0.9 (3H, H18') representing the terminal methyl group of the oleoyl chain; (c) the presence of 4 protons at δ = 3.2-3.5 (m, 4H, H3, H5), which are deshielded because they are next to the nitrogen atoms of the amide group at N^4, indicating presence of one amide bond, and the successful conjugation of the fatty acids to spermine N^4 position; (d) The two protons at δ = 2.1-2.3 (m, 2H, H2') which are deshielded because they are next to the carbonyl group of the amide, proving the conjugation of the oleoyl residue to spermine; (e) the presence of 4 protons at δ = 2.7-2.8 (m, 4H, H8, H10) which are deshielded because they are next to the free secondary amine group at position N^9; (f) 4 protons at δ = 3.6-3.8 (m, 4H, H1, H12), deshielded because they are next to the imide groups of the protected terminal amines; (g) the aromatic protons of the phthalimide protecting groups at δ = 7.7-7.8 (8 protons). The HMQC shows: (a) the cross-peak of H2' proton with C2' carbon at δ = 33.1, which is the δ of the carbon next to amide carbonyl (b) the cross-peak of H1' and H12' protons with C1 and C12 carbons at δ = 35.3-35.9, which is δ of carbons next to imide carbonyls (c) the cross-peak of H3, H5, H8, and H10 protons with C3, C5, C8, C10 carbons at δ = 45.2-50.6, which are the chemical shifts of carbons next to amide and amine groups. Taken together with the HRMS shown in Figure 3 of 1,12-diphthalimido-N^4-oleoyl-4,9-diazadodecane, these results prove that the target compound was synthesized successfully.

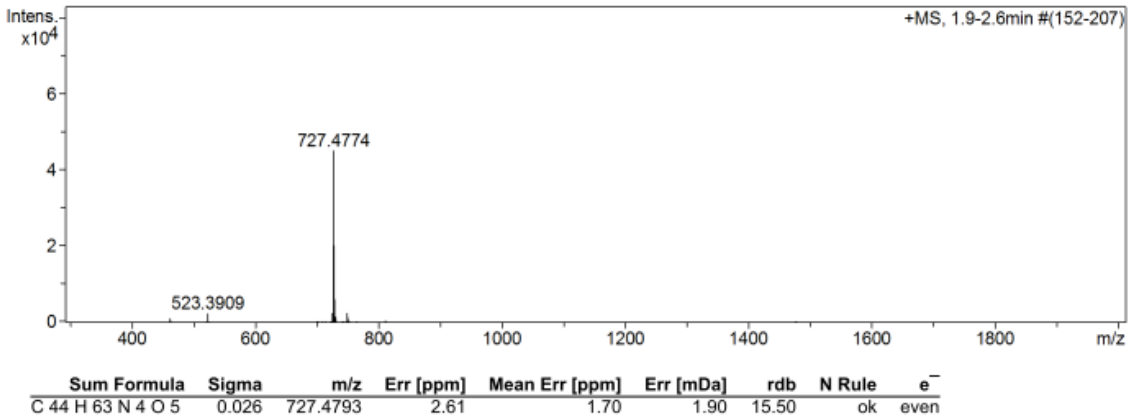

Figure 3. HRMS of protonated $(M+H)^+$ 1,12-Diphthalimido-N^4-oleoyl-4,9-diazadodecane $C_{44}H_{63}N_4O_5$ with *m/z* = 727.4774.

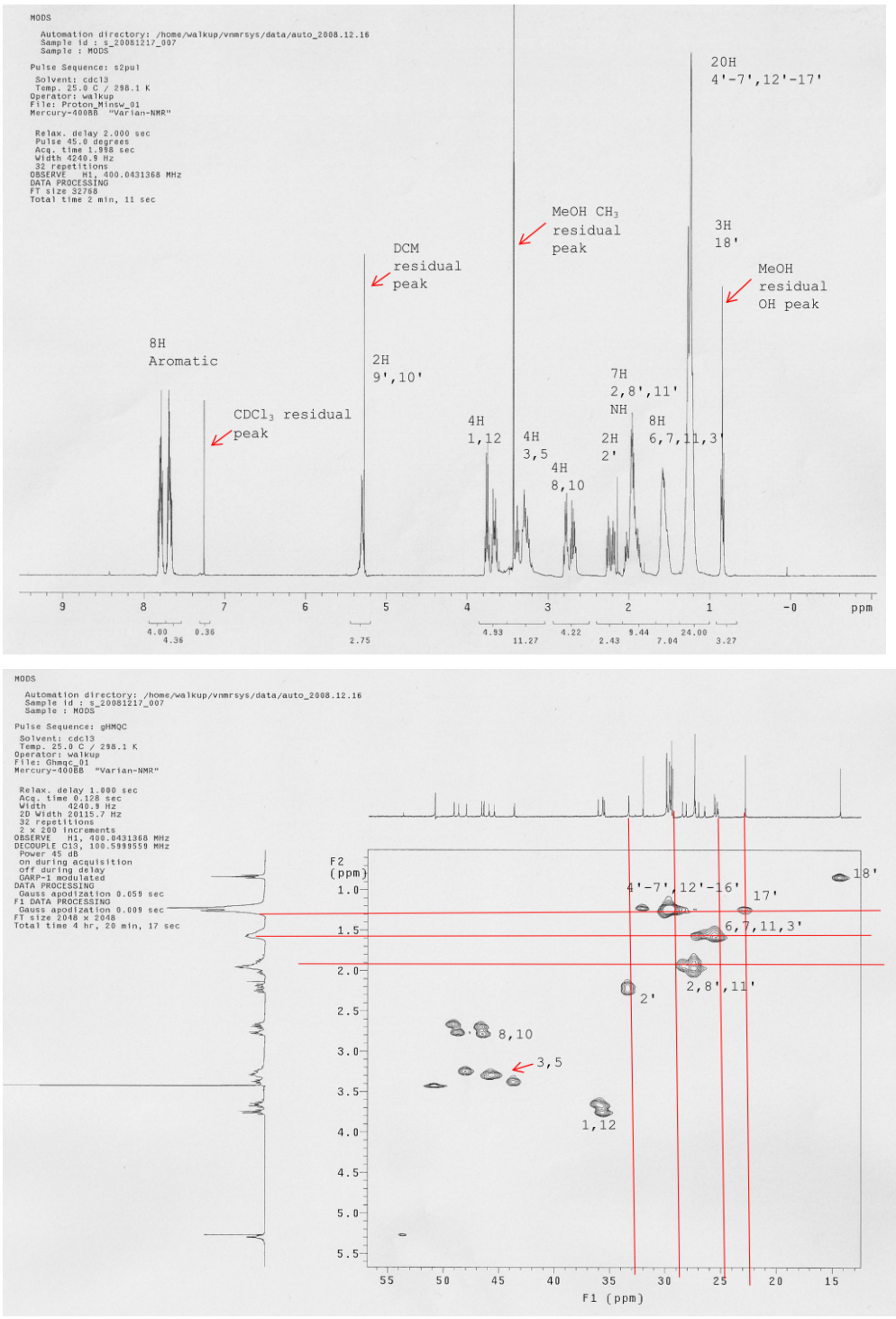

Figure 4. Upper: ^{1}H NMR of 1,12-diphthalimido-*N*^{4}-oleoyl-4,9-diazadodecane. Lower: HMQC NMR. The number of protons (peak integration) and the numbering of the associated carbons are shown in ^{1}H NMR chart. The numbering of the assigned carbons is shown in HMQC chart next to each cross-peak.

The HRMS of LinOS is shown in Figure 5. Figure 6 shows the ^{1}H NMR (upper) and HMQC (lower) assignments of LinOS. The numbering convention is that the spermine residue is the parent residue, the linoleoyl carbon numbers are primed, and the oleoyl carbon numbers are double primed, which is the IUPAC convention for numbering side chains (alphabetical priority for side chains). The most important features necessary to identify the target compound include: (a) the presence of the double bonds protons (6 protons at δ = 5.3, H9', H10', H12', H13', H9'', H10'') which correspond to the two double bonds of the linoleoyl chain and the one double bond of the oleoyl chain; (b) the presence of 8 protons at δ = 3.2-3.4 (8H, H3, H5, H8, H10), which are deshielded because they are next to the nitrogen atoms of the amide groups, indicating the successful conjugation of the fatty acids to the spermine N^4 and N^9; (c) 6 protons at δ = 0.9 (6H, H18', H18'') representing the two terminal methyl groups of the two conjugated fatty acids; (d) 4 protons at δ = 2.6-2.8 (4H, H1, H12) representing protons of two CH_2 groups deshielded because they are next to an amine group, indicating that the primary amine groups are deprotected; (e) the total proton integration which fits the formulae of LinOS, including the four protons of the amine groups at δ = 1.8-2.0.

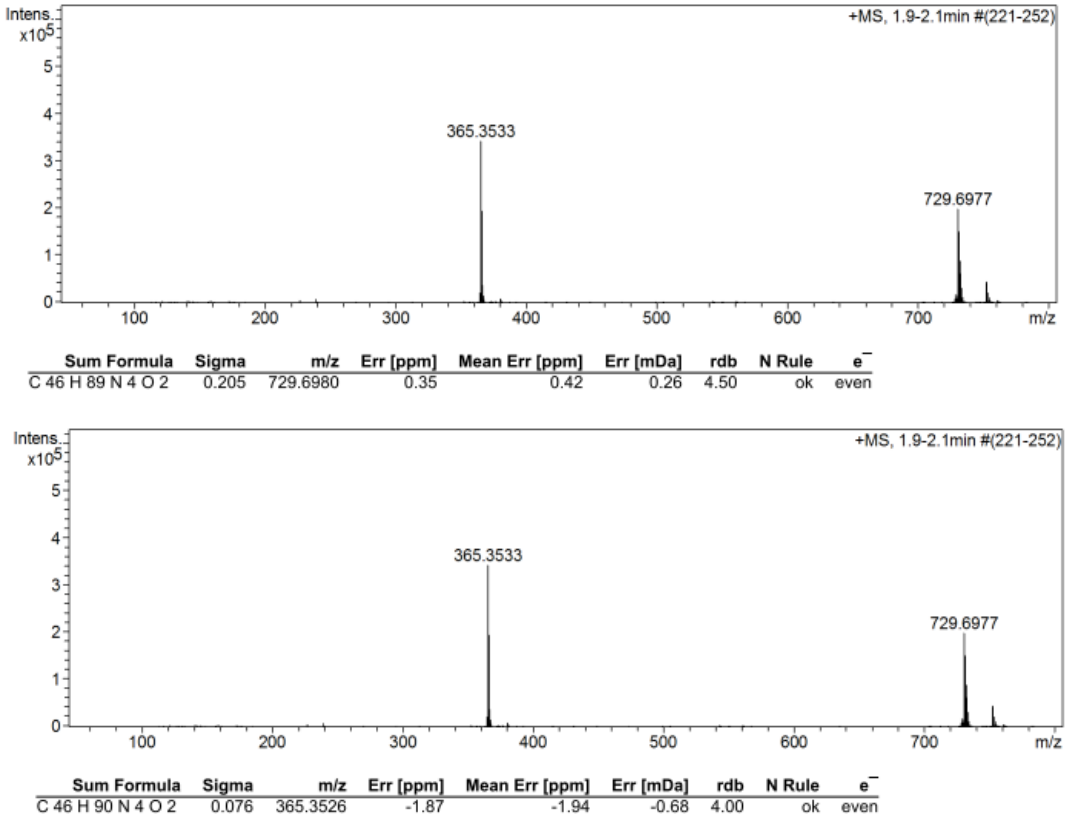

Figure 5. HRMS of LinOS $C_{46}H_{88}N_4O_2$. The upper spectrum shows the protonated LinOS, $C_{46}H_{89}N_4O_2$, $(M+H)^+$ with *m/z* = 729.6980. The lower spectrum shows the doubly protonated LinOS $C_{46}H_{90}N_4O_2$ $(M+2H)^{2+}$ with *m/z* = 365.3533.

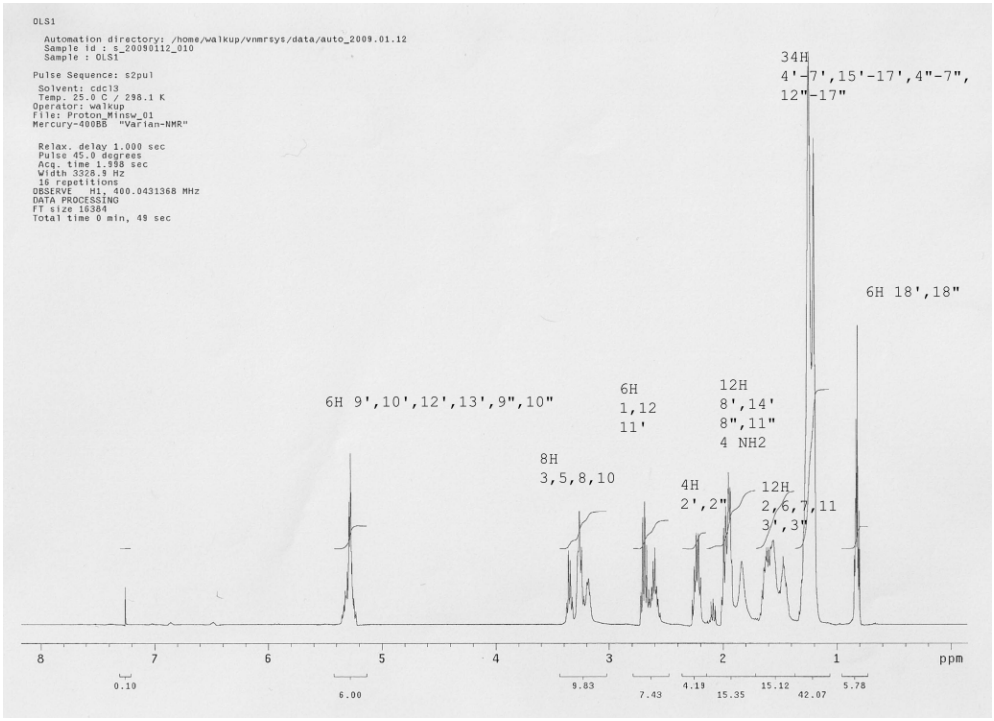

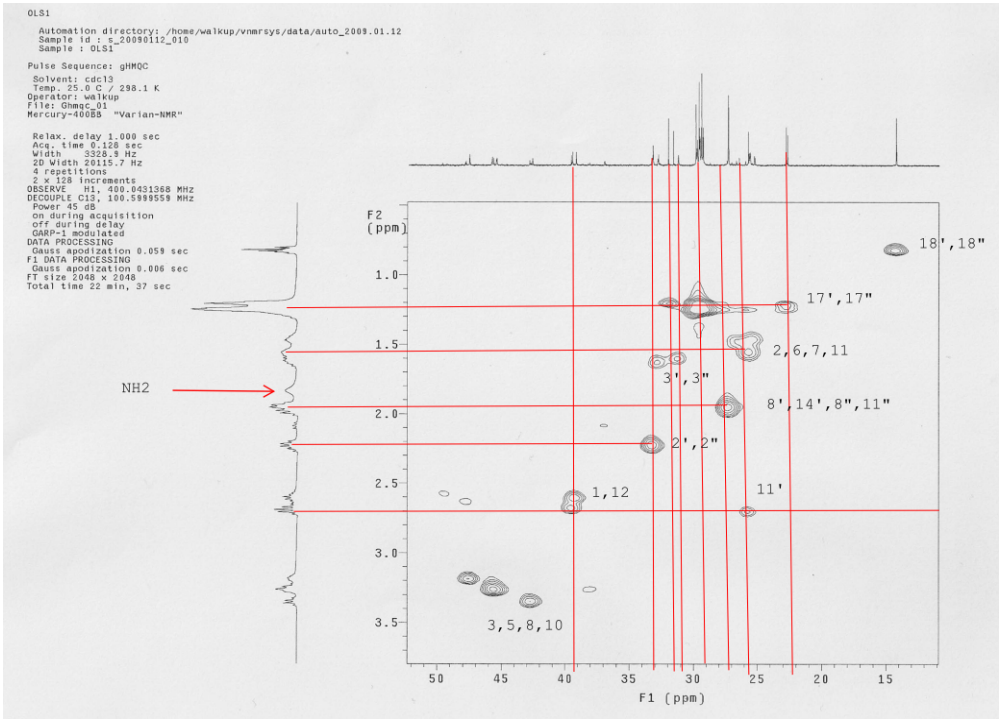

Figure 6. Upper: ^{1}H NMR of LinOS. Lower: HMQC NMR of LinOS. The number of protons (peak integration) and the numbering of the associated carbons are shown in ^{1}H NMR chart. The numbering of the assigned carbons is shown in HMQC chart next to each cross-peak.

Figure 6 (lower) shows the HMQC of LinOS. The assignments of ^{1}H-NMR and ^{13}C-NMR of LinOS can be verified, as seen from the cross-peaks representing the protons H1 and H12 with carbons C1 and C12 at δ = 38.9-39.3. The cross-peaks of protons of H3, H5, H8, and H10 to the carbons at δ = 42.4-47.6, as well as the cross-peaks of protons H2' and H2" and the carbons at δ = 33.0-36.7, indicate the presence of the amide groups and the conjugation of the fatty acids to the parent spermine. The absence of any cross-peaks of the NH_2 protons at δ = 1.8-1.9 (^{1}H-NMR) verifies the presence of the deprotected terminal primary NH_2 protons. Taken together, in addition to the HRMS results shown in Figure 5, it can be concluded that the target compound (LinOS) has been synthesised successfully.

3.1. Transfection studies of HeLa cells stably expressing EGFP

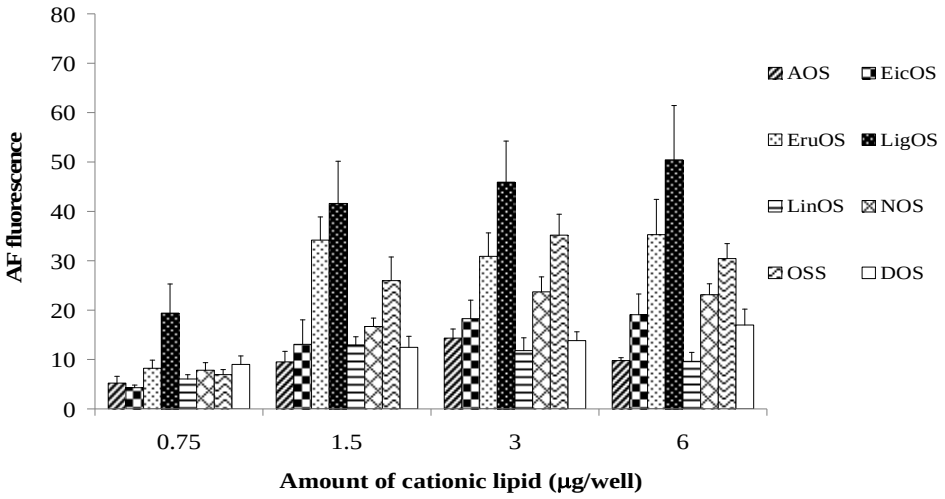

Figure 7. siEGFP-AF delivery to HeLa cells expressed as the normalized values of the AF647 geometric mean fluorescence (AF fluorescence) 48 h post-transfection of HeLa cells with the lipoplexes prepared with seven asymmetrical spermine fatty acid conjugates and symmetrical DOS. The amount of siEGFP-AF was kept constant at 15 pmol/well (15 nM).

Figure 7 shows siRNA siEGFP-AF delivery to HeLa cells as evaluated by the normalized geometric mean fluorescence of AF647 covalently bound to siEGFP. The amount of siRNA delivered (at 6 μg cationic lipid/well) as measured by AF647 fluorescence was 30, 17, and 10 for the C18 fatty acid conjugates OSS, DOS, and LinOS respectively which was related inversely to increases in the number of C=C double bonds in the C18 fatty acids. Increasing the number of unsaturation sites in C24 fatty acids also decreased siRNA delivery (at 6 μg cationic lipid/well, *N/P* = 21.4) normalized AF647 fluorescence was 50 and 23 for LigOS and ><urls><related-urls><url><Go to ISI>://WOS:A1996UF04900016</url></rel one to EicOS and AOS respectively, resulted in a decrease in siRNA delivery, from 19 to 10 at 6 μg

cationic lipid/well (p = 0.0001), and from 18 to 14 at 3 μg/well (p = 0.0163) for EicOS and AOS respectively. Increasing the chain length (EruOS, 22:1 and NOS, 24:1), while keeping the number of C=C double bonds constant, caused an increase in siRNA delivery compared to shorter DOS 18:1 and EicOS 20:1. At a cationic lipid concentration of 6 μg/well, AF647 fluorescence was 17, 19, 35, and 23; and at 3 μg/well: 14, 18, 31, and 24 for DOS, EicOS, EruOS, and NOS respectively. Comparing saturated LigOS (with lignoceroyl chain, 24:0) and OSS (with stearoyl chain 18:0) shows that an increase in the chain length from C18 (OSS) to C24 (LigOS) resulted in an increase in AF647 fluorescence from 30 to 50 respectively (p < 0.0001).

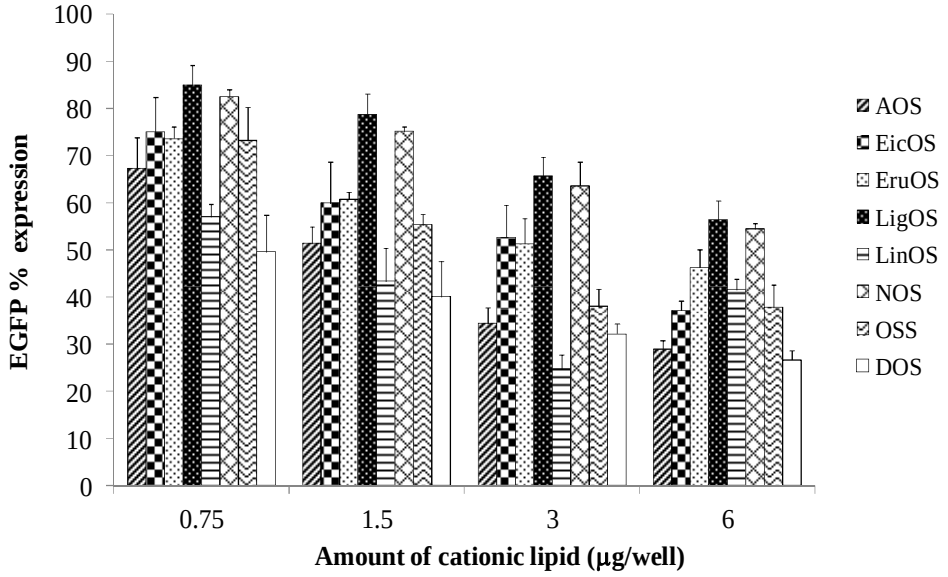

Figure 8. EGFP expression percentage calculated 48 h post-transfection of HeLa cells with the lipoplexes prepared with seven asymmetrical spermine fatty acid conjugates and symmetrical DOS. The amount of siEGFP-AF was kept constant at 15 pmol/well (15 nM).

Figure 8 shows the reduction of EGFP expression in HeLa cells 48 h post-transfection with lipoplexes of siEGFP and the synthesized asymmetrical fatty acid derivatives of spermine. C18 fatty acids with one or two unsaturation sites resulted in better reduction in EGFP expression. Thus, LinOS (3 μg/well, *N/P* = 11.9) gave 24% EGFP expression, DOS (6 μg/well, *N/P* = 23.8) gave 27% EGFP, compared to OSS (with one stearoyl 18:0) which at 3 μg/well gave 38% EGFP and at 6 μg/well gave 38% EGFP. Increasing the number of unsaturation sites in C20 fatty acids resulted in better reduction in EGFP expression (down to 37% and 29% at 6 μg/well, p < 0.0001; 52% and 34% at 3 μg/well; p < 0.0001 for EicOS and AOS respectively). There was no significant statistical difference (p > 0.05) between LigOS and NOS with respect to their effects on EGFP expression. Increasing the chain length of the

fatty acid spermine derivatives from C18 to C24 while keeping number of C=C double bonds constant generally resulted in higher levels of EGFP across the series of compounds, with EGFP expression reduced to 26%, 38%, 51%, and 54% at 6 μg/well of DOS, EicOS, EruOS, and NOS respectively. There were no differences between EicOS and EruOS at 0.75, 1.5, and 3 μg/well. Increasing the chain length from C18 to C24 in OSS and LigOS respectively resulted in higher levels of EGFP expression at different concentrations of lipids. At 6 μg/well, OSS resulted in EGFP expression of 38% while LigOS resulted in EGFP expression of 56% ($p < 0.0001$). The efficiency of gene silencing achieved with LinOS (76%, corresponding to 24% EGFP percentage expression), DOS (73%), and OSS (62%) is comparable to that of commercially available reagents TransIT-TKO (4 μL/well, 75%) and Lipofectamine 2000 (2 μL/well, 69%) used in the presence of serum (10% FCS) and in accordance with the manufacturers' instructions for optimal efficiency. The quantitative FACS data (Figures 7 and 8) are better illustrated by the flow cytometric graphs comprised of individual histograms (Figure 9).

Representative FACS results (Figure 9) are shown with the typical graphs: forward scatter/side-scatter (FSC/SSC) dot graph showing the gating of the healthy cell population, the profile with the AF647 gate, and the profile with the EGFP gate. These data are representative in that they are typical and reflect a single delivery and gene silencing experiment (from 1 of 9 wells). The conditions shown are without (as a control) and with siEGFP-AF. A qualitative analysis of the control cells (Figure 9a) shows a healthy and homogeneous population of EGFP fluorescing cells, with weak autofluorescence excluded out of the AF647 gate. Delivery of siEGFP-AF (15 nM, 15 pmol/well) was 6-fold greater with LigOS (6 μg/well) than with LinOS (3 μg/well). However, gene silencing was greater with LinOS lipoplexes than with those prepared with LigOS (shown in Figure 9 and statistics in Figure 8). Thus, these flow cytometry experiments are also good representatives of cationic lipids showing high delivery with low gene silencing (LigOS), and low delivery with good silencing (LinOS). The commercial transfection reagents TransIT-TKO and Lipofectamine 2000 show very high delivery, but their silencing is no better than that achieved with LinOS (3 μg/well) (Figure 9). Clearly, intracellular delivery and gene silencing are controlled by different processes and therefore functional siRNA delivery is affected by lipoplexes of different cationic lipids to varying extents.[171]

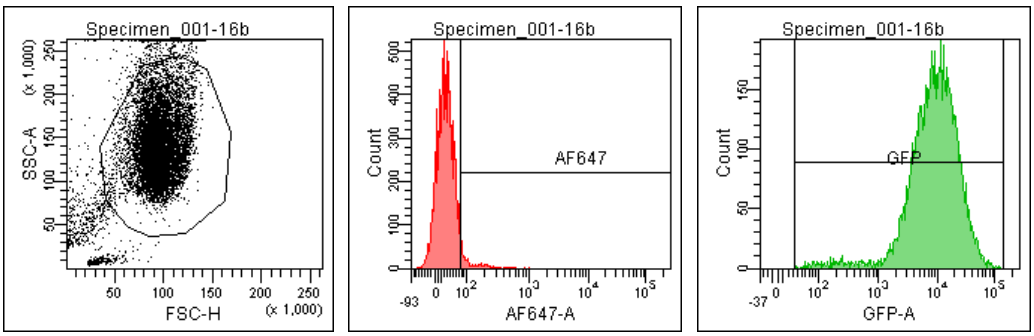

(9a) Control

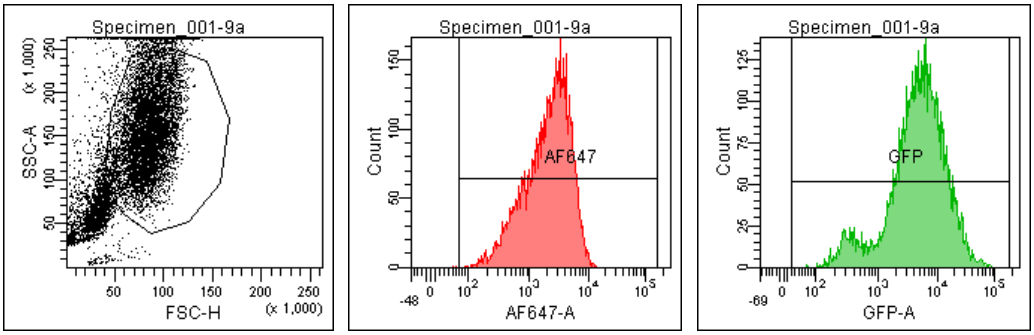

(9b) LigOS

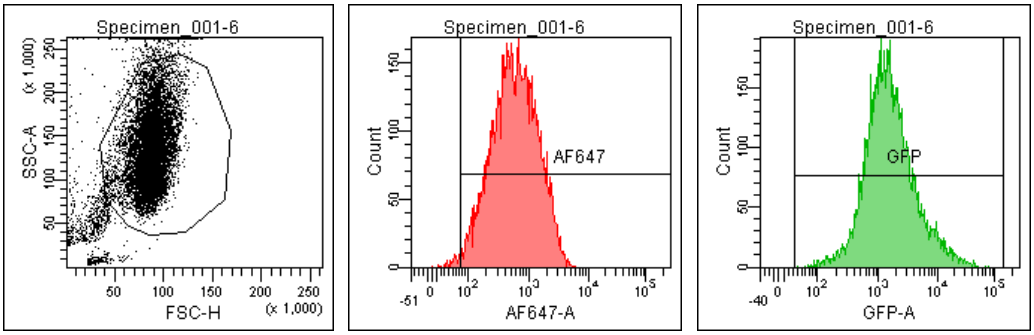

(9c) LinOS

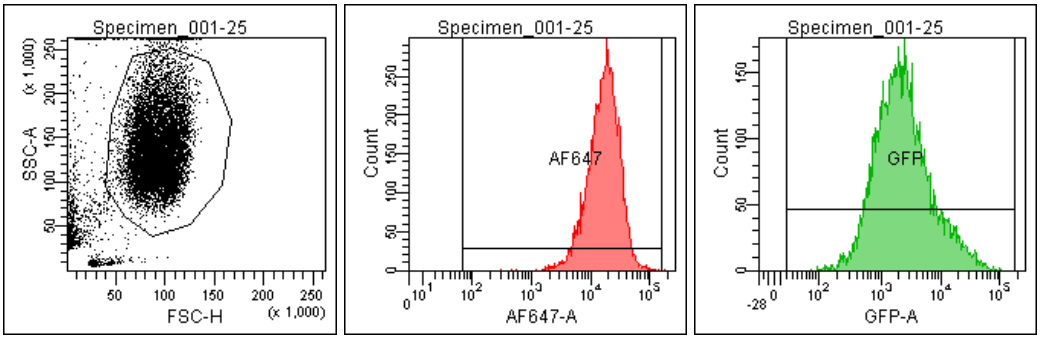

(9d) TransIT-TKO

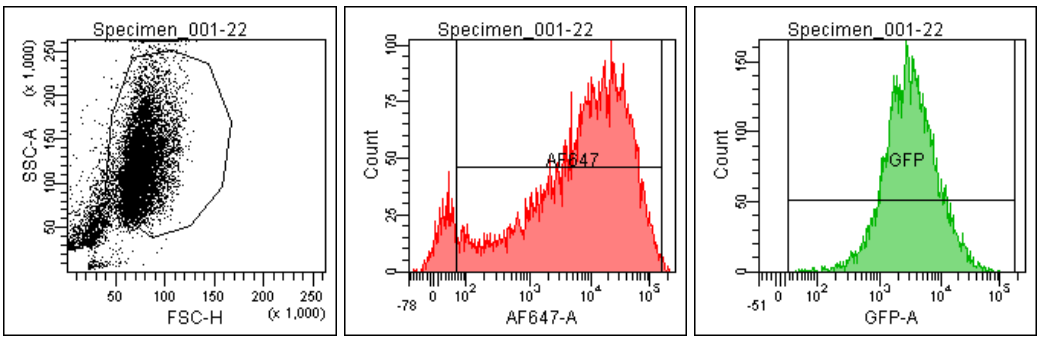

(9e) Lipofectamine 2000

Figure 9. Gated FACS analysis of delivery of siEGFP-AF (15 nM, 15 pmol/well) and EGFP expression in HeLa cells (compared to control) 48 h post-transfection with lipoplexes of LigOS (6 µg/well) and LinOS (3 µg/well). Positive controls come with the commercial transfection reagents TransIT-TKO and Lipofectamine 2000. The AF647 gate (red) typically shows >95% of parent-gated cells with delivery of siEGFP-AF lipoplexes prepared with asymmetrical spermine fatty acid conjugates. The EGFP gate (green, values measured by geometric mean fluorescence relative to control) shows silencing to ~20% with LinOS lipoplexes, and to ~55% with LigOS lipoplexes even though delivery is essentially quantitative with the latter.

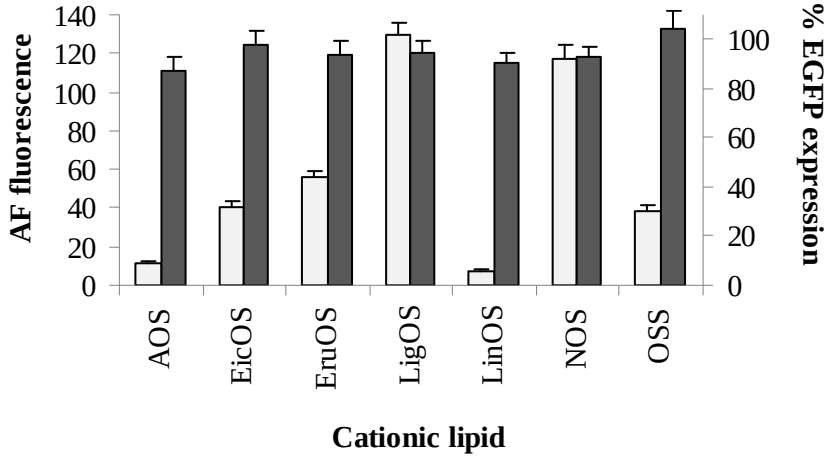

Figure 10. EGFP expression percentage (dark grey bars) calculated 48 h post-transfection of HeLa cells with the lipoplexes prepared with asymmetrical spermine fatty acid conjugates and siNC-AF (15 pmol/well, 15 nM). siNC-AF fluorescence shows siRNA delivery (white bars). Cationic lipid amounts used were those that resulted in the best reduction in EGFP expression: AOS (6 µg/well), EicOS (6 µg/well), EruOS (6 µg/well), LigOS (6 µg/well), LinOS (3 µg/well), NOS (6 µg/well), and OSS (6 µg/well).

The EGFP expression and siNC-AF delivery are shown in Figure 10. The amounts of lipids used were those which resulted in the best reduction in EGFP expression with respect to each cationic lipid (Figure 8). The data show that while the delivery of siNC-AF for each cationic lipid, at the specified concentration, was with comparable efficiency to the delivery results of siEGFP-AF (Figure 7), there was no significant effect (a maximum of 10% reduction) on EGFP expression percentage. Thus, the reduction in EGFP expression after transfection with siEGFP-AF lipoplexes is mainly due to sequence-specific EGFP knock-down mediated by the delivered siEGFP-AF, and not due to any cationic lipid-related effects, e.g. toxicity.

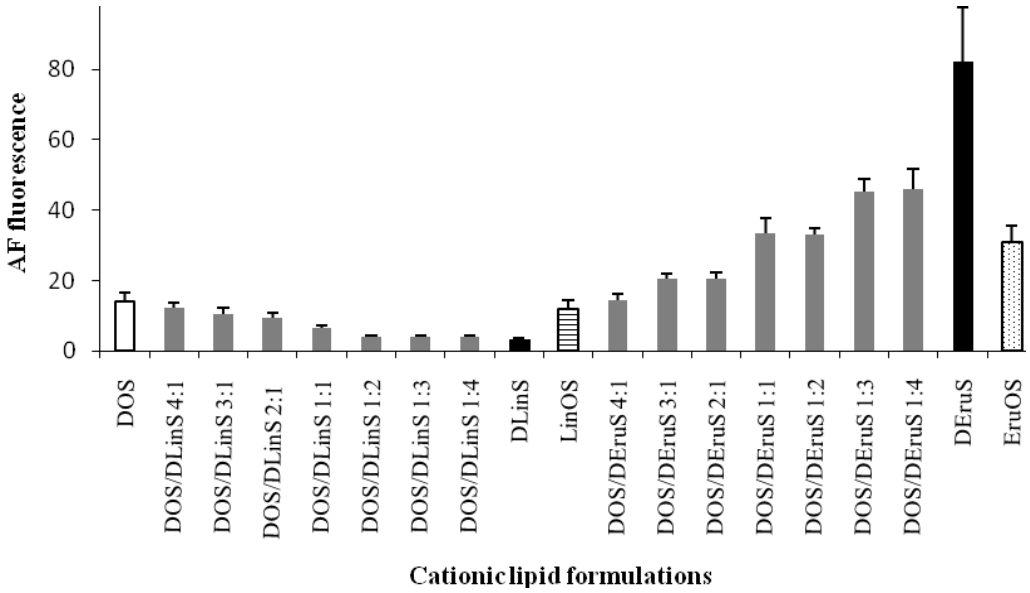

Figure 11. siEGFP-AF delivery to HeLa cells expressed as the normalized values of the geometric mean fluorescence of AF647 48 h post-transfection of HeLa cells with the mixtures of lipoplexes prepared with DOS/DLinS or DOS/DEruS at different molar ratios (total lipid weight 3 μg/well). The amount of siEGFP-AF was kept constant at 15 pmol/well (15 nM).

Mixtures of cationic lipids have been reported to enhance DNA transfection through synergy.[224] Figure 11 shows siEGFP-AF delivery with lipoplexes of mixtures of DOS/DLinS and DOS/DEruS at different molar ratios of the symmetrical spermine derivatives, as well as comparing their siEGFP-AF delivery with the delivery by the asymmetrical LinOS and EruOS. DOS lipoplexes resulted in AF647 fluorescence of 14 (normalized) and DLinS resulted in delivery of 3. The mixtures of DOS/DLinS of molar ratio 4:1 to 1:4, resulted in AF647 fluorescence of intermediate values between those of DOS and DLinS. When compared to LinOS, the siEGFP-AF delivery with the DOS/DLinS 1:1 lipoplexes resulted in lower AF647 delivery (7 and 12 for DOS/DLinS 1:1 and LinOS respectively, $p < 0.0001$). The mixtures of DOS/DEruS of molar ratio 4:1 to 1:4, resulted in AF647 fluorescence of

intermediate values between those of DOS (14) and DEruS (82). There was no statistical significant difference between DOS/DEruS 1:1and EruOS (33 and 31 respectively, $p = 0.64$). The mixtures mostly behave in a way which reflects the behaviour of the individual components (Figure 11). DLinS shows the lowest uptake, consistent with the results (Figure 11) where lipids containing more double bonds show lower uptake. DEruS has the highest uptake, also consistent with the results in Figure 11 where the longer and more saturated lipid chains, EruOS, LigOS, and NOS show higher uptake. However, these mixtures of cationic lipids displayed no synergy in siEGFP-AF delivery as found with DNA transfection.[224]

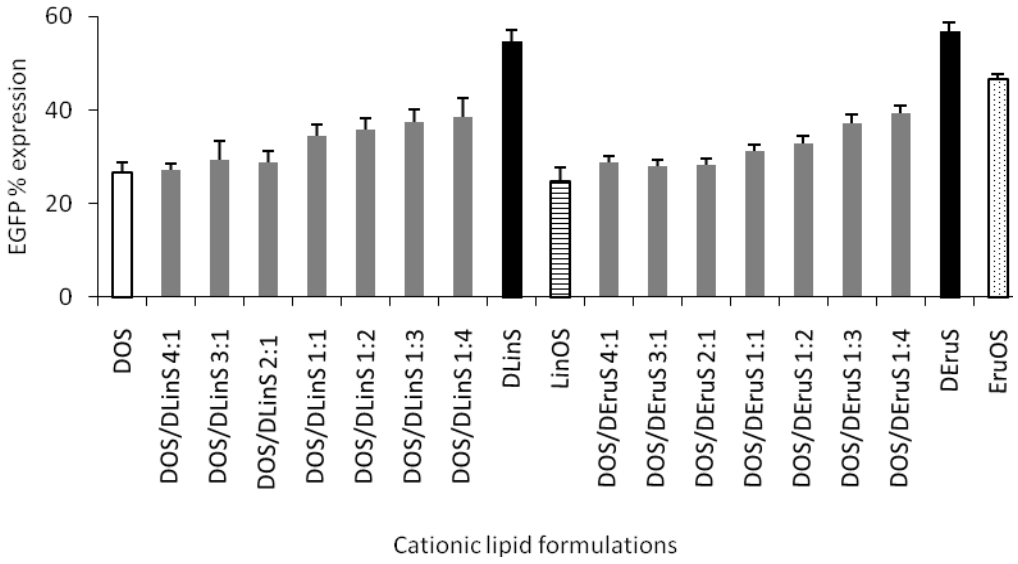

Figure 12. EGFP expression percentage measured 48 h post-transfection of HeLa cells with the lipoplexes prepared with mixtures of DOS/DLinS or DOS/DEruS at different molar ratios (total lipid weight 3 μg/well). The amount of siEGFP-AF was kept constant at 15 pmol/well (15 nM).

Figure 12 shows the reduction in EGFP expression 48 h post-transfection with lipoplexes of mixtures of DOS/DLinS and DOS/DEruS at different molar ratios of the symmetrical spermine derivatives, as well as the EGFP expression resulting from transfection with lipoplexes of the asymmetrical LinOS and EruOS. The mixtures of DOS/DLinS of molar ratio 4:1 to 1:4, resulted in EGFP expression of intermediate values between those of DOS and DLinS, with EGFP expression increasing with the increase in DLinS content in the mixture. When compared to LinOS, the EGFP expression with the DOS/DLinS 1:1 lipoplexes resulted in EGFP expression of 34% compared to LinOS 24% (3 μg/well, $p < 0.0001$). The mixtures of DOS/DEruS of molar ratio 4:1 to 1:4, resulted in EGFP expression of intermediate values between those of DOS and DEruS. Contrary to the results obtained

with DOS/DLinS 1:1 and LinOS, EruOS resulted in higher EGFP expression (47%) compared to the DOS/DEruS 1:1 mixture (31%, $p < 0.0001$). The gene silencing of lipoplexes composed solely of DLinS (55%), and of DEruS (57%) show limited inhibition of EGFP expression (Figure 12). The mixtures mostly show gene silencing dominated by DOS rather than reflecting the percentage composition of the individual components. This is also found in the covalent binding of erucoyl and oleoyl chains in the spermine conjugate EruOS (gene silencing to 47%), but incorporating two different C18 acyl chains in the asymmetrical LinOS, linoleoyl and oleoyl, affords the best gene silencing (24%).

3.2. Confocal microscopy cell imaging

Figure 13a shows non-transfected (control) HeLa cells expressing EGFP (green) within the cell membrane (blue). Figures 13b and 13d show HeLa cells only 4 h post-transfection with lipoplexes of siEGFP-AF and LinOS (3 µg/well). Figure 13b shows that while siEGFP-AF (red) has been delivered, EGFP is still strongly expressed throughout the cell. In Figure 13d, the green channel was turned-off to better visualize the red colour representing siEGFP-conjugated dye AF647 (siEGFP-AF). Note that the lower cell shows higher uptake compared to the upper cell. In Figure 13c, EGFP (green) is barely detectable at 48 h post-transfection, compared to the control untransfected cells shown in Figure 13a. Scattered red dots indicate that siEGFP-AF is still present 48 h post-transfection. Taken together, the photomicrographs shown in Figure 13 demonstrate the apparent efficient uptake of lipoplexes of siEGFP-AF and LinOS (3 µg/well) and the subsequent very dramatic reduction (knock-down) of EGFP expression, at least up to 48 h post-transfection. Of interest is that LinOS (at 3 and even at 6 µg/well, Figure 7) shows the lowest siRNA delivery, but with siEGFP-AF held constant at 15 pmol/well (15 nM), LinOS (3 µg/well) forms the most efficient lipoplexes for gene silencing (Figure 8) even though this high efficacy is not reflected in high delivery.

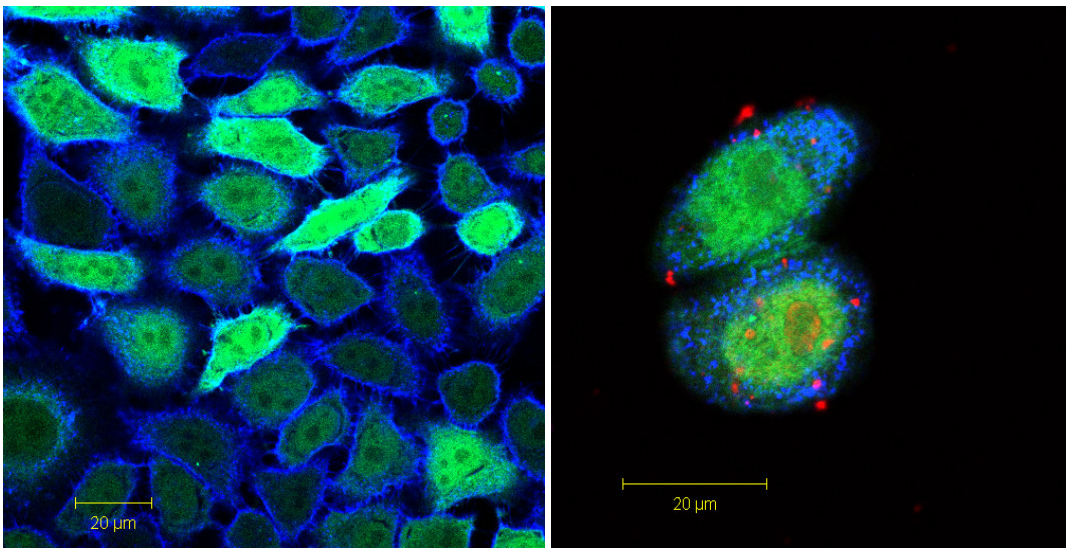

(13a) (13b)

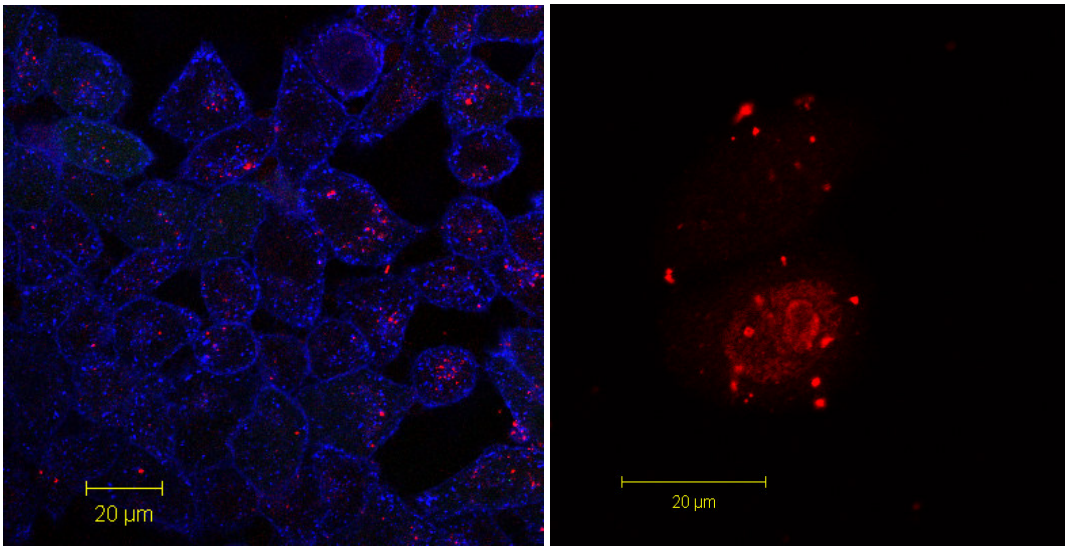

(13c) (13d)

Figure 13. Confocal photomicrographs of HeLa cells before and after transfection of siEGFP-AF with LinOS (3 µg/well). The cell membrane is stained with Alexa Fluor 555 (blue). Representative pictures are shown. (13a) Untransfected HeLa cells stably expressing EGFP (green). (13b) Detection of siEGFP-AF (red dots), only 4 h post-transfection. (13c) EGFP expression with the green channel on as in (13a) and (13b), monitored 48 h post-transfection. EGFP expression is largely reduced (cf FACS data, Figure 13b). (13d) as (13b) with the FACS green and blue channels turned off for clarity.

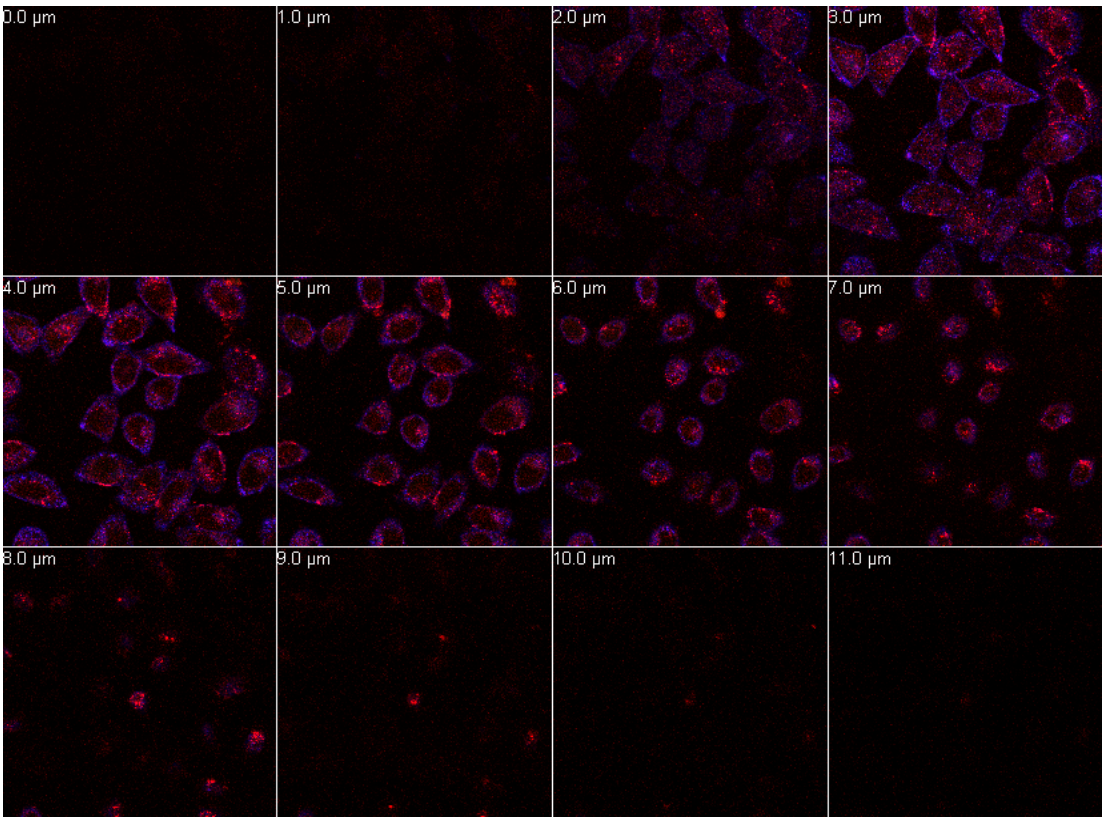

Figure 14. A Z-stack confocal photomicrograph gallery of photomicrographs representing 12 Z-sections in HeLa cells transfected with lipoplexes of LinOS (3 µg/well) and siEGFP-AF (15 pmol). EGFP fluorescence (green), cell membrane stained with WGA-Alexa Fluor 555 (blue), and Alexa Fluor 647 (red) represents tagged siRNA delivery.

In order to further highlight the intracellular detection of siEGFP-AF monitored 48 h post-transfection (Figure 13c) where there is almost no detectable EGFP expression (with the green channel turned on), a Z-stack gallery was recorded through a monolayer of transfected HeLa cells (Figure 14). Z-Stacks are a series of successive optical sections acquired at different positions along the Z-axis (in 1.0 µm slices). The first optical section was taken slightly lower than the surface of the cells attached to the cover slip, then the sections were recorded while slicing through to the opposite surface. Figure 14 shows that majority of the red colour (representing siRNA delivery) is present inside the cell, the blue colour representing cell membrane is only present at the perimeter of the cells, and occasionally the red colour is present simultaneously with the blue colour indicating Alexa Fluor 647 (red) (bound to siRNA) within the membrane. While slicing along the Z-axis, there is no blue colour in the middle of the cells where there is red. Minko and co-workers have recently reported the use of Z-stack photomicrographs to determine the orientation of the delivered

siRNA, where a NuLight DY-547 fluorophore tagged siRNA was delivered to A2780 human ovarian cancer cells by surface neutral, but internally cationic polyamidoamine dendrimers.[225]

3.3. Particle size, zeta-potential measurements, and siRNA binding (RiboGreen intercalation assay)

Table 1. Particle diameter, ζ-potential, and siRNA binding assay of fatty acid amides of spermine measured at the cationic lipid/siRNA ratios that showed best knock-down of EGFP (all shown as mean ± SD).

Cationic lipid	Diameter (nm)	ζ-potential (mV)	% fluorescence of RiboGreen
AOS	292 ± 36	49 ± 1	4 ± 1
EicOS	273 ± 11	55 ± 2	2 ± 1
EruOS	286 ± 29	51 ± 2	2 ± 1
LigOS	241 ± 26	59 ± 6	1 ± 1
LinOS	225 ± 20	53 ± 3	4 ± 1
NOS	291 ± 26	40 ± 4	1 ± 1
OSS	145 ± 7	56 ± 2	5 ± 1

DLS was used to measure the particle sizes (Table 1) of the lipoplexes prepared at the cationic lipid/siRNA ratio that resulted in the largest reduction in EGFP expression. The size range is 145-292 nm (OSS to AOS respectively) which is in agreement with the size range of lipoplexes previously reported to transfect successfully in cell culture.[214] The particle size could determine the main route of cellular entry, with lipoplexes <300 nm likely to enter via clathrin-mediated endocytosis, and lipoplexes >500 nm entering cells via caveoli-mediated endocytosis.[214, 215] However, the entry route for functional siRNA delivery might be by fusion with the cell membrane rather than via an endocytic pathway, as demonstrated using selective inhibitors.[171] The ζ-potentials of the prepared lipoplexes (Table 1) are all positive (40-59 mV). Such a net positive charge on the lipoplex surface is important in promoting lipoplex-lipoplex repulsion, thus preventing aggregation. The RiboGreen siRNA binding assay results (Table 1) show that the asymmetrical spermine conjugates are able to bind siRNA almost completely, with the fluorescence of RiboGreen dye reduced to values of 1-5% of the control. The two free terminal primary amine groups of the acylated spermine conjugates are practically fully protonated at physiological pH 7.4.

3.4. Cell viability assays

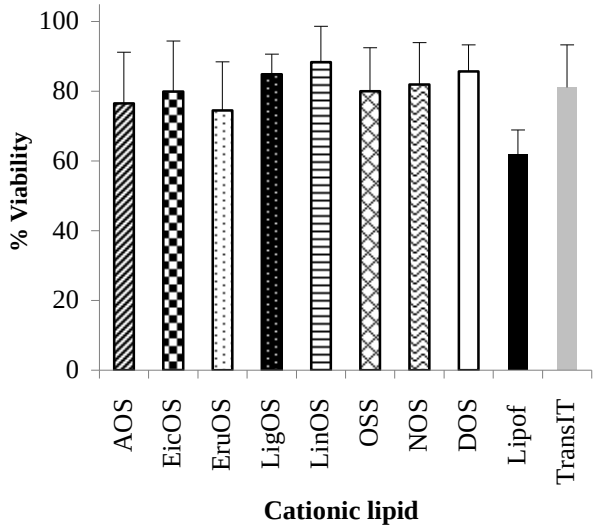

Figure 15. Cell viability (alamarBlue assay) 48 h post-transfection of HeLa cells with the lipoplexes prepared with spermine fatty acid conjugates, using 6,500 cells/well, and transfection with lipoplexes was 24 h after seeding the cells. The amount of siNC was kept constant (1.5 pmol/well, 15 nM) and amounts of lipids were adjusted accordingly to the same cationic lipid/siRNA ratio that resulted in the best reduction in EGFP expression: AOS (0.6 μg/well), EicOS (0.6 μg/well), EruOS (0.6 μg/well), LigOS (0.6 μg/well), LinOS (0.3 μg/well), NOS (0.6 μg/well), and OSS (0.6 μg/well); compared with DOS (0.6 μg/well), Lipofectamine 2000 (Lipof, 0.2 μL/well), and TransIT-TKO (0.4 μL/well).

For pragmatic cell viability assays, the transfection conditions in 24-well format were downscaled to 96-well format, after establishing that 4,000-6,500 cells/well was an optimal range for reproducible results and in order to avoid problems of overconfluency. To keep the ratios and concentrations the same, the cell number, weight of cationic lipid, and amount of siRNA were each reduced to one tenth of their original values. The two cell viability assay conditions employed reflect the experimental conditions used in gene silencing (0.5 h between seeding and transfection) and in confocal microscopy where the time after seeding was 24 h to allow the cells to attach well and distribute evenly on the cover slips. In comparison, when using FACS to quantify gene silencing, there was no requirement for a long time between seeding and transfection as there was no requirement for better attachment to cover slips.

For the experiments whose results are shown in Figure 15, the weight of lipid chosen was based on the ratio of lipid/siEGFP-AF that resulted in the best reduction in EGFP expression as seen in Figure 8. The percentage cell viabilities, shown in Figure 14, indicate that transfection of HeLa cells with lipoplexes of siRNA and the synthesized asymmetrical spermine derivatives resulted in cell viabilities above 74%, with LinOS (0.3 μg/well) resulting in 88% viability and DOS 85% viability (0.6 μg/well) which is comparable to TransIT-TKO (81%) and better than Lipofectamine 2000 (62%).

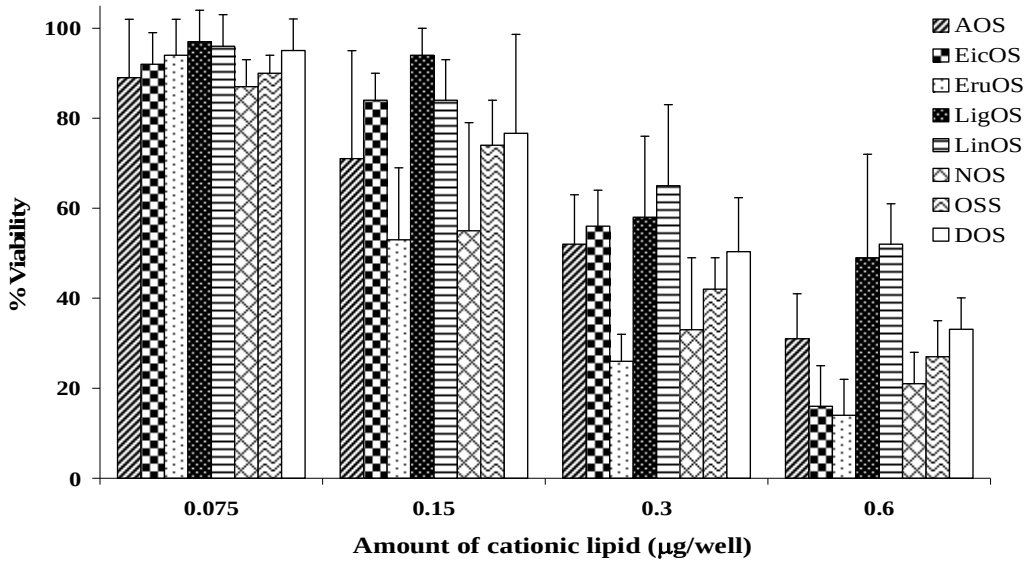

Figure 16. Cell viability (alamarBlue assay) 48 h post-transfection of HeLa cells with the lipoplexes prepared with spermine cationic lipids using 4,000 cells/well and transfection 0.5 h after seeding. The amount of siRNA (siNC) was kept constant at 1.5 pmol/well (15 nM) and amounts of cationic lipids were adjusted accordingly.

Figure 16 shows the cell viabilities after transfection of HeLa cells using a lower number of cells (4,000 cell/well in 96-well format) and carrying out the transfection within 0.5 h of seeding the cells, aiming to make the transfection conditions harsher for the cells, such that individual differences between each of the cationic lipids at their different concentrations can be compared. Figure 16 also shows that increasing the amounts of lipids per well from 0.075 to 0.6 μg resulted in a decrease in cell viability. The viabilities resulting from transfection with lipoplexes of LinOS and DOS (the cationic lipids that showed the best reduction in EGFP expression as shown in Figure 8) were reduced from 96% to 84% to 65% to 52% (LinOS) and from 95% to 77% to 50% to 33% (DOS) at 0.075, 0.15, 0.3, and 0.6 μg/well respectively. The lowest cell viabilities were due to transfection with EruOS lipoplexes (from 94%, 53%, 26%, and 14% at 0.075, 0.15, 0.3, and 0.6 μg/well of EruOS respectively).

In this Chapter, seven asymmetrical lipopolyamines based on spermine, possessing two primary amines were designed, synthesized, purified, and tested in a variety of physico-chemical and cell biological assays. These are novel divalent cationic lipids. Assessment using both flow cytometry and fluorescence microscopy in human HeLa cells, measuring both delivery of the fluorescently tagged siRNA and silencing the EGFP signal in a stably transfected cell line, allowed quantitation of the differences between asymmetrical cationic lipids, selected mixtures of their symmetrical counterparts, and comparison with commercially available non-viral delivery agents. In this Chapter, the design of this series of novel spermine based cationic lipids involved making variations in the hydrophobic domain by changing the type of fatty acids conjugated to the parent spermine molecule. Koynova et al. reported the impact of changing the hydrophobic moiety of cationic lipids on DNA transfection efficiency.[147] Data from 20 cationic phosphatidylcholine (PC) derivatives show that the chain saturation state and chain length, representing hydrophobic volume and cationic lipid hydrophilic-lipophilic balance (HLB), are major factors that determine DNA transfection efficiency, with variations in efficiency by more than two orders of magnitude, and also that lipid chain asymmetry has a strong impact on DNA transfection efficiency while keeping the HLB of cationic lipids constant.[147]

Non-viral DNA vectors prepared from cationic lipids that are composed of asymmetrical fatty acid chains have been reported to have higher in vitro[153] and/or in vivo[226] efficiencies in comparison with their symmetrical counterparts. Several hypotheses have been put forward to explain the superior DNA transfection efficiency of asymmetrical cationic lipids. Ali et al. reported that fatty chain asymmetry in membrane lipids affects the physical environment of liquid-crystalline bilayers.[223] PCs showing a relatively large difference in chain length (larger asymmetry, e.g. 18:0/8:0 or 18:0/10:0 PCs) resulted in 20-25% greater in-plane elasticity compared to PCs with less asymmetry (16:0-18:1 PCs) and to symmetrical PCs (di18:1). Heyes et al.[153] suggested that the difference in length between the fatty chains allows for better overlapping within biological lipid bilayers following the work of Balasubramaniam et al. who proposed that asymmetrical lipids have increased fusogenicity.[227]

The effect on DNA transfection efficiency of changing the saturation state in one chain was reported by Koynova et al.[228] Comparing two asymmetric cationic phospholipid derivatives, oleoyldecanoylethyl-PC (C18:1/C10:0) and stearoyldecanoylethyl-PC (C18:0/C10:0), resulted in the former compound with the oleoyl chain showing 50-fold more DNA transfection efficiency than the latter with the saturated stearoyl chain. This DNA transfection efficiency result was attributed to the enhanced fusibility of the (C18:1/C10:0) lipid with cellular lipid membranes, and to the facilitated release of DNA due to phase reorganization, lamellar to non-lamellar transitions, and extensive phase coexistence as a

result of lipid mixing at physiological temperatures.[228] The processes of siRNA lipoplex delivery (uptake) and gene silencing are different from each other and different from DNA transfection. The results of EGFP expression gene-silencing show that siRNA lipoplexes self-assembled with lipopolyamines possessing one or two centres of unsaturation in the acyl chains (e.g. DOS, LinOS) lead to more gene silencing compared to similar lipoplexes containing saturated chains of the same length (e.g. stearoyl in OSS). siRNA uptake was highest with the symmetrical DEruS.

Synergistic effects of mixtures of cationic lipids have also been reported to enhance DNA transfection. However, mixtures of *N*-[1-(2,3-dimyristoyloxy)propyl]-*N*,*N*,*N*-trimethylammonium (DMTAP) and *N*-[1-(2,3-dioleoyloxy)propyl]-*N*,*N*,*N*-trimethylammonium (DOTAP) show intermediate values of DNA transfection efficiencies compared to using pure parent lipids as a linear function of lipid mixture composition.[224] Enhanced DNA transfection following the use of lipid mixtures is possibly due to the change of the hydrophobic volumes of the lipids, related to the average hydrophobicity of the mixture and/or the heterogeneous distribution of the hydrophobic domains of the mixtures. Also, the presence of more than one lipid results in an increase in the degrees of freedom of lipoplex-membrane interactions eventually leading to better fusogenicity.[224] siRNA lipoplex formation and delivery do not necessarily follow the same constraints as those of DNA lipoplexes due to the significant structural differences between DNA and siRNA regarding molecular weight and rigidity. Thus, the aforementioned hypotheses regarding DNA self-assembled lipoplexes should be applied cautiously to siRNA lipoplexes.

The use of mixtures e.g. DOS/DLinS and DOS/DEruS, at different molar ratios of the symmetrical spermine derivatives, afforded similar or lower siEGFP-AF delivery in comparison with their related asymmetrical cationic lipids (LinOS and EruOS). Reduction in EGFP expression 48 h after transfection with lipoplexes prepared from mixtures of these symmetrical cationic lipids was poorer than that achieved with the related asymmetrical cationic lipid LinOS, but better than that achieved with EruOS. In the alamarBlue assay, cell viability of LinOS lipoplexes was 88%. LinOS is an excellent, efficient, non-toxic cationic lipid in HeLa cells, comparable or superior to commercially available reagents TransIT-TKO and Lipofectamine 2000.

The amount of siEGFP-AF delivered to HeLa cells was lower with more C=C double bonds in the lipid moiety. Increasing the chain length, while keeping the number of C=C constant, caused an increase in siRNA delivery. C18 fatty acids with one or two unsaturation sites resulted in better reduction in EGFP expression and increasing the number of unsaturation sites in C20 fatty acids also resulted in better reduction in EGFP expression in HeLa cells 48 h post-transfection. Increasing the chain length of the fatty acid spermine

derivatives from C18 to C24 while keeping the number of C=C double bonds constant was generally less efficient for gene silencing. It is shown that reduction in EGFP expression after transfection with siEGFP-AF lipoplexes was due to sequence-specific EGFP knock-down mediated by the delivered siEGFP-AF, and not due to any cationic lipid-related effects, e.g. toxicity. It is concluded that the effects of different hydrophobic domains are not equal on intracellular delivery of siRNA and on gene silencing by siRNA. Control of these processes can be achieved with different N^4,N^9-diacyl spermines where gene silencing is efficiently demonstrated using lipoplexes of LinOS, and relatively higher siEGFP-AF delivery is demonstrated using LigOS.

4. Conclusions

In this Chapter, seven asymmetrical N^4,N^9-diacyl spermine conjugates were designed, synthesized, characterized by NMR and HRMS, and investigated in vitro in HeLa cells for siEGFP-AF delivery and EGFP gene knock-down. One oleoyl chain was kept constant in all the asymmetrical conjugates while the other fatty acid chain was varied in length and/or saturation state. The SAR study revealed that asymmetrical conjugates with longer fatty acid chains (e.g. in LigOS and NOS), results in more siEGFP-AF intracellular delivery compared to conjugates with less chain length (e.g. LinOS). Also, the spermine conjugates with one saturated chain (e.g. OSS) resulted in better siEGFP-AF delivery compared to their unsaturated analogues (LinOS). Interestingly, EGFP silencing did not essentially directly relate to the amount of siEGFP-AF delivered. LinOS lipoplexes resulted in reduction of EGFP expression to 24% (3 μg lipid/well) and LigOS reduced EGFP expression to 56% (6 μg lipid/well), while LigOS resulted in 4-fold more delivery than LinOS. The SAR study showed that generally having one or two double bonds in the conjugated fatty acid chains enhance the resultant gene-silencing of the delivered siEGFP-AF when compared to saturated chains of same length. The cell viability 48 h post-transfection was above 74%, with LinOS at the best lipid/siNC ratio resulting in 88% cell viability.

In the next Chapter, coformulating asymmetrical LinOS with the neutral lipids cholesterol and DOPE will be investigated, aiming to enhance the amount of siEGFP-AF delivered to the cells, and evaluating the subsequent reduction of EGFP expression. These coformulation approaches will be carried out while maintaining the simple procedure for preparing the lipoplexes, i.e. lipid mixtures will be prepared without carrying out the traditional liposomal preparation protocols.

Chapter Five Quantitative silencing of EGFP reporter gene by self-assembled siRNA lipoplexes of mixtures of LinOS or DOS with either cholesterol or DOPE

1. Introduction

Small (or short) interfering RNA (siRNA) is a double-stranded RNA (dsRNA), typically 21-25 nucleotides per strand. Sequence-specific post-transcriptional gene silencing by siRNA has many potential therapeutic applications[1] as well as being an important tool in the study of functional genomics.

Gene silencing mediated by siRNA requires that the siRNA is protected from various exo- and endo-nucleases[44] and is delivered intact to the cytoplasm of the target cell.[39] The negative charges of the siRNA phosphate backbone must be masked to facilitate the siRNA-vector complex (lipoplex) binding to the cell membrane which is then followed by cellular entry of the lipoplex mainly via endocytosis and to a lesser extent by membrane fusion.[171] Thus, a vector is needed to fulfil these requirements. Non-viral vectors used for gene delivery (DNA based) and gene silencing by siRNA or shRNA include lipid-based vectors, polymer-based vectors e.g. polyethylenimine, carbohydrate-based polymers e.g. cyclodextrin and chitosan, dendrimers e.g. polyamidoamine[225] and polypropylenimine, and polypeptides.[82, 229-231] Lipid-based non-viral vectors are widely used for siRNA delivery.[196, 198, 218] Fatty acid derivatives of spermine (symmetrical N^1,N^{12}-diacyl and N^4,N^9-diacyl) were previously synthesized and tested for their ability to deliver non-silencing siRNA in vitro,[170, 182, 216] while in Chapter 4, the novel asymmetrical LinOS showed high gene-silencing efficiency.

In this Chapter, the formulations of the new spermine diacyl fatty acid derivative N^4-linoleoyl-N^9-oleoyl-1,12-diamino-4,9-diazadodecane (LinOS) are characterized in preparing self-assembled lipoplexes with siRNA either on its own (without a helper lipid) or in co-formulae with cholesterol or DOPE, and without pre-formulation of liposomes. The prepared lipoplexes were evaluated for their efficiency in delivering siRNA, in mediating gene-silencing, and for their effects on cell viability.

2. Material and methods

2.1. Materials and general methods

Chemicals were purchased from Sigma-Aldrich (Gillingham, UK) and solvents were purchased from Fisher Scientific UK (Loughborough, UK). All chemicals and cell culture media were purchased as described in Chapter 2 (Section 2.1). HeLa cells stably expressing EGFP were obtained from the Cell Service at Cancer Research UK (CRUK, London

Research Institute, Clare Hall Laboratories, South Mimms, London, UK). The high resolution (HR) time-of-flight mass spectra (MS) were obtained on a Bruker Daltonics micrOTOF mass spectrometer using electrospray ionisation (ESI). AllStars negative control siRNA (siNC) and it tagged with Alexa Fluor 647 (siNC-AF) at the 3'-position were purchased from Qiagen (Crawley, UK) as was siRNA against EGFP labelled with Alexa Fluor 647 (siEGFP-AF) at the 3'-position of the sense strand.

2.2. N^4-Linoleoyl-N^9-oleoyl-1,12-diamino-4,9-diazadodecane (LinOS) and N^4,N^9-dioleoyl-1,12-diamino-4,9-diazadodecane (DOS)

The authenticity of N^4-linoleoyl-N^9-oleoyl-1,12-diamino-4,9-diazadodecane (LinOS) was confirmed (HRMS, found $(M+H)^+$ 729.6980, $C_{46}H_{89}N_4O_2$ requires $(M+H)^+$ 729.6986) and N^4,N^9-dioleoyl-1,12-diamino-4,9-diazadodecane (DOS) (HRMS, found $(M+H)^+$ 731.7162, $C_{46}H_{91}N_4O_2$ requires $(M+H)^+$ 731.7137) by the HRMS of homogenous samples.

2.3. siRNA lipoplex preparation

LinOS, DOS, cholesterol, and DOPE were prepared as ethanolic solutions. For LinOS and DOS mixtures with cholesterol and DOPE, the required volumes of the ethanolic solutions of the single lipids were mixed together. To prepare the lipoplexes, two working liquids A and B were prepared. Liquid A was prepared by adding the required amount of siRNA (siEGFP-AF, siNC-AF, or siNC) to OptiMEM I media, such that the concentration of siRNA was adjusted to 1 pmol/µL. Liquid B was prepared by adding the required volume of lipid ethanolic solution to OptiMEM I media, such that the final concentration of LinOS or DOS was 0.75 µg/µL followed by mixing on a vortex mixer for 3 s. Liquid A was added to liquid B and they were mixed on a vortex mixer for 3 s. The lipoplex preparation was then simply allowed to stand for 20 min at 20 °C to allow lipoplex formation by charge neutralization and equilibration. TransIT-TKO was prepared according to the supplier's (Mirus) instructions.

2.4. Experimental Protocols

Transfection experiments were carried out on HeLa cells stably expressing EGFP using the protocol described in Chapter 2 (Section 2.4). Flow cytometry (FACS analysis) was carried out as described in Chapter 2 (Section 2.5). Confocal microscopy cell imaging was carried out as described in Chapter 2 Section 2.6. Cell viability assay was carried out as described in Chapter 2 (Section 2.7). Particle size and ζ-potential measurements were carried out as described in Chapter 2 (Section 2.8). Statistical analysis was carried out as described in Chapter 2 (Section 2.10).

2.8. Cryo-transmission electron microscopy (Cryo-TEM)

siNC lipoplexes were prepared with LinOS/Chol 1:2 (0.75 μg LinOS per 3.75 pmol siNC, *N/P* = 11.9) in 10 mM HEPES buffer. Cryo-transmission electron microscopy (Cryo-TEM) was kindly performed by J. M. Mantell (*School of Biochemistry and Wolfson Bioimaging Facility,* University of Bristol, *Bristol BS8 1TD,*). A sample (5 μL) was pipetted onto a previously glow discharged, lacy carbon-coated copper grid (Electron Microscopy Services). The excess was blotted and the sample plunge frozen into liquid ethane using a Vitrobot plunge freezer (FEI Company). The sample was transferred to a Gatan 626 Cryotransfer holder and the lipoplexes were examined at a temperature of approximately −170 °C in a FEI Tecnai 20 Transmission Electron Microscope operating at 200kV.

3. Results and discussion

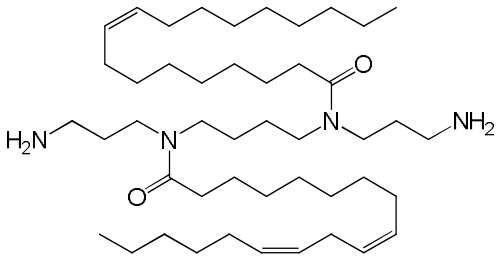

(1a)

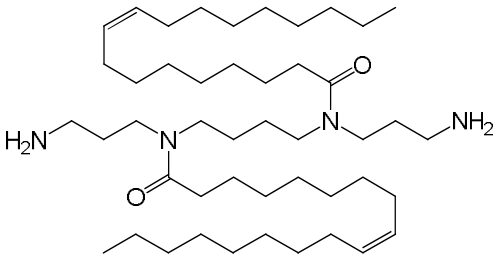

(1b)

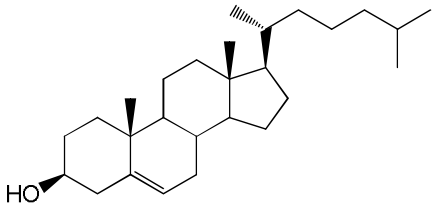

(1c)

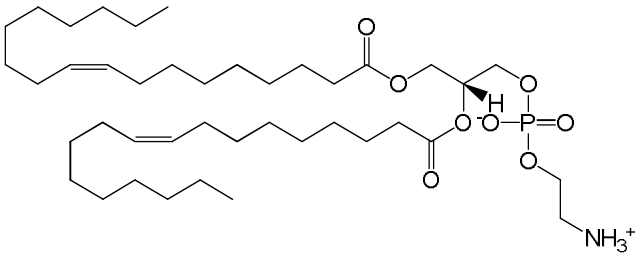

(1d)

Figure 1. (a) N^4-Linoleoyl-N^9-oleoyl-1,12-diamino-4,9-diazadodecane (LinOS), (b) N^4,N^9-dioleoyl-1,12-diamino-4,9-diazadodecane (DOS), (c) cholesterol, (d) 1,2-dioleoyl-*sn*-glycero-3-phosphoethanolamine (DOPE).

The lipid dispersions in Opti-MEM media were prepared by addition of ethanolic solutions of the single lipids (Figure 1) or lipid mixtures to Opti-MEM followed by brief mixing on a vortex mixer. This simple procedure avoids the use of sonication or extrusion techniques which are used to prepare single lamellar vesicles and/or reduce the size of the prepared lipid vesicles. This procedure can be considered as an even more direct method than the ethanol injection vesicle protocol.[232, 233]

Figure 2 shows the effect of changing the N^4-linoleoyl-N^9-oleoyl-1,12-diamino-4,9-diazadodecane/ cholesterol (LinOS/Chol) molar ratio on the delivery of siEGFP-AF or siNC-AF in the transfected HeLa cells measured by flow cytometry (FACS). The highest siEGFP-AF delivery was achieved with lipoplexes having a LinOS/Chol molar ratio of 1:2, as these lipoplexes resulted in normalized Alexa Fluor 647 (AF647) fluorescence of 250. The difference between the value obtained by lipoplexes of LinOS/Chol 1:2 and the closest value of 165 of lipoplexes of LinOS/Chol 1:3 was statistically significant (p = 0.0005). Decreasing the molar ratio of LinOS/Chol from 3:1 to 1:2, i.e. increasing the amount of cholesterol in the mixtures, resulted in an increase in the AF647 fluorescence from 11 to 250 respectively. Co-formulation with cholesterol in the lipoplexes of LinOS/Chol 1:2 resulted in a significant increase of AF647 fluorescence when compared with lipoplexes of LinOS only, from 6 with LinOS lipoplexes to 250 with LinOS/Chol 1:2 lipoplexes which means a ~42-fold increase in siEGFP-AF delivery. The cholesterol data column (Chol) shows that cholesterol alone did not result in any significant siEGFP-AF delivery. Lipoplexes of siNC-AF and LinOS/Chol 1:2 resulted in comparable delivery of siNC-AF when compared with lipoplexes of siEGFP-AF and LinOS/Chol 1:2, Alexa Fluor 647 fluorescence of 268 and 250 respectively (p = 0.28).

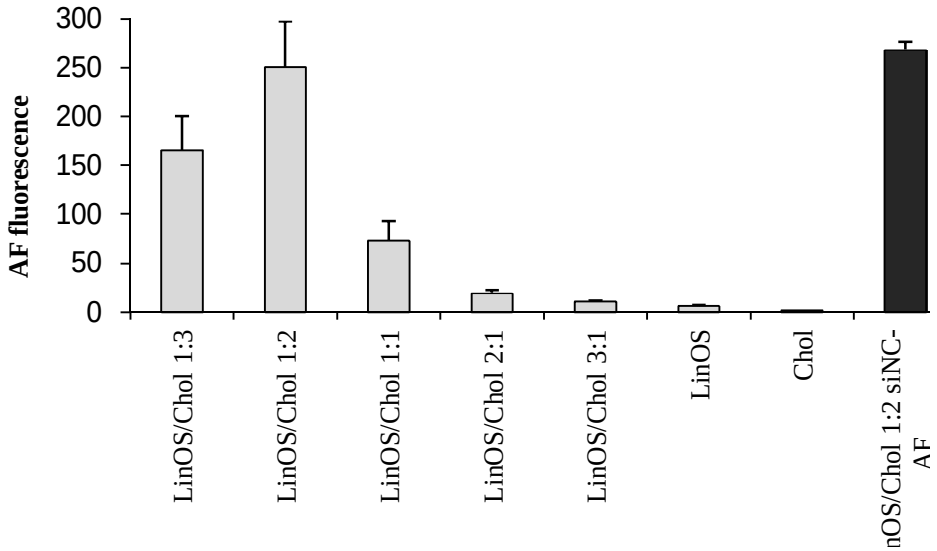

Figure 2. siEGFP-AF delivery to HeLa cells expressed as the normalized values of the geometric mean fluorescence intensity of Alexa Fluor 647 (AF fluorescence) 48 h post-transfection of HeLa cells with the lipoplexes prepared with LinOS/Chol and either siEGFP-AF at different LinOS/Chol ratios or siNC-AF at LinOS/Chol 1:2 (per well, the amounts of LinOS, siEGFP-AF, and siNC-AF were kept constant at 0.75 µg, 15 pmol, and 15 pmol respectively, *N/P* = 3.0). The LinOS/Chol ratio is the molar ratio. Light grey columns represent lipoplexes prepared with siEGFP-AF, the black column represents lipoplexes of LinOS/Chol 1:2 with siNC-AF.

Figure 3 shows the effect of changing the LinOS/Chol molar ratio from 3:1 to 1:3 on the percentage expression of EGFP in the transfected HeLa cells measured by FACS. The best lipoplexes were those having LinOS/Chol ratio of 1:2, as they resulted in a reduction of EGFP percentage expression to 20%, statistically significant when compared to the reduction of EGFP obtained by lipoplexes of LinOS/Chol 1:3 (26%, $p = 0.0024$) and LinOS/Chol 1:1 (27%, $p = 0.0001$) which were the second best in terms of EGFP expression reduction. Co-formulation with cholesterol in lipoplexes of LinOS/Chol 1:2 resulted in reducing the EGFP percentage expression from 32% for lipoplexes of LinOS only to 20% ($p = 0.0001$). The cholesterol data column (Figure 3) shows that siEGFP-AF only formulated with cholesterol did not have any significant effect on EGFP expression (100% ± 5). Lipoplexes of siNC-AF and LinOS/Chol 1:2 likewise did not result in any reduction in EGFP expression (105% ± 5). Transfection of siEGFP-AF with the commercial reagent TransIT-TKO resulted in EGFP expression of only 20%. There was no statistically significant difference between the percentage reductions of EGFP expression due to transfection with lipoplexes of LinOS/Chol 1:2 and TransIT-TKO ($p > 0.05$).

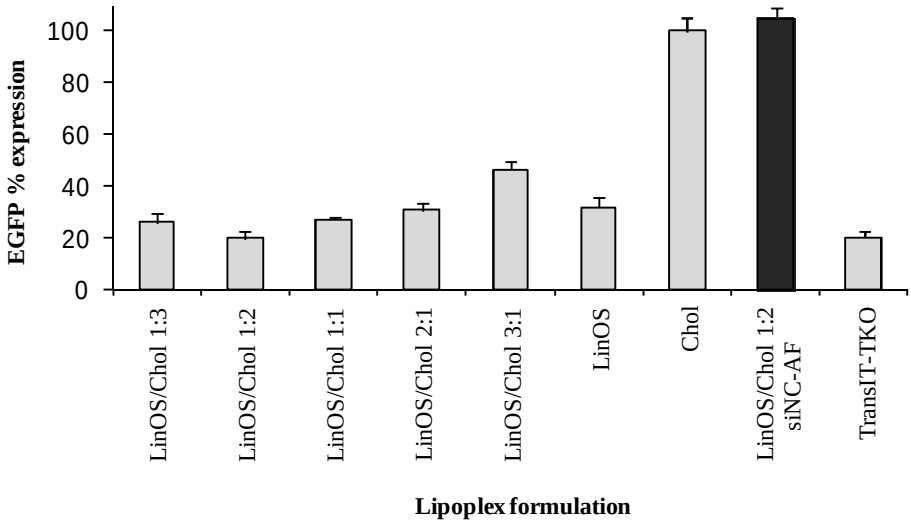

Figure 3. EGFP percentage expression calculated 48 h post-transfection of HeLa cells with the lipoplexes prepared with LinOS/Chol and either siEGFP-AF at different LinOS/Chol ratios or siNC-AF at LinOS/Chol 1:2 (per well, the amounts of LinOS, siEGFP-AF, and siNC-AF were kept constant at 0.75 µg, 15 pmol, and 15 pmol respectively, *N/P* = 3.0). Light grey columns represent lipoplexes prepared with siEGFP-AF, the black column represents lipoplexes of LinOS/Chol 1:2 with siNC-AF.

LinOS/Chol 1:2 lipoplexes with siEGFP-AF resulted in both highest siRNA delivery and most efficient reduction of EGFP (from 100% to 20%). The reduction of EGFP with

LinOS/Chol lipoplexes having different LinOS/Chol ratios is affected by the amount of siEGFP-AF delivered. However, it can be seen that although siRNA delivery with lipoplexes of LinOS/Chol of molar ratio 1:2 and 3:1 was 250 and 11 respectively (~23-fold), the reduction of EGFP was to 20% and to 46% (~2-fold). Thus, it is difficult to predict the functional biological activity of siRNA based solely on the amount delivered. One explanation is that siRNA lipoplexes might be delivered via different cellular internalization pathways such as clathrin- or caveolin-mediated endocytosis and/or membrane fusion. A recent report showed that the functional delivery of siRNA lipoplexes is not necessarily via endocytic pathways, but rather might be due to another cellular internalization mechanism such as membrane fusion.[171] Although the amounts of siRNA delivered might vary largely, the resultant reduction in EGFP may not correspond exactly with that same large variation.

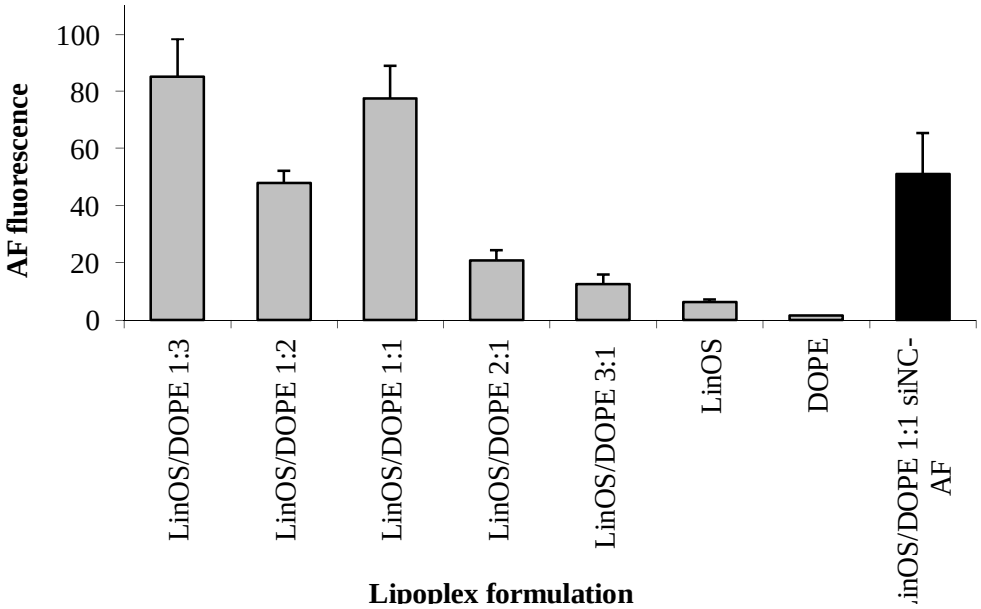

Figure 4. siEGFP-AF delivery to HeLa cells expressed as the normalized values of the geometric mean fluorescence intensity of AF647 48 h post-transfection with the lipoplexes prepared with LinOS/DOPE and siEGFP-AF at different LinOS/DOPE ratios (per well, the amounts of LinOS and siEGFP-AF were kept constant at 0.75 µg and 15 pmol respectively, *N/P* = 3.0). Light grey columns represent lipoplexes prepared with siEGFP-AF, the black column represents lipoplexes of LinOS/DOPE 1:1 with siNC-AF.

Figure 4 shows the effect of changing the LinOS/1,2-dioleoyl-*sn*-glycero-3-phosphoethanolamine (DOPE) molar ratio from 1:3 to 3:1 on the delivery of siEGFP-AF or siNC-AF in the transfected HeLa cells. Co-formulation with DOPE in the lipoplexes of LinOS/DOPE resulted in a significant increase of normalized AF647 fluorescence when

compared with lipoplexes of LinOS only, from 6 with LinOS only to 85 and 78 respectively (p = 0.24) for lipoplexes of LinOS/DOPE 1:3 and 1:1 which gave the highest AF647 fluorescence. Lipoplexes of LinOS/DOPE 1:2 and 2:1 (molar ratios) resulted in AF647 fluorescence of 48 and 21 respectively (p = 0.0001). The DOPE data column shows that siEGFP-AF formulation with DOPE only did not result in any significant siEGFP-AF delivery. Lipoplexes of siNC-AF and DOPE/Chol 1:1 resulted in AF647 fluorescence of 51.

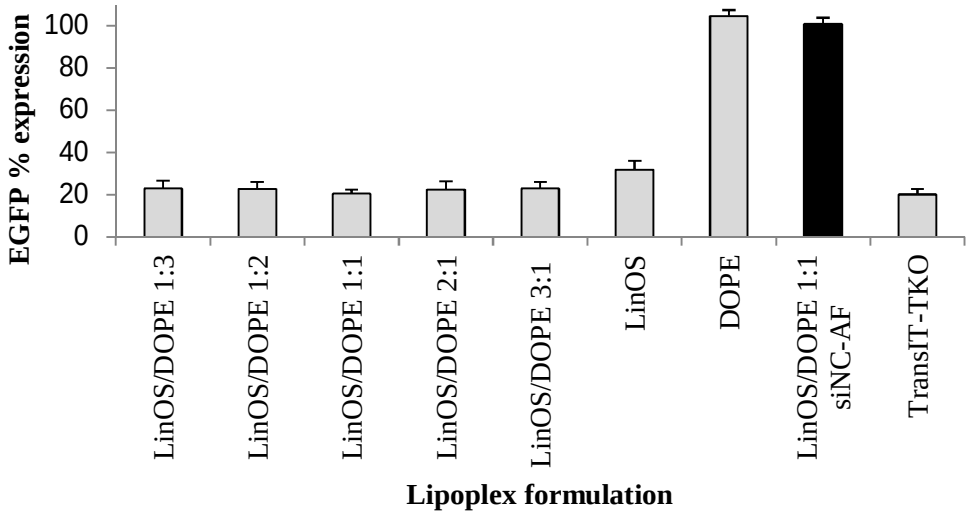

Figure 5. EGFP percentage expression calculated 48 h post-transfection of HeLa cells with the lipoplexes prepared with LinOS/DOPE and siEGFP-AF at different LinOS/DOPE ratios (per well, the amounts of LinOS and siEGFP-AF were kept constant at 0.75 µg and 15 pmol respectively, *N/P* = 3.0). Light grey columns represent lipoplexes prepared with siEGFP-AF, the black column represents lipoplexes of LinOS/DOPE 1:1 with siNC-AF.

Figure 5 shows the effect of changing the LinOS/DOPE molar ratio from 1:3 to 3:1on the percentage expression of EGFP in the transfected HeLa cells. There were very little differences between the percentage expressions of EGFP after transfection with the LinOS/DOPE lipoplexes at all LinOS/DOPE ratios, with LinOS/DOPE 1:1 lipoplexes resulting in EGFP percentage expression of 21%, and no statistically significant difference was found between any of the EGFP percentage expressions resulting from the transfection with the LinOS/DOPE lipoplexes. Co-formulation with DOPE in the lipoplexes of LinOS/DOPE 1:1 resulted in reducing the EGFP percentage expression from 32% for lipoplexes of LinOS to 21% (p = 0.0001). The DOPE data column shows that formulating siEGFP-AF with DOPE only did not result in any significant effect on EGFP expression (105% ± 3). Lipoplexes of siNC-AF and LinOS/DOPE 1:1 did not result in any reduction in

EGFP expression (101% ± 3). There was no statistically significant difference between the percentage expressions of EGFP after transfection with lipoplexes of LinOS/DOPE 1:1 and TransIT-TKO (p = 0.49). Although the amount of delivered siEGFP-AF increased markedly with the addition of DOPE, the differences in the delivered amount did not reflect significant differences in the reduction of EGFP corresponding to the differences in the delivered amount. For example, lipoplexes of LinOS/DOPE 1:1 and 3:1 delivered siEGFP-AF with values of 78 and 12 respectively, and reduced EGFP (from 100%) to 21% and 23% word><keyword>ohese data, as discussed above with LinOS/Chol lipoplexes, reflect the possibility of the presence of a specific functional mechanism which results in the required specific gene silencing.[171]

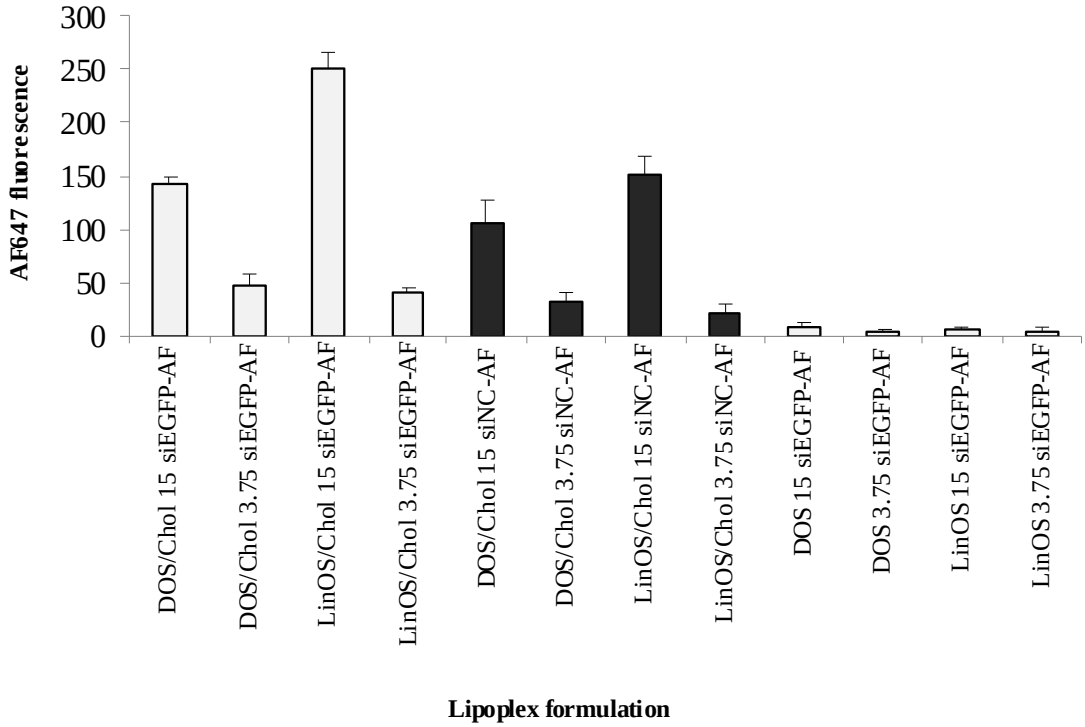

Figure 6. siEGFP-AF delivery to HeLa cells 48 h post-transfection with the lipoplexes prepared with LinOS/Chol 1:2 or DOS/Chol 1:2 at *N/P* = 3.0 or *N/P* = 11.9 (per well, the amounts of LinOS and DOS were kept constant at 0.75 μg). Lipoplexes names ending in 15 and 3.75 represent lipoplexes prepared with 15 pmol and 3.75 pmol respectively of siEGFP-AF or siNC-AF. Light grey columns represent lipoplexes prepared with siEGFP-AF, black columns represent lipoplexes prepared with siNC-AF.

Figure 6 shows the effect of changing the *N/P* charge ratio from 3.0 to 11.9 by means of reducing the amount of siEGFP-AF (or siNC-AF) from 15 pmol/well of 24-well plates to 3.75 pmol/well, on the normalized AF647 fluorescence in the transfected cells. A comparison between the LinOS/Chol 1:2 lipoplexes and N^4,N^9-dioleoyl-1,12-diamino-4,9-

diazadodecane/cholesterol (DOS/Chol) 1:2 lipoplexes at *N/P* = 3.0 and 11.9 is also shown. The AF647 fluorescence is significantly higher in the case of lipoplexes prepared with 15 pmol siEGFP-AF or siNC-AF when compared to the lipoplexes prepared with 3.75 pmol siEGFP-AF or siNC-AF at *N/P* = 11.9. siEGFP-AF lipoplexes LinOS/Chol 15 and LinOS/Chol 3.75 resulted in AF647 fluorescence of 250 and 41 respectively and $p = 0.0001$, siNC-AF lipoplexes LinOS/Chol 15 and LinOS/Chol 3.75 resulted in AF647 fluorescence of 151 and 23 respectively and $p = 0.0001$. siEGFP-AF lipoplexes of DOS/Chol 15 and DOS/Chol 3.75 resulted in AF647 fluorescence of 144 and 48 respectively and $p = 0.0001$, siNC-AF lipoplexes of DOS/Chol 15 and DOS/Chol 3.75 resulted in AF647 fluorescence of 106 and 32 respectively and $p = 0.0001$. Lipoplexes of LinOS/Chol 15 showed the highest AF647 fluorescence. The delivery of AF647 results from transfecting HeLa cells with lipoplexes co-formulated with cholesterol were significantly higher than those achieved on transfection with only DOS or LinOS lipoplexes (DOS 15, DOS 3.75, LinOS 15, and LinOS 3.75, Figure 6 the four columns on the right) of siEGFP-AF.

Figure 7 shows the effect of changing the *N/P* charge ratio from 3.0 to 11.9 by reducing the amount of siEGFP-AF (or siNC-AF) from 15 pmol/well to 3.75 pmol/well (24-well plates), on the percentage of EGFP expression in the transfected HeLa cells (48 h post-transfection) investigated together with a comparison between LinOS/Chol 1:2 lipoplexes and DOS/Chol 1:2 lipoplexes at *N/P* = 3.0 and 11.9. The amounts of LinOS and DOS were kept constant at 0.75 µg. Transfecting HeLa cells with lipoplexes of siEGFP-AF and LinOS/Chol 1:2 did not show a significant decrease in the efficiency of transfection on decreasing the amount of siEGFP-AF from 15 pmol/well to 3.75 pmol/well. Thus, lipoplexes of LinOS/Chol 15 and LinOS/Chol 3.75 resulted in EGFP percentage expression of 20% and 21% respectively with $p = 0.42$. Lipoplexes of DOS/Chol 1:2 showed a significant change of EGFP percentage expression from 21% for DOS/Chol 15 to 28% for DOS/Chol 3.75 lipoplexes (with siEGFP-AF 15 pmol and 3.75 pmol respectively). There were no statistically significant differences between the EGFP percentage expression on transfection with lipoplexes of siEGFP-AF with either DOS/Chol 15 or LinOS/Chol 15 (21% and 20% respectively, $p = 0.42$). However, transfection with lipoplexes of LinOS/Chol 3.75 resulted in a lower EGFP percentage expression (21%) compared to lipoplexes of DOS/Chol 3.75 (28%), $p = 0.0001$. Transfection with lipoplexes of siNC-AF (15 pmol or 3.75 pmol) with DOS/Chol 1:2 or LinOS/Chol 1:2 did not result in any significant reduction of the EGFP expression. However, delivery of siEGFP-AF in co-formulations of DOS or LinOS with cholesterol led to statistically significant enhancement of gene silencing, i.e. a large reduction in EGFP percentage expression in the transfected HeLa cells: DOS/Chol 15, DOS/Chol 3.75, LinOS/Chol 15, and LinOS/Chol 3.75 were 21%, 28%, 20%, and 21% (each ± 2%) respectively, compared to DOS 15, DOS 3.75, LinOS 15, and LinOS 3.75 lipoplexes which

resulted in EGFP percentage expressions of 37%, 38%, 32%, and 35% (each ±5%) respectively, showing significant improvements in the gene silencing on mixing with cholesterol (p = 0.0001 for all four respectively). With EGFP having a half-life of ~24 h,[234] gene silencing to 20% (48 h post-transfection) is essentially quantitative as the fluorescence which equates to 20% EGFP expression is the residual EGFP after two half-lives.

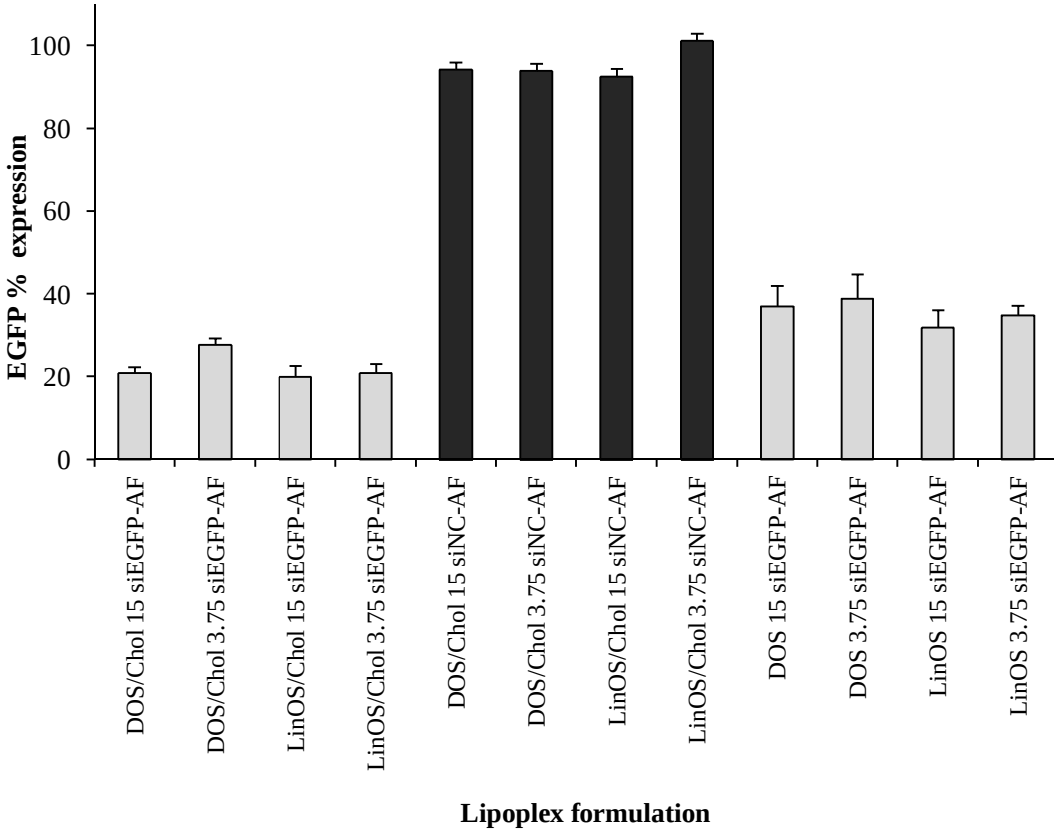

Figure 7. EGFP percentage expression 48 h post-transfection with lipoplexes prepared with LinOS/Chol 1:2 or DOS/Chol 1:2 at *N/P* = 3.0 or *N/P* = 11.9 (per well, the amounts of LinOS and DOS were kept constant at 0.75 μg). Lipoplex names followed by 15 and 3.75 represent lipoplexes prepared with 15 pmol and 3.75 pmol respectively of siEGFP-AF or siNC-AF. Light grey columns represent lipoplexes prepared with siEGFP-AF. Black columns represent lipoplexes prepared with siNC-AF.

Figure 6 shows that the amount of siEGFP-AF delivered with either DOS/Chol or LinOS/Chol lipoplexes prepared with 15 pmol siEGFP-AF was higher by ~3-fold and 5-fold respectively when compared to lipoplexes prepared with 3.75 pmol siEGFP-AF. However, the reduction in EGFP expression (Figure 7) of the DOS/Chol or LinOS/Chol lipoplexes prepared with either 15 pmol or 3.75 pmol only varied slightly.

Table 1. Effect of formulation on the particle size, polydispersity index (PDI), and ζ-potential of lipoplexes of LinOS, DOS, DOS/Chol, LinOS/Chol, and LinOS/DOPE mixtures. All lipoplexes were prepared with either 15 pmol siNC (*N/P* = 3.0) or 3.75 pmol siNC (*N/P* = 11.9) except for LinOS/DOPE which was prepared with 15 pmol siNC only (*N/P* = 3.0). The cationic lipid/helper lipid ratios which resulted in the best reduction in EGFP expression post-transfection with siEGFP-AF lipoplexes were selected (Figures 3, 5, and 7) (n = 2, triplicates of duplicates).

Lipoplex formulation	**Particle size (nm) Mean ± SD**	**PDI Mean ± SD**	**ζ-Potential (+mV) Mean ± SD**
DOS/Chol 1:2 15 pmol siNC	106 ± 19	0.35 ± 0.04	58 ± 4
DOS/Chol 1:2 3.75 pmol siNC	127 ± 8	0.37 ± 0.02	60 ± 5
LinOS/Chol 1:2 15 pmol siNC	113 ± 13	0.34 ± 0.05	60 ± 4
LinOS/Chol 1:2 3.75 pmol siNC	118 ± 6	0.35 ± 0.06	56 ± 1
DOS 15 pmol siNC	356 ± 37	0.48 ± 0.06	56 ± 2
DOS 3.75 pmol siNC	192 ± 10	0.32 ± 0.05	52 ± 4
LinOS 15 pmol siNC	294 ± 25	0.41 ± 0.06	53 ± 3
LinOS 3.75 pmol siNC	194 ± 9	0.33 ± 0.04	60 ± 3
LinOS/DOPE 1:1 15 pmol siNC	685 ± 83	0.66 ± 0.08	64 ± 4

Self-assembled lipoplexes of siRNA and cholesterol co-formulations with DOS or LinOS resulted in particle size in the range of 106-127 nm. There were a slight increase in particle size in lipoplexes of DOS/Chol 1:2 from 106 nm to 127 nm upon decreasing the amount of siRNA from 15 pmol to 3.75 pmol (increasing *N/P* charge ratio from 3.0 to 11.9), $p = 0.0317$. There was no statistically significant difference between the particle sizes of lipoplexes of LinOS/Chol 1:2 with either 15 or 3.75 pmol ($p = 0.41$). The type of cationic lipid used (DOS or LinOS) in the cholesterol mixtures did not have a significant effect on the resulting particle size at the same *N/P* charge ratio (same amount of siRNA), where DOS/Chol and LinOS/Chol lipoplexes at *N/P* = 3.0 (15 pmol siRNA) resulted in particle size of 106 and 113 respectively ($p = 0.47$), and DOS/Chol and LinOS/Chol lipoplexes at *N/P* = 11.9 (3.75 pmol siRNA) resulted in particle size of 127 and 118 respectively ($p = 0.05$). Lipoplexes prepared with siRNA and either DOS or LinOS, without any helper lipid, have a particle size in the range of 192-356 nm. There was a statistically significant difference between the DOS and

the LinOS lipoplex particle sizes (356 and 294 respectively, $p = 0.0068$) at $N/P = 3.0$ (15 pmol siRNA). At $N/P = 11.9$, the type of cationic lipid did not affect the particle size, with lipoplexes of DOS and LinOS having particle sizes of 192 and 194 respectively ($p = 0.72$). Increasing the N/P charge ratio to 11.9 (lowering the siRNA amount from 15 to 3.75 pmol) reduced the lipoplexes particle size from 356 to 192 nm (DOS, $p = 0.0001$) and 294 to 194 nm (LinOS, $p = 0.0001$). Co-formulation with cholesterol resulted in significant reduction of the prepared lipoplexes size, when comparing the lipoplexes of each cationic lipid with or without cholesterol. The particle sizes of DOS/Chol 15, DOS/Chol 3.75, LinOS/Chol 15 , LinOS/Chol 3.75 (106, 127, 113, and 118 nm respectively) are significantly reduced compared to DOS 15, DOS 3.75, LinOS 15, and LinOS 3.75 (356 nm; $p = 0.0001$, 192 nm; $p = 0.0001$, 294 nm; $p = 0.0001$, and 194 nm; $p = 0.0001$ respectively). The lipoplexes of LinOS/DOPE 1:1 and 15 pmol siRNA (N/P =3.0) had the relatively larger particle size of 685 nm compared to the other lipoplex formulations.

The ζ-potentials of the prepared lipoplexes were all positive and in the range 53-64 mV. There was no significant effect of the co-formulation with cholesterol on the ζ-potentials of their prepared lipoplexes compared to the lipoplexes of their cationic lipids without cholesterol. The presence of DOPE caused no or only a very slight increase in the lipoplex ζ-potential (+64 mV) when compared to the other lipoplexes prepared with the same amount of siRNA (15 pmol) at the same $N/P = 3.0$.

Lipoplex size is an important factor in transfection efficiency though it is not the only determinant factor.[213] Cationic cholesterol derivatized liposomes complexed with siRNA have a size range of 150-500 nm,[172] where selected siRNA lipoplexes were used either to deliver fluorescently tagged scrambled siRNA to different cell lines including HeLa cells, or to deliver siRNA silencing GFP in a 293T cell line that stably expresses GFP. Lipoplex size affects the main route of cellular entry where smaller lipoplexes (diameter < 300 nm) are likely to enter by clathrin-mediated endocytosis, while larger particles (diameter > 500 nm) enter cells by caveoli-mediated endocytosis.[214, 215] Also, the entry route that results in functional siRNA mediated gene knock-down might be by fusion with the plasma membrane rather than the endocytosis pathway.[171] In a report earlier this year, functional delivery of lipoplexes of oligonucleotides in two cell lines, including a HeLa S3 cell line, was found to be by membrane fusion.[235] The authors concluded that lipoplexes internalized in cells by direct membrane fusion improve the functional delivery of oligonucleotide cargoes because they might avoid the endosomal escape step which is the rate-limiting step for many pDNA and siRNA delivery vectors. However, the lipoplex size used in that study was 869 nm.[235]

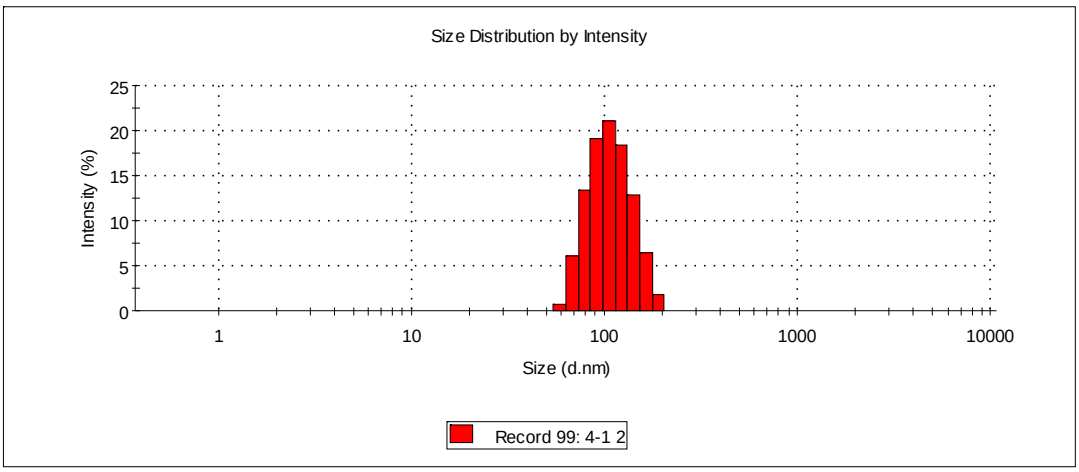

(8a)

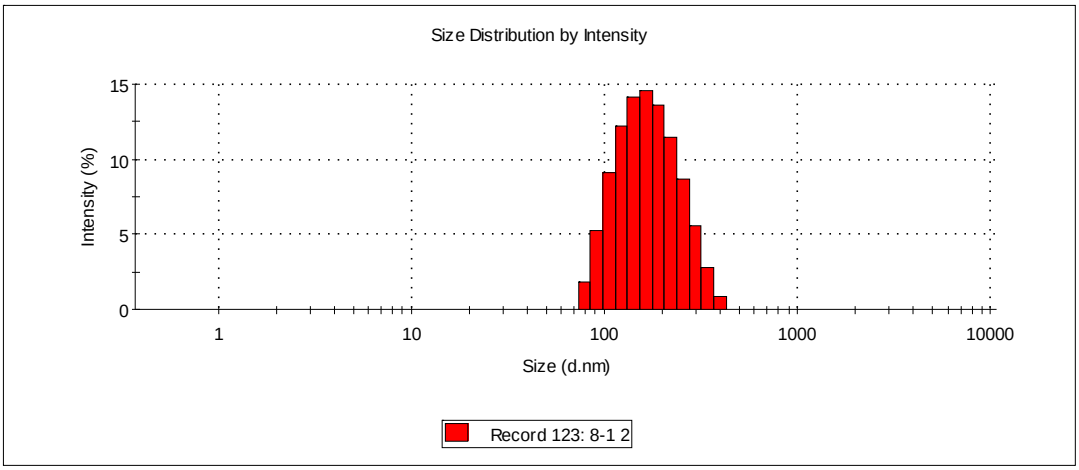

(8b)

Figure 8. (a) Particle size distribution (DLS) for LinOS/Chol 1:2 lipoplexes prepared with 3.75 pmol siNC (*N/P* = 11.9), the hydrodynamic diameter is 117 nm (polydispersity index, PDI = 0.31). (b) Particle size distribution (DLS) for LinOS (only) lipoplexes prepared with 3.75 pmol siNC (*N/P* = 11.9), the hydrodynamic diameter is 187 nm (PDI = 0.38) for the shown lipoplexes.

Shown in Figure 8 are monomodal populations of LinOS/Chol 1:2 and LinOS (only) lipoplexes. The polydispersity indices (PDI) of the lipoplexes (Table 1) prepared with LinOS or DOS cholesterol mixtures were 0.35-0.37. There was no effect of changing the siRNA amount in the LinOS/Chol or DOS/Chol lipoplexes on the PDI. The PDI of lipoplexes prepared with the cationic lipids only varied from 0.32–0.48. Decreasing the amount of siRNA (thus increasing *N/P* from 3.0 to 11.9) in LinOS or DOS lipoplexes resulted in a decrease in the PDI from 0.48 to 0.32 and 0.41 to 0.33 respectively (p = 0.0217 and 0.0005). The lipoplexes of LinOS/DOPE 1:1 resulted in a higher PDI of 0.66.

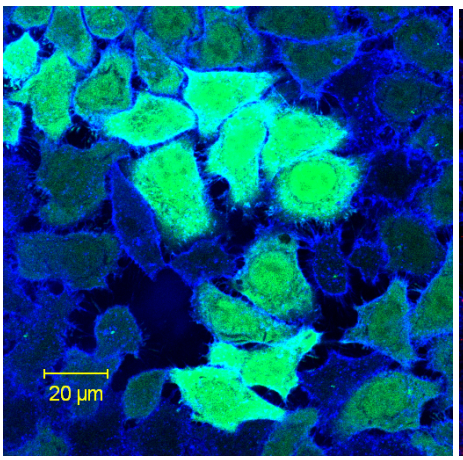

(9a)

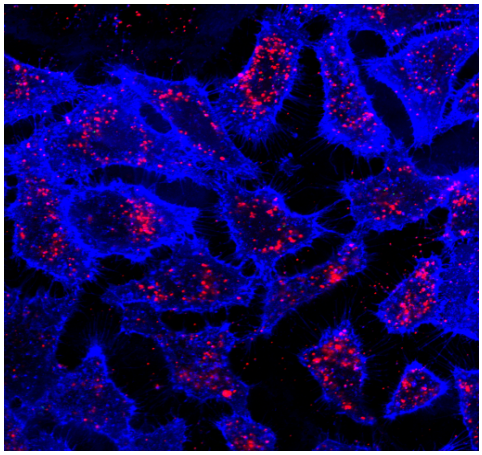

(9b)

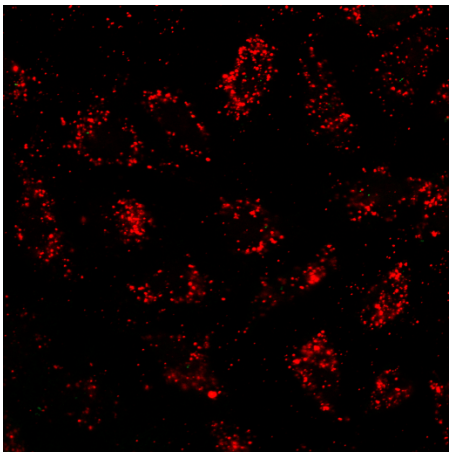

(9c)

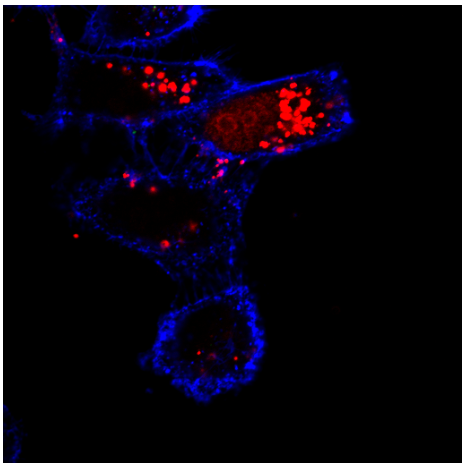

(9d)

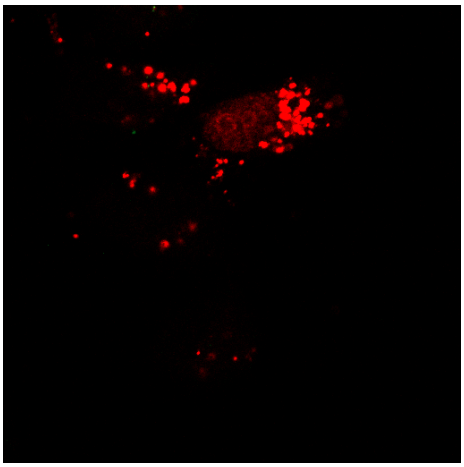

(9e)

Figure 9. Confocal photomicrographs. EGFP fluorescence (green), cell membrane stained with WGA-Alexa Fluor 555 (blue), and Alexa Fluor 647 (red) shows tagged siEGFP-AF delivery. (a) Control non-transfected HeLa cells, (b) HeLa cells 48 h post-transfection with lipoplexes of LinOS/Chol 1:2 and siEGFP-AF (3.75 pmol), (c) as (d) with the red channel only, (d) and (e) magnified HeLa cells 48 h post-transfection, as in (b) and (c) respectively.

Confocal photomicrographs show control non-transfected HeLa cells, Figure 9a the EGFP (green colour) contained within the cell membrane (blue colour). Post-transfection (48 h) with siEGFP-AF, the EGFP expression was reduced (Figure 9b 63x objective, scan zoom 1.0) as the green colour largely faded away and the red colour represents the delivered siEGFP-AF. Figure 9c is as Figure 9b with the red channel only turned on for better visualization of the delivered siEGFP-AF. Figure 9d is a zoomed photomicrograph (63x objective, 1.7 scan zoom), and Figure 9e is as Figure 9d with the red channel only turned on. Figure 9b and Figure 9d show the reduction of EGFP expression compared to control cells, with the red colour of delivered siEGFP-AF. The photomicrographs in Figure 9 prove that siEGFP-AF was delivered to the EGFP-stably transfected HeLa cells, and also that EGFP gene expression was silenced.

Z-Stacks are a series of successive optical sections acquired at different positions across the Z-axis defining the thickness of the sample perpendicular to the sample's horizontal XY plane and therefore they are useful for visualizing three-dimensional structures. To characterize the intracellular delivery of siEGFP-AF further, Z-stack photomicrographs were recorded through a monolayer of transfected HeLa cells (Figure 10). In order to record such a stack, the experiment was set up such that the first optical section was recorded slightly lower than the surface of the cells attached to the cover slip, then the sections were recorded while slicing through to the opposite surface. This arrangement allows to identify whether the red colour (representing siRNA delivery) is present inside the cell, where there will be no blue colour (representing cell membrane) associated with the red colour, or the red colour is present on/in the cell membrane, in this case the red colour will be present simultaneously with the blue colour of the cell membrane. It can be seen in the series of Z-stack photomicrographs starting from the top left (Figure 10), that the red colour appears in the centre of the cells, the blue colour is present only in the perimeter of the cells, and there is no simultaneous blue colour in the middle of the cells where there is red. Thus, it is concluded that the majority of the delivered siRNA is present inside the HeLa cells. Minko and co-workers have reported the use of Z-stack photomicrographs to characterize the orientation of the delivered siRNA, where a siRNA tagged with NuLight DY-547 fluorophore was delivered to A2780 human ovarian cancer cells by surface neutral while internally cationic polyamidoamine dendrimers.[225]

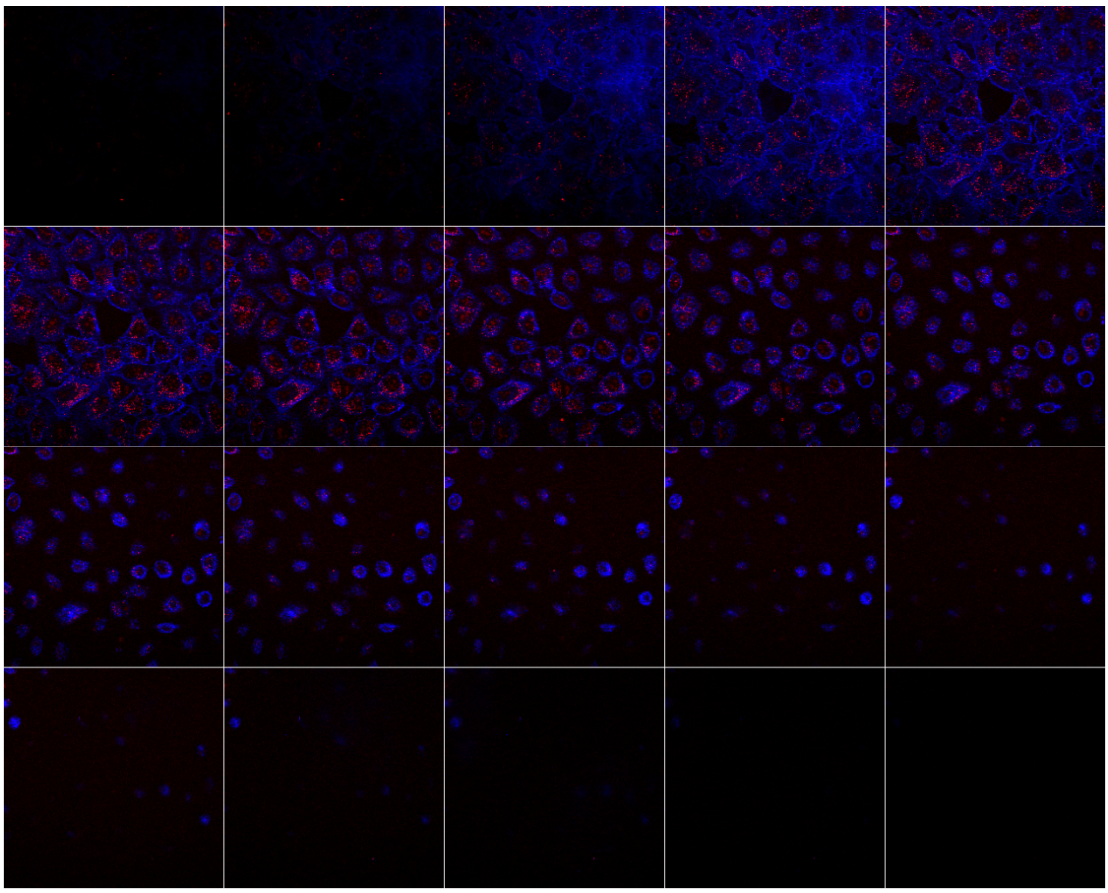

Figure 10. Z-Stack confocal photomicrographs. EGFP fluorescence (green), cell membrane stained with WGA-Alexa Fluor 555 (blue), and Alexa Fluor 647 (red) represents tagged siRNA delivery. A Z-stack series of photomicrographs representing 20 Z-sections in HeLa cells transfected with lipoplexes of LinOS/Chol 1:2 and siEGFP-AF (3.75 pmol).

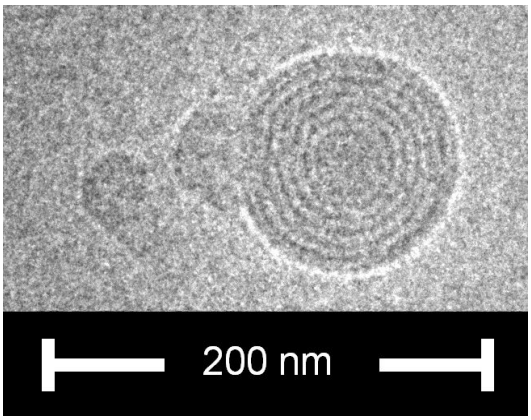

Figure 11. Cryo-TEM of LinOS/Chol (1:2) siRNA lipoplexes.

Lipoplexes prepared with LinOS/Chol 1:2 and siRNA form spherical multilamellar arrangements (Figure 11) with a size of ~100 nm which is in good agreement with the particle size measured by DLS (Table 1) of the same lipoplexes. The constant distance between lamellar repeats is ~6 nm, with the electron-dense layers fitting a monolayer of siRNA. Recent cryo-TEM photomicrographs of lipidic aminoglycoside derivatives/siRNA self-assembled lamellar complexes show concentric onion-like structures with the distance between the lamellar repeats being 7 nm.[236] Such siRNA lipoplexes promote efficient siRNA delivery and RNA interference.

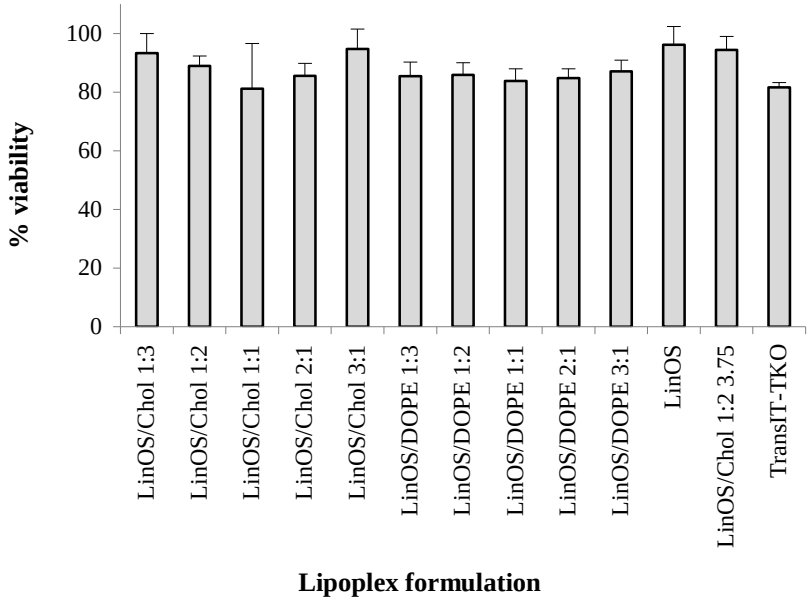

Figure 12. Viability of transfected HeLa cells measured using the alamarBlue assay 48 h post-transfection with lipoplexes prepared with siNC and either LinOS/Chol or LinOS/DOPE at different LinOS/neutral lipid ratios. All were assayed at 1.5 pmol siNC/well (15 nM), 6,500 cells/well, except LinOS/Chol 1:2 3.75 which had only 0.375 pmol siNC/well (3.75 nM).

Transfection of HeLa cells with lipoplexes of LinOS/Chol and LinOS/DOPE at different molar ratios and 1.5 pmol siRNA in 96-well plates (Figure 12), *N/P* = 3.0, resulted in cell viabilities of 81-95% of the control cells. The viability resulting from transfection using LinOS (only) lipoplexes was 96% at *N/P* = 3.0. Transfection with LinOS/Chol 1:2 3.75 resulted in viability of 94%, higher than that of LinOS/Chol 1:2 (89%, $p = 0.0205$). These values are significantly higher than the cell viability on transfection with TransIT-TKO (82%, $p = 0.0001$ for both). There were small differences in viabilities between LinOS/Chol lipoplexes (81-95%) and LinOS/DOPE lipoplexes (84-87%). Although the amount of lipoplexes chosen in this assay was only one tenth that used in the 24-well plate assays (for

delivery and gene silencing experiments), the siRNA concentration was kept constant in the culture medium in all experiments, i.e. either 15 nM or 3.75 nM.

In this Chapter, the efficiency of both siRNA delivery and the gene silencing by siRNA lipoplexes prepared from mixtures of LinOS or DOS with either cholesterol or DOPE neutral helper lipids was evaluated. LinOS and DOS are derivatives of the naturally occurring polyamine, spermine, that has been conjugated to the naturally occurring C18 unsaturated fatty acids: oleic acid (18:1) and/or linoleic acid (18:2). The design of LinOS and DOS is based on the hypothesis that using such natural moieties as the building blocks in the synthetic lipid will result in more benign (less toxic) cationic lipids and that better interactions (mixing) with bilayers of both the cell membrane and the endosomal membranes of target cells will increase cellular delivery efficiency and endosomal escape.

Cholesterol and DOPE are widely used as helper lipids in DNA liposome and lipoplex preparations,[237] mainly due to their ability to promote non-lamellar lipid arrangements and thus facilitate membrane fusion upon cellular internalization. Herein is reported an important increase in both siRNA delivery and the resultant gene silencing efficiency with an increase in the cholesterol content of the lipoplexes (Figure 2 and Figure 3). Cholesterol enhances transfection with DNA lipoplexes by increasing DNase resistance and cholesterol nanodomains are known to form in lipoplexes having $\geq$ 52% of molar cholesterol content. [238, 239] The presence of cholesterol domains in the lipoplexes prepared with $\geq$ 60% molar cholesterol content was suggested to result in an increasing resistance to lipoplex aggregation in the presence of 50% serum, and decreased albumin binding to the lipoplexes led to better interaction (fusion) with the cell membrane.[239] Cholesterol and DOPE facilitate the conversion of the lipoplex lamellar phase (L_α) into the non-lamellar inverted hexagonal (H_{II}) and cubic phases which play an important role in membrane fusion.[237, 240, 241] In early and elegant siRNA SNALP delivery studies, MacLachlan and co-workers reported on the importance of the saturation of C=C along the lipids chains.[158] They found that, in an series of symmetrical 1,2-dialkyloxy-*N*,*N*-dimethyl-3-aminopropane analogues, as C=C saturation increased, lamellar phase (L_α) to non-lamellar inverted hexagonal (H_{II}) phase transition temperatures increased, an indicator of decreasing fusogenicity, and that less fusogenic particles are more readily internalized by cells, but with lower gene silencing efficiency. They also argued that as electrostatic binding is a precursor to uptake, the pK_a values of the cationic lipid will be important. Their results support an siRNA transfection model in which endosomal release, mediated by fusion with the endosomal membrane, results in cytoplasmic translocation of the siRNA payload.[158] Whilst fully agreeing with their argument, in addition to the two (different) unsaturated acyl chains (18:2 and 18:1) of LinOS, cholesterol, a known membrane fusogen[242] was also incorporated in the efficient lipoplex formulations.

Lipoplexes containing LinOS/DOPE showed enhanced gene silencing (Figure 5) compared to LinOS lipoplex formulations lacking any helper lipid. However, LinOS/DOPE lipoplexes showed less siEGFP-AF delivery (Figure 4) when compared to LinOS/Chol lipoplexes (Figure 2). Lipoplexes containing cholesterol have also been found to be more effective in vivo than those containing DOPE.[243-247] The particle size of LinOS/Chol lipoplexes that resulted in the best balance between gene silencing and siEGFP-AF delivery were measured (Table 1). These LinOS/Chol lipoplexes were much smaller than the LinOS/DOPE lipoplexes (Table 1). DOPE containing lipoplexes reportedly showed immediate loss of integrity in the presence of serum which might explain the higher efficiency of cholesterol containing lipoplexes in vivo.[246] Thus, lipoplexes of LinOS/Chol at 1:2 ratio resulted in the best siEGFP-AF delivery and gene silencing. Further investigation with respect to the effect of decreasing the amount of complexed siRNA from 15 pmol to 3.75 pmol at LinOS/Chol 1:2 ratio showed the amount of siEGFP-AF delivered was down to 20-33%. The symmetrical spermine conjugate DOS, which was demonstrated to form siRNA lipoplexes that efficiently silence EGFP (Chapter 2), was chosen to prepare lipoplexes with the DOS/Chol ratio of 1:2, experimentally determined to be the best for LinOS/Chol, to investigate the effect of changing the cationic lipid on the siEGFP-AF delivery and EGFP knock-down. Figure 6 shows that both LinOS and DOS mixtures with cholesterol markedly increased siEGFP-AF delivery, with LinOS/Chol lipoplexes resulting in more enhanced siEGFP-AF delivery. The reduction of EGFP expression was essentially the same at both siEGFP-AF concentrations used and for both formulae. Although lipoplexes prepared with 3.75 pmol siEGFP-AF have a lower amount of siRNA, they therefore have a higher *N/P* charge ratio, *N/P* = 11.9 compared with *N/P* = 3.0 for lipoplexes prepared with 15 pmol siEGFP-AF which may play a role in the interactions with cell membranes hence promoting gene silencing. The differences seen between lipoplexes of LinOS/Chol and DOS/Chol can be attributed to the difference between the fatty acids in LinOS and DOS. LinOS contains one oleoyl chain (18:1, one *Z*-double bond) and one linoleoyl (18:2, two *Z*-double bonds) while DOS contains two oleoyl chains. The differences in the hydrophobic volume of these cationic lipids will affect the transfection efficiency of lipoplexes,[147, 226, 227] and LinOS lipoplexes were better than DOS lipoplexes in EGFP silencing in HeLa cells. Lipoplexes prepared with scrambled siNC-AF had good delivery efficiency, but they did not result in any significant gene silencing, therefore the reduction in EGFP expression on transfection with siEGFP-AF lipoplexes is due to sequence specific gene silencing, and not due to any off target or lipid related effects e.g. toxicity. The cell viability (Figure 12) shows that the lipoplexes were well tolerated by HeLa cells with viabilities ≥ 81%, and the best viability (94%) for lipoplexes containing cholesterol was achieved with LinOS/Chol 1:2 prepared with 0.375 pmol siRNA.

4. Conclusions

The new cationic lipid LinOS was characterized and evaluated for its ability to deliver siRNA to HeLa cells, and for its effect on gene silencing efficiency. LinOS was used to prepare self-assembled lipoplexes with siRNA, either alone, or in a co-formula with cholesterol or DOPE at various ratios of the cationic lipid/helper lipid. The lipoplexes co-formulated with cholesterol resulted in particle size that is smaller than the particle size of lipoplexes co-formulated with DOPE. The lipoplexes co-formulated with either cholesterol or DOPE were superior to those without cholesterol in terms of efficiency of siRNA delivery, with the lipoplexes having LinOS/Chol ratio 1:2 resulting in the highest delivery. These lipoplexes resulted in better gene silencing than the lipoplexes of LinOS, and comparable to the commercial transfecting agent TransIT-TKO in the presence of 10% FCS in the HeLa cell culture media. The self-assembled lipoplexes resulted in cell viability that is larger than 80% in HeLa cells. LinOS/Chol 1:2, without any liposomal pre-formulation steps, achieves siRNA delivery to ~100% of cells, best gene silencing, and with up to 94% cell viability. These results show that LinOS/Chol forms self-assembled lipoplexes with siRNA, and LinOS/Chol (1:2) is a promising non-viral non-toxic non-viral vector for siRNA.

The importance of the different mechanisms of lipoplex cell entry is now a key topic for investigation. Earlier this year, Juliano and co-workers reported functional delivery of oligonucleotide lipoplexes was by membrane fusion.[235] This route of entry brought improved functional delivery of oligonucleotide cargoes. However, Langer and co-workers have reported that there are at least two routes of entry. The well-established endocytic pathway and membrane fusion.[171] Therefore, there is a need to optimise the delivery of siRNA cargoes and to uncover aspects of the mechanisms of cellular entry.

Chapter Six On consideration of mechanisms

1. Introduction

In Chapters 2-5, a series of fatty acid spermine conjugates and fatty acid guanidinylated spermine conjugates were synthesized, characterized, and evaluated in vitro as non-viral vectors for siRNA delivery. In order to enhance the efficiency of the lipoplexes and to investigate the underlying mechanisms affecting the efficiency of siRNA delivery and EGFP knock-down, a series of 'proof of concept' experiments was designed and carried-out. The contribution of endosomal escape to the delivery and gene silencing efficiency, the packing of the lipoplexes, the effect of using more than one helper lipid in the lipoplex formulation, and changing the type of the cationic head-group from amine to guanidine in the lipoplexes containing cholesterol are key variables. Among different pathways for intracellular delivery of lipoplexes, endocytosis and the subsequent escape of the lipoplexes were studied extensively.[215, 237, 248-251] In the field of lipid mediated DNA delivery, endocytosis was found to be a determinant factor in the efficiency of the transgene expression.[250] Lipoplexes may enter cells via another independent pathway (in addition to endocytosis), which may be by lipid mixing which itself depends on the lipoplex structure.[252] Related to siRNA delivery and endosomal escape, the use of a neutral helper lipid that enhances the fusogenicity of the lipoplexes is one possible approach to improve the outcome of transfection. The effect of using a cholesterol and DOPE mixture in the same lipoplex preparation on the transfection process is also worth investigating. Another strategy is to facilitate endosomal escape by using a molecule that responds to the decrease in pH in the endosome, e.g. cholesteryl hemisuccinate (CHS) which shows pH-dependent release characteristics in liposomes.[253]

The properties of the cationic head-group affect its behaviour with respect to nucleic acid binding, its interaction with different anionic groups extracellularly and on the cell membrane, lipid polymorphism and its endosomal escape characteristics.[125, 153, 254] In order to differentiate between endocytic and non-endocytic (e.g. membrane fusion) intracellular delivery pathways, decreasing the temperature to 4-6 °C is known to block the various endocytic pathways (clathrin and caveolin dependent).[171] More importantly, as it has been shown in the previous Chapters, as delivery is not necessarily related to the subsequent gene silencing quantitatively, and while various intracellular delivery pathways might be involved in the internalization process, not all of them are essentially involved in the resulting gene silencing.[171] Thus, preventing endocytosis by decreasing the transfection temperature should allow us to differentiate between the contribution of endocytosed lipoplexes and lipoplexes internalized by other mechanisms such as membrane fusion.

2. Materials and methods

Dextran sulfate (DS) (molecular weight > 500,000 Da) and cholesteryl hemisuccinate (CHS) were purchased from Sigma-Aldrich. All solvents and other chemicals were purchased as described in Chapter 2 (Section 2.1).

2.1. Experimental protocols

The lipoplexes containing individual cationic lipids were prepared as described above in Chapter 2 (Section 2.4). The lipoplexes containing individual cationic lipids/Chol mixtures were prepared as described in Chapter 5 (Section 2.3), with the cationic lipid/Chol 1:2 molar ratio and the cationic lipid amount 0.75 μg/well kept constant.

2.2. Preparation of lipoplexes containing Chol/DOPE

Ethanolic solutions of the individual cationic lipids, cholesterol, and DOPE were mixed to result in the required molar ratio of cationic lipid/Chol/DOPE. Two liquid preparations (A and B) were then prepared. Liquid A was prepared by adding the ethanolic solution containing the lipid mixture to Opti-MEM serum free medium in an Eppendorf microtube, and then mixed on a vortex mixer for 2-3 s. Liquid B was prepared by adding the required volume of siRNA master solution to serum free Opti-MEM medium in an Eppendorf microtube, and then mixing briefly. The lipoplexes were prepared by adding the required volumes of liquid B to liquid A containing the required amounts of lipids in an Eppendorf microtube, followed by mixing on a vortex mixer for 2-3 s, and then left for 20 min at 20 °C for the lipoplexes to form.

2.3. Preparation of lipoplexes containing CHS

Ethanolic solutions of the individual cationic lipids, cholesterol, and CHS were mixed to yield the required molar ratio of either cationic lipid/CHS or cationic lipids/CHS/Chol. Two liquid preparations (A and B) were then prepared. Liquid A was prepared by adding the ethanolic solution containing the lipid mixture to Opti-MEM serum free medium in an Eppendorf microtube, and then was mixed on a vortex mixer for 2-3 s. Liquid B was prepared by adding the required volume of siRNA master solution to serum free Opti-MEM medium in an Eppendorf microtube, and then mixing briefly. The lipoplexes were prepared by adding the required volumes of liquid B to liquid A containing the required amounts of lipids in an Eppendorf microtube, followed by mixing on a vortex mixer for 2-3 s, and then left for 20 min at 20 °C for the lipoplexes to form.

2.4. Preparation of lipoplexes containing DS

Ethanolic solutions of the individual cationic lipids and cholesterol were mixed to result in the required molar ratio of cationic lipid/Chol. Two liquid preparations (A and B) were then prepared. Liquid A was prepared by adding the ethanolic solution containing the lipid mixture to Opti-MEM serum free medium in an Eppendorf microtube, and then mixed on a vortex mixer for 2-3 s. Liquid B was prepared by adding the required volumes of master solutions of siRNA and DS to serum free Opti-MEM medium in an Eppendorf microtube, and mixing briefly. The lipoplexes were prepared by adding the required volumes of liquid B to liquid A containing the required amounts of the lipids in an Eppendorf microtube, followed by mixing on a vortex mixer for 2-3 s, and leaving for 20 min at 20 °C for the lipoplexes to form.

2.5. Cell culture and transfection experiments in the presence of 10% or 50% serum

The cell culture and transfection experiments in 10% serum were carried out as described in Chapter 2 (Section 2.4). The cell culture and transfection experiments in 50% serum were carried out as described in Chapter 2 (Section 2.4), except that on day of transfection, the medium in each well was aspirated and replaced with DMEM containing 50% FCS. The lipoplexes were then added to each well and the plates were incubated for 4 h in 5% CO_2 at 37 °C. The cell culture medium from each well was then removed, and replaced with DMEM containing 10% FCS, and the plates were incubated for a further 44 h in 5% CO_2 at 37 °C.

2.6. Cell culture and transfection experiments at different temperatures

Cells were trypsinized at a confluency of 80-90% and seeded at a density of 65,000 cells/well in 24-well plates and were then incubated for 24 h at 37 °C, 5% CO_2. Prior to transfection, the plates were incubated for 1 h at 37, 22, or 6 °C. The lipoplex solutions were then added to wells containing DMEM (10% FCS) such that the final volume in each well was 1 mL, and the plates were incubated at 37, 22, or 6 °C for 4 h to allow for the intracellular delivery. The media from each well were then aspirated and the cells were washed twice with PBS. DMEM (10% FCS) was then added to each well (1 mL) and all the plates were incubated at 37 °C for 44 h prior to FACS analysis.

2.7. FACS analysis

Preparation of the cells for FACS analysis and measurement of delivery and gene silencing were carried out as described in Chapter 2 (Section 2.5).

3. Results and discussion

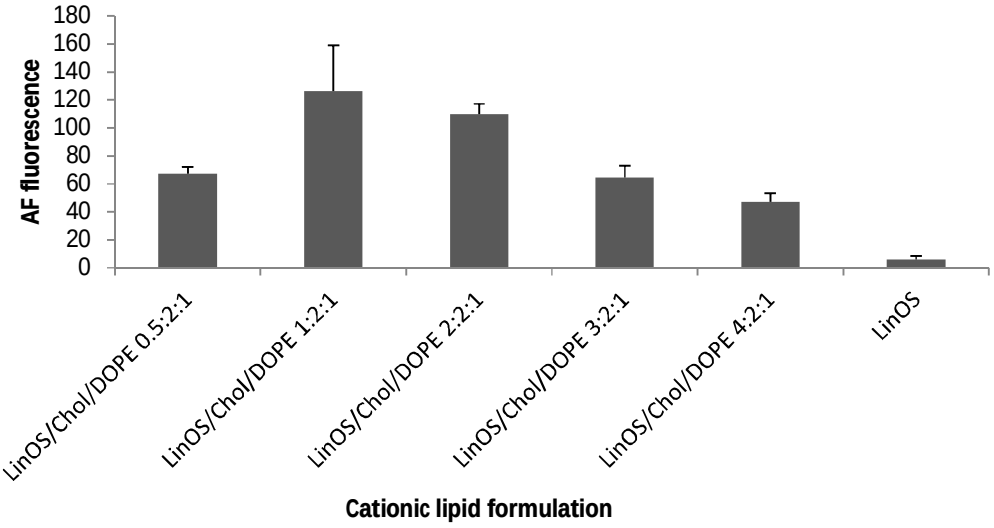

Figure 1. siEGFP-AF delivery 48 h post-transfection with lipoplexes prepared using mixtures of LinOS with cholesterol and DOPE. Delivery was compared to that of LinOS without any helper lipids. The *N/P* ratio of 3.0 was kept constant by using 0.75 µg LinOS and 15 pmol siEGFP-AF constant in all lipoplex formulations while varying the Chol/DOPE mixture molar ratio with respect to LinOS, and Chol/DOPE molar ratio was kept constant at 2:1 in all experiments.

Figure 1 shows the effect of preparing the lipoplexes with LinOS/Chol/DOPE mixtures. The molar ratio of Chol/DOPE was kept constant at 2:1 while the amount of LinOS was varied. The LinOS/Chol/DOPE is the molar ratio of the three lipids in the mixture. The Chol/DOPE ratio was preliminary chosen based on the previous results which showed that LinOS/Chol 1:2 and LinOS/DOPE 1:1 were the best in terms of siEGFP-AF delivery among LinOS/Chol and LinOS/DOPE mixtures respectively. All the LinOS/Chol/DOPE lipoplexes resulted in increased siEGFP-AF delivery, with LinOS/Chol/DOPE 1:2:1 lipoplexes resulting in the best delivery, showing ~20-fold increase compared to LinOS only lipoplexes. However, the delivery of siEGFP-AF with LinOS/Chol 1:2 (Chapter 5, Figure 2) resulted in an ~40-fold increase in siEGFP-AF delivery compared to LinOS lipoplexes, i.e. better than LinOS/Chol/DOPE.

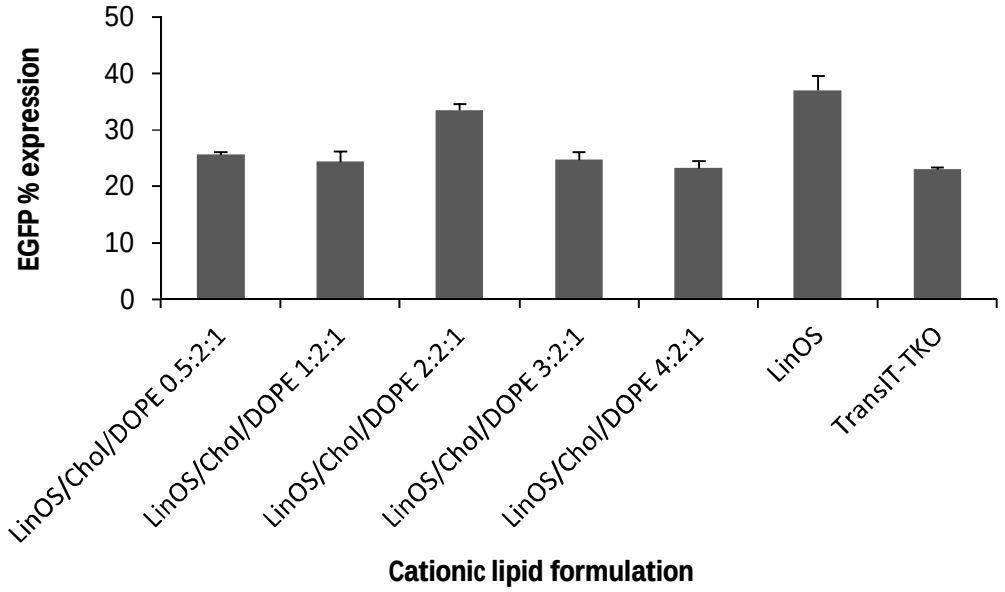

Figure 2. EGFP percentage expression 48 h post-transfection with lipoplexes prepared using mixtures of LinOS with cholesterol and DOPE. EGFP percentage expression was compared to that of LinOS without any helper lipids. The *N/P* ratio of 3.0 was kept constant by using 0.75 µg LinOS and 15 pmol siEGFP-AF constant in all lipoplex formulations while varying the Chol/DOPE weight. Chol/DOPE molar ratio was kept constant at 2:1.

Figure 2 shows the effect of preparing the lipoplexes with LinOS/Chol/DOPE mixtures on EGFP expression. The molar ratio of Chol/DOPE was kept constant at 2:1 while the amount of LinOS was varied. The Chol/DOPE ratio was preliminary chosen based on the previous results (Chapter 5) which showed that LinOS/Chol 1:2 and LinOS/DOPE 1:1 were the best in terms of EGFP silencing among LinOS/Chol and LinOS/DOPE mixtures respectively. Compared to LinOS (37% EGFP expression), all LinOS/Chol/DOPE mixtures resulted in enhanced reduction in EGFP expression (reduced to 23-26%), except 2:2:1 lipoplexes which resulted in 34% EGFP percentage expression.

The rationale of using Chol/DOPE mixtures was to evaluate the combining of the roles of both helper lipids. The results in Figures 1 and 2 taken together, show that while using LinOS/Chol/DOPE mixtures resulted in significant enhancement of siEGFP-AF delivery and reduction in EGFP expression, there was no advantage found on using the Chol/DOPE mixture over using the LinOS/Chol 1:2 mixture (Chapter 5, Figures 2 and 3).

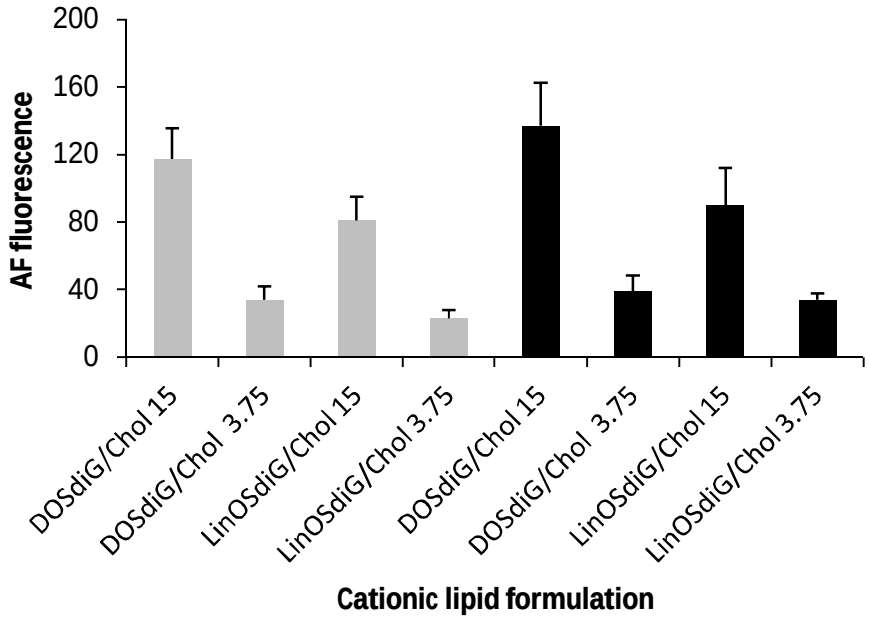

Figure 3. siEGFP-AF and siNC-AF delivery 48 h post-transfection with lipoplexes prepared using DOSdiG/Chol 1:2 and LinOSdiG/Chol 1:2 mixtures (0.75 µg/well cationic lipid). Light grey bars represent siEGFP-AF delivery, black bars represent siNC-AF delivery. Lipoplex formulae suffixed with 15 are prepared with 15 pmol of siRNA (*N/P* = 2.7), while those suffixed with 3.75 are prepared with 3.75 pmol siRNA (*N/P* = 10.7).

siEGFP-AF delivery (Figure 3) with lipoplexes prepared with DOSdiG/Chol and LinOSdiG/Chol 1:2 mixtures. siEGFP-AF amount was 15 or 3.75 pmol, with the *N/P* = 2.7 and 10.7 respectively. The cationic lipid/Chol ratio was chosen based on the efficiency of LinOS/Chol 1:2 lipoplexes (Chapter 5). The results show that using 15 pmol siEGFP-AF resulted in more delivery compared to 3.75 pmol siEGFP-AF. Compared to using DOSdiG and LinOSdiG 0.75 µg/15 pmol siEGFP-AF (Chapter 3, Figure 8), there is a clear enhancement of delivery of ~20-fold. The black bars show that the delivery of siNC-AF lipoplexes is comparable with that of the siEGFP-AF lipoplexes (grey bars).

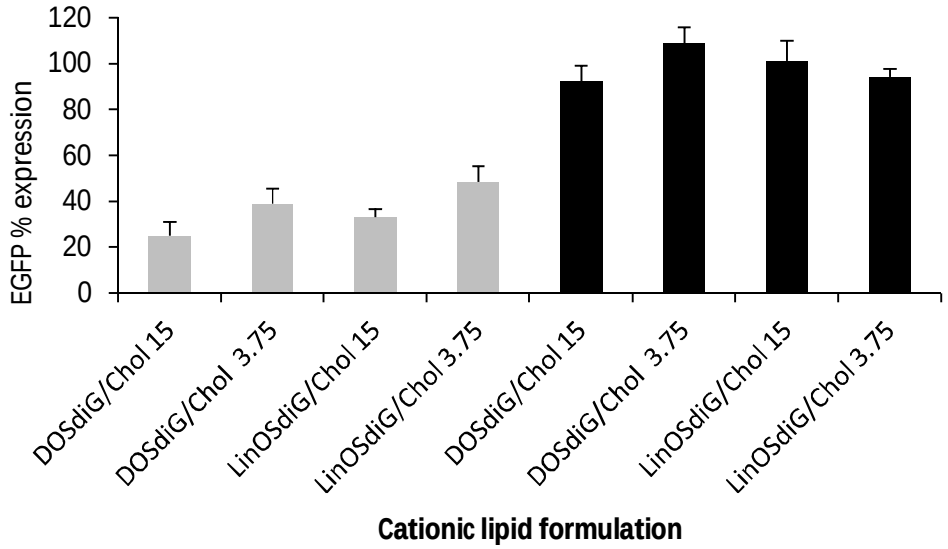

Figure 4. EGFP percentage expression 48 h post-transfection with lipoplexes prepared using DOSdiG/Chol and LinOSdiG/Chol mixtures. Light grey bars represent siEGFP-AF delivery, while black bars represent siNC-AF delivery. Lipoplex formulae suffixed with 15 are prepared with 15 pmol of siRNA (*N/P* = 2.7), while those suffixed with 3.75 are prepared with 3.75 pmol siRNA (*N/P* = 10.7).

EGFP percentage expression is shown in Figure 4, 48 h post-transfection with lipoplexes prepared with DOSdiG/Chol and LinOSdiG/Chol 1:2 mixtures, siEGFP-AF amount was 15 or 3.75 pmol. The results show that there was a significant reduction of EGFP expression by using the cholesterol mixtures (expression reduced to 25-33%) when compared to DOSdiG or LinOSdiG 0.75 µg/15 pmol siEGFP-AF (Chapter 3, Figure 9) lipoplexes which resulted in EGFP percentage expression of 50-65%. Lowering the amount of siEGFP-AF in the lipoplexes from 15 to 3.75 pmol resulted in decreasing the efficiency of EGFP silencing (expression only reduced to 39-48%). Using 15 pmol siEGFP-AF, there was no significant difference between DOSdiG/Chol and LinOSdiG/Chol lipoplexes (p = 0.06). Transfection with siNC-AF lipoplexes showed that there is no significant change in EGFP expression.

Using the guanidine conjugates DOSdiG/Chol and LinOSdiG/Chol, in comparison to using DOS/Chol and LinOS/Chol in Chapter 5, was to investigate if changing the type of the cationic head-group (from amine to guanidine), which hypothetically affects the packing of the cationic lipid due to changing the size of the polar head-group relative to the hydrophobic portion, would have an effect on the delivery and/or gene silencing. The results show that although formulation with cholesterol enhanced both delivery and transfection, the DOS/Chol and LinOS/Chol 1:2 mixtures (Chapter 5, Figure 6) were significantly better in delivery (at 15 pmol siEGFP-AF, DOS/Chol, DOSdiG/Chol, LinOS/Chol, and LinOSdiG/Chol resulted

in 169, 117, 250, and 81 AF647 fluorescence respectively) and also better in gene silencing especially at 3.75 pmol siEGFP-AF (DOS/Chol, DOSdiG/Chol, LinOS/Chol, and LinOSdiG/Chol resulted in 29, 39, 23, and 48% EGFP expression respectively). Thus, the results show that using the guanidine conjugates did not offer any significant advantage over using the polyamine conjugates with respect to delivery and/or gene silencing.

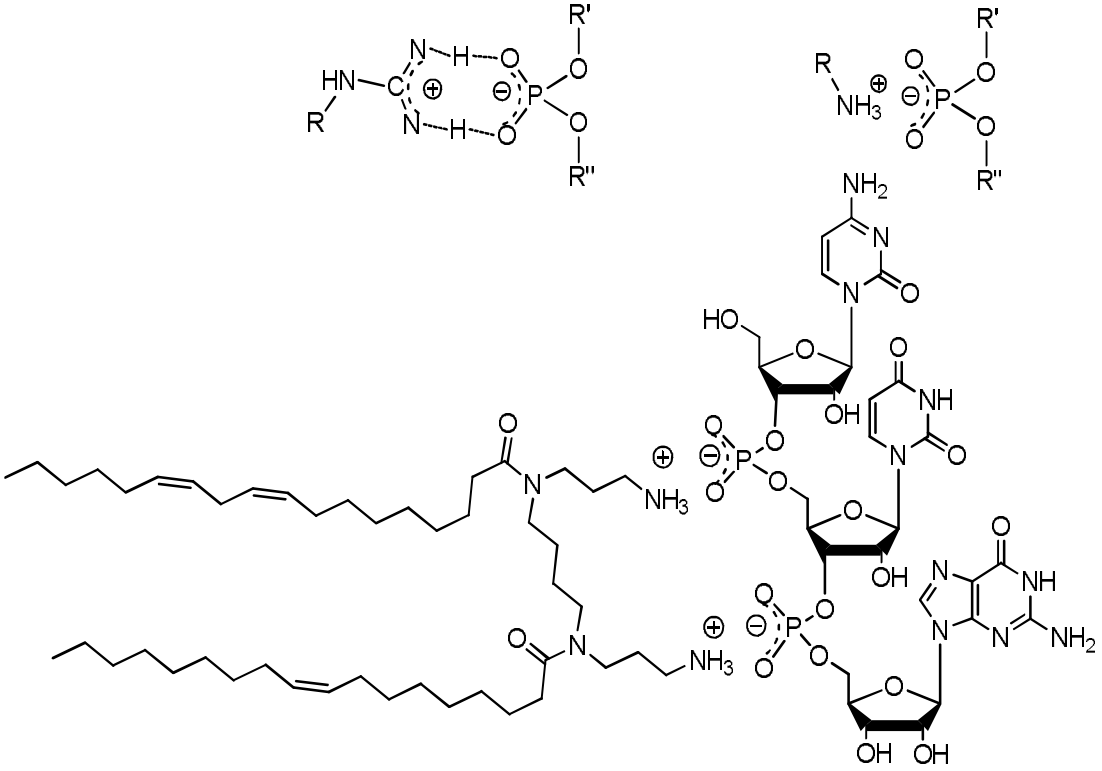

Figure 5. Upper: bidentate hydrogen bonding of guanidinium group (left) vs. electrostatic interaction of the ammonium group both interacting with a phosphate group. Lower: LinOS showing electrostatic binding to 5'-3' CUG found in the sense strand of siEGFP.

In contrast to the protonated amine group which interacts electrostatically with the phosphate groups, the guanidinium group forms bidentate hydrogen bonds, and the electrostatic interaction between the positively charged guanidinium and the negatively charged phosphate (Figure 5).[201] Although this interaction of guanidinium functional groups in the bulk of aqueous buffers can be weak, it is strong upon approaching cell membranes, and thus guanidine groups have the advantage of enhancing the binding to negatively charged cell membranes.[201, 255, 256] Guanidine groups are also known to have a negligible hydration shell in contrast to ammonium groups.[257, 258] Cationic lipid hydration state, which is in part affected by the cationic head hydration and bulkiness, was related to the efficiency of transfection in vivo in mouse lungs.[132]

More efficient transfection was achieved with the lipids that had polar head-groups resulting in closer polar domain association and less hydration (e.g. due to H-bonds), in addition to having acyl *cis*-unsaturated fatty chains conjugated to the polar head-groups. These lipids had the greatest imbalance between the polar head-groups and the hydrophobic domain's cross-sectional area. The hydration of the head group as well as the hydrocarbon tail packing also determines the stability of the interaction of the cationic lipid with polynucleotides.[160] In addition, changing the type of the polar head-group will affect the shape parameter of the lipid. The lipid shape parameter (also known as the packing parameter) is defined by the equation:

$$S = \frac{V_{HC}}{L_{HC} . A_O}$$

where S is the shape parameter, V_{HC} the volume of hydrophobic hydrocarbon chain, L_{HC} the length of the hydrocarbon chain, and A_O the surface area of the polar head-group. Lipids that have $S \leq 0.5$ are cone-shaped and tend to form micelles in aqueous media. A value of $0.5 \leq S \leq 1$ indicates cylindrical shape and tendency towards formation of lipid bilayers. When $S \geq 1$, this suggests inverted cone shape and a tendency to form inverted structures such as reversed micelles or hexagonal phases (Figure 6).[125] The formation of inverted hexagonal phases (H_{II}) is known to enhance membrane fusion, whether upon intracellular delivery and/or during lipoplex endosomal escape.[125] Decreased head-group hydration results in reducing the space available to water and so reduces the cross-sectional area of the polar head-group, and resulting in $S > 1$. Conjugating unsaturated fatty acids also increases the tendency to form inverted structures (and $S > 1$).

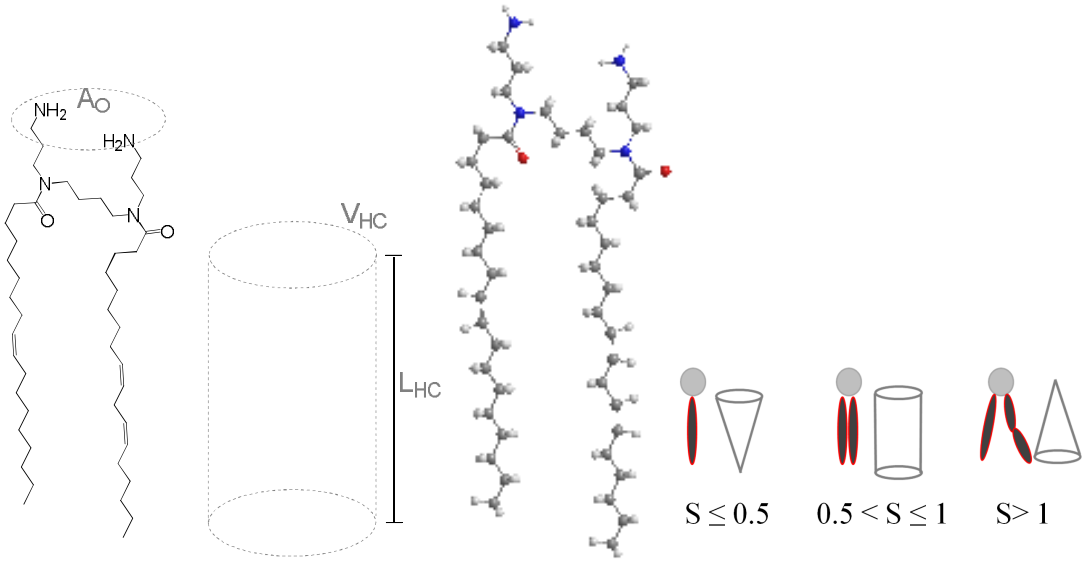

Figure 6. Shape (packaging) parameter of cationic lipids.

The difference between DOS/DOSdiG and LinOS/LinOSdiG is in the cationic head-groups. Although the guanidine group was reported previously to increase transfection efficiency,[204, 206] it is the effect of the guanidine group on the lipid's hydration and shape as a whole that is important in determining its efficiency, and hence the advantages gained by guanidinylation were not evident in DOSdiG and LinOSdiG in comparison with their amine counterparts.

Cholesterol

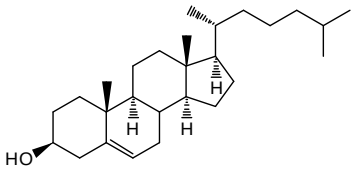

Cholesteryl hemisuccinate (non-ionized)

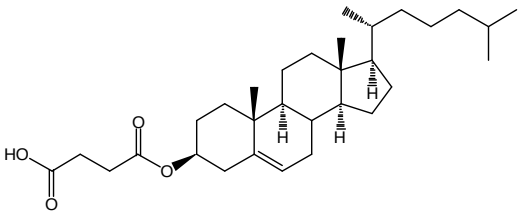

Cholesteryl hemisuccinate (ionized)

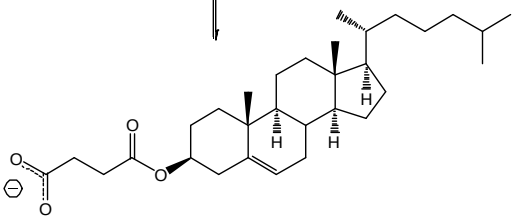

Figure 7. Cholesteryl hemisuccinate can take either an ionized or non-ionized form. At acidic pH = p*K*a ~4.3, 50% of the CHS population is ionized and 50% is non-ionized.

CHS is used as a fusogenic lipid in some liposomal preparations[259] because it promotes phase change from lamellar/bilayer to the inverted hexagonal phase H_{II}, in the endosomal compartment due to the decreasing pH, typically at pH ≤ 4.3 which is approximately the p*K*a of succinic acid.[260] As shown in Figure 7, as the acidity increases in endosomes towards pH ~4.3, the CHS ionized form which is predominant at physiological pH 7.4 starts to change to the non-ionized form. This change affects the shape of the CHS molecule, as the ionized form has a polar head and adopts a cylindrical shape promoting bilayer formation.[260] The non-ionized form lacks the polar head, while the hydrophobic steroid part is unchanged and adopts an inverted cone shape (Figure 6), thus promoting H_{II} phase formation which enhances the fusogenic characteristic of CHS. During formulation of the lipoplexes and during

intracellular entry, the pH is approximately 7.4 and thus CHS is ionized (deprotonated), promoting bilayer formation in the lipoplexes. Once the lipoplexes are in the endosomes and the pH starts to decrease (towards 5.5), CHS starts to be protonated changing to the non-ionized form which enhances fusogenicity. Therefore, CHS was used to prepare mixtures with LinOS and LinOS/Chol, aiming to enhance endosomal escape of the lipoplexes and the release of the siEGFP-AF cargo of the lipoplexes into the cytoplasm.

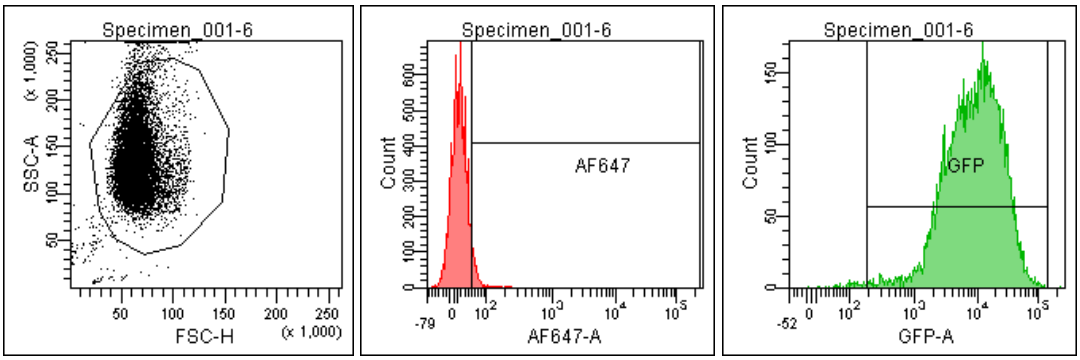

(8a) Control

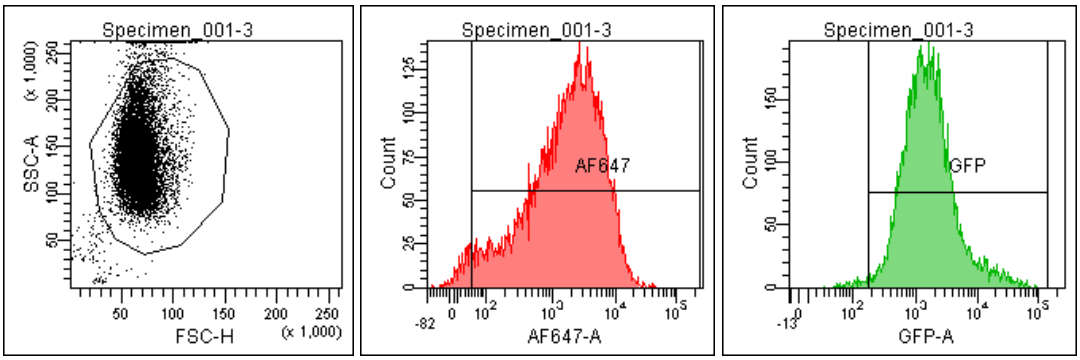

(8b) LinOS/CHS/Chol 1:1:1 (7.5 pmol siEGFP-AF)

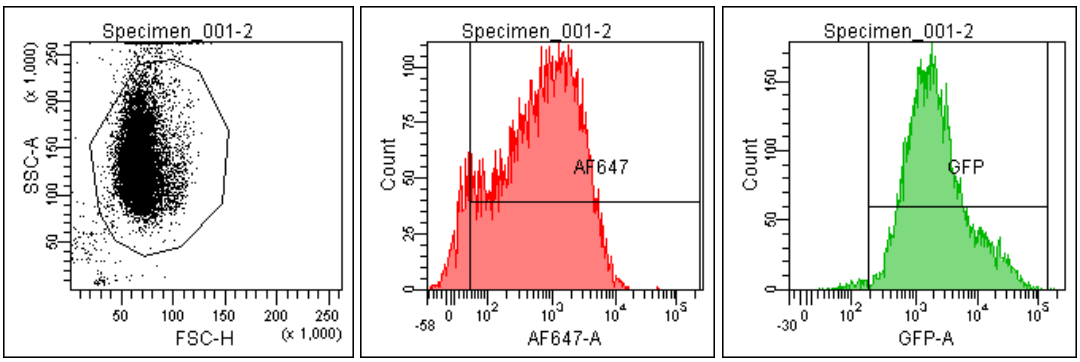

(8c) LinOS/CHS 1:1 (7.5 pmol siEGFP-AF)

Figure 8. FACS data for (a) control non-transfected cells, and transfected cells with (b) LinOS/CHS/Chol 1:1:1 and (c) LinOS/CHS 1:1 (molar ratios) (at 7.5 pmol siEGFP-AF) showing siEGFP-AF delivery (middle column) and EGFP silencing (right column). LinOS is 0.75 μg/well.

The representative FACS data in Figure 8 show the effect of formulating the lipoplexes with CHS. Relative to control cells (Figure 8a), there was an increase in both siEGFP-AF delivery and efficiency of EGFP silencing with the lipoplexes of LinOS/CHS/Chol 1:1:1 and LinOS/CHS 1:1 (molar ratios) (Figure 8b and 8c respectively). There was better delivery with LinOS/CHS/Chol relative to LinOS/CHS (Figure 8b and 8c, middle column). The EGFP silencing was slightly better with LinOS/ CHS/Chol lipoplexes compared to lipoplexes of LinOS/CHS only (Figure 8b and 8c, right column).

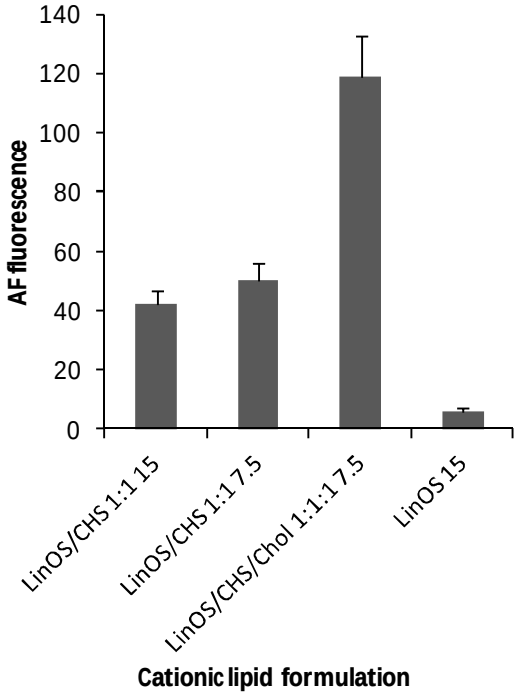

Figure 9. siEGFP-AF delivery 48 h post-transfection with lipoplexes prepared using LinOS and LinOS mixtures with cholesterol and/or CHS. Molar ratios are used, lipoplexes suffixed 15 and 7.5 are prepared with 15 and 7.5 pmol of siEGFP-AF respectively (LinOS is 0.75 μg/well).

siEGFP-AF delivery is shown in Figure 9 48 h post-transfection with lipoplexes of LinOS, LinOS/CHS 1:1 and LinOS/CHS/Chol 1:1:1 (molar ratios). Also shown is the effect of decreasing the siEGFP-AF amount from 15 to 7.5 pmol for LinOS/CHS 1:1 lipoplexes. Preparing the lipoplexes with LinOS/CHS 1:1 resulted in a significant increase of siEGFP-AF delivery (~6-9-fold) compared to LinOS only. Lowering the amount of siEGFP-AF from 15 to 7.5 pmol in LinOS/CHS 1:1 lipoplexes resulted in a slight significant increase in delivery (from 42 to 50, $p = 0.03$). Lipoplexes of LinOS/CHS/Chol 1:1:1 clearly resulted in the best delivery (Figure 8).

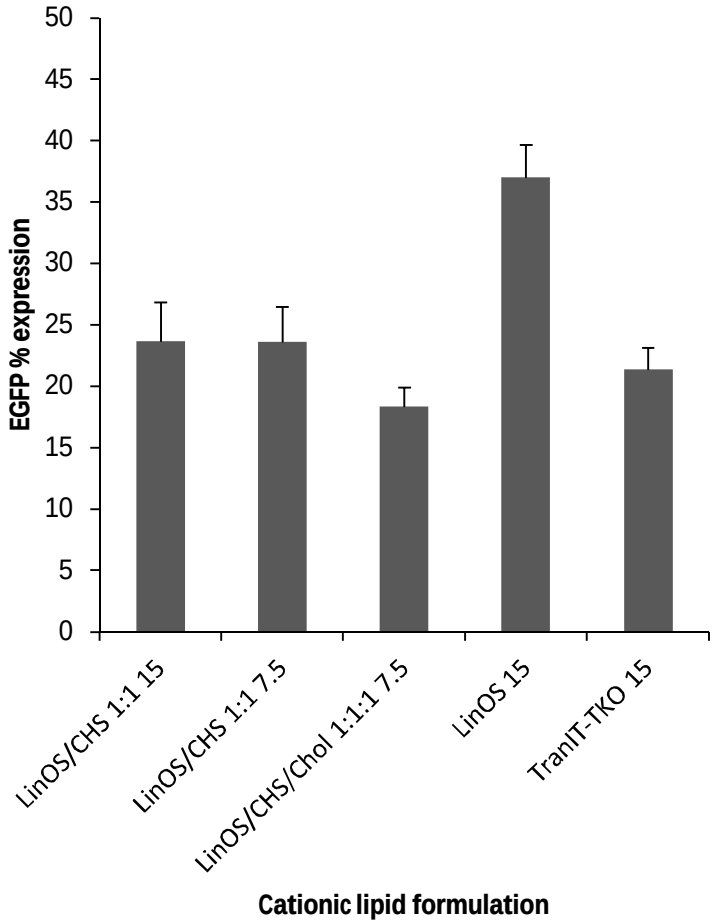

Figure 10. EGFP percentage expression 48 h post-transfection with lipoplexes prepared using LinOS and LinOS mixtures with cholesterol and/or CHS. Lipoplexes suffixed with 15 and 7.5 are prepared with 15 and 7.5 pmol of siEGFP-AF respectively (LinOS is 0.75 µg/well).

The EGFP percentage expression 48 h post-transfection with LinOS, LinOS/CHS, and LinOS/CHS/Chol lipoplexes are shown in Figure 10. Compared to LinOS lipoplexes (0.75 µg, 15 pmol siRNA), all lipoplexes containing CHS resulted in an enhanced reduction of EGFP expression. The lipoplexes of LinOS/CHS/Chol 1:1:1 resulted in the best gene silencing, reducing EGFP expression to 18%, compared to 23% with TransIT-TKO (p = 0.0001, formulated with 15 pmol siEGFP-AF).

The molar ratio LinOS/CHS/Chol 1:1:1 was chosen to be as close as possible to that of the efficient lipoplexes LinOS/Chol 1:2. LinOS/CHS 1:1 lipoplexes were prepared to investigate if the effect of LinOS/CHS/Chol 1:1:1 is solely due to CHS or cholesterol is contributing to the effects on delivery and gene silencing. It is clear that adding cholesterol to the lipoplexes formulation enhanced delivery and gene knock-down. A formula of LinOS/CHS 1:2 was not

prepared (in analogy to the efficient LinOS/Chol 1:2) because each CHS molecule at pH 7.4 carries one negative charge, while LinOS carries 2 positive charges at the same pH, thus the LinOS/CHS 1:2 will be neutral with no excess of positive charges to bind electrostatically the siRNA or to promote stability of the lipoplexes (due to a positive ζ-potential).

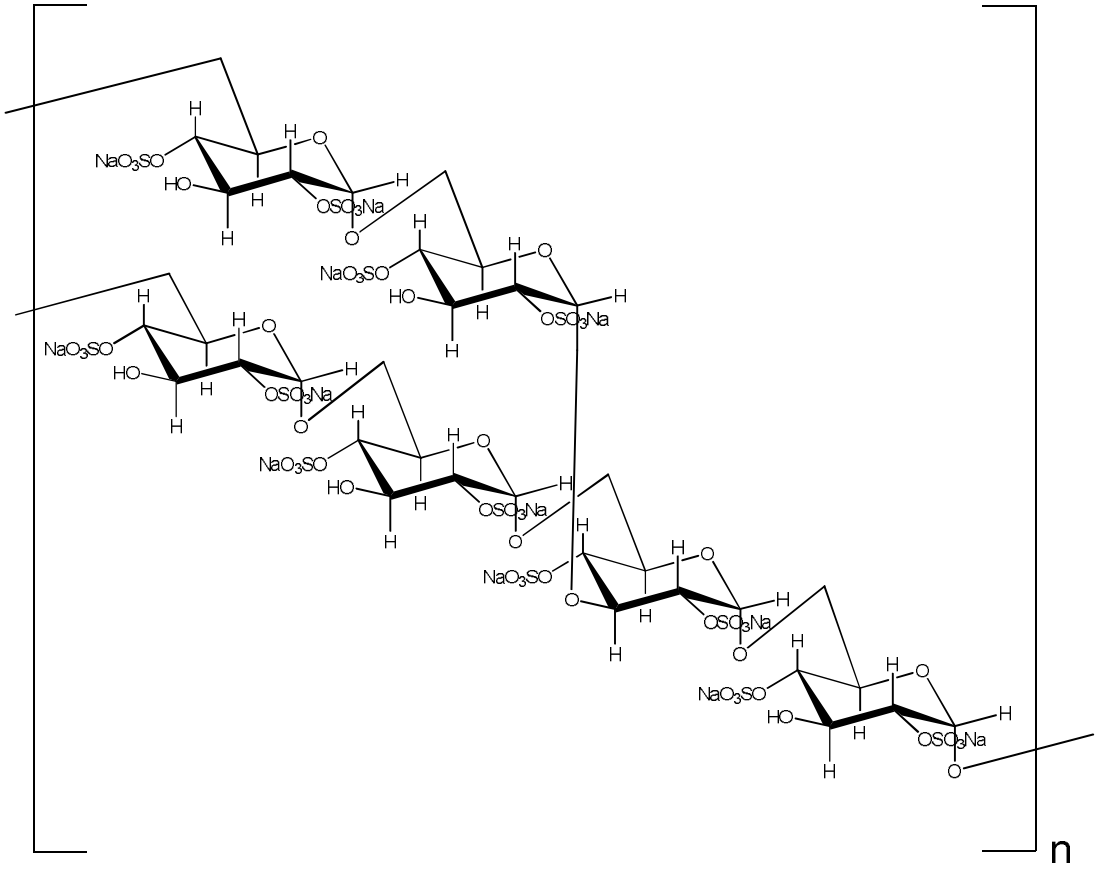

Figure 11. DS is a polymer (n = 1-~500) of α-1,6-linked D-glucopyranose modified with side-chains (branches) of D-glucopyranose with (α-1,3) linkages to the parent chain and an average length of 3 units of glucose. DS has approximately 17% sulfur (~2.3 sulfate groups per glucose unit).

DS (Figure 11) is a highly negatively charged polymer, due to its sulfated glucose units. DS has approximately 2 sulfate units per glucose unit and therefore two p*K*a values. The first has a negative p*K*a value and the other has p*K*a < 2,[261] which makes the DS practically and essentially 100% ionized at pH 7.4. Thus, because DS is a polymer, it is rationalized that the packing of siRNA lipoplexes will be changed in the presence of DS, which will affect lipoplex stability, the distribution of the siRNA cargo within the lipoplex, and/or transfection efficiency. In two recent reports, adding additional DNA cargo to siRNA lipoplexes resulted in enhanced gene silencing both in vivo [262] and in vitro to mouse melanoma cell lines.[168] The

addition of the DNA (a negatively charged biopolymer) was found to enhance gene silencing of lipid/liposomal delivery systems but not polymer based systems, a difference which was attributed to the different physicochemical characteristics of lipoplexes and polyplexes, e.g. polyplexes do not form lamellar structures. Adding DNA cargo resulted in more homogenous distribution of the nucleic acids (DNA and siRNA) within the lipid matrix of the polyplexes, and also resulted in better release characteristics (i.e. less stability) when the lipoplexes were challenged in vitro with anionic heparan sulfate. As DNA and DS are both highly negatively charged polymers, DS was chosen to investigate its effects on lipoplex formulation. Interestingly, during the progress of the current work, a recent paper by the same research group mentioned above using various anionic polymers to formulate siRNA lipoplexes was published.[263] The lipoplexes containing the anionic polymers (including dextran sulfate) were evaluated in vitro in mouse melanoma cells (B16-Luc) stably expressing luciferase, and in vivo in female C57BL/6 mice.[263]

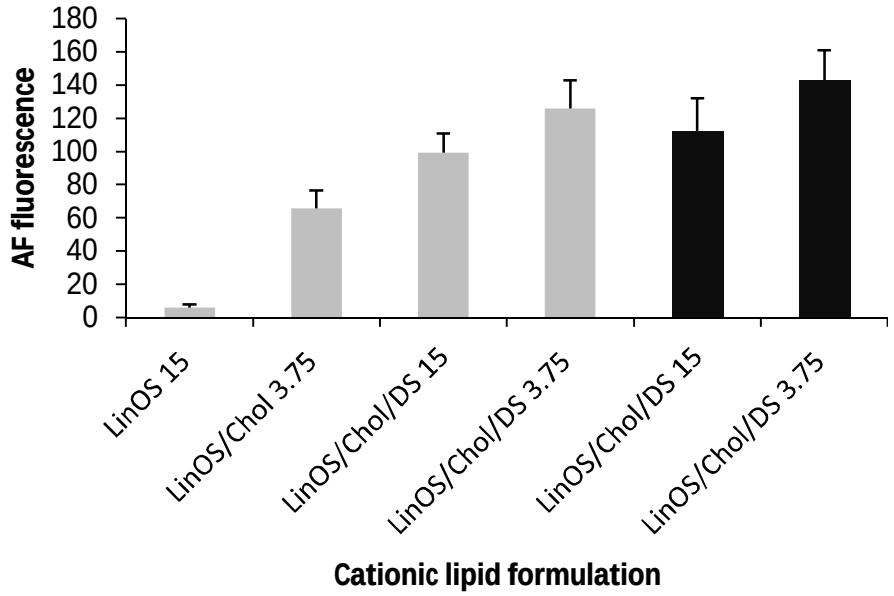

Figure 12. siEGFP-AF delivery (grey bars) 48 h post-transfection with lipoplexes prepared using LinOS and LinOS mixtures with cholesterol and/or dextran sulfate (DS). Lipoplexes suffixed with 15 and 3.75 are prepared with 15 and 3.75 pmol of siEGFP-AF. Black bars represent siNC-AF delivery.

Although the DNA remained the most efficient cargo, the most efficient anionic polymer, polyglutamate, showed marked efficiency compared to the lipoplexes without any anionic polymer. In the current work, DS showed an enhancement in delivery and slight enhancement of gene silencing, which is evidence, as a proof of concept, of the potential for improvement of LinOS/Chol lipoplexes.

The effect of adding dextran sulfate (DS) to LinOS/Chol lipoplexes on siEGFP-AF delivery is shown in Figure 12. The LinOS/Chol ratio was 1:2, and the amount of DS used was such that it provides an equal number of negative charges as 15 pmol/well siRNA. Thus, the *N/P* ratio of these lipoplexes will be half that of the lipoplexes without DS. There was an enhancement in delivery with the lipoplexes containing DS. Interestingly, delivery with 15 pmol siEGFP-AF was lower than that with 3.75 pmol. This might be due to the higher positive charge (*N/P* = 2.4) of the LinOS/Chol/DS 3.75 lipoplexes, while the LinOS/Chol/DS 15 lipoplexes will have a lower *N/P* ratio (*N/P* = 1.5) with the presence of the highly negatively charged DS, which will in turn affect the latter lipoplex's ability to bind to the negatively charged cell membranes. The black columns show that the delivery of siNC-AF lipoplexes was comparable to that of the siEGFP-AF lipoplexes (grey columns).

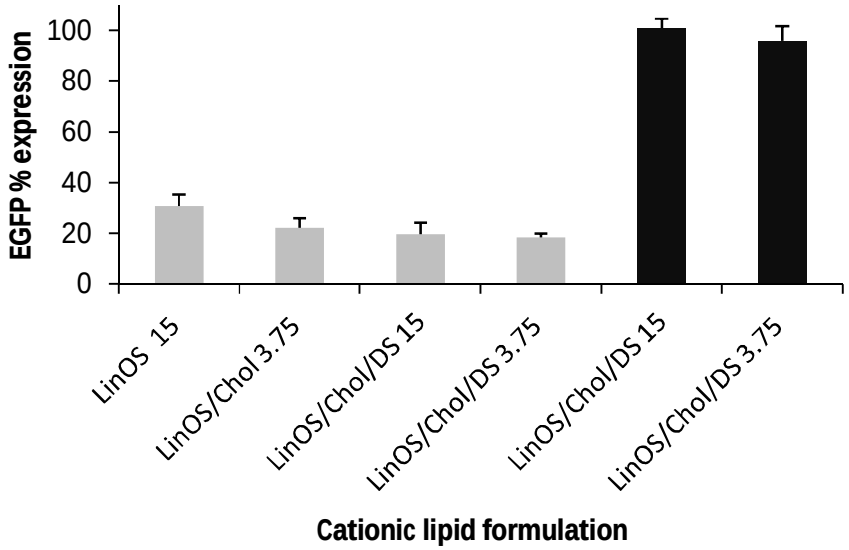

Figure 13. EGFP percentage expression 48 h post-transfection with siEGFP-AF lipoplexes (grey bars) and siNC-AF (black bars) prepared using LinOS and LinOS mixtures with cholesterol and/or dextran sulfate (DS). Lipoplexes suffixed with 15 and 3.75 are prepared with 15 and 3.75 pmol of siRNA.

The effect of adding DS to LinOS/Chol lipoplexes on EGFP expression 48 h post-transfection is shown in Figure 13. The addition of DS resulted in slight enhancement of gene silencing compared to the LinOS/Chol 1:2 lipoplexes. LinOS/Chol/DS and LinOS/Chol lipoplexes prepared with 3.75 pmol siEGFP-AF reduced EGFP expression to 18 and 21, p = 0.03. The EGFP expression was not practically affected with transfection with siNC-AF lipoplexes, showing that the EGFP silencing with siEGFP-AF lipoplexes is not related to non-specific effects of LinOS/Chol/DS formulation. Figure 14 shows representative FACS

data where the addition of DS to LinOS/Chol 1:2 (at 3.75 pmol siEGFP-AF) caused an enhanced delivery (Figure 14b, middle column) relative to the lipoplexes without DS (Figure 14c, middle column).

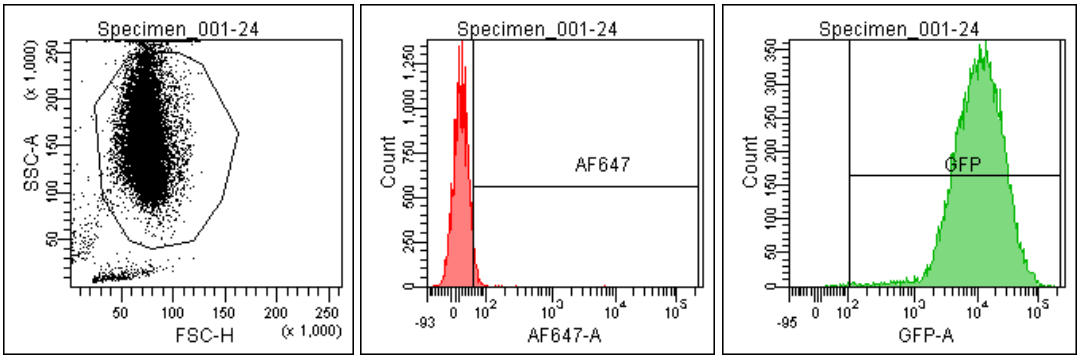

(14a) Control HeLa cells

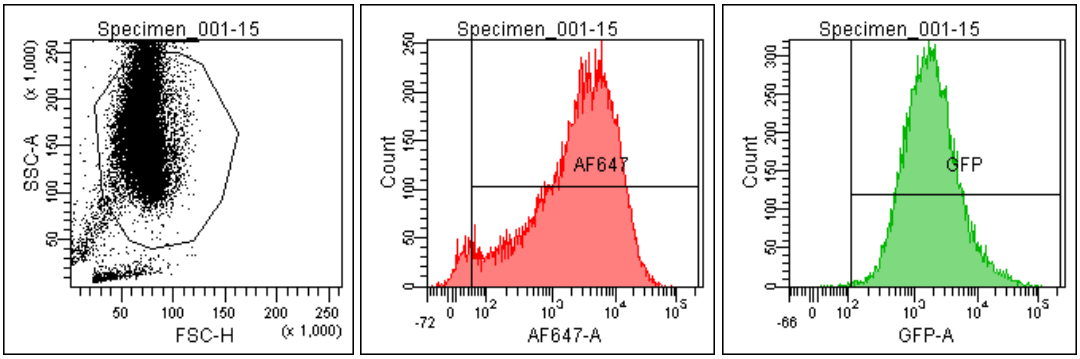

(14b) LinOS/Chol 1:2 3.75 pmol siEGFP-AF + DS

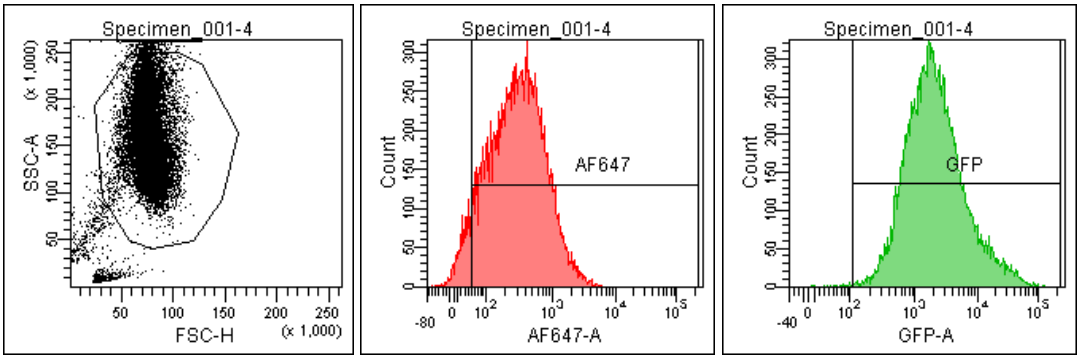

(14c) LinOS/Chol 1:2 3.75 pmol siEGFP-AF

Figure 14. Representative data showing siEGFP-AF (3.75 pmol) delivery and EGFP-AF silencing of LinOS/Chol 1:2, (a) control HeLa cells, (b) with and (c) without DS.

There was efficient EGFP silencing compared to control non-transfected cells (Figure 14a, right column), and adding DS to the lipoplex formulation caused a marked increase in the delivery of siEGFP-AF as shown in Figure 14b and 14c (middle column).

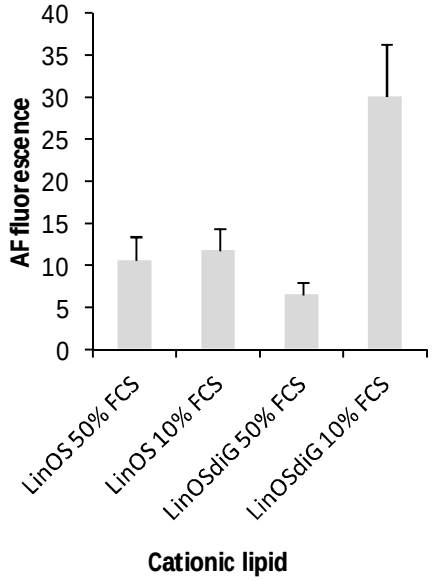

(15a)

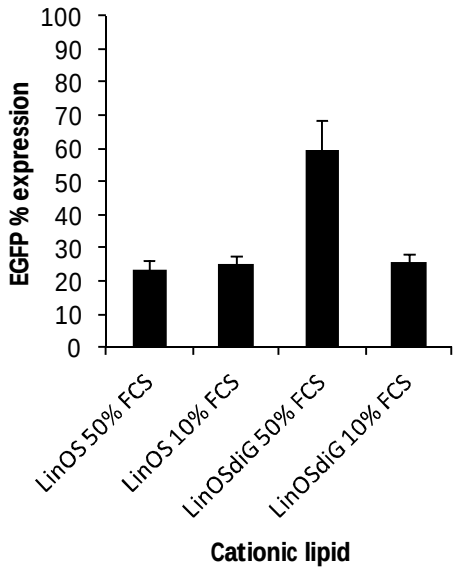

(15b)

Figure 15. LinOS (3 μg/well) and LinOSdiG (6 μg/well) transfection in the presence of 50% or 10% FCS, at 15 nM siEGFP-AF (a) siEGFP-AF delivery and (b) EGFP expression percentage, 48 h post-transfection. The transfection duration was 4 h in the presence of 50% FCS and was 48 h in the presence of 10% FCS.

The presence of serum in the cell culture medium, commonly 10-15% and up to 50% of the culture medium, during transfection with lipoplexes was found to decrease the transfection efficiency.[264-266] Figure 15 shows the effect of increasing the serum content of the cell culture medium (DMEM) from 10% to 50% on siEGFP-AF delivery and EGFP silencing. The percentage of 50% v/v serum in DMEM was chosen based on the fact that approximately half of human blood is serum by percentage, thus 50% serum in the transfection medium is one step further on towards investigating the expected lipoplexes performance in vivo. Practically, 50% serum is considered by some research groups as 100% serum, i.e. 100% relative to the percentage of serum in blood.[267] LinOS (3 μg/well) and LinOSdiG (6 μg/well) were chosen as LinOS was the best asymmetrical lipospermine, and LinOSdiG was the best among the guanidinylated conjugates. The two cationic lipids also were chosen to have different cationic head-groups (amine and guanidine), as this may affect the interaction with the increased content of serum. Increasing the amount of serum to 50% increased the stress on the lipoplex stability, in a similar manner to the destabilizing factors that can be present in vivo, where serum is known to affect negatively transfection efficiency, with the exception of pulmonary delivery which can benefit from an increase in lipoplex

size.[109, 246, 268] Serum contains proteins (e.g. albumin and fibrinogen), heparin, and lipoproteins that can bind to cationic lipids, causing aggregation of lipoplexes, resulting in size changes and changes in the zeta-potential from positive to negative values.[246, 269] siEGFP-AF delivery was higher with LinOS than with LinOSdiG ($p = 0.02$). EGFP expression was reduced to 24% with LinOS, which is approximately similar to the reduction of EGFP expression in the presence of only 10% FCS serum at the same concentration of LinOS (Chapter 4, Figure 7). LinOSdiG reduced the expression to only 59%, and the difference from LinOS was statistically significant ($p = 0.001$). It is clear that while the transfection duration lasted 4 h before replacing the culture media with fresh media, LinOS retained its activity in 50% serum, while LinOSdiG showed reduced gene-silencing compared to that obtained in 10% FCS (Chapter 3, Figure 9). Thus, LinOS is a good candidate for future in vivo experiments.

The EGFP half-life ($t_{1/2}$) is reported to be ~24 h,[234, 270-272] ($t_{1/2}$ is the time required for the fluorescence of a given amount of EGFP to be reduced to 50%), thus the fluorescence will be reduced to ~25% of its original value after two half-lives (48 h). Therefore, lipoplexes showing reduction of EGFP expression to values ≤ 25% 48 h post-transfection (e.g. Figures 10, 13, and 15) completely inhibit EGFP expression (100% gene silencing).

The effects of carrying out transfection at different temperatures (37, 22, and 6 °C) on siEGFP-AF delivery are shown in Figure 16. The amounts of siEGFP-AF and LinOS were kept constant at 15 pmol and 0.75 µg respectively. The delivery of both LinOS and LinOS/Chol 1:2 lipoplexes was significantly decreased at 22 °C and 6 °C compared to delivery at 37 °C. At 6 °C, the delivery was decreased to values of 1 and 3 of LinOS and LinOS/Chol lipoplexes respectively, as compared to values of 6 and 34 respectively at 37 °C.

Figure 17 shows the EGFP expression 48 h post-transfection with LinOS and LinOS/Chol 1:2 siEGFP-AF lipoplexes. The results show that the gene silencing efficiency of both LinOS and LinOS/Chol decreased with decreasing temperature, from 24 and 21 at 37 °C to 64 and 40 at 6 °C respectively. At 22 °C, the LinOS lipoplexes were affected more than LinOS/Chol lipoplexes (EGFP expression reduced to 59% and 21% respectively). Lowering the temperature during the experimental work on cells in culture is a known method for inhibiting temperature dependent (and thereby energy dependent) endocytosis.[171, 252, 273]

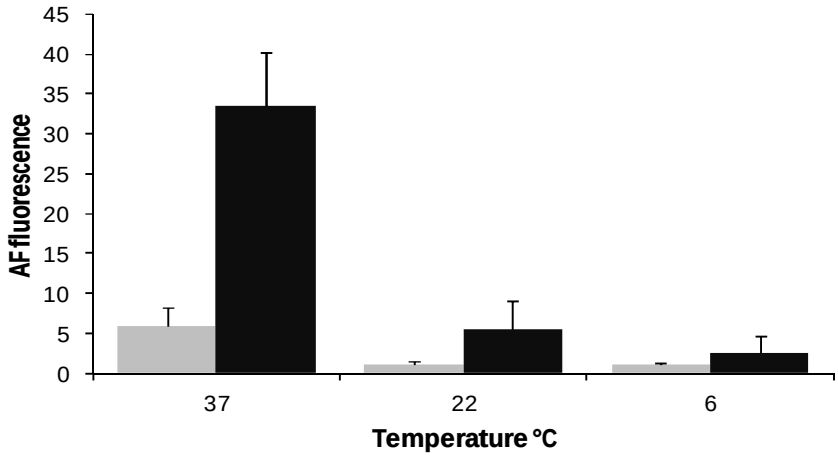

Figure 16. siEGFP delivery 48 h post-transfection with lipoplexes of either LinOS (6 µg/15 pmol siEGFP-AF) represented as grey bars, or lipoplexes of LinOS/Chol 1:2 (LinOS 0.75 µg/15 pmol siEGFP-AF) represented as black bars. Transfection was carried out at 37, 22, and 6 °C for 4 h.

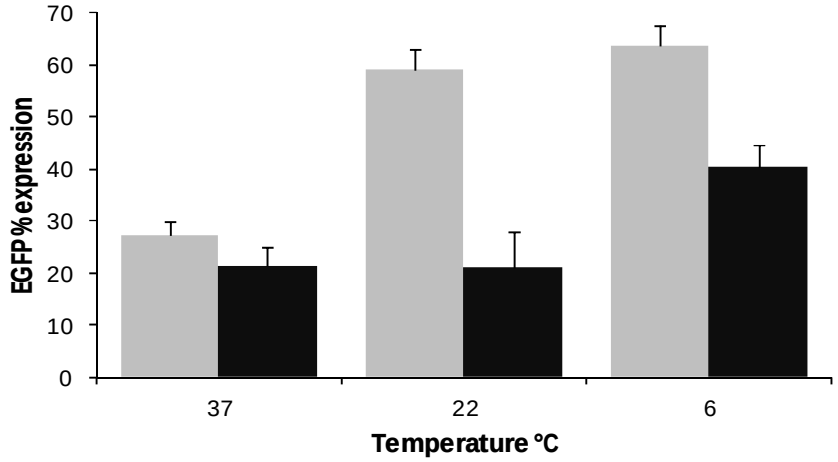

Figure 17. EGFP percentage expression 48 h post-transfection with lipoplexes of either LinOS (6 µg/15 pmol siEGFP-AF) represented as grey bars, or lipoplexes of LinOS/Chol 1:2 (LinOS 0.75 µg/15 pmol siEGFP-AF) represented as black bars. Transfection was carried out at 37, 22, and 6 °C for 4 h.

These results suggest that only a tiny fraction of the delivered siRNA is responsible for the gene silencing effect. For example, the delivery of LinOS/Chol lipoplexes was decreased by ~ 10-fold by changing the temperature from 37 to 6 °C, while EGFP expression changed only

from 21% to 40% at 37 and 6 °C respectively. While gene silencing is sensitive to temperature change, endocytosis and the mechanism responsible for functional siRNA delivery are different. These results agree with the results recently reported[171] by Lu et al., where the functional delivery of siRNA lipoplexes, prepared with the cationic lipid commercial transfection reagent DharmaFECT 1, was found to be temperature sensitive, but independent on different endocytic pathways. They also reported that even though the majority of siRNA lipoplexes reside in the endosomes, membrane fusion is the major functional siRNA lipoplex delivery mechanism.

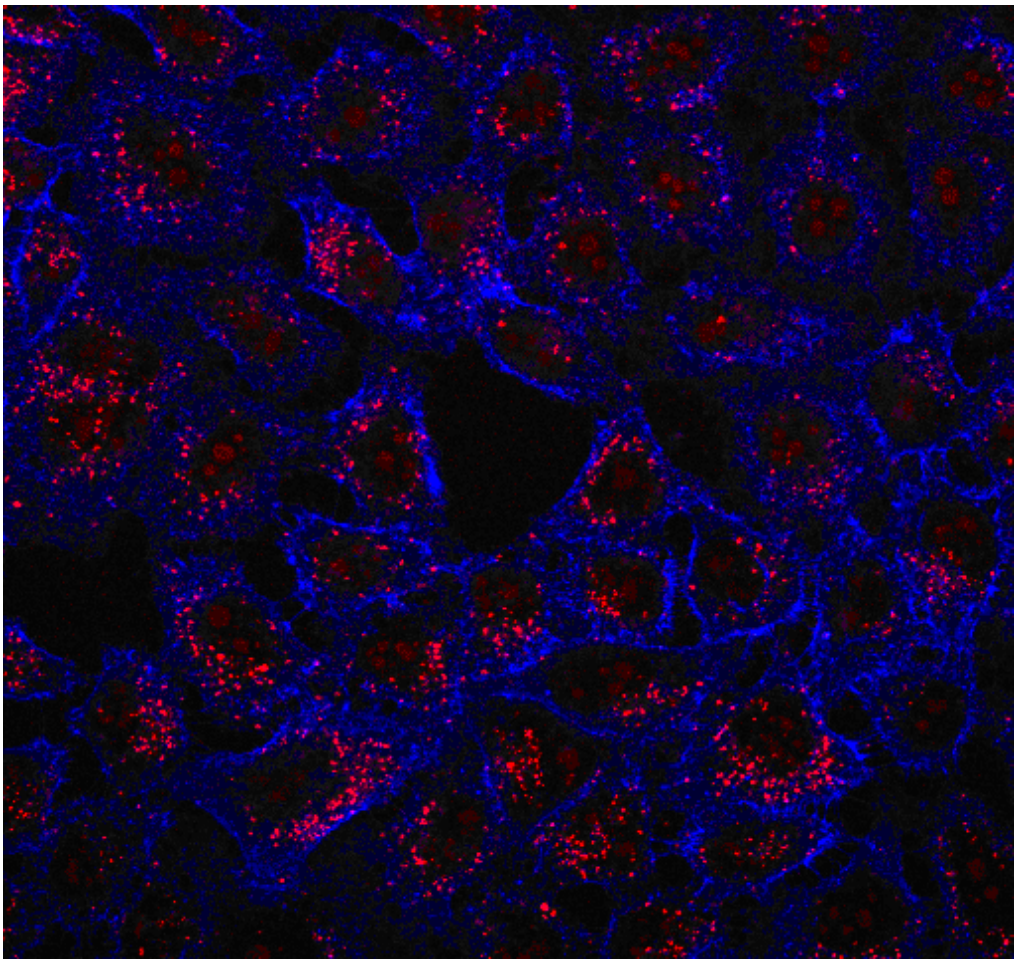

Figure 18. siEGFP-AF lipoplexes of LinOS/Chol 1:2 48 h post transfection in HeLa cells.

The cellular internalization and distribution of lipoplexes of LinOS/Chol 1:2 prepared with siEGFP-AF in HeLa cells 48 h post transfection is shown in Figure 18. Two population of siEGFP-AF appear. One population appears as relatively larger red dots, indicating an increased localization in specific areas inside the cells. The second population appears as a homogenous distribution of a less bright-red colour which might be located in the

nuclear/perinuclear areas. The presence of such two different populations suggests that either they result from two or more different internalization mechanisms, or they resulted from different intracellular distribution processes after being uptaken by the cells. Taken together with the effect of lowering temperature during the transfection process (shown in Figures 16 and 17), Figure 18 further points to the possibility of the existence of more than one internalization mechanism for these lipoplexes.

4. Conclusions

In this Chapter, different approaches to understanding the molecular mechanisms with a view to improving the efficiency of delivery and/or gene silencing of the lipoplexes prepared with selected spermine conjugates have been considered. The selection of the conjugates and their mixtures with helper lipids was based on their high efficiency (e.g. LinOS/Chol 1:2) or specific property (e.g. guanidine head-groups in DOSdiG and LinOSdiG). Mixing cholesterol and DOPE did not result in a significant enhancement of delivery or gene silencing relative to LinOS/Chol 1:2 lipoplexes, although the mixture resulted in a significant increase in efficiency compared to LinOS lipoplexes. Cholesterol mixtures with DOSdiG and LinOSdiG were much more efficient than lipoplexes prepared with the cationic lipids only, however, no significant advantage of changing the nature of the head-group, from amine to guanidine, was observed. The inclusion of the pH sensitive CHS in the formulation resulted in enhancement of gene silencing. Formulating the lipoplexes with the anionic polymer DS resulted in a slight increase of silencing efficiency. Both CHS and DS formulation approaches are promising for further optimization of the lipoplexes. Investigating the cellular entry of siRNA lipoplexes by carrying out transfection at decreasing temperatures showed that delivery was significantly decreased (10-fold) and that whilst the subsequent silencing was also decreased, this was by a much lesser extent. Therefore, it is concluded that a temperature sensitive mechanism, aside from endocytosis, is responsible for the majority of functional siRNA delivery.

Conclusions

In this thesis, a focussed and critical overview of siRNA delivery, the need for siRNA studies of non-viral vectors, and the potential for siRNA lipoplexes in difficult-to-treat diseases was presented. Five discrete sets of experiments were carried out in order to answer SAR and mechanism-of-action questions with regard to siRNA delivery and gene silencing.

Firstly, five symmetrical lipospermines were prepared by conjugating fatty acids of various chain length and oxidation state (C12:0, C18:0, C18:1 Δ^9, C18:2 $\Delta^{9,12}$, C22:1 Δ^{13}) to the naturally occurring polyamine, spermine (1,12-diamino-4,9-diazadodecane). They were evaluated for their siRNA delivery, gene knock-down efficiency, and effect on cell viability. siRNA delivery could not be related directly to gene silencing efficiency as N^4,N^9-dierucoyl spermine (DES) resulted in higher siRNA delivery compared to N^4,N^9-dioleoyl spermine (DOS). EGFP silencing in HeLa cells stably expressing EGFP showed that the unsaturated fatty acid conjugates are more efficient than the saturated fatty acid ones, with DOS resulting in the most efficient gene silencing in the presence of 10% FCS. The alamarBlue cell viability assay showed that the symmetrical spermine conjugates resulted in good cell viability (75%-85% compared to the commercial controls Lipofectamine 2000 and TransIT-TKO), except N^4,N^9-dilauroyl spermine (DLauS) which resulted in low cell viability (50% at 3 μg DLauS/well). Thus, unsaturated fatty acid conjugates of spermine are efficient and non-toxic non-viral vectors for siRNA mediated gene silencing. The best gene silencing was with the symmetrical conjugates that have two C18 chains with one double bond on each chain (oleoyl, silencing EGFP to 19%), followed by linoleoyl chains with two double bonds per chain (silencing EGFP to 28%).

The effect of changing the type of the cationic head-group from a primary amine to a guanidine group was investigated by synthesizing four guanidine derivatives of selected N^4,N^9-diacylated spermines. These guanidine-containing cationic lipids bound siRNA efficiently and formed lipoplexes with lipoplex diameters in the nanometre size-range. Two cationic lipids with C18 unsaturated chains, N^1,N^{12}-diamidino-N^4,N^9-dioleoylspermine and N^1,N^{12}-diamidino-N^4-linoleoyl-N^9-oleoylspermine, were more efficient in terms of EGFP gene silencing compared to cationic lipids with shorter C12 (12:0, lauroyl) and very long C22 (22:1 Δ^{13}, erucoyl) chains. N^1,N^{12}-Diamidino-N^4-linoleoyl-N^9-oleoylspermine (LinOSdiG) siRNA lipoplexes resulted in EGFP gene silencing to 26%, in the presence of 10% FCS, and satisfactory cell viability (64%). The EGFP gene silencing was comparable with that obtained with TransIT-TKO (down to 23%). Changing the cationic head-group to the guanidine did not offer a significant advantage in siRNA delivery or in EGFP gene silencing over the lipospermines with terminal primary amine groups. Guanidinylated N^4,N^9-diacylated

spermines that have fatty chains 18:1/18:1 (symmetrical) or 18:1/18:2 (asymmetrical) are good candidates for non-viral delivery of siRNA to HeLa cells using self-assembled lipoplexes, but they do not show any significant advantages despite their increased basicity and the formation of double the number of salt-bridges (four compared to two primary amines) to the siRNA and cell membrane anionic groups.

The symmetrical spermine conjugates with two 18:1 chains showed the best balance between siRNA delivery, EGFP gene silencing to 19%, and high cell viability (78%). Thus, seven asymmetrical N^4,N^9-diacyl spermines were synthesized and one oleoyl chain was chosen to be held constant. These lipospermines were evaluated as siRNA non-viral vectors, and were compared to molar mixtures of selected symmetrical N^4,N^9-diacyl spermines, keeping the total weight of the cationic lipid constant (3 μg/well). These lipospermines bound siRNA efficiently and formed lipoplexes with particle diameters in the nanometre size-range. Intracellular delivery of siRNA and EGFP gene silencing differ with varying the fatty acid chain lengths and saturation state. N^4-Linoleoyl-N^9-oleoyl-1,12-diamino-4,9-diazadodecane (LinOS) resulted in the best gene silencing, while LigOS (with one lignoceroyl 24:0 chain and one oleoyl) resulted in the best siRNA delivery. Lipospermines with two unsaturated fatty chains generally resulted in better EGFP gene silencing, while the conjugates with one saturated chain resulted in better siRNA delivery. Increasing the lipid chain-length also resulted in increased siRNA delivery. LinOS EGFP gene silencing (24 % with 3 μg/well, compared to 27% with 6 μg DOS under same experimental conditions of transfection) was comparable with or superior to that achieved with the commercially available non-viral vectors TransIT-TKO (25%) and Lipofectamine 2000 (31%), although siRNA delivery was much higher with these two commercial reagents. Thus, delivery and gene silencing are governed by significantly different factors. The asymmetrical lipospermines were well tolerated by the HeLa cells under the normal transfection conditions (cell viabilities typically >74%, LinOS 88%).

The use of the mixtures DOS/DLinS and DOS/DEruS at different molar ratios did not enhance siRNA delivery when compared to the corresponding asymmetrical cationic lipids LinOS and EruOS. EGFP gene silencing with LinOS was better than any of the DOS/DLinS mixtures, while the mixture of 1:1 DOS/DEruS resulted in better EGFP gene expression reduction. Thus, although no definitive rule can describe the superiority of using mixtures over asymmetrical lipospermines or vice versa, it is clear that both approaches can offer an advantage in terms of the resulting gene silencing. These results can be compared and contrasted with the use of mixtures for DNA delivery (gene delivery/gene therapy) where synergy was observed.

It is concluded that not only are siRNA delivery and siRNA mediated gene silencing controlled by different factors, but also that DNA delivery has different vector requirements. It is clear that siRNA delivery and gene silencing are not the same, and the facile comparison with DNA delivery i.e. “all polynucleotides are similar” is precisely that, facile.

siRNA lipoplexes were prepared by the direct mixing of siRNA and mixtures of LinOS with either cholesterol or DOPE (as a neutral lipid) at various molar ratios of the lipids. The effects of varying the lipid formulation and changing of the *N/P* ratio on the intracellular delivery of siRNA to HeLa cells and on the EGFP gene silencing were evaluated. The presence of either cholesterol or DOPE in the mixture resulted in a significant increase in siRNA delivery, as well as enhanced EGFP silencing. LinOS/Chol mixture (1:2) resulted in the highest siRNA delivery, as well as the best gene EGFP silencing (reduced to 20%) at an *N/P* ratio of 3.0. Decreasing the amount of siRNA from 15 pmol to 3.75 pmol while keeping the LinOS/Chol amount constant, thus increasing the *N/P* ratio to 11.9, resulted in decreasing the amount of delivered siRNA, while the reduction of EGFP was comparable to that obtained with 15 pmol (*N/P* = 3.0) of siRNA. Cholesterol mixtures with the symmetrical cationic lipid DOS at 1:2 DOS/Chol, *N/P* = 3.0 (15 pmol siRNA) resulted in less efficient siRNA delivery than with LinOS/Chol 1:2, and comparable delivery at *N/P* = 11.9 (3.75 pmol siRNA). The EGFP gene silencing was comparable with 1:2 mixtures of either LinOS or DOS with cholesterol (lipoplexes prepared with 15 pmol siRNA), but LinOS/Chol mixture showed better EGFP gene silencing when the siRNA amount was reduced to 3.75 pmol. Particle size determination by DLS showed that the lipoplex diameters for cholesterol mixtures were in the range 106-118 nm, compared to 194-356 nm for the lipoplexes prepared with the spermine conjugates only, and to 685 nm for the 1:1 LinOS/DOPE mixture.

Confocal microscopy showed successful siRNA delivery and EGFP knock-down, and Z-stack photomicrographs showed that the delivered siRNA is distributed intracellularly. Cell viability assay (alamarBlue) showed that the prepared lipoplexes resulted in cell viabilities ≥ 81%, with LinOS/Chol (1:2) resulting in viability of 85% and 94% at siRNA amounts 15 pmol and 3.75 pmol respectively. These results show that co-formulation with the helper lipids cholesterol or DOPE resulted in enhanced siRNA delivery and EGFP silencing. siRNA lipoplexes of LinOS/Chol mixtures prepared by the direct mixing of the lipid mixture and siRNA, without any preceding pre-formulation steps of the lipid mixtures, resulted in enhanced siRNA delivery and EGFP knock-down, with very good cell viability (81-95%). Thus, LinOS/Chol (1:2) mixture is a promising candidate as an siRNA non-viral vector.

Different approaches to further improve the performance of selected lipoplex formulations and to understand their mechanisms of action were carried out. The selection of the conjugates and their mixtures with helper lipids was based either on their high efficiency (e.g.

LinOS/Chol 1:2) or on a specific property (e.g. guanidine head-groups in DOSdiG and LinOSdiG). Mixing cholesterol and DOPE did not result in a significant enhancement of delivery or gene silencing relative to LinOS/Chol 1:2 lipoplexes, although the mixture resulted in significant increase in efficiency compared to LinOS lipoplexes at the same *N/P* ratio. Cholesterol mixtures with DOSdiG and LinOSdiG were much more efficient than the lipoplexes prepared with the cationic lipids only. However, no significant advantage of changing the type of head group, from amine to guanidine, was found. The inclusion of the pH sensitive cholesteryl hemisuccinate (CHS) in the lipoplex formulation resulted in an enhancement of gene silencing. Formulating the lipoplexes with the anionic polymer dextran sulfate (DS), resulted in a slight increase of gene silencing efficiency. Both CHS and DS formulation approaches are promising for further optimization of the lipoplexes. Carrying out transfection experiments in 50% FCS, showed that LinOS (with terminal primary amine groups) did not lose its efficiency, while LinOSdiG showed decreased efficiency compared to transfection in 10% FCS. Thus, the amine group is potentially more promising for future applications in vivo. Investigating the mechanism of cellular entry of the siRNA lipoplexes by carrying out transfection at decreasing temperatures, showed that the delivery was significantly decreased (10-fold at 6 °C), but whilst the subsequent gene silencing was also decreased, this was to a much lower extent (by 25%, from ~80% to ~60% silencing corresponding to ~20% and ~40% EGFP expression respectively). From these results it was concluded that a temperature sensitive mechanism aside from endocytosis is responsible for a large part of functional siRNA delivery.

In summary, several lipopolyamines were designed to achieve effective siRNA delivery, efficient gene-silencing, and minimum toxicity to cells. Symmetrical DOS achieved efficient gene-silencing while symmetrical DEruS showed enhanced delivery. DOS is as good as the two leading (gold standard) non-viral transfection reagents TransIT-TKO and Lipofectamine 2000 for gene silencing and for cell viability. Notwithstanding the huge siRNA delivery of TransIT-TKO and Lipofectamine 2000, the novel asymmetrical LinOS was developed which achieved complete gene silencing, still with excellent cell viability, and yet with significantly lower siRNA delivery. Coformulation of LinOS with cholesterol further enhanced its efficiency. Finally, as the half-life ($t_{1/2}$) of EGFP is ~24 h, then 25% of EGFP will be present 48 h post-transfection (after two half-lives of EGFP) which when compared to the gene silencing 48 h post-transfection with DOS and LinOS (20-24% expression of EGFP) leads to the conclusion that the biosynthesis of EGFP is 100% inhibited.

References (in the style of *Mol. Pharmaceutics*)

1. Blagbrough, I. S.; Zara, C. Animal models for target diseases in gene therapy - using DNA and siRNA delivery strategies. *Pharm. Res.* **2009**, *26*, 1-18.
2. van der Krol, A. R.; Mur, L. A.; Beld, M.; Mol, J.; Stuitje, A. R. Flavonoid genes in Petunia: addition of a limited number of gene copies may lead to a suppression of gene expression. *Plant Cell* **1990**, *2*, 291-299.
3. Napoli, C.; Lemieux, C.; Jorgensen, R. Introduction of a chimeric chalcone synthase gene into Petunia results in reversible co-suppression of homologous genes *in trans*. *Plant Cell* **1990**, *2*, 279-289.
4. Vanblokland, R.; Vandergeest, N.; Mol, J. N. M.; Kooter, J. M. Transgene-mediated suppression of chalcone synthase expression in Petunia hybrida results from an increase in RNA turnover. *Plant J.* **1994**, *6*, 861-877.
5. Metzlaff, M.; Odell, M.; Cluster, P. D.; Flavell, R. B. RNA-mediated RNA degradation and chalcone synthase A silencing in Petunia. *Cell* **1997**, *88*, 845-854.
6. Fire, A.; Xu, S. Q.; Montgomery, M. K.; Kostas, S. A.; Driver, S. E.; Mello, C. C. Potent and specific genetic interference by double-stranded RNA in Caenorhabditis elegans. *Nature* **1998**, *391*, 806-811.
7. Elbashir, S. M.; Harborth, J.; Lendeckel, W.; Yalcin, A.; Weber, K.; Tuschl, T. Duplexes of 21-nucleotide RNAs mediate RNA interference in cultured mammalian cells. *Nature* **2001**, *411*, 494-498.
8. Cogoni, C.; Macino, G. Post-transcriptional gene silencing across kingdoms. *Curr. Opin. Genet. Dev.* **2000**, *10*, 638-643.
9. Sontheimer, E. J. Assembly and function of RNA silencing complexes. *Nat. Rev. Mol. Cell Bio.* **2005**, *6*, 127-138.
10. Collins, R. E.; Cheng, X. D. Structural and biochemical advances in mammalian RNAi. *J. Cell. Biochem.* **2006**, *99*, 1251-1266.
11. Hutvagner, G.; Simard, M. J. Argonaute proteins: Key players in RNA silencing. *Nat. Rev. Mol. Cell Bio.* **2008**, *9*, 22-32.
12. Gaynor, J. W.; Campbell, B. J.; Cosstick, R. RNA interference: A chemist's perspective. *Chem. Soc. Rev.* **2010**, *39*, 4169-4184.
13. Liu, Q. H.; Paroo, Z. Biochemical principles of small RNA pathways. *Annu. Rev. Biochem.* **2010**, *79*, 295-319.
14. Haley, B.; Zamore, P. D. Kinetic analysis of the RNAi enzyme complex. *Nat. Struct. Mol. Biol.* **2004**, *11*, 599-606.

15. Hutvagner, G. Small RNA asymmetry in RNAi: Function in RISC assembly and gene regulation. *FEBS Lett.* **2005**, *579*, 5850-5857.
16. Wang, H. W.; Noland, C.; Siridechadilok, B.; Taylor, D. W.; Ma, E. B.; Felderer, K.; Doudna, J. A.; Nogales, E. Structural insights into RNA processing by the human RISC-loading complex. *Nat. Struct. Mol. Biol.* **2009**, *16*, 1148-1153.
17. Wahid, F.; Shehzad, A.; Khan, T.; Kim, Y. Y. MicroRNAs: synthesis, mechanism, function, and recent clinical trials. *Biochim. Biophys. Acta Mol. Cell Res.* **2010**, *1803*, 1231-1243.
18. Paddison, P. J.; Caudy, A. A.; Bernstein, E.; Hannon, G. J.; Conklin, D. S. Short hairpin RNAs (shRNAs) induce sequence-specific silencing in mammalian cells. *Genes Dev.* **2002**, *16*, 948-958.
19. Rao, D. D.; Vorhies, J. S.; Senzer, N.; Nemunaitis, J. siRNA vs. shRNA: Similarities and differences. *Adv. Drug Del. Rev.* **2009**, *61*, 746-759.
20. Freier, S. M.; Kierzek, R.; Jaeger, J. A.; Sugimoto, N.; Caruthers, M. H.; Neilson, T.; Turner, D. H. Improved free-energy parameters for predictions of RNA duplex stability. *Proc. Natl. Acad. Sci. U.S.A.* **1986**, *83*, 9373-9377.
21. Freier, S. M.; Altmann, K. H. The ups and downs of nucleic acid duplex stability: structure-stability studies on chemically-modified DNA:RNA duplexes. *Nucleic Acids Res.* **1997**, *25*, 4429-4443.
22. Beverly, M. B. Applications of mass spectrometry to the study of siRNA. *Mass Spectrom. Rev.* **2010**, 10.1002/mas.20260.
23. Shah, S. A.; Brunger, A. T. The 1.8 angstrom crystal structure of a statically disordered 17 base-pair RNA duplex: principles of RNA crystal packing and its effect on nucleic acid structure. *J. Mol. Biol.* **1999**, *285*, 1577-1588.
24. Rana, T. M. Illuminating the silence: understanding the structure and function of small RNAs. *Nat. Rev. Mol. Cell Bio.* **2007**, *8*, 23-36.
25. Banan, M.; Puri, N. The ins and outs of RNAi in mammalian cells. *Curr. Pharm. Biotechnol.* **2004**, *5*, 441-450.
26. Hickerson, R. P.; Vlassov, A. V.; Wang, Q.; Leake, D.; Ilves, H.; Gonzalez-Gonzalez, E.; Contag, C. H.; Johnston, B. H.; Kaspar, R. L. Stability study of unmodified siRNA and relevance to clinical use. *Oligonucleotides* **2008**, *18*, 345-354.
27. Layzer, J. M.; McCaffrey, A. P.; Tanner, A. K.; Huang, Z.; Kay, M. A.; Sullenger, B. A. In vivo activity of nuclease-resistant siRNAs. *RNA* **2004**, *10*, 766-771.
28. Turner, J. J.; Jones, S. W.; Moschos, S. A.; Lindsay, M. A.; Gait, M. J. MALDI-TOF mass spectral analysis of siRNA degradation in serum confirms an RNAse A-like activity. *Mol. Biosyst.* **2007**, *3*, 43-50.

29. Volkov, A. A.; Kruglova, N. y. S.; Meschaninova, M. I.; Venyaminova, A. G.; Zenkova, M. A.; Vlassov, V. V.; Chernolovskaya, E. L. Selective protection of nuclease-sensitive sites in siRNA prolongs silencing effect. *Oligonucleotides* **2009**, *19*, 191-202.
30. Melnikova, I. RNA-based therapies. *Nat. Rev. Drug Discov.* **2007**, *6*, 863-864.
31. Skoblov, M. Prospects of antisense therapy technologies. *Mol. Biol.* **2009**, *43*, 917-929.
32. Ghosal, A.; Kabir, A. H.; Mandal, A. RNA interference and its therapeutic potential. *Cent. Eur. J. Med.* **2011**, *6*, 137-147.
33. Cheng, H.; Luo, C.; Wu, X.; Zhang, Y.; He, Y.; Wu, Q.; Xia, Y.; Zhang, J. shRNA targeting PLCε inhibits bladder cancer growth in vitro and In vivo. *Urology* **2011**, *78*.
34. Qin, X.-J.; Dai, D.-J.; Gao, Z.-G.; Huan, J.-L.; Zhu, L. Effect of lentivirus-mediated shRNA targeting VEGFR-3 on proliferation, apoptosis and invasion of gastric cancer cells. *Int. J. Mol. Med.* **2011**, *28*, 761-768.
35. Liu, Q.-S.; Zhang, J.; Liu, M.; Dong, W.-G. Lentiviral-mediated miRNA against liver-intestine cadherin suppresses tumor growth and invasiveness of human gastric cancer. *Cancer Sci.* **2010**, *101*, 1807-1812.
36. Bumcrot, D.; Manoharan, M.; Koteliansky, V.; Sah, D. W. Y. RNAi therapeutics: A potential new class of pharmaceutical drugs. *Nat. Chem. Biol.* **2006**, *2*, 711-719.
37. Aleku, M.; Schulz, P.; Keil, O.; Santel, A.; Schaeper, U.; Dieckhoff, B.; Janke, O.; Endruschat, J.; Durieux, B.; Roeder, N.; Loeffler, K.; Lange, C.; Fechtner, M.; Moepert, K.; Fisch, G.; Dames, S.; Arnold, W.; Jochims, K.; Giese, K.; Wiedenmann, B.; Scholz, A.; Kaufmann, J. Atu027, a liposomal small interfering RNA Formulation targeting protein kinase N3, inhibits cancer progression. *Cancer Res.* **2008**, *68*, 9788-9798.
38. Behlke, M. A. Progress towards in vivo use of siRNAs. *Mol. Ther.* **2006**, *13*, 644-670.
39. Whitehead, K. A.; Langer, R.; Anderson, D. G. Knocking down barriers: advances in siRNA delivery. *Nat. Rev. Drug Discovery* **2009**, *8*, 129-138.
40. Reischl, D.; Zimmer, A. Drug delivery of siRNA therapeutics: Potentials and limits of nanosystems. *Nanomed. Nanotechnol. Biol. Med.* **2009**, *5*, 8-20.
41. van de Water, F. M.; Boerman, O. C.; Wouterse, A. C.; Peters, J. G. P.; Russel, F. G. M.; Masereeuw, R. Intravenously administered short interfering RNA accumulates in the kidney and selectively suppresses gene function in renal proximal tubules. *Drug Metab. Disposition* **2006**, *34*, 1393-1397.

42. Ruponen, M.; Ronkko, S.; Honkakoski, P.; Pelkonen, J.; Tammi, M.; Urtti, A. Extracellular glycosaminoglycans modify cellular trafficking of lipoplexes and polyplexes. *J. Biol. Chem.* **2001**, *276*, 33875-33880.
43. Singh, A. K.; Kasinath, B. S.; Lewis, E. J. Interaction of polycations with cell-surface negative charges of epithelial-cells. *Biochim. Biophys. Acta* **1992**, *1120*, 337-342.
44. Watts, J. K.; Deleavey, G. F.; Damha, M. J. Chemically modified siRNA: Tools and applications. *Drug Discov. Today* **2008**, *13*, 842-855.
45. Behlke, M. A. Chemical modification of siRNAs for in vivo use. *Oligonucleotides* **2008**, *18*, 305-319.
46. Hall, A. H. S.; Wan, J.; Shaughnessy, E. E.; Shaw, B. R.; Alexander, K. A. RNA interference using boranophosphate siRNAs: structure-activity relationships. *Nucleic Acids Res.* **2004**, *32*, 5991-6000.
47. Ui-Tei, K.; Naito, Y.; Zenno, S.; Nishi, K.; Yamato, K.; Takahashi, F.; Juni, A.; Saigo, K. Functional dissection of siRNA sequence by systematic DNA substitution: modified siRNA with a DNA seed arm is a powerful tool for mammalian gene silencing with significantly reduced off-target effect. *Nucleic Acids Res.* **2008**, *36*, 2136-2151.
48. Chiu, Y. L.; Rana, T. M. siRNA function in RNAi: A chemical modification analysis. *RNA* **2003**, *9*, 1034-1048.
49. Bell, N. M.; Micklefield, J. Chemical modification of oligonucleotides for therapeutic, bioanalytical and other applications. *ChemBioChem* **2009**, *10*, 2691-2703.
50. Corey, D. R. Chemical modification: The key to clinical application of RNA interference? *J. Clin. Invest.* **2007**, *117*, 3615-3622.
51. Nishina, K.; Unno, T.; Uno, Y.; Kubodera, T.; Kanouchi, T.; Mizusawa, H.; Yokota, T. Efficient in vivo delivery of siRNA to the liver by conjugation of alpha-tocopherol. *Mol. Ther.* **2008**, *16*, 734-740.
52. Lorenz, C.; Hadwiger, P.; John, M.; Vornlocher, H. P.; Unverzagt, C. Steroid and lipid conjugates of siRNAs to enhance cellular uptake and gene silencing in liver cells. *Bioorg. Med. Chem. Lett.* **2004**, *14*, 4975-4977.
53. Soutschek, J.; Akinc, A.; Bramlage, B.; Charisse, K.; Constien, R.; Donoghue, M.; Elbashir, S.; Geick, A.; Hadwiger, P.; Harborth, J.; John, M.; Kesavan, V.; Lavine, G.; Pandey, R. K.; Racie, T.; Rajeev, K. G.; Rohl, I.; Toudjarska, I.; Wang, G.; Wuschko, S.; Bumcrot, D.; Koteliansky, V.; Limmer, S.; Manoharan, M.; Vornlocher, H. P. Therapeutic silencing of an endogenous gene by systemic administration of modified siRNAs. *Nature* **2004**, *432*, 173-178.

54. Wolfrum, C.; Shi, S.; Jayaprakash, K. N.; Jayaraman, M.; Wang, G.; Pandey, R. K.; Rajeev, K. G.; Nakayama, T.; Charrise, K.; Ndungo, E. M.; Zimmermann, T.; Koteliansky, V.; Manoharan, M.; Stoffel, M. Mechanisms and optimization of in vivo delivery of lipophilic siRNAs. *Nat. Biotechnol.* **2007**, *25*, 1149-1157.

55. Eguchi, A.; Dowdy, S. F. siRNA delivery using peptide transduction domains. *Trends Pharmacol. Sci.* **2009**, *30*, 341-345.

56. Muratovska, A.; Eccles, M. R. Conjugate for efficient delivery of short interfering RNA (siRNA) into mammalian cells. *FEBS Lett.* **2004**, *558*, 63-68.

57. Moschos, S. A.; Jones, S. W.; Perry, M. M.; Williams, A. E.; Erjefalt, J. S.; Turner, J. J.; Barnes, P. J.; Sproat, B. S.; Gait, M. J.; Lindsay, M. A. Lung delivery studies using siRNA conjugated to TAT(48-60) and penetratin reveal peptide induced reduction in gene expression and induction of innate immunity. *Bioconj. Chem.* **2007**, *18*, 1450-1459.

58. Kim, S. H.; Jeong, J. H.; Lee, S. H.; Kim, S. W.; Park, T. G. PEG conjugated VEGF siRNA for anti-angiogenic gene therapy. *J. Control. Release* **2006**, *116*, 123-129.

59. Xia, C. F.; Zhang, Y.; Boado, R. J.; Pardridge, W. M. Intravenous siRNA of brain cancer with receptor targeting and avidin-biotin technology. *Pharm. Res.* **2007**, *24*, 2309-2316.

60. Chu, T. C.; Twu, K. Y.; Ellington, A. D.; Levy, M. Aptamer mediated siRNA delivery. *Nucleic Acids Res.* **2006**, *34*.

61. Li, M. J.; Bauer, G.; Michienzi, A.; Yee, J. K.; Lee, N. S.; Kim, J.; Li, S.; Castanotto, D.; Zaia, J.; Rossi, J. J. Inhibition of HIV-1 infection by lentiviral vectors expressing Pol III-promoted anti-HIV RNAs. *Mol. Ther.* **2003**, *8*, 196-206.

62. Sliva, K.; Schnierle, B. S. Selective gene silencing by viral delivery of short hairpin RNA. *Virol. J.* **2010**, *7*, 248.

63. Atkinson, H.; Chalmers, R. Delivering the goods: viral and non-viral gene therapy systems and the inherent limits on cargo DNA and internal sequences. *Genetica* **2010**, *138*, 485-98.

64. Chen, Y.; Du, D.; Wu, J.; Chan, C. P.; Tan, Y.; Kung, H. F.; He, M. L. Inhibition of hepatitis B virus replication by stably expressed shRNA. *Biochem. Biophys. Res. Commun.* **2003**, *311*, 398-404.

65. Kumar, A.; Panda, S. K.; Durgapal, H.; Acharya, S. K.; Rehman, S.; Kar, U. K. Inhibition of Hepatitis E virus replication using short hairpin RNA (shRNA). *Antiviral Res.* **2010**, *85*, 541-550.

66. Bushman, F. D. Retroviral integration and human gene therapy. *J. Clin. Invest.* **2007**, *117*, 2083-2086.

67. Brummelkamp, T. R.; Bernards, R.; Agami, R. Stable suppression of tumorigenicity by virus-mediated RNA interference. *Cancer Cell* **2002**, *2*, 243-247.
68. Anesti, A. M.; Peeters, P. J.; Royaux, I.; Coffin, R. S. Efficient delivery of RNA Interference to peripheral neurons in vivo using herpes simplex virus. *Nucleic Acids Res.* **2008**, *36*.
69. Manjunath, N.; Wu, H.; Subramanya, S.; Shankar, P. Lentiviral delivery of short hairpin RNAs. *Adv. Drug Del. Rev.* **2009**, *61*, 732-745.
70. Carlson, M. E.; Hsu, M.; Conboy, I. M. Imbalance between pSmad3 and Notch induces CDK inhibitors in old muscle stem cells. *Nature* **2008**, *454*, 528-532.
71. Yoo, J. Y.; Kim, J. H.; Kwon, Y. G.; Kim, E. C.; Kim, N. K.; Choi, H. J.; Yun, C. O. VEGF-specific short hairpin RNA-expressing oncolytic adenovirus elicits potent inhibition of angiogenesis and tumor growth. *Mol. Ther.* **2007**, *15*, 295-302.
72. Xia, H.; Mao, Q.; Eliason, S. L.; Harper, S. Q.; Martins, I. H.; Orr, H. T.; Paulson, H. L.; Yang, L.; Kotin, R. M.; Davidson, B. L. RNAi suppresses polyglutamine-induced neurodegeneration in a model of spinocerebellar ataxia. *Nat. Med.* **2004**, *10*, 816-820.
73. Berkowitz, R.; Ilves, H.; Lin, W. Y.; Eckert, K.; Coward, A.; Tamaki, S.; Veres, G.; Plavec, I. Construction and molecular analysis of gene transfer systems derived from bovine immunodeficiency virus. *J. Virol.* **2001**, *75*, 3371-3382.
74. Kuhlmann, K. F.; Gouma, D. J.; Wesseling, J. G. Adenoviral gene therapy for pancreatic cancer: where do we stand? *Dig. Surg.* **2008**, *25*, 278-292.
75. Descamps, D.; Benihoud, K. Two key challenges for effective adenovirus-mediated liver gene therapy: innate immune responses and hepatocyte-specific transduction. *Curr. Gene Ther.* **2009**, *9*, 115-127.
76. Nayak, S.; Herzog, R. W. Progress and prospects: Immune responses to viral vectors. *Gene Ther.* **2010**, *17*, 295-304.
77. Raper, S. E.; Chirmule, N.; Lee, F. S.; Wivel, N. A.; Bagg, A.; Gao, G. P.; Wilson, J. M.; Batshaw, M. L. Fatal systemic inflammatory response syndrome in a ornithine transcarbamylase deficient patient following adenoviral gene transfer. *Mol. Genet. Metab.* **2003**, *80*, 148-158.
78. Howe, S. J.; Mansour, M. R.; Schwarzwaelder, K.; Bartholomae, C.; Hubank, M.; Kempski, H.; Brugman, M. H.; Pike-Overzet, K.; Chatters, S. J.; de Ridder, D.; Gilmour, K. C.; Adams, S.; Thornhill, S. I.; Parsley, K. L.; Staal, F. J.; Gale, R. E.; Linch, D. C.; Bayford, J.; Brown, L.; Quaye, M.; Kinnon, C.; Ancliff, P.; Webb, D. K.; Schmidt, M.; von Kalle, C.; Gaspar, H. B.; Thrasher, A. J. Insertional mutagenesis combined with acquired somatic mutations causes leukemogenesis following gene therapy of SCID-X1 patients. *J. Clin. Invest.* **2008**, *118*, 3143-3150.

79. Hacein-Bey-Abina, S.; von Kalle, C.; Schmidt, M.; Le Deist, F.; Wulffraat, N.; McIntyre, E.; Radford, I.; Villeval, J. L.; Fraser, C. C.; Cavazzana-Calvo, M.; Fischer, A. A serious adverse event after successful gene therapy for X-linked severe combined immunodeficiency. *New Engl. J. Med.* **2003**, *348*, 255-256.
80. Qasim, W.; Gaspar, H. B.; Thrasher, A. J. Progress and prospects: Gene therapy for inherited immunodeficiencies. *Gene Ther.* **2009**, *16*, 1285-1291.
81. Sheridan, C. Gene therapy finds its niche. *Nat. Biotechnol.* **2011**, *29*, 121-128.
82. Mintzer, M. A.; Simanek, E. E. Nonviral vectors for gene delivery. *Chem. Rev.* **2009**, *109*, 259-302.
83. Torchilin, V. P.; Rammohan, R.; Weissig, V.; Levchenko, T. S. TAT peptide on the surface of liposomes affords their efficient intracellular delivery even at low temperature and in the presence of metabolic inhibitors. *Proc. Natl. Acad. Sci. U.S.A.* **2001**, *98*, 8786-8791.
84. Torchilin, V. P.; Levchenko, T. S.; Rammohan, R.; Volodina, N.; Papahadjopoulos-Sternberg, B.; D'Souza, G. G. Cell transfection in vitro and in vivo with nontoxic TAT peptide-liposome-DNA complexes. *Proc. Natl. Acad. Sci. U.S.A.* **2003**, *100*, 1972-1977.
85. Snyder, E. L.; Dowdy, S. F. Cell penetrating peptides in drug delivery. *Pharm. Res.* **2004**, *21*, 389-393.
86. Gait, M. J. Peptide-mediated cellular delivery of antisense oligonucleotides and their analogues. *Cell. Mol. Life Sci.* **2003**, *60*, 844-853.
87. Eguchi, A.; Akuta, T.; Okuyama, H.; Senda, T.; Yokoi, H.; Inokuchi, H.; Fujita, S.; Hayakawa, T.; Takeda, K.; Hasegawa, M.; Nakanishi, M. Protein transduction domain of HIV-1 TAT protein promotes efficient delivery of DNA into mammalian cells. *J. Biol. Chem.* **2001**, *276*, 26204-26210.
88. Foerg, C.; Merkle, H. P. On the biomedical promise of cell penetrating peptides: Limits versus prospects. *J. Pharm. Sci.* **2008**, *97*, 144-162.
89. Mäe, M.; Andaloussi, S. E.; Lehto, T.; Langel, Ü. Chemically modified cell-penetrating peptides for the delivery of nucleic acids. *Expert Opin. Drug Deliv.* **2009**, *6*, 1195-1205.
90. Frankel, A. D.; Pabo, C. O. Cellular uptake of the TAT protein from human immunodeficiency virus. *Cell* **1988**, *55*, 1189-1193.
91. Vives, E.; Brodin, P.; Lebleu, B. A truncated HIV-1 TAT protein basic domain rapidly translocates through the plasma membrane and accumulates in the cell nucleus. *J. Biol. Chem.* **1997**, *272*, 16010-16017.

92. Jones, A. T. Macropinocytosis: searching for an endocytic identity and role in the uptake of cell penetrating peptides. *J. Cell. Mol. Med.* **2007**, *11*, 670-684.
93. Patel, L. N.; Zaro, J. L.; Shen, W. C. Cell penetrating peptides: Intracellular pathways and pharmaceutical perspectives. *Pharm. Res.* **2007**, *24*, 1977-1992.
94. Crombez, L.; Aldrian-Herrada, G.; Konate, K.; Nguyen, Q. N.; McMaster, G. K.; Brasseur, R.; Heitz, F.; Divita, G. A new potent secondary amphipathic cell-penetrating peptide for siRNA delivery into mammalian cells. *Mol. Ther.* **2009**, *17*, 95-103.
95. Kim, W. J.; Christensen, L. V.; Jo, S.; Yockman, J. W.; Jeong, J. H.; Kim, Y. H.; Kim, S. W. Cholesteryl oligoarginine delivering vascular endothelial growth factor siRNA effectively inhibits tumor growth in colon adenocarcinoma. *Mol. Ther.* **2006**, *14*, 343-350.
96. Lundberg, P.; El-Andaloussi, S.; Sutlu, T.; Johansson, H.; Langel, U. Delivery of short interfering RNA using endosomolytic cell-penetrating peptides. *FASEB J.* **2007**, *21*, 2664-2671.
97. Simeoni, F.; Morris, M. C.; Heitz, F.; Divita, G. Insight into the mechanism of the peptide-based gene delivery system MPG: Implications for delivery of siRNA into mammalian cells. *Nucleic Acids Res.* **2003**, *31*, 2717-2724.
98. Zeineddine, D.; Papadimou, E.; Chebli, K.; Gineste, M.; Liu, J.; Grey, C.; Thurig, S.; Behfar, A.; Wallace, V. A.; Skerjanc, I. S.; Puceat, M. Oct-3/4 dose dependently regulates specification of embryonic stem cells toward a cardiac lineage and early heart development. *Dev. Cell* **2006**, *11*, 535-546.
99. Davidson, T. J.; Harel, S.; Arboleda, V. A.; Prunell, G. F.; Shelanski, M. L.; Greene, L. A.; Troy, C. M. Highly efficient small interfering RNA delivery to primary mammalian neurons induces microRNA-like effects before mRNA degradation. *J. Neurosci.* **2004**, *24*, 10040-10046.
100. Turner, J. J.; Jones, S.; Fabani, M. M.; Ivanova, G.; Arzumanov, A. A.; Gait, M. J. RNA targeting with peptide conjugates of oligonucleotides, siRNA and PNA. *Blood Cells. Mol. Dis.* **2007**, *38*, 1-7.
101. Chiu, Y. L.; Ali, A.; Chu, C. Y.; Cao, H.; Rana, T. M. Visualizing a correlation between siRNA localization, cellular uptake, and RNAi in living cells. *Chem. Biol.* **2004**, *11*, 1165-1175.
102. Hassani, Z.; Lemkine, G. F.; Erbacher, P.; Palmier, K.; Alfama, G.; Giovannangeli, C.; Behr, J. P.; Demeneix, B. A. Lipid-mediated siRNA delivery down-regulates exogenous gene expression in the mouse brain at picomolar levels. *J. Gene Med.* **2005**, *7*, 198-207.

103. Grayson, A. C.; Doody, A. M.; Putnam, D. Biophysical and structural characterization of polyethylenimine-mediated siRNA delivery in vitro. *Pharm. Res.* **2006**, *23*, 1868-1876.

104. Spagnou, S.; Miller, A. D.; Keller, M. Lipidic carriers of siRNA: Differences in the formulation, cellular uptake, and delivery with plasmid DNA. *Biochemistry* **2004**, *43*, 13348-13356.

105. Bolcato-Bellemin, A. L.; Bonnet, M. E.; Creusatt, G.; Erbacher, P.; Behr, J. P. Sticky overhangs enhance siRNA-mediated gene silencing. *Proc. Natl. Acad. Sci. U.S.A.* **2007**, *104*, 16050-16055.

106. Moghimi, S. M.; Symonds, P.; Murray, J. C.; Hunter, A. C.; Debska, G.; Szewczyk, A. A two-stage poly(ethylenimine)-mediated cytotoxicity: implications for gene transfer/therapy. *Mol. Ther.* **2005**, *11*, 990-995.

107. Werth, S.; Urban-Klein, B.; Dai, L.; Hobel, S.; Grzelinski, M.; Bakowsky, U.; Czubayko, F.; Aigner, A. A low molecular weight fraction of polyethylenimine (PEI) displays increased transfection efficiency of DNA and siRNA in fresh or lyophilized complexes. *J. Control. Release* **2006**, *112*, 257-270.

108. Boussif, O.; Lezoualc'h, F.; Zanta, M. A.; Mergny, M. D.; Scherman, D.; Demeneix, B.; Behr, J. P. A versatile vector for gene and oligonucleotide transfer into cells in culture and in vivo: polyethylenimine. *Proc. Natl. Acad. Sci. U.S.A.* **1995**, *92*, 7297-7301.

109. Philipp, A.; Zhao, X.; Tarcha, P.; Wagner, E.; Zintchenko, A. Hydrophobically modified oligoethylenimines as highly efficient transfection agents for siRNA delivery. *Bioconj. Chem.* **2009**, *20*, 2055-2061.

110. Bajaj, A.; Kondaiah, P.; Bhattacharya, S. Synthesis and gene transfection efficacies of PEI-cholesterol-based lipopolymers. *Bioconj. Chem.* **2008**, *19*, 1640-1651.

111. Breunig, M.; Hozsa, C.; Lungwitz, U.; Watanabe, K.; Umeda, I.; Kato, H.; Goepferich, A. Mechanistic investigation of poly(ethyleneimine)-based siRNA delivery: disulfide bonds boost intracellular release of the cargo. *J. Control. Release* **2008**, *130*, 57-63.

112. Mao, S.; Sun, W.; Kissel, T. Chitosan-based formulations for delivery of DNA and siRNA. *Adv. Drug Del. Rev.* **2010**, *62*, 12-27.

113. Liu, X.; Howard, K. A.; Dong, M.; Andersen, M. O.; Rahbek, U. L.; Johnsen, M. G.; Hansen, O. C.; Besenbacher, F.; Kjems, J. The influence of polymeric properties on chitosan/siRNA nanoparticle formulation and gene silencing. *Biomaterials* **2007**, *28*, 1280-1288.

114. Katas, H.; Alpar, H. O. Development and characterisation of chitosan nanoparticles for siRNA delivery. *J. Control. Release* **2006**, *115*, 216-225.

115. Menuel, S.; Fontanay, S.; Clarot, I.; Duval, R. E.; Diez, L.; Marsura, A. Synthesis and Complexation Ability of a Novel Bis-(guanidinium)-tetrakis-(beta-cyclodextrin) Dendrimeric Tetrapod as a Potential Gene Delivery (DNA and siRNA) System. Study of Cellular siRNA Transfection. *Bioconj. Chem.* **2008**, *19*, 2357-2362.

116. Hu-Lieskovan, S.; Heidel, J. D.; Bartlett, D. W.; Davis, M. E.; Triche, T. J. Sequence-specific knockdown of EWS-FLI1 by targeted, nonviral delivery of small interfering RNA inhibits tumor growth in a murine model of metastatic Ewing's sarcoma. *Cancer Res.* **2005**, *65*, 8984-8992.

117. Zhu, L.; Mahato, R. I. Lipid and polymeric carrier-mediated nucleic acid delivery. *Expert Opin. Drug Deliv.* **2010**, *7*, 1209-1226.

118. Dufès, C.; Uchegbu, I. F.; Schätzlein, A. G. Dendrimers in gene delivery. *Adv. Drug Del. Rev.* **2005**, *57*, 2177-2202.

119. Zinselmeyer, B. H.; Mackay, S. P.; Schatzlein, A. G.; Uchegbu, I. F. The lower-generation polypropylenimine dendrimers are effective gene-transfer agents. *Pharm. Res.* **2002**, *19*, 960-967.

120. Fischer, D.; Li, Y.; Ahlemeyer, B.; Krieglstein, J.; Kissel, T. In vitro cytotoxicity testing of polycations: influence of polymer structure on cell viability and hemolysis. *Biomaterials* **2003**, *24*, 1121-1131.

121. Sonawane, N. D.; Szoka, F. C.; Verkman, A. S. Chloride accumulation and swelling in endosomes enhances DNA transfer by polyamine-DNA polyplexes. *J. Biol. Chem.* **2003**, *278*, 44826-44831.

122. Taratula, O.; Savla, R.; He, H. X.; Minko, T. Poly(propyleneimine) dendrimers as potential siRNA delivery nanocarrier: From structure to function. *Int. J. Nanotech.* **2011**, *8*, 36-52.

123. Perez, A. P.; Romero, E. L.; Morilla, M. J. Ethylendiamine core PAMAM dendrimers/siRNA complexes as in vitro silencing agents. *Int. J. Pharm.* **2009**, *380*, 189-200.

124. Felgner, P. L.; Gadek, T. R.; Holm, M.; Roman, R.; Chan, H. W.; Wenz, M.; Northrop, J. P.; Ringold, G. M.; Danielsen, M. Lipofection: A highly efficient, lipid-mediated DNA-transfection procedure. *Proc. Natl. Acad. Sci. U.S.A.* **1987**, *84*, 7413-7417.

125. Martin, B.; Sainlos, M.; Aissaoui, A.; Oudrhiri, N.; Hauchecorne, M.; Vigneron, J. P.; Lehn, J. M.; Lehn, P. The design of cationic lipids for gene delivery. *Curr. Pharm. Des.* **2005**, *11*, 375-394.

126. Bhattacharya, S.; Bajaj, A. Advances in gene delivery through molecular design of cationic lipids. *Chem. Commun.* **2009**, 4632-4656.
127. Shirazi, R. S.; Ewert, K. K.; Leal, C.; Majzoub, R. N.; Bouxsein, N. F.; Safinya, C. R. Synthesis and characterization of degradable multivalent cationic lipids with disulfide-bond spacers for gene delivery. *Biochim. Biophys. Acta Biomembr.* **2011**, *1808*, 2156-2166.
128. Guenin, E.; Herve, A. C.; Floch, V.; Loisel, S.; Yaouanc, J. J.; Clement, J. C.; Ferec, C.; des Abbayes, H. Cationic phosphonolipids containing quaternary phosphonium and arsonium groups for DNA transfection with good efficiency and low cellular toxicity. *Angew. Chem. Int. Ed.* **2000**, *39*, 629-631.
129. Floch, V.; Loisel, S.; Guenin, E.; Herve, A. C.; Clement, J. C.; Yaouanc, J. J.; des Abbayes, H.; Ferec, C. Cation substitution in cationic phosphonolipids: A new concept to improve transfection activity and decrease cellular toxicity. *J. Med. Chem.* **2000**, *43*, 4617-4628.
130. Hasegawa, S.; Hirashima, N.; Nakanishi, M. Comparative study of transfection efficiency of cationic cholesterols mediated by liposomes-based gene delivery. *Bioorg. Med. Chem. Lett.* **2002**, *12*, 1299-1302.
131. Felgner, J. H.; Kumar, R.; Sridhar, C. N.; Wheeler, C. J.; Tsai, Y. J.; Border, R.; Ramsey, P.; Martin, M.; Felgner, P. L. Enhanced gene delivery and mechanism studies with a novel series of cationic lipid formulations. *J. Biol. Chem.* **1994**, *269*, 2550-2561.
132. Bennett, M. J.; Aberle, A. M.; Balasubramaniam, R. P.; Malone, J. G.; Malone, R. W.; Nantz, M. H. Cationic lipid-mediated gene delivery to murine lung: Correlation of lipid hydration with in vivo transfection activity. *J. Med. Chem.* **1997**, *40*, 4069-4078.
133. Sen, J.; Chaudhuri, A. Design, syntheses, and transfection biology of novel non-cholesterol-based guanidinylated cationic lipids. *J. Med. Chem.* **2005**, *48*, 812-820.
134. Gao, H.; Hui, K. M. Synthesis of a novel series of cationic lipids that can act as efficient gene delivery vehicles through systematic heterocyclic substitution of cholesterol derivatives. *Gene Ther.* **2001**, *8*, 855-863.
135. Schmid, N.; Behr, J. P. Location of spermine and other polyamines on DNA as revealed by photoaffinity cleavage with polyaminobenzenediazonium salts. *Biochemistry* **1991**, *30*, 4357-4361.
136. Bernstein, H.-G.; Müller, M. The cellular localization of the l-ornithine decarboxylase/polyamine system in normal and diseased central nervous systems. *Prog. Neurobiol.* **1999**, *57*, 485-505.

137. Janne, J.; Poso, H.; Raina, A. Polyamines in rapid growth and cancer. *Biochim. Biophys. Acta* **1978**, *473*, 241-293.
138. Fozard, J. R.; Part, M. L.; Prakash, N. J.; Grove, J.; Schechter, P. J.; Sjoerdsma, A.; Koch-Weser, J. L-Ornithine decarboxylase: An essential role in early mammalian embryogenesis. *Science* **1980**, *208*, 505-508.
139. Pegg, A. E.; Seely, J. E.; Poso, H.; della Ragione, F.; Zagon, I. A. Polyamine biosynthesis and interconversion in rodent tissues. *Fed. Proc.* **1982**, *41*, 3065-3072.
140. Pegg, A. E.; McCann, P. P. Polyamine metabolism and function. *Am. J. Physiol.* **1982**, *243*, C212-221.
141. Janne, J.; Alhonen, L.; Leinonen, P. Polyamines - from molecular-biology to clinical-applications. *Ann. Med.* **1991**, *23*, 241-259.
142. Hougaard, D. M. Polyamine cytochemistry: localization and possible functions of polyamines. *Int. Rev. Cytol.* **1992**, *138*, 51-88.
143. Behr, J. P.; Demeneix, B.; Loeffler, J. P.; Perez-Mutul, J. Efficient gene transfer into mammalian primary endocrine cells with lipopolyamine-coated DNA. *Proc. Natl. Acad. Sci. U.S.A.* **1989**, *86*, 6982-6986.
144. Moradpour, D.; Schauer, J. I.; Zurawski, V. R.; Wands, J. R.; Boutin, R. H. Efficient gene transfer into mammalian cells with cholesteryl-spermidine. *Biochem. Biophys. Res. Commun.* **1996**, *221*, 82-88.
145. Geall, A. J.; Eaton, M. A. W.; Baker, T.; Catterall, C.; Blagbrough, I. S. The regiochemical distribution of positive charges along cholesterol polyamine carbamates plays significant roles in modulating DNA binding affinity and lipofection. *FEBS Lett.* **1999**, *459*, 337-342.
146. Fujiwara, T.; Hasegawa, S.; Hirashima, N.; Nakanishi, M.; Ohwada, T. Gene transfection activities of amphiphilic steroid-polyamine conjugates. *Biochim. Biophys. Acta Biomembr.* **2000**, *1468*, 396-402.
147. Koynova, R.; Tenchov, B.; Wang, L.; MacDonald, R. C. Hydrophobic moiety of cationic lipids strongly modulates their transfection activity. *Mol. Pharmaceutics* **2009**, *6*, 951-958.
148. Incani, V.; Lavasanifar, A.; Uludag, H. Lipid and hydrophobic modification of cationic carriers on route to superior gene vectors. *Soft Matter* **2010**, *6*, 2124-2138.
149. Koynova, R.; Tenchov, B. Cationic phospholipids: structure-transfection activity relationships. *Soft Matter* **2009**, *5*, 3187-3200.
150. Floch, V.; Legros, N.; Loisel, S.; Guillaume, C.; Guilbot, J.; Benvegnu, T.; Ferrieres, V.; Plusquellec, D.; Ferec, C. New biocompatible cationic amphiphiles derivative

from glycine betaine: A novel family of efficient nonviral gene transfer agents. *Biochem. Biophys. Res. Commun.* **1998**, *251*, 360-365.

151. Wang, J.; Guo, X.; Xu, Y.; Barron, L.; Szoka, F. C., Jr. Synthesis and characterization of long chain alkyl acyl carnitine esters. Potentially biodegradable cationic lipids for use in gene delivery. *J. Med. Chem.* **1998**, *41*, 2207-2215.
152. Laxmi, A. A.; Vijayalakshmi, P.; Kaimal, T. N.; Chaudhuri, A.; Ramadas, Y.; Rao, N. M. Novel non-glycerol-based cytofectins with lactic acid-derived head groups. *Biochem. Biophys. Res. Commun.* **2001**, *289*, 1057-1062.
153. Heyes, J. A.; Niculescu-Duvaz, D.; Cooper, R. G.; Springer, C. J. Synthesis of novel cationic lipids: Effect of structural modification on the efficiency of gene transfer. *J. Med. Chem.* **2002**, *45*, 99-114.
154. Lindner, L. H.; Brock, R.; Arndt-Jovin, D.; Eibl, H. Structural variation of cationic lipids: Minimum requirement for improved oligonucleotide delivery into cells. *J. Control. Release* **2006**, *110*, 444-456.
155. Xu, Y. H.; Szoka, F. C. Mechanism of DNA release from cationic liposome/DNA complexes used in cell transfection. *Biochemistry* **1996**, *35*, 5616-5623.
156. Ghonaim, H. M.; Ahmed, O. A. A.; Pourzand, C.; Blagbrough, I. S. Varying the chain length in N^4,N^9-diacyl spermines: non-viral lipopolyamine vectors for efficient plasmid DNA formulation. *Mol. Pharmaceutics* **2008**, *5*, 1111-1121.
157. McGregor, C.; Perrin, C.; Monck, M.; Camilleri, P.; Kirby, A. J. Rational approaches to the design of cationic gemini surfactants for gene delivery. *J. Am. Chem. Soc.* **2001**, *123*, 6215-6220.
158. Heyes, J.; Palmer, L.; Bremner, K.; MacLachlan, I. Cationic lipid saturation influences intracellular delivery of encapsulated nucleic acids. *J. Control. Release* **2005**, *107*, 276-287.
159. Hattori, Y.; Hagiwara, A.; Ding, W.; Maitani, Y. NaCl improves siRNA delivery mediated by nanoparticles of hydroxyethylated cationic cholesterol with amido-linker. *Bioorg. Med. Chem. Lett.* **2008**, *18*, 5228-5232.
160. Rao, N. M.; Gopal, V. Cationic lipids for gene delivery in vitro and in vivo. *Expert Opin. Ther. Pat.* **2006**, *16*, 825-844.
161. Ilies, M. A.; Seitz, W. A.; Johnson, B. H.; Ezell, E. L.; Miller, A. L.; Thompson, E. B.; Balaban, A. T. Lipophilic pyrylium salts in the synthesis of efficient pyridinium-based cationic lipids, gemini surfactants, and lipophilic oligomers for gene delivery. *J. Med. Chem.* **2006**, *49*, 3872-3887.

162. Zhu, L.; Lu, Y.; Miller, D. D.; Mahato, R. I. Structural and formulation factors influencing pyridinium lipid-based gene transfer. *Bioconj. Chem.* **2008**, *19*, 2499-2512.

163. Medvedeva, D. A.; Maslov, M. A.; Serikov, R. N.; Morozova, N. G.; Serebrenikova, G. A.; Sheglov, D. V.; Latyshev, A. V.; Vlassov, V. V.; Zenkova, M. A. Novel cholesterol-based cationic lipids for gene delivery. *J. Med. Chem.* **2009**, *52*, 6558-6568.

164. Guo, X.; Szoka, F. C. Chemical approaches to triggerable lipid vesicles for drug and gene delivery. *Acc. Chem. Res.* **2003**, *36*, 335-341.

165. Chen, H. G.; Zhang, H. Z.; McCallum, C. M.; Szoka, F. C.; Guo, X. Unsaturated cationic ortho esters for endosome permeation in gene delivery. *J. Med. Chem.* **2007**, *50*, 4269-4278.

166. Bajaj, A.; Kondaiah, P.; Bhattacharya, S. Effect of the nature of the spacer on gene transfer efficacies of novel thiocholesterol derived gemini lipids in different cell lines: A structure-activity investigation. *J. Med. Chem.* **2008**, *51*, 2533-2540.

167. Koynova, R.; Tarahovsky, Y. S.; Wang, L.; MacDonald, R. C. Lipoplex formulation of superior efficacy exhibits high surface activity and fusogenicity, and readily releases DNA. *Biochim. Biophys. Acta Biomembr.* **2007**, *1768*, 375-386.

168. Rhinn, H.; Largeau, C.; Bigey, P.; Kuen, R. L.; Richard, M.; Scherman, D.; Escriou, V. How to make siRNA lipoplexes efficient? Add a DNA cargo. *Biochim. Biophys. Acta Gen. Subjects* **2009**, *1790*, 219-230.

169. McLaggan, D.; Adjimatera, N.; Sepcic, K.; Jaspars, M.; MacEwan, D. J.; Blagbrough, I. S.; Scott, R. H. Pore forming polyalkylpyridinium salts from marine sponges versus synthetic lipofection systems: distinct tools for intracellular delivery of cDNA and siRNA. *BMC Biotechnol.* **2006**, *6*.

170. Ghonaim, H. M.; Li, S.; Blagbrough, I. S. N^1,N^{12}-Diacyl spermines: SAR studies on non-viral lipopolyamine vectors for plasmid DNA and siRNA formulation. *Pharm. Res.* **2010**, *27*, 17-29.

171. Lu, J. J.; Langer, R.; Chen, J. Z. A novel mechanism is involved in cationic lipid-mediated functional siRNA delivery. *Mol. Pharmaceutics* **2009**, *6*, 763-771.

172. Han, S. E.; Kang, H.; Shim, G. Y.; Suh, M. S.; Kim, S. J.; Kim, J. S.; Oh, Y. K. Novel cationic cholesterol derivative-based liposomes for serum-enhanced delivery of siRNA. *Int. J. Pharm.* **2008**, *353*, 260-269.

173. Zaghloul, E. M.; Viola, J. R.; Zuber, G.; Smith, C. I.; Lundin, K. E. Formulation and delivery of splice-correction antisense oligonucleotides by amino acid modified polyethylenimine. *Mol. Pharmaceutics* **2010**, *7*, 652-663.

174. Klein, E.; Leborgne, C.; Ciobanu, M.; Klein, J.; Frisch, B.; Pons, F.; Zuber, G.; Scherman, D.; Kichler, A.; Lebeau, L. Nucleic acid transfer with hemifluorinated polycationic lipids. *Biomaterials* **2010**, *31*, 4781-4788.
175. Alexander, L. M.; Sánchez-Martín, R. M.; Bradley, M. Knocking (anti)-sense into cells: The microsphere approach to gene silencing. *Bioconj. Chem.* **2009**, *20*, 422-426.
176. del Pino, P.; Munoz-Javier, A.; Vlaskou, D.; Rivera Gil, P.; Plank, C.; Parak, W. J. Gene silencing mediated by magnetic lipospheres tagged with small interfering RNA. *Nano Lett.* **2010**, *10*, 3914-3921.
177. Mok, H.; Veiseh, O.; Fang, C.; Kievit, F. M.; Wang, F. Y.; Park, J. O.; Zhang, M. pH-Sensitive siRNA nanovector for targeted gene silencing and cytotoxic effect in cancer cells. *Mol. Pharmaceutics* **2010**, *7*, 1930-1939.
178. Asasutjarit, R.; Lorenzen, S. I.; Sirivichayakul, S.; Ruxrungtham, K.; Ruktanonchai, U.; Ritthidej, G. C. Effect of solid lipid nanoparticles formulation compositions on their size, zeta potential and potential for in vitro type pHIS-HIV-Hugag transfection. *Pharm. Res.* **2007**, *24*, 1098-1107.
179. Nefkens, G. H. L. Synthesis of phthaloyl amino-acids under mild conditions. *Nature* **1960**, *185*, 309-309.
180. Sosnovsky, G.; Lukszo, J. In the search for new anticancer drugs .16. selective protection and deprotection of primary amino-groups in spermine, spermidine and other polyamines. *Z. Naturforsch. B* **1986**, *41*, 122-129.
181. Fauchet, V.; Bourel, L.; Tarter, A.; Sergheraert, C. Solid-phase synthesis of trypanothione disulfide *Bioorg. Med. Chem. Lett.* **1994**, *4*, 2559-2562.
182. Soltan, M. K.; Ghonaim, H. M.; El Sadek, M.; Abou Kull, M.; El-Aziz, L. A.; Blagbrough, I. S. Design and synthesis of N^4,N^9-disubstituted spermines for non-viral siRNA delivery - Structure-activity relationship studies of siFection efficiency versus toxicity. *Pharm. Res.* **2009**, *26*, 286-295.
183. Jones, L. J.; Yue, S. T.; Cheung, C. Y.; Singer, V. L. RNA quantitation by fluorescence-based solution assay: RiboGreen reagent characterization. *Anal. Biochem.* **1998**, *265*, 368-374.
184. Skloot, R.,*The immortal life of Henrietta Lacks*. Macmillan: London, UK, 2010.
185. Lee, J. S.; Green, J. J.; Love, K. T.; Sunshine, J.; Langer, R.; Anderson, D. G. Gold, poly(β-amino ester) nanoparticles for small interfering RNA delivery. *Nano Lett.* **2009**, *9*, 2402-2406.

186. Tschuch, C.; Schulz, A.; Pscherer, A.; Werft, W.; Benner, A.; Hotz-Wagenblatt, A.; Barrionuevo, L. S.; Lichter, P.; Mertens, D. Off-target effects of siRNA specific for GFP. *BMC Mol. Biol.* **2008**, *9*.

187. Tsien, R. Y. The green fluorescent protein. *Annu. Rev. Biochem.* **1998**, *67*, 509-544.

188. Yang, T. T.; Cheng, L. Z.; Kain, S. R. Optimized codon usage and chromophore mutations provide enhanced sensitivity with the green fluorescent protein. *Nucleic Acids Res.* **1996**, *24*, 4592-4593.

189. Royant, A.; Noirclerc-Savoye, M. Stabilizing role of glutamic acid 222 in the structure of Enhanced Green Fluorescent Protein. *J. Struct. Biol.* **2011**, *174*, 385-390.

190. Blagbrough, I. S.; Metwally, A. A.; Geall, A. J., Measurement of polyamine pKa values. In *Polyamines: methods and protocols*, Pegg, A. E.; Casero Jr., R. A., Eds.; Springer Science, Humana Press, New York, USA: New York, 2011; Vol. 720, pp 493-503.

191. Ahmed, O. A. A.; Pourzand, C.; Blagbrough, I. S. Varying the unsaturation in N^4,N^9-dioctadecanoyl spermines: Nonviral lipopolyamine vectors for more efficient plasmid DNA formulation. *Pharm. Res.* **2006**, *23*, 31-40.

192. Gaucheron, J.; Santaella, C.; Vierling, P. Highly fluorinated lipospermines for gene transfer: Synthesis and evaluation of their in vitro transfection efficiency. *Bioconj. Chem.* **2001**, *12*, 114-128.

193. Rasmussen, E. S. Use of fluorescent redox indicators to evaluate cell proliferation and viability. *In Vitro Mol. Toxicol.* **1999**, *12*, 47-58.

194. Gonzalez, R. J.; Tarloff, J. B. Evaluation of hepatic subcellular fractions for Alamar blue and MTT reductase activity. *Toxicol. In Vitro* **2001**, *15*, 257-259.

195. Goegan, P.; Johnson, G.; Vincent, R. Effects of serum protein and colloid on the alamarBlue assay in cell cultures. *Toxicol. In Vitro* **1995**, *9*, 257-266.

196. Schroeder, A.; Levins, C. G.; Cortez, C.; Langer, R.; Anderson, D. G. Lipid-based nanotherapeutics for siRNA delivery. *J. Intern. Med.* **2010**, *267*, 9-21.

197. Wu, S. Y.; McMillan, N. A. J. Lipidic systems for in vivo siRNA delivery. *AAPS J.* **2009**, *11*, 639-652.

198. Tseng, Y.-C.; Mozumdar, S.; Huang, L. Lipid-based systemic delivery of siRNA. *Adv. Drug Deliv. Rev.* **2009**, *61*, 721-731.

199. Mevel, M.; Breuzard, G.; Yaouanc, J. J.; Clement, J. C.; Lehn, P.; Pichon, C.; Jaffres, P. A.; Midoux, P. Synthesis and transfection activity of new cationic phosphoramidate lipids: High efficiency of an imidazolium derivative. *Chembiochem* **2008**, *9*, 1462-1471.

200. Rothbard, J. B.; Jessop, T. C.; Lewis, R. S.; Murray, B. A.; Wender, P. A. Role of membrane potential and hydrogen bonding in the mechanism of translocation of guanidinium-rich peptides into cells. *J. Am. Chem. Soc.* **2004**, *126*, 9506-9507.

201. Wender, P. A.; Galliher, W. C.; Goun, E. A.; Jones, L. R.; Pillow, T. H. The design of guanidinium-rich transporters and their internalization mechanisms. *Adv. Drug Del. Rev.* **2008**, *60*, 452-472.

202. Radchatawedchakoon, W.; Watanapokasin, R.; Krajarng, A.; Yingyongnarongkul, B. E. Solid phase synthesis of novel asymmetric hydrophilic head cholesterol-based cationic lipids with potential DNA delivery. *Biorg. Med. Chem.* **2010**, *18*, 330-342.

203. Chen, Y. C.; Sen, J.; Bathula, S. R.; Yang, Q.; Fittipaldi, R.; Huang, L. Novel cationic lipid that delivers siRNA and enhances therapeutic effect in lung cancer cells. *Mol. Pharmaceutics* **2009**, *6*, 696-705.

204. Santel, A.; Aleku, M.; Keil, O.; Endruschat, J.; Esche, V.; Fisch, G.; Dames, S.; Loffler, K.; Fechtner, M.; Arnold, W.; Giese, K.; Klippel, A.; Kaufmann, J. A novel siRNA-lipoplex technology for RNA interference in the mouse vascular endothelium. *Gene Ther.* **2006**, *13*, 1222-1234.

205. Kim, T. I.; Lee, M.; Kim, S. W. A guanidinylated bioreducible polymer with high nuclear localization ability for gene delivery systems. *Biomaterials* **2010**, *31*, 1798-1804.

206. Bromberg, L.; Raduyk, S.; Hatton, T. A.; Concheiro, A.; Rodriguez-Valencia, C.; Silva, M.; Alvarez-Lorenzo, C. Guanidinylated polyethyleneimine-polyoxypropylene-polyoxyethylene conjugates as gene transfection agents. *Bioconj. Chem.* **2009**, *20*, 1044-1053.

207. Theodossiou, T. A.; Pantos, A.; Tsogas, I.; Paleos, C. M. Guanidinylated dendritic molecular transporters: Prospective drug delivery systems and application in cell transfection. *Chemmedchem* **2008**, *3*, 1635-1643.

208. Higashi, T.; Khalil, I. A.; Maiti, K. K.; Lee, W. S.; Akita, H.; Harashima, H.; Chung, S. K. Novel lipidated sorbitol-based molecular transporters for non-viral gene delivery. *J. Control. Release* **2009**, *136*, 140-147.

209. Varghese, O. P.; Kisiel, M.; Martinez-Sanz, E.; Ossipov, D. A.; Hilborn, J. Synthesis of guanidinium-modified hyaluronic acid hydrogel. *Macromol. Rapid Commun.* **2010**, *31*, 1175-1180.

210. Vigneron, J. P.; Oudrhiri, N.; Fauquet, M.; Vergely, L.; Bradley, J. C.; Basseville, M.; Lehn, P.; Lehn, J. M. Guanidinium-cholesterol cationic lipids: Efficient vectors for the transfection of eukaryotic cells. *Proc. Natl. Acad. Sci. U.S.A.* **1996**, *93*, 9682-9686.

211. Feichtinger, K.; Zapf, C.; Sings, H. L.; Goodman, M. Diprotected triflylguanidines: A new class of guanidinylation reagents. *J. Org. Chem.* **1998**, *63*, 3804-3805.

212. Feichtinger, K.; Sings, H. L.; Baker, T. J.; Matthews, K.; Goodman, M. Triurethane-protected guanidines and triflyldiurethane-protected guanidines: New reagents for guanidinylation reactions. *J. Org. Chem.* **1998**, *63*, 8432-8439.

213. Ross, P. C.; Hui, S. W. Lipoplex size is a major determinant of in vitro lipofection efficiency. *Gene Ther.* **1999**, *6*, 651-659.

214. Marchini, C.; Montani, M.; Amici, A.; Amenitsch, H.; Marianecci, C.; Pozzi, D.; Caracciolo, G. Structural stability and increase in size rationalize the efficiency of lipoplexes in serum. *Langmuir* **2009**, *25*, 3013-3021.

215. Hoekstra, D.; Rejman, J.; Wasungu, L.; Shi, F.; Zuhorn, I. Gene delivery by cationic lipids: In and out of an endosome. *Biochem. Soc. Trans.* **2007**, *35*, 68-71.

216. Ghonaim, H. M.; Li, S.; Blagbrough, I. S. Very long chain N^4,N^9-diacyl spermines: Non-viral lipopolyamine vectors for efficient plasmid DNA and siRNA delivery. *Pharm. Res.* **2009**, *26*, 19-31.

217. Cornish, J.; Callon, K. E.; Lin, C. Q. X.; Xiao, C. L.; Mulvey, T. B.; Cooper, G. J. S.; Reid, I. R. Trifluoroacetate, a contaminant in purified proteins, inhibits proliferation of osteoblasts and chondrocytes. *Am. J. Physiol-Endoc. M.* **1999**, *277*, E779-E783.

218. Stanton, M. G.; Colletti, S. L. Medicinal chemistry of siRNA delivery. *J. Med. Chem.* **2010**, *53*, 7887-7901.

219. Tattrie, N. H.; Bennett, J. R.; Cyr, R. Maximum and minimum values for lecithin classes from various biological sources. *Can. J. Biochem.* **1968**, *46*, 819-824.

220. Marai, L.; Kuksis, A. Molecular species of lecithins from erythrocytes and plasma of man. *J. Lipid Res.* **1969**, *10*, 141-152.

221. Huang, C.; Li, S. Calorimetric and molecular mechanics studies of the thermotropic phase behavior of membrane phospholipids. *Biochim. Biophys. Acta Rev. Biomembr.* **1999**, *1422*, 273-307.

222. Beermann, C.; Mobius, M.; Winterling, N.; Schmitt, J.; Boehm, G. *sn*-Position determination of phospholipid-linked fatty acids derived from erythrocytes by liquid chromatography electrospray ionization ion-trap mass spectrometry. *Lipids* **2005**, *40*, 211-218.

223. Ali, S.; Smaby, J. M.; Momsen, M. M.; Brockman, H. L.; Brown, R. E. Acyl chain-length asymmetry alters the interfacial elastic interactions of phosphatidylcholines. *Biophys. J.* **1998**, *74*, 338-348.

224. Wang, L.; MacDonald, R. C. Synergistic effect between components of mixtures of cationic amphipaths in transfection of primary endothelial cells. *Mol. Pharmaceutics* **2007**, *4*, 615-623.
225. Patil, M. L.; Zhang, M.; Taratula, O.; Garbuzenko, O. B.; He, H.; Minko, T. Internally cationic polyamidoamine PAMAM-OH dendrimers for siRNA delivery: effect of the degree of quaternization and cancer targeting. *Biomacromolecules* **2009**, *10*, 258-266.
226. Nantz, M. H.; Dicus, C. W.; Hilliard, B.; Yellayi, S.; Zou, S. M.; Hecker, J. G. The benefit of hydrophobic domain asymmetry on the efficacy of transfection as measured by in vivo imaging. *Mol. Pharmaceutics* **2010**, *7*, 786-794.
227. Balasubramaniam, R. P.; Bennett, M. J.; Aberle, A. M.; Malone, J. G.; Nantz, M. H.; Malone, R. W. Structural and functional analysis of cationic transfection lipids: The hydrophobic domain. *Gene Ther.* **1996**, *3*, 163-172.
228. Koynova, R.; Wang, L.; MacDonald, R. C. An intracellular lamellar-nonlamellar phase transition rationalizes the superior performance of some cationic lipid transfection agents. *Proc. Natl. Acad. Sci. U.S.A.* **2006**, *103*, 14373-14378.
229. Blagbrough, I. S.; Ghonaim, H. M., Polyamines and their conjugates for gene and siRNA delivery. In *Biological aspects of biogenic amines, polyamines and conjugates*, Dandrifosse, G., Eds.; Research Signpost: India, 2009; Vol. pp 81-112.
230. Wang, J.; Lu, Z.; Wientjes, M. G.; Au, J. L. S. Delivery of siRNA therapeutics: Barriers and carriers. *AAPS J.* **2010**, *12*, 492-503.
231. Yuan, X.; Naguib, S.; Wu, Z. Recent advances of siRNA delivery by nanoparticles. *Expert Opin. Drug Deliv.* **2011**, *8*, 521-536.
232. Kremer, J. M. H.; Esker, M. W. J.; Pathmamanoharan, C.; Wiersema, P. H. Vesicles of variable diameter prepared by a modified injection method. *Biochemistry* **1977**, *16*, 3932-3935.
233. Bakht, O.; Pathak, P.; London, E. Effect of the structure of lipids favoring disordered domain formation on the stability of cholesterol-containing ordered domains (lipid rafts): Identification of multiple raft-stabilization mechanisms. *Biophys. J.* **2007**, *93*, 4307-4318.
234. Corish, P.; Tyler-Smith, C. Attenuation of green fluorescent protein half-life in mammalian cells. *Protein Eng.* **1999**, *12*, 1035-1040.
235. Ming, X.; Sato, K.; Juliano, R. L. Unconventional internalization mechanisms underlying functional delivery of antisense oligonucleotides via cationic lipoplexes and polyplexes. *J. Control. Release* **2011**, *153*, 83-92.

236. Desigaux, L.; Sainlos, M.; Lambert, O.; Chevre, R.; Letrou-Bonneval, E.; Vigneron, J. P.; Lehn, P.; Lehn, J. M.; Pitard, B. Self-assembled lamellar complexes of siRNA with lipidic aminoglycoside derivatives promote efficient siRNA delivery and interference. *Proc. Natl. Acad. Sci. U.S.A.* **2007**, *104*, 16534-16539.

237. Wasungu, L.; Hoekstra, D. Cationic lipids, lipoplexes and intracellular delivery of genes. *J. Control. Release* **2006**, *116*, 255-264.

238. Xu, L.; Anchordoquy, T. J. Cholesterol domains in cationic lipid/DNA complexes improve transfection. *Biochim. Biophys. Acta Biomembr.* **2008**, *1778*, 2177-2181.

239. Xu, L.; Anchordoquy, T. J. Effect of cholesterol nanodomains on the targeting of lipid-based gene delivery in cultured cells. *Mol. Pharmaceutics* **2010**, *7*, 1311-1317.

240. Tenchov, B. G.; MacDonald, R. C.; Siegel, D. P. Cubic phases in phosphatidylcholine-cholesterol mixtures: Cholesterol as membrane "fusogen". *Biophys. J.* **2006**, *91*, 2508-2516.

241. Margineanu, A.; De Feyter, S.; Melnikov, S.; Marchand, D.; van Aerschot, A.; Herdewijn, P.; Habuchi, S.; De Schryver, F. C.; Hofkens, J. Complexation of lipofectamine and cholesterol-modified DNA sequences-studied by single-molecule fluorescence techniques. *Biomacromolecules* **2007**, *8*, 3382-3392.

242. Tenchov, B. G.; MacDonald, R. C.; Siegel, D. P. Cubic phases in phosphatidylcholine-cholesterol mixtures: Cholesterol as membrane fusogen *Biophys. J.* **2006**, *91*, 2508-2516.

243. Templeton, N. S.; Lasic, D. D.; Frederik, P. M.; Strey, H. H.; Roberts, D. D.; Pavlakis, G. N. Improved DNA: Liposome complexes for increased systemic delivery and gene expression. *Nat. Biotech.* **1997**, *15*, 647-652.

244. Sternberg, B.; Hong, K. L.; Zheng, W. W.; Papahadjopoulos, D. Ultrastructural characterization of cationic liposome-DNA complexes showing enhanced stability in serum and high transfection activity in vivo. *Biochim. Biophys. Acta Biomembr.* **1998**, *1375*, 23-35.

245. Li, S.; Tseng, W. C.; Stolz, D. B.; Wu, S. P.; Watkins, S. C.; Huang, L. Dynamic changes in the characteristics of cationic lipidic vectors after exposure to mouse serum: Implications for intravenous lipofection. *Gene Ther.* **1999**, *6*, 585-594.

246. Simberg, D.; Weisman, S.; Talmon, Y.; Faerman, A.; Shoshani, T.; Barenholz, Y. The role of organ vascularization and lipoplex-serum initial contact in intravenous murine lipofection. *J. Biol. Chem.* **2003**, *278*, 39858-39865.

247. Hirsch-Lerner, D.; Zhang, M.; Eliyahu, H.; Ferrari, M. E.; Wheeler, C. J.; Barenholz, Y. Effect of "helper lipid" on lipoplex electrostatics. *Biochim. Biophys. Acta Biomembr.* **2005**, *1714*, 71-84.

248. Girao da Cruz, M. T.; Simoes, S.; Pires, P. P. C.; Nir, S.; Pedroso de Lima, M. C. Kinetic analysis of the initial steps involved in lipoplex-cell interactions: Effect of various factors that influence transfection activity. *Biochim. Biophys. Acta* **2001**, *1510*, 136-151.

249. Zuhorn, I. S.; Kalicharan, R.; Hoekstra, D. Lipoplex-mediated transfection of mammalian cells occurs through the cholesterol-dependent clathrin-mediated pathway of endocytosis. *J. Biol. Chem.* **2002**, *277*, 18021-18028.

250. Prasad, T. K.; Rangaraj, N.; Rao, N. M. Quantitative aspects of endocytic activity in lipid-mediated transfections. *FEBS Lett.* **2005**, *579*, 2635-2642.

251. Rejman, J.; Bragonzi, A.; Conese, M. Role of clathrin- and caveolae-mediated endocytosis in gene transfer mediated by lipo- and polyplexes. *Mol. Ther.* **2005**, *12*, 468-474.

252. Resina, S.; Prevot, P.; Thierry, A. R. Physico-chemical characteristics of lipoplexes influence cell uptake mechanisms and transfection efficacy. *PLoS One* **2009**, *4*.

253. Cho, S. M.; Lee, H. Y.; Kim, J. C. pH-dependent release property of dioleoylphosphatidyl ethanolamine liposomes. *Korean J. Chem. Eng.* **2008**, *25*, 390-393.

254. Kearns, M. D.; Donkor, A. M.; Savva, M. Structure-transfection activity studies of novel cationic choesterol-based amphiphiles. *Mol. Pharmaceutics* **2008**, *5*, 128-139.

255. Onda, M.; Yoshihara, K.; Koyano, H.; Ariga, K.; Kunitake, T. Molecular recognition of nucleotides by the guanidinium unit at the surface of aqueous micelles and bilayers. A comparison of microscopic and macroscopic interfaces. *J. Am. Chem. Soc.* **1996**, *118*, 8524-8530.

256. Springs, B.; Haake, P. Equilibrium-constants for association of guanidinium and ammonium-ions with oxyanions - effect of changing basicity of oxyanion. *Bioorg. Chem.* **1977**, *6*, 181-190.

257. Mason, P. E.; Neilson, G. W.; Dempsey, C. E.; Barnes, A. C.; Cruickshank, J. M. The hydration structure of guanidinium and thiocyanate ions: Implications for protein stability in aqueous solution. *Proc. Natl. Acad. Sci. U.S.A.* **2003**, *100*, 4557-4561.

258. Hol, P.; Streefland, L.; Blandamer, M. J.; Engberts, J. Kinetic medium effects of cationic cosolutes in aqueous solution: The effects of alkylammonium bromides on the neutral hydrolysis of 1-benzoyl-1,2,4-triazole. *J. Chem. Soc. Perk. Trans. 2* **1997**, 485-488.

259. Hafez, I. M.; Ansell, S.; Cullis, P. R. Tunable pH-sensitive liposomes composed of mixtures of cationic and anionic lipids. *Biophys. J.* **2000**, *79*, 1438-1446.

260. Hafez, I. M.; Cullis, P. R. Cholesteryl hemisuccinate exhibits pH sensitive polymorphic phase behavior. *Biochim. Biophys. Acta Biomembr.* **2000**, *1463*, 107-114.

261. Reis, C. P.; Ribeiro, A. J.; Veiga, F.; Neufeld, R. J.; Damge, C. Polyelectrolyte biomaterial interactions provide nanoparticulate carrier for oral insulin delivery. *Drug Deliv.* **2008**, *15*, 127-139.

262. Khoury, M.; Louis-Plence, P.; Escriou, V.; Noel, D.; Largeau, C.; Cantos, C.; Scherman, D.; Jorgensen, C.; Apparailly, F. Efficient new cationic liposome formulation for systemic delivery of small interfering RNA silencing tumor necrosis factor alpha in experimental arthritis. *Arthritis Rheum.* **2006**, *54*, 1867-1877.

263. Schlegel, A.; Largeau, C.; Bigey, P.; Bessodes, M.; Lebozec, K.; Scherman, D.; Escriou, V. Anionic polymers for decreased toxicity and enhanced in vivo delivery of siRNA complexed with cationic liposomes. *J. Control. Release* **2011**, *152*, 393-401.

264. Vitiello, L.; Bockhold, K.; Joshi, P. B.; Worton, R. G. Transfection of cultured myoblasts in high serum concentration with DODAC:DOPE liposomes. *Gene Ther.* **1998**, *5*, 1306-1313.

265. Wasan, E. K.; Harvie, P.; Edwards, K.; Karlsson, G.; Bally, M. B. A multi-step lipid mixing assay to model structural changes in cationic lipoplexes used for in vitro transfection. *Biochim. Biophys. Acta* **1999**, *1461*, 27-46.

266. Turek, J.; Dubertret, C.; Jaslin, G.; Antonakis, K.; Scherman, D.; Pitard, B. Formulations which increase the size of lipoplexes prevent serum-associated inhibition of transfection. *J. Gene Med.* **2000**, *2*, 32-40.

267. Zhang, Y.; Anchordoquy, T. J. The role of lipid charge density in the serum stability of cationic lipid/DNA complexes. *Biochim. Biophys. Acta Biomembr.* **2004**, *1663*, 143-157.

268. Wasungu, L.; Scarzello, M.; van Dam, G.; Molema, G.; Wagenaar, A.; Engberts, J. B.; Hoekstra, D. Transfection mediated by pH-sensitive sugar-based gemini surfactants; potential for in vivo gene therapy applications. *J. Mol. Med.* **2006**, *84*, 774-784.

269. Zelphati, O.; Uyechi, L. S.; Barron, L. G.; Szoka, F. C., Jr. Effect of serum components on the physico-chemical properties of cationic lipid/oligonucleotide complexes and on their interactions with cells. *Biochim. Biophys. Acta* **1998**, *1390*, 119-133.

270. Wahlers, A.; Schwieger, M.; Li, Z.; Meier-Tackmann, D.; Lindemann, C.; Eckert, H. G.; von Laer, D.; Baum, C. Influence of multiplicity of infection and protein stability

on retroviral vector-mediated gene expression in hematopoietic cells. *Gene Ther.* **2001**, *8*, 477-486.

271. Barrow, J.; Bernardo, A. S.; Hay, C. W.; Blaylock, M.; Duncan, L.; Mackenzie, A.; McCreath, K.; Kind, A. J.; Schnieke, A. E.; Colman, A.; Hart, A. W.; Docherty, K. Purification and characterization of a population of EGFP-expressing cells from the developing pancreas of a neurogenin3/EGFP transgenic mouse. *Organogenesis* **2005**, *2*, 22-27.

272. Paganin-Gioanni, A.; Bellard, E.; Escoffre, J. M.; Rols, M. P.; Teissie, J.; Golzio, M. Direct visualization at the single-cell level of siRNA electrotransfer into cancer cells. *Proc. Natl. Acad. Sci. U.S.A.* **2011**, *108*, 10443-10447.

273. Ruozi, B.; Montanari, M.; Vighi, E.; Tosi, G.; Tombesi, A.; Battini, R.; Restani, C.; Leo, E.; Forni, F.; Vandelli, M. A. Flow cytometry and live confocal analysis for the evaluation of the uptake and intracellular distribution of FITC-ODN into HaCaT cells. *J. Liposome Res.* **2009**, *19*, 241-251.

Output arising from this research

15 abstracts (including two invited Orals and an invited Poster) and 2 refereed papers:

1. Efficient siRNA delivery and effective gene silencing by lipoplexes
Metwally, AA; Pourzand, C; Blagbrough, IS
3rd International Cellular Delivery of Therapeutic Macromolecules (CDTM) Symposium, Cardiff, UK, 26-29 June 2010.
Drug Discovery Today Volume: 15 Issue: 23-24 Pages: 1090 Meeting Abstract: A29 2010

2. Efficient siRNA delivery and gene silencing by unsymmetrical fatty acid amides of spermine
Metwally, AA; Pourzand, C; Blagbrough, IS
Academy Pharmaceutical Sciences. 1-3 September 2010.
Journal of Pharmacy and Pharmacology Volume: 62 Issue: 10 Pages: 1220-1221 2010
(Invited Oral Symposium)

3. Efficient siRNA delivery and effective gene silencing by lipospermine lipoplexes
Metwally AA, Pourzand C, Blagbrough IS
2nd APGI International Conference. Innovation in Drug Delivery: From Preformulation to Development through Innovative Evaluation Process.
Aix-en-Provence, France, 3-6 October 2010, #207 p 300

4. siRNA delivery and gene silencing by unsymmetrical fatty acid amides of spermine
Metwally AA, Pourzand C, Blagbrough IS
2nd APGI International Conference. Innovation in Drug Delivery: From Preformulation to Development through Innovative Evaluation Process.
Aix-en-Provence, France, 3-6 October 2010, #208 p 301

5. Efficient siRNA delivery and effective gene silencing by lipoplexes
Metwally AA, Pourzand C, Blagbrough IS
25th Annual Meeting of the American Association of Pharmaceutical Scientists and PSWC, New Orleans, LA, 14-18 November 2010.
Pharmaceutical Research Volume: 27 Issue: 11 SUPPL. Nov 2010

6. siRNA delivery to effect efficient gene silencing: opportunities with self-assembly lipoplexes of unsymmetrical fatty acid amides of spermine
Metwally AA, Pourzand C, Blagbrough IS
25th Annual Meeting of the American Association of Pharmaceutical Scientists and PSWC, New Orleans, LA, 14-18 November 2010.
Pharmaceutical Research Volume: 27 Issue: 11 SUPPL. Nov 2010

7. Practical synthesis of unsymmetrical fatty acid conjugates of spermine for siRNA delivery
Metwally AA, Pourzand C, Blagbrough IS
RSC UK-China Symposium, Burlington House, Piccadilly, London, 22 Nov 2010 (Invited Poster)

8. Efficient siRNA delivery and gene silencing by unsymmetrical fatty acid amides of spermine
Metwally AA, Pourzand C, Blagbrough IS
2nd International Conference on the Role of Polyamines and their Analogs in Cancer and other Diseases, Poster Abstracts, Tivoli, Rome, Italy, 1-6 December 2010

9. Binding sites for polyamine conjugates – where therapy meets chemistry
Blagbrough IS, Metwally AA, Ghonaim HM
2nd International Conference on the Role of Polyamines and their Analogs in Cancer and other Diseases, Oral Abstracts, Tivoli, Rome, Italy, 1-6 December 2010

10. Models for target diseases with RNAi therapy – self-assembly siRNA delivery strategies
Blagbrough IS, Metwally AA, Ghonaim HM
38th Annual Meeting and Exposition of the Controlled Release Society, National Harbor, MD, 30 July-3 Aug 2011

11. Efficient siRNA delivery and gene silencing by symmetrical fatty acid conjugates of spermine
Metwally AA, Pourzand C, Blagbrough IS
Academy Pharmaceutical Sciences. Nottingham, UK, 31 August-2 September 2011.
Journal of Pharmacy and Pharmacology Volume: 63 Issue: 10 Pages: #38 2011 (Invited Oral Symposium)

12. Synthesis and evaluation of N^4,N^9-fatty acid conjugates of N^1,N^{12}-diamidino-spermine as non-viral siRNA delivery vectors
Metwally AA, Blagbrough IS
Academy Pharmaceutical Sciences. Nottingham, UK, 31 August-2 September 2011.
Journal of Pharmacy and Pharmacology Volume: 63 Issue: 10 Pages: #39 2011

13. siRNA lipoplex stability with glycosaminoglycans (GAGs)
Alhusein N, Metwally AA, Blagbrough IS
Academy Pharmaceutical Sciences. Nottingham, UK, 31 August-2 September 2011.
Journal of Pharmacy and Pharmacology Volume: 63 Issue: 10 Page: #49 2011

14. Synthesis and evaluation of N^4,N^9-di-fatty acid conjugates of N^1,N^{12}-diamidino-spermine as non-viral siRNA delivery vectors
Metwally AA, Blagbrough IS
25th Annual Meeting of the American Association of Pharmaceutical Scientists, Washington, DC, 23-27 October 2011.
Pharmaceutical Research Volume: 28 Issue: 12 SUPPL. Pages: #895, 2011 #W4379

15. Efficient siRNA delivery and gene silencing by symmetrical fatty acid conjugates of spermine Metwally AA, Pourzand C, Blagbrough IS
25th Annual Meeting of the American Association of Pharmaceutical Scientists, Washington, DC, 23-27 October 2011.
Pharmaceutical Research Volume: 28 Issue: 12 SUPPL. Pages: #896, 2011 #W4380

#1 A A Metwally, C Pourzand, and I S Blagbrough, Efficient gene silencing by self-assembled complexes of siRNA and symmetrical fatty acid amides of spermine, *Pharmaceutics*, **2011**, *3*, 125-140 doi:10.3390/pharmaceutics3020125.

#2 A A Metwally and I S Blagbrough, Self-assembled lipoplexes of short interfering RNA (siRNA) using spermine-based fatty acid amide guanidines: Effect on gene silencing efficiency, *Pharmaceutics*, **2011**, *3*, 406-424 doi:10.3390/pharmaceutics3030406.

Efficient siRNA delivery and effective gene silencing by lipoplexes

Metwally AA, Pourzand C, Blagbrough IS
Department of Pharmacy and Pharmacology, University of Bath, Bath BA2 7AY, U.K.

siRNA is double-stranded RNA typically 21-24 nucleotide base-pairs long. Gene silencing by siRNA has gained wide acceptance in genomics and is already in different phases of clinical trials as a potential therapeutic. Long chain fatty acid conjugates of spermine have previously been synthesized and evaluated in our research group for both gene and siRNA delivery [1, 2]. We report the synthesis of two novel unsymmetrical N^4,N^9-difatty acid conjugates of the naturally occurring polyamine spermine with the aim of developing structure-activity relationships for their potential as non-viral, self-assembly vectors for siRNA delivery. After transfection with lipoplexes of Alexa Fluor® 647-labelled siRNA (a 24-mer from Qiagen), silencing EGFP expression, both the efficiency of delivery and the effectiveness of knock-down (gene silencing) were evaluated in HeLa cells stably expressing EGFP. Analysis was by FACS 48 h post transfection. All transfection experiments were carried-out in DMEM containing 10% foetal calf serum.

The efficiency of intracellular delivery was measured by the (normalized) fluorescence of Alexa Fluor® 647-labelled siRNA; N^4,N^9-dioleoylspermine (DOS) showed 150% of the delivery efficiency achieved with N^4-linoleoyl-N^9-oleoylspermine (LOS). However, knock-down results show that LOS is more effective with a reduction of EGFP expression levels from control (100%) to 25 ± 3% at a concentration of 3 µg/well (N/P = 11, n = 3 and triplicate replicates). Under the same experimental conditions, DOS reduced EGFP expression to 27 ± 2% at a concentration of 6 µg/well (N/P = 22) and to 32 ± 2% at a concentration of 3 µg/well (N/P = 11). Cell viability was measured as the percentage of viable cells using the Alamar Blue® assay [3]. The results show that at 3 µg/well LOS cell viability is 83 ± 4%, at 6 µg/well LOS cell viability is 46 ± 8%, while at 6 µg/well DOS cell viability is only 32 ± 9%. Transfection of cells with Lipofectamine™ 2000 resulted in reduction of EGFP expression to 37 ± 3%, with cell viability of 91 ± 6%.

We conclude from these results that the unsymmetrical lipopolyamine LOS is an excellent transfecting agent for the delivery of siRNA producing effective gene silencing in the presence of 10% foetal calf serum.

We thank the Egyptian Government for a fully-funded studentship to AAM.

1 Ghonaim, H.M. et al. (2009) Very Long Chain N^4,N^9-Diacyl Spermines: Non-Viral Lipopolyamine Vectors for Efficient Plasmid DNA and siRNA Delivery. Pharm. Res. 26, 19-31
2 Ghonaim, H.M. et al. (2010) N^1,N^{12}-Diacyl Spermines: SAR Studies on Non-viral Lipopolyamine Vectors for Plasmid DNA and siRNA Formulation. Pharm. Res. 27, 17-29
3 Asasutjarit, R. et al. (2007) Effect of Solid Lipid Nanoparticles Formulation Compositions on Their Size, Zeta Potential and Potential for In Vitro pHIS-HIV-Hugag Transfection. Pharm. Res. 24, 1098-1107

3rd International Cellular Delivery of Therapeutic Macromolecules (CDTM) Symposium, Cardiff, UK, 26-29 June 2010.
Drug Discovery Today Volume: 15 Issue: 23-24 Pages: 1090-1090 Meeting Abstract: A29 2010

Efficient siRNA delivery and gene silencing by unsymmetrical fatty acid amides of spermine

Metwally AA, Pourzand C, Blagbrough IS
Department of Pharmacy and Pharmacology, University of Bath, Bath BA2 7AY, U.K.

INTRODUCTION

Gene silencing by siRNA i.e. synthetic dsRNA of 21-24 nucleotides, is already an important biological tool in the study of gene function and it also has many potential therapeutic applications for difficult-to-treat diseases [1].

Long-chain fatty acid amides of the naturally occurring polyamine spermine have previously been synthesized and evaluated in our research group for both pDNA and siRNA delivery [2-5]. Our SAR studies of long- (C18) and very-long (C20 and longer) fatty acid [6] conjugates of spermine are important in investigating the enhancement of siRNA delivery and of gene silencing.

AIMS

To study the SAR of novel unsymmetrical long- and very-long chain fatty acid spermine conjugates that will be evaluated for their efficiencies of siRNA delivery and gene knock-down.

MATERIALS AND METHODS

N^4-Arachidonoyl-N^9-oleoylspermine (AOS), N^4-lignoceroyl-N^9-oleoylspermine (LIGOS), and N^4-linoleoyl-N^9-oleoylspermine (LINOS) were prepared using DCC coupling of the corresponding carboxylic acids, after di-*N*-phthalimido protection of the primary amines. All transfection studies were carried out in the presence of foetal calf serum (FCS), 10% in DMEM on HeLa cells stably expressing enhanced green fluorescent protein (EGFP). siRNA concentration in each well of 24-well plates was 15 nM. Mean geometric fluorescence intensity of Alexa Fluor® 647 labelled-siRNA and EGFP was measured by FACS analysis 48 h post transfection. The alamarBlue® assay [7] was used to evaluate cytotoxicity. 6000 cells/well were incubated for 44 h post transfection then alamarBlue® reagent was added to the culture media and cells were incubated for a further 3.5 h.

RESULTS AND DISCUSSION

Gated FACS analysis (of living cells) showed that LIGOS has the highest siRNA delivery as measured by the normalized geometric mean fluorescence of Alexa Fluor® 647 (4-fold more compared to AOS and LINOS). However, more reduction in EGFP expression, in HeLa cells stably expressing EGFP, was achieved on siRNA delivery with AOS (to 34%, N/P = 21) and LINOS (to 29%, N/P = 11) compared to a reduction to 56% achieved with LIGOS (N/P = 18). Unsaturated fatty acid amide (linoleoyl; 18:2; arachidonoyl; 20:4) spermine conjugates showed higher knock-down efficiencies compared to (saturated) lignoceroyl (24:0) spermine conjugates.

This knock-down effect might be due to the ability of unsaturated chains to enhance fusion with endosomal membranes and thereby to facilitate endosomal escape [2], a key factor in the efficiency of siRNA mediated knockdown by lipoplexes [2-6]. Although LIGOS gave better siRNA delivery, its relatively low knockdown (to 56%) means that whilst saturated fats might enhance delivery, unsaturated fats specifically enhance endosomal escape of the delivered siRNA.

AlamarBlue® cytotoxicity evaluation showed that LINOS was less cytotoxic to HeLa cells (72% cell viability) compared to AOS (32%) and LIGOS (63%). The lower cell viability obtained with AOS may be attributed to the increased number (4) of C=C double bonds which has been reported to be a cause of cytotoxicity [8]. Under the same experimental settings, Lipofectamine™ 2000 reduced EGFP expression to 34%, with cell viability of 82%.

CONCLUSIONS

N^4-Linoleoyl-N^9-oleoylspermine (LINOS) is an efficient vector for the delivery of siRNA producing effective gene silencing even in the presence of FCS.

ACKNOWLEDGMENTS

We thank the Egyptian Government for a fully-funded studentship to AAM.

REFERENCES

[1] I.S. Blagbrough and C. Zara, "Animal models for target diseases in gene therapy - using DNA and siRNA delivery strategies" *Pharm. Res.*, **26** (2009) 1-18.

[2] O.A. Ahmed, C. Pourzand, and I.S. Blagbrough, "Varying the unsaturation in N^4,N^9-dioctadecanoyl spermines: nonviral lipopolyamine vectors for more efficient plasmid DNA formulation" *Pharm. Res.*, **23** (2006) 31-40.

[3] D. McLaggan, *et al.*, "Pore forming polyalkylpyridinium salts from marine sponges versus synthetic lipofection systems: distinct tools for intracellular delivery of cDNA and siRNA" *BMC Biotechnol*. **6**, (2006).

[4] M.K. Soltan *et al*., "Design and synthesis of N^4,N^9-disubstituted spermines for non-viral siRNA delivery - structure-activity relationship studies of siFection efficiency versus toxicity" *Pharm. Res.*, **26** (2009) 286-295.

[5] H.M. Ghonaim, S. Li, and I.S. Blagbrough, "N^1,N^{12}-diacyl spermines: SAR studies on non-viral lipopolyamine vectors for plasmid DNA and siRNA formulation" *Pharm. Res.*, **27** (2010) 17-29.

[6] H.M. Ghonaim, S. Li, and I.S. Blagbrough, "Very long chain N^4,N^9-diacyl spermines: non-viral lipopolyamine vectors for efficient plasmid DNA and siRNA delivery" *Pharm. Res.*, **26** (2009) 19-31.

[7] R. Asasutjarit, *et al.*, "Effect of solid lipid nanoparticles formulation compositions on their size, zeta potential and potential for in vitro type pHIS-HIV-Hugag transfection" *Pharm. Res.*, **24** (2007) 1098-1107.

[8] T.M. Lima, C.C. Kanunfre, C. Pompéia, R. Verlengia, and R. Curi, "Ranking the toxicity of fatty acids on Jurkat and Raji cells by flow cytometric analysis" *Toxicol. In Vitro*, **16** (2002) 741–747.

EFFICIENT siRNA DELIVERY AND EFFECTIVE GENE SILENCING BY LIPOSPERMINE LIPOPLEXES

Abdelkader A. Metwally, Charareh Pourzand, and Ian S. Blagbrough

Department of Pharmacy and Pharmacology, University of Bath, Bath BA2 7AY, U.K.
E-mail: prsisb@bath.ac.uk

Purpose: To develop structure-activity relationships of two novel unsymmetrical N^4,N^9-difatty acid conjugates of the naturally occurring polyamine spermine for their potential as non-viral, self-assembly vectors for siRNA delivery.

Methods: Synthesis of the unsymmetrical fatty acid spermine conjugates was achieved by stepwise DCC/DMAP coupling of fatty acids to N^1,N^{12} protected spermine. Alexa Fluor® 647-labelled siRNA silencing EGFP expression (a 24-mer) was custom synthesized by Qiagen. All transfection experiments were carried-out in DMEM containing 10% FCS. The efficiency of delivery and the effectiveness of knock-down were evaluated in HeLa cells stably expressing EGFP by FACS analysis 48 h post transfection. Cell viability was measured as the percentage of viable cells using the alamarBlue® assay.

Results: N^4,N^9-Dioleoylspermine (DOS) showed 150% more delivery efficiency compared to N^4-linoleoyl-N^9-oleoylspermine (LINOS). However, knock-down results show that LINOS is more effective with a reduction of EGFP expression levels from control (100%) to 25 ± 3% at 3 µg/well (N/P = 11). DOS reduced EGFP expression to 27 ± 2% at a concentration of 6 µg/well (N/P = 22) and to 32 ± 2% at a concentration of 3 µg/well (N/P = 11). N^4-Lignoceroyl-N^9-oleoyl-spermine (LIGOS) showed 400% more delivery compared to LINOS while reducing EGFP expression to 56 ± 4%. At 3 µg/well LINOS cell viability is 65 ± 18%, while at 6 µg/well DOS cell viability is only 33 ± 7%. Cell transfection with Lipofectamine™ 2000 reduced EGFP expression to 37 ± 3%, with cell viability 84 ± 10%.

Conclusions: Unsymmetrical lipopolyamine LINOS is an excellent transfecting agent for the delivery of siRNA producing effective gene silencing in the presence of 10% FCS. The efficiency of delivery is not necessarily a direct measure of gene silencing efficiency.

Acknowledgments: We thank the Egyptian Government for a fully-funded studentship to AAM.

2nd APGI International Conference. Innovation in Drug Delivery: From Preformulation to Development through Innovative Evaluation Process.
Aix-en-Provence, France, 3-6 October 2010, #208 p 301.

siRNA DELIVERY AND GENE SILENCING BY UNSYMMETRICAL FATTY ACID AMIDES OF SPERMINE

Abdelkader A. Metwally, Charareh Pourzand, and Ian S. Blagbrough
Department of Pharmacy and Pharmacology, University of Bath, Bath BA2 7AY, U.K.
E-mail: prsisb@bath.ac.uk

Purpose: The evaluation of siRNA delivery and gene silencing efficiencies using novel unsymmetrical long- and very-long chain fatty acid spermine conjugates.
Methods: We prepared N^4-arachidonoyl-N^9-oleoylspermine (AOS), N^4-lignoceroyl-N^9-oleoylspermine (LIGOS), and N^4-linoleoyl-N^9-oleoylspermine (LINOS). All transfection studies were carried out in the presence of 10% FCS in DMEM on HeLa cells stably expressing enhanced green fluorescent protein (EGFP). siRNA concentration was 15 nM. Mean geometric fluorescence intensity of Alexa Fluor® 647 labelled-siRNA and EGFP was measured by FACS analysis 48 h post transfection. Cytotoxicity was evaluated using the alamarBlue® assay.
Results: Living cells were gated for FACS analysis which showed that LIGOS gave the highest siRNA delivery, 4-fold more compared to AOS and LINOS (measured by the normalized Alexa Fluor® 647 geometric mean fluorescence). More reduction in EGFP expression was achieved on siRNA delivery with AOS (to 29%, N/P = 21) and LINOS (to 25%, N/P = 11) compared to a reduction to 56% achieved with LIGOS (N/P = 18). Unsaturated fatty acid amide (linoleoyl; 18:2; arachidonoyl; 20:4) spermine conjugates showed higher silencing efficiencies compared to (saturated) lignoceroyl (24:0) spermine conjugates. AlamarBlue® cytotoxicity evaluation showed that LINOS was less cytotoxic to HeLa cells (65% cell viability) compared to AOS (31%) and LIGOS (49%). The lower cell viability obtained with AOS may be attributed to the increased number (4) of C=C double bonds which has been reported to be a cause of cytotoxicity. Under the same experimental settings, Lipofectamine™ 2000 reduced EGFP expression to 37 ± 3%, with cell viability of 84 ± 10%.
Conclusions: N^4-Linoleoyl-N^9-oleoylspermine (LINOS) is an efficient vector for siRNA delivery and effective gene silencing.
Acknowledgments: We thank the Egyptian Government for a fully-funded studentship to AAM.

2nd APGI International Conference. Innovation in Drug Delivery: From Preformulation to Development through Innovative Evaluation Process.
Aix-en-Provence, France, 3-6 October 2010.

EFFICIENT siRNA DELIVERY AND EFFECTIVE GENE SILENCING BY LIPOPLEXES

Abdelkader A. Metwally, Charareh Pourzand, and Ian S. Blagbrough

Department of Pharmacy and Pharmacology, University of Bath, Bath BA2 7AY, U.K.

PURPOSE

We report the synthesis and biological activity of two novel unsymmetrical N^4,N^9-difatty acid conjugates of the naturally occurring polyamine spermine, with the aim of developing structure-activity relationships for their potential as non-viral, self-assembly vectors for siRNA delivery.

METHODS

Transfection experiments

Lipoplexes of Alexa Fluor® 647-labelled siRNA silencing EGFP expression were prepared at different N/P ratios. The efficiency of delivery and the effectiveness of knock-down (gene silencing) were evaluated in HeLa cells stably expressing EGFP. All transfection experiments were carried-out in DMEM containing 10% foetal calf serum (FCS) in 24-well plates. Analysis of fluorescence intensity was out FACS 48 h post transfection.

Cytotoxicity assay by alamarBlue®

Lipoplexes were added to HeLa cells in the same manner as the above transfection protocol with the exception of adjusting the amount of siRNA to the 96-well format. The % viability is calculated according to alamarBlue® manufacturer instructions.

RESULTS

The efficiency of intracellular delivery was measured by the (normalized) fluorescence of Alexa Fluor® 647-labelled siRNA; N^4,N^9-dioleoylspermine (DOS) showed 150% of the delivery efficiency achieved with N^4-linoleoyl-N^9-oleoylspermine (LOS). However, knock-down results show that LOS is more effective with a reduction of EGFP expression levels from control (100%) to 25 ± 3% at a concentration of 3 µg/well (N/P = 11, n = 3 and triplicate replicates). Under the same experimental conditions, DOS reduced EGFP expression to 27 ± 2% at a concentration of 6 µg/well (N/P = 22) and to 32 ± 2% at a concentration of 3 µg/well (N/P = 11). Cell viability results show that at 3 µg/well LOS cell viability is 83 ± 4%, at 6 µg/well LOS cell viability is 46 ± 8%, while at 6 µg/well DOS cell viability is only 32 ± 9%. Transfection of cells with Lipofectamine™ 2000 resulted in reduction of EGFP expression to 37 ± 3%, with cell viability of 91 ± 6%.

CONCLUSIONS

Unsymmetrical lipopolyamine LOS is an excellent transfecting agent for the delivery of siRNA producing effective gene silencing (even with FCS).

We thank the Egyptian Government for a fully-funded studentship to AAM.

siRNA DELIVERY TO EFFECT EFFICIENT GENE SILENCING: OPPORTUNITIES WITH SELF-ASSEMBLY LIPOPLEXES OF UNSYMMETRICAL FATTY ACID AMIDES OF SPERMINE

Abdelkader A. Metwally, Charareh Pourzand, and Ian S. Blagbrough
Department of Pharmacy and Pharmacology, University of Bath, Bath BA2 7AY, UK
E-mail: prsisb@bath.ac.uk

Purpose: Our aim is to study the SAR of novel unsymmetrical long- and very-long chain fatty acid spermine conjugates evaluating their efficiencies in siRNA delivery and gene silencing.
Methods: N^4-Arachidonoyl-N^9-oleoylspermine (AOS), N^4-lignoceroyl-N^9-oleoylspermine (LIGOS), and N^4-linoleoyl-N^9-oleoylspermine (LINOS) were prepared using DCC coupling of the corresponding carboxylic acids, after N^4,N^9-diphthalimido protection of the primary amines. All transfection studies were carried out in the presence of 10% FCS in DMEM on HeLa cells stably expressing enhanced green fluorescent protein (EGFP). siRNA concentration in each well of 24-well plates was 15 nM. Mean geometric fluorescence intensity of Alexa Fluor® 647 labelled-siRNA and EGFP was measured by FACS analysis 48 h post transfection. Cytotoxicity was evaluated using the alamarBlue® assay.
Results: Gated FACS analysis of living cells showed that LIGOS has the highest siRNA delivery as measured by the normalized geometric mean fluorescence of Alexa Fluor® 647 (4-fold more compared to AOS and LINOS). However, more reduction in EGFP expression was achieved on siRNA delivery with AOS (to 34%, N/P = 21) and LINOS (to 29%, N/P = 11) compared to a reduction to 56% achieved with LIGOS (N/P = 18). Unsaturated fatty acid amide (linoleoyl; 18:2; arachidonoyl; 20:4) spermine conjugates showed higher silencing efficiencies compared to (saturated) lignoceroyl (24:0) spermine conjugates. LIGOS gave better siRNA delivery, however its relatively low knockdown (to 56%) means that whilst incorporating a saturated chain might enhance delivery, unsaturated chains specifically enhance the endosomal escape of the delivered siRNA due to the ability of unsaturated chains to enhance fusion with endosomal membranes. AlamarBlue® cytotoxicity evaluation showed that LINOS was less cytotoxic to HeLa cells (72% cell viability) compared to AOS (32%) and LIGOS (63%). The lower cell viability obtained with AOS may be attributed to the increased number (4) of C=C double bonds which has been reported to be a cause of cytotoxicity. Under the same experimental conditions, Lipofectamine™ 2000 reduced EGFP expression to 34%, with cell viability of 82%.
Conclusions: N^4-Linoleoyl-N^9-oleoylspermine (LINOS) is an excellent vector for siRNA delivery and efficient gene silencing working through lipoplex self-assembly.
Acknowledgments: We thank the Egyptian Government for a fully-funded studentship to AAM.

Practical synthesis of unsymmetrical fatty acid conjugates of spermine for siRNA delivery

Abdelkader A. Metwally, Charareh Pourzand, and Ian S. Blagbrough*

Department of Pharmacy and Pharmacology, University of Bath, Bath BA2 7AY, U.K.

We have designed, synthesized, and purified C12 to C18 unsymmetrical fatty acid amides of the tetraamine spermine (lipospermines), conjugates containing two different fatty acid chains at the N^4- and N^9-positions of spermine. Spermine contains two primary and two secondary amine functional groups which require orthogonal protection to synthesize unsymmetrical N^4,N^9-diacylated lipospermines. One approach to their synthesis is to protect the primary amine functional groups as phthalimides, followed by BOC protection of one secondary amine. The first fatty acid was introduced by HOBT/DCC coupling to the free secondary amine followed by BOC deprotection and then conjugation with the second long-chain fatty acid. Another practical approach uses DMAP/DCC to conjugate stoichometrically (40%) only one fatty acid to the diphthalimide of spermine. After purifying from a small amount of the diacylated product, conjugating the second fatty acid avoids BOC introduction and TFA-mediated BOC deprotection. After hydrazine deprotection of the phthalimides, the six unsymmetrical lipospermines were characterized. One fatty acid chain was kept constant as oleoyl (C18) in conjugates of: arachidonic (C20), erucic (C22), lignoceric (C24), linoleic (C18), nervonic (C24), and stearic (C18) acids. HeLa cells stably expressing EGFP were transfected by lipoplexes of lipospermine with siRNA to silence EGFP production. SAR of fatty acid chain length and saturation state were studied. Unsaturated fatty acids were more efficient in knocking down EGFP, while saturated fatty acids enhanced siRNA delivery. These results show that unsymmetrical lipospermines are promising non-viral vectors.

We thank the Egyptian Government (through Ain Shams University) for a fully-funded studentship to AAM.

Efficient siRNA delivery and gene silencing by unsymmetrical fatty acid amides of spermine

Abdelkader A. Metwally, Charareh Pourzand, and Ian S. Blagbrough
Department of Pharmacy and Pharmacology, University of Bath, Bath BA2 7AY, U.K.

Gene knock-down, gene silencing using siRNA (synthetic dsRNA of 21-25 base pairs), has many potential therapeutic applications for difficult-to-treat diseases [1]. We have designed, synthesized, and evaluated long-chain (C18) and very-long (C20 and C24) fatty acid amides of the naturally occurring polyamine spermine for siRNA delivery and gene knock-down [2]. Our latest spermine conjugates are unsymmetrical, possessing two different fatty acid chains conjugated at the N^4- and N^9-positions. They are designed upon the observation that most mammalian diacylglycerols are composed of chains with different length or oxidation state. Phospholipids usually have one unsaturated acyl chain in the *sn*-2-position, and so we kept mono-oleoyl as a constant feature in our novel unsymmetrical diacylspermine conjugates: N^4-arachidonoyl-N^9-oleoylspermine (AOS), N^4-lignoceroyl-N^9-oleoylspermine (LIGOS), N^4-linoleoyl-N^9-oleoylspermine (LINOS), and N^4-nervonoyl-N^9-oleoylspermine (NOS) evaluating their efficiencies with respect to siRNA delivery and gene knock-down. Synthesis of these unsymmetrical polyamine amides was achieved by DCC/DMAP catalysed coupling of the corresponding carboxylic acids, after protection of spermine primary amines with phthalimide. Thus, using oleic acid (1.1 eq.) and N^1,N^{12}-diphthalimido spermine (1.0 eq., 24 h, 20 ^{o}C) gave the N^4-mono-oleoyl conjugate, 50% yield after flash chromatography. Under the same conditions, the second long-chain fatty acid was then added. Deprotection was by refluxing with hydrazine (10% v/v) in THF:DCM (1:1 v/v, 4 h) followed by flash column chromatography (40% over both steps). Transfection studies were carried out in the presence of 10% foetal calf serum (FCS) in DMEM. HeLa cells stably expressing enhanced green fluorescent protein (EGFP) were transfected with siRNA at a concentration of 15 nM. Mean geometric fluorescence intensity of Alexa Fluor® 647 labelled-siRNA and of EGFP was measured by FACS analysis 48 h post transfection. The alamarBlue® assay was used to evaluate cell viability where 6000 cells/well of 96-well plates were incubated for 44 h post transfection followed by adding alamarBlue® to the media and incubation for 3.5 h.

FACS analysis results indicated that LIGOS has the highest siRNA delivery – 4-fold more compared to AOS and LINOS. However, more reduction in EGFP expression was achieved with AOS (to 34%, N/P = 21) and LINOS (to 29%, N/P = 11) compared to a reduction to 56% achieved with LIGOS (N/P = 18), and to 54% with NOS (N/P = 18). Unsaturated fatty acid spermine conjugates (linoleoyl; 18:2; arachidonoyl; 20:4) showed higher knock-down efficiencies compared to the lignoceroyl (24:0) or nervonoyl (24:1) conjugates. This knock-down effect may be due to the unsaturated chains' ability to enhance fusion with endosomal membranes and thereby to facilitate endosomal escape [3]. Though LIGOS and NOS were almost equivalent in gene silencing, the siRNA delivered by LIGOS lipoplexes was twice that of NOS, in other words, NOS (24:1) achieved the same knock-down as LIGOS (24:0) with half the amount of siRNA. AlamarBlue® cell viability evaluation showed that LINOS was less cytotoxic to HeLa cells (72% cell viability) at the N/P ratio that showed the best knock-down efficiency, compared to AOS (32%), LIGOS (63%), and NOS (22%). The lower cell viability obtained with AOS and NOS (compared to LIGOS) may be attributed to the presence of C=C double bonds which relatively increases the cytotoxicity among other factors [4]. Using the same experimental conditions, Lipofectamine^{TM} 2000 reduced EGFP expression to 34% while cell viability was 82%. N^4-Linoleoyl-N^9-oleoylspermine (LINOS) is an efficient vector for the delivery of siRNA producing effective gene silencing even in the presence of FCS showing protection in the self-assembled nanoparticle from RNase.

We acknowledge financial support from the Egyptian Government (studentship to A.A.M.).

[1] *Blagbrough I S, Zara C (2009) Animal models for target diseases in gene therapy - using DNA and siRNA delivery strategies. Pharm. Res. 26:1-18.*

[2] *Ghonaim H G, Li S, Blagbrough I S (2009) Very long chain N^4,N^9-diacyl spermines: non-viral lipopolyamine vectors for plasmid DNA and siRNA formulation. Pharm. Res. 26:19-31.*

[3] *Ahmed O A, Pourzand C, Blagbrough I S (2006) Varying the unsaturation in N^4,N^9-dioctadecanoyl spermines: nonviral lipopolyamine vectors for more efficient plasmid DNA formulation. Pharm. Res. 23:31-40.*

[4] *Lima T M, Kanunfre C C, Pompéia C, Verlengia R, Curi R (2002) Ranking the toxicity of fatty acids on Jurkat and Raji cells by flow cytometric analysis. Toxicol. In Vitro 16:741-747.*

Binding sites for polyamine conjugates – where therapy meets chemistry

Ian S. Blagbrough, Abdelkader A. Metwally, and Hassan M. Ghonaim

Department of Pharmacy and Pharmacology, University of Bath, Bath BA2 7AY, U.K.

prsisb@bath.ac.uk

Polyamine conjugates are found widely distributed as natural products in plants, bacteria, invertebrates, and in mammals. Although free polyamines are simple linear structures, often characterised by C-3 spacers derived from *S*-adenosylMet (SAM), or C-4, putrescine from Orn or Arg, or C-5, cadaverine from Lys, it is their pattern of positive charges as a result of their differing pK_a values which, together with their three dimensional shape, brings about their intrinsic biological activity. Such molecules display high affinity for a range of binding sites. Whilst this may lead to some therapeutic possibilities, it is also likely to lead to non-specificity, and even non-selectivity, so-called "dirty drugs" with no (or limited) therapeutic value. The covalent attachment of side-chains through a variety of functional groups allows higher binding affinity and therefore more selectivity. The simple amide, being neutral, takes away the possibility of a positive charge. However, the guanidine, being the most basic functional group in medicinal chemistry, ensures the presence of a positive charge across the pH range. Taken together with hydrogen bonding potential and van der Waals' lipid-lipid non-bonding interactions arising from the conjugated moieties, means that a wide range of polyamine conjugates are now known that have roles or potential roles in therapy.

Placing 4-6 positive charges around a 3D-template gives powerful antibiotic action, although with side-effects e.g. ototoxicity (permanent deafness). Such polyamine conjugates, amino-glycosides e.g. tobramycin, neomycin, find widespread use in hospitals. As the polycationic polyamines have been known since their discovery to bind to polyanionic DNA, as in sperm, it is not surprising that they can interfere with various cancers. Affinity and cytotoxicity can both be improved by the addition of an anthracene or acridine intercalator moiety. Capping the N-termini with alkyl moieties has given rise to a large number of analogues, N^1,N^{11}-diethylnorspermine (DENSPM) being one of the more famous. One interesting effect of *R*,*R*-dihydroxy-N^1,N^{14}-diethylhomospermine (from DEHSPM) is as an anti-diarrhoeal. Increasing the spacing between the two central secondary amines and adding longer chain alkyl or aromatic end-groups turns the anti-cancer activity into anti-malarial activity.

Spider and wasp venoms contain a plethora of polyamine amides. These toxins are typically use-dependent voltage-sensitive cation channel blockers. They are reversible paralysing

toxins which can cross the blood-brain barrier when it is compromised in stroke. Although they do not need to be specific or even selective as invertebrate toxins, they show selectivity for potassium/sodium/calcium i.e. cation channel blockers. We can therefore modify these polyamine amides, with molecular weights in drug-space (below 500 Da), to probe for selective cation channel block of interest in various CNS disorders and especially in stroke. It is unlikely, without an extremely efficient delivery vehicle, that these polyamine conjugates acting as reversible channel blockers will become commercial insecticides.

Microbes have solved the problems of insoluble and toxic ferric ion by generating iron chelating systems, siderophores that complex (sequester) ferric ion for solubilisation and transport. These siderophores are rich in polyamine and polyamide moieties e.g. parabactin, agrobactin, desferrioxamine B. Phytosiderophores are low molecular weight ion-chelators endogenous to plants e.g. the triamine triacid nicotianamine. These polyamine conjugates are important as probes to investigate iron transport and the roles of iron in infection, and as lead compounds for the potential treatment for haemochromatosis (β-thalassemia). DNA intercalator anthraquinones bound to metal chelating polyamines (ethylenediamines) that are complexed with cupric ions act as synthetic DNase. Alternatively, using acridine for RNA intercalation, or adding a 19-mer of DNA complementary to the RNA sequence adjacent to the desired site for scission, and two units of ethylenediamine yields synthetic RNases.

As part of our detailed studies of the SAR of polynucleotide delivery, we have a focus on using lipopolyamine conjugates for non-viral gene and small interfering RNA (siRNA) delivery, potential medicines for siRNA delivery to its site of action in the cytosol. We are investigating the design, synthesis, formulation, and delivery of fluorescent siRNA by self-assembly of nanoparticles measuring gene silencing efficiency. We aim to silence the biosynthesis of selected proteins that are signals for cancers to grow or for selected causes of inflammation. With regard to vector specificity, surprisingly, DNA transfer reagents cannot be used under similar conditions to achieve efficient and non-toxic delivery of siRNA.

We acknowledge financial support from the Egyptian Government (studentships to A.A.M. and H.M.G.).

Models for Target Diseases with RNAi Therapy – Self-assembly siRNA Delivery Strategies

Ian S. Blagbrough,* Abdelkader A. Metwally, and Hassan M. Ghonaim

Department of Pharmacy and Pharmacology, University of Bath, Bath BA2 7AY, U.K.
prsisb@bath.ac.uk

ABSTRACT SUMMARY

Animal models for RNA interference (RNAi) therapy are outlined together with evidence that this approach works from a Phase 1 clinical trial against age-related macular degeneration. A novel strategy of lipoplex self-assembly is shown to be an efficient, non-toxic method for delivering siRNA to cells in the presence of serum.

INTRODUCTION

Many animal models e.g. rodents, and primates are now being investigated to pave the way for RNAi clinical trials [1]. In 1998, Fire and Mello published the mechanism for the degradation of mRNA transcribed from a specific gene in a sequence specific manner [2], a discovery for which they were rapidly awarded the Nobel Prize in Physiology or Medicine (2006). Since then, and also rapidly, research relating to possible therapeutic applications of RNAi has reached the clinical trial stage. Activating the RNAi pathway results in reduction of gene expression (knock-down) by the intracellular delivery of either short hairpin RNA (shRNA) or small interfering RNA (siRNA), a process called sequence specific post-transcriptional gene silencing. siRNAs can be used together with hematopoietic stem cell transplants stably to modulate gene expression in non-human primates and hence potentially to treat blood diseases e.g. HIV-1 [1]. Non-human primate models e.g. macaque, common marmoset, owl monkey are used for preclinical delivery vector safety and efficacy trials. Li and Tang evaluated SARS coronavirus potent (in vitro) siRNA inhibitors for efficacy and safety in a rhesus macaque (*M. mulatta*) SARS, where three dosing regimens which showed siRNA-mediated anti-SARS efficacy were evaluated as either prophylactic or therapeutic regimens [3]. Takeshita and Ochiya have reviewed the first in vivo delivery of siRNA (2002) achieved by the "hydrodynamic" technique in which naked siRNA is administered in large volumes of a physiological solution under high pressure into the tail vein of mice [4]. The efficacy of this delivery method was evaluated by co-injecting mice with plasmids that express the luciferase gene as a reporter along with an siRNA against luciferase mRNA [4]. A phase 1 clinical trial for the treatment of choroidal neovascularization secondary to neovascular age-related macular degeneration has recently been reported, evaluating the tolerability and safety of single ascending intravitreal doses of (naked) siRNA in a proof-of-principle of the biological activity of the specified siRNA [5]. Apart from tail vein and ocular delivery, a carrier (a vector e.g. positively charged atelocollagen [4]) offers advantages for efficient delivery of the polynucleotide therapeutic to target cells [6]. The main functions of such a vector are to protect the RNA from serum nuclease degradation, to secure the efficient intracellular delivery of RNA, and to target a desired cell/tissue type if required. Moving from in vitro experiments to in vivo clinical trials requires the use of non-human models to ensure the safety and the efficient intracellular delivery of siRNA/shRNA.

We aim to design and evaluate our lipopolyamines [7-9], developing this strategy as a safe (non-toxic) and efficient non-viral approach clinically effective delivery of RNAi technologies. The synthesized lipopolyamine vectors are prepared by conjugating two long fatty acid chains to the N^4- and N^9-amine functional groups of the symmetrical polyamine spermine. The properties of the synthesized lipospermines can be varied by changing the length and oxidation state of the fatty acid. We report the synthesis of five symmetrical lipospermines, characterized and tested for their safety and efficacy.

EXPERIMENTAL METHODS

Synthesis of lipospermines

N^4,N^9-Dierucoylspermine **1**, N^4,N^9-dilauroylspermine **2**, N^4,N^9-dilinoleoylspermine **3**, N^4,N^9-dioleoylspermine **4**, and N^4,N^9-distearoylspermine **5** were prepared using either DCC coupling of the corresponding carboxylic acids or coupling with the corresponding acyl chlorides, after di-*N*-phthalimido protection of the primary amines with subsequent deprotection by hydrazinolysis. They were all purified to homogeneity and showed satisfactory spectroscopic and spectrometric data, including: **1**, HRMS m/z, ESI found $(M+1)^+$ 843.8355, $C_{54}H_{106}N_4O_2$ requires $(M+1)^+$

843.8316; **2**, HRMS m/z, ESI found $(M+1)^+$ 567.5553, $C_{34}H_{70}N_4O_2$ requires $(M+1)^+$ 567.5572; **3**, HRMS m/z, ESI found $(M+1)^+$ 727.6851, $C_{46}H_{86}N_4O_2$ requires $(M+1)^+$ 727.6824; **4**, HRMS m/z, ESI found $(M+1)^+$ 731.7174, $C_{46}H_{90}N_4O_2$ requires $(M+1)^+$ 731.7137; **5**, HRMS m/z, ESI found $(M+1)^+$ 735.7428, $C_{46}H_{94}N_4O_2$ requires $(M+1)^+$ 735.7450.

Transfection experiments

All transfection studies were carried out in the presence of 10% FCS in DMEM on HeLa cells stably expressing green fluorescent protein (GFP). Cells were seeded at 65,000 cells/well 24 h prior to transfection. siRNA concentration in each well of 24-well plates was 15 nM. Mean geometric fluorescence intensity of Alexa Fluor® 647 (AF) labeled-siRNA and of GFP was measured by FACS analysis 48 h post transfection. FACS measurements were carried out on the gated population of healthy cells. The reduction in GFP expression was calculated as:

$$\%GFP = \frac{GFP\ fluorescen\ ce\ of\ transfecte\ d\ cells}{GFP\ fluorescen\ ce\ of\ control\ cells} x100$$

Cell viability assay

The alamarBlue® assay [10] was used to evaluate cell viability after transfection. HeLa cells were incubated in 96-well plates for 44 h post transfection then alamarBlue® reagent was added to the culture media and cells were incubated for a further 3.5 h. Percentage viability was calculated by measuring absorbance at λ = 570 nm and 600 nm using a VersaMax microplate reader and performing calculations according to the alamarBlue® supplier's instructions.

RESULTS AND DISCUSSION

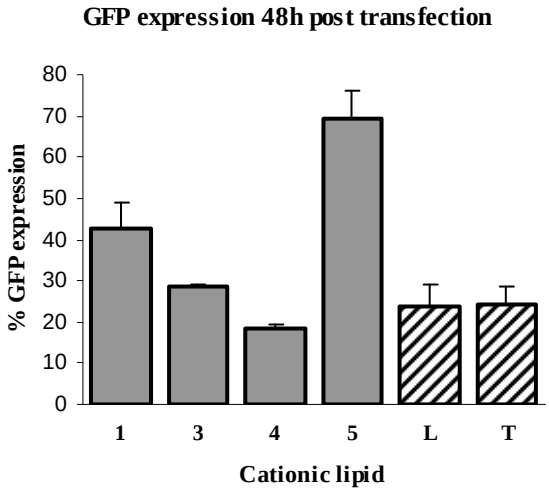

Fig. 1. Knock-down of GFP expression in HeLa cells. Values are mean ± SD (n = 6) for erucoyl **1** (6 μg/well), linoleoyl **3** (1.5 μg/well), oleoyl **4** (6 μg/well), and stearoyl **5** (6 μg/well), and commercially available transfection agents Lipofectamine 2000 (**L**, 2 μL/well) and TransIT TKO (**T**, 4 μL/well).

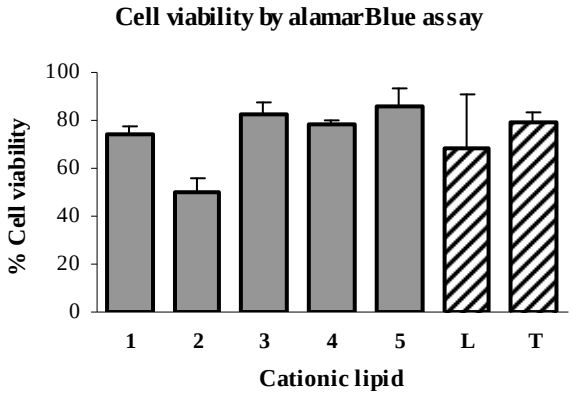

Fig. 2. Cell viability in HeLa cells mediated by fatty acid amides of spermine compared with the commercially available transfection agents Lipofectamine 2000 (**L,** 0.2 μL/well) and TransIT TKO **(T, 0.**4 μL/well). Values are presented as mean ± SD (n = 6) using erucoyl **1** (0.6 μg/well), lauroyl **2** (0.3 μg/well), linoleoyl **3** (0.15 μg/well), oleoyl **4** (0.6 μg/well), and stearoyl **5** (0.6 μg/well) in 96-well plates.

siRNA delivery was evaluated by the amount of AF fluorescence 48 h post-transfection with lipospermine/ siRNA lipoplexes. **1** showed the highest AF fluorescence (159 normalized units) at 6 μg of **1**, lipoplexes of **4** showed 17 normalized units at 6 μg of **4**. There was a direct proportionality between the amount of a specific fatty acid spermine conjugate and the intensity of AF fluorescence delivered. Fatty acids with long chains and one double bond, 22:1 and 18:1, resulted in a general trend of higher fluorescence for the same amount of lipid used. At 6 μg, **4** resulted in AF fluorescence twice that of **5**. The least fluorescence (least delivery) was achieved with **2** (lauroyl 12:0) which was the most toxic conjugate.

The most efficient knock-down of GFP expression in HeLa cells 48 h post-transfection (Fig. 1) (>80%) was achieved with N^4,N^9-dioleoylspermine **4**. This conjugate together with N^4,N^9-dilinoleoylspermine **3** were the least toxic in the alamarBlue® assay (Fig. 2), and comparing favourably with the commercially available transfection agents Lipofectamine 2000 (**L**) and TransIT TKO (**T**).

CONCLUSIONS

Lipoplexes of siRNA and N^4,N^9-difatty acid amides of spermine resulted in successful siRNA delivery and gene silencing of GFP in HeLa cells. Variation of the chain length or saturation state of the fatty acids affected both the siRNA delivery and gene silencing efficiency where non-saturated fatty acids C18:1, C18:2, and C22:1 showed more efficient knock-down compared to that achieved with the saturated fatty acids C12:0 and C18:0.

REFERENCES

1. Blagbrough, I. S.; Zara, C. *Pharm. Res.* **2009**, 26, 1-18.
2. Fire, A.; Xu, S. Q.; Montgomery, M. K.; Kostas, S. A.; Driver, S. E.; Mello, C. C. *Nature* **1998**, 391, 806-811.
3. Li, B. J.; Tang, Q. Q. *Nat. Med.* **2005,** 11, 944-951.
4. Takeshita, F.; Ochiya, T. *Cancer Sci.* **2006**, 97, 689-696.
5. Kaiser, P. K.; Symons, R. C. A.; Shah, S. M.; Quinlan, E. J.; Tabandeh, H.; Do, D. V.; Reisen, G.; Lockridge, J. A.; Short, B.; Guerciolini, R.; Nguyen, Q. D. *Am. J. Ophthalmol.* **2010**, 150, 33-39.
6. Whitehead, K. A.; Langer, R.; Anderson, D. G. *Nat. Rev. Drug Discov.* **2009**, 8**,** 129-138.
7. McLaggan, D.; Adjimatera, N.; Sepčić, K.; Jaspars, M.; MacEwan, D. J,; Blagbrough, I. S.; Scott, R. H. *BMC Biotechnol.* **2006**, 6, doi: 10.1186/1472-6750-6-6.
8. Soltan, M. K.; Ghonaim, H. M.; El Sadek, M.; Abou Kull, M.; El-Aziz, L. A.; Blagbrough, I. S. *Pharm. Res.* **2009**, 26, 286-295.
9. Ghonaim, H. M.; Li, S.; Blagbrough, I. S. *Pharm. Res.* **2009**, 26, 19-31.
10. Asasutjarit, R.; Lorenzen, S.; Sirivichayakul, S.; Ruxrungtham, K.; Ruktanonchai, U.; Ritthidej, G. C. *Pharm. Res.* **2007**, 24, 1098-1107.

ACKNOWLEDGMENTS

We acknowledge the financial support of the Egyptian Government (fully-funded studentships to A.A.M. and H.M.G.). We are grateful to Dr C. Pourzand (University of Bath) for helpful discussions.

Efficient siRNA delivery and gene silencing by symmetrical fatty acid conjugates of spermine

Metwally AA, Pourzand C, and Blagbrough IS
Department of Pharmacy and Pharmacology, University of Bath, Bath BA2 7AY, UK

INTRODUCTION

Gene silencing by siRNA is an important tool in the study of gene function with many potential therapeutic applications [1]. In this study, five spermine fatty acid conjugates were synthesized, characterized, and evaluated for their ability to deliver siRNA to knock down green fluorescent protein (GFP) expression in transfected HeLa cells that stably express GFP.

AIMS

To study the SAR of the five synthetic spermine fatty acid conjugates and to evaluate these vectors for their efficiencies of siRNA delivery and gene knock-down.

MATERIALS AND METHODS

The N^4,N^9-di-fatty acid spermine conjugates were prepared using DCC coupling of the corresponding carboxylic acids (erucic, lauric, linoleic, oleic, and stearic), after di-*N*-phthalimido protection of the primary amines. Particle size was measured by DLS and zeta-potential was determined by measuring electrophoretic mobility of the lipoplexes. All transfection studies were carried out in the presence of foetal calf serum (FCS) 10% in DMEM on HeLa cells stably expressing GFP. siRNA concentration in each well of 24-well plates was 15 pmol/well. FACS analysis was carried out 48 h post transfection to measure mean geometric fluorescence intensity of Alexa Fluor® 647 labelled-siRNA and GFP. The alamarBlue® assay [2] was used to evaluate cytotoxicity.

RESULTS AND DISCUSSION

The particle size of the prepared lipoplexes was in the range 145-353 nm, and all the lipoplexes showed a positive zeta-potential. After FACS gating of healthy cells, siRNA delivery did not relate directly to gene silencing efficiency as N^4,N^9-dierucoyl spermine resulted in higher siRNA delivery (9-fold) compared to N^4,N^9-dioleoyl spermine. GFP silencing in HeLa cells showed that the unsaturated fatty acid amides are more efficient than saturated fatty acid amides, with N^4,N^9-dioleoyl spermine resulting in the most efficient gene silencing (reduced GFP to 19%) followed by N^4,N^9-dilinoleoyl spermine (reduced GFP to 28%) in the presence of 10% FCS. The alamarBlue assay showed that spermine fatty acid amides have good viability (75%-85% compared to control), except N^4,N^9-dilauroyl spermine with its lower cell viability of 50% at N/P = 15. These results show that unsaturated fatty acid amides of spermine of chain length C18 are efficient, non-toxic, non-viral vectors for siRNA mediated gene silencing in HeLa cells.

CONCLUSIONS

The symmetrical lipopolyamines N^4,N^9-dioleoyl spermine and N^4,N^9-dilinoleoyl spermine are efficient non-viral siRNA delivery vectors producing effective gene silencing even in the presence of FCS.

ACKNOWLEDGMENTS

We thank the Egyptian Government for a fully-funded studentship to AAM. We thank Dr Olivier Reelfs (KCL) for helpful discussions.

REFERENCES

[1] I.S. Blagbrough and C. Zara, “Animal models for target diseases in gene therapy - using DNA and siRNA delivery strategies” *Pharm. Res.*, **26** (2009) 1-18.

[2] R. Asasutjarit, *et al.*, “Effect of solid lipid nanoparticles formulation compositions on their size, zeta potential and potential for in vitro type pHIS-HIV-Hugag transfection” *Pharm. Res.*, **24** (2007) 1098-1107.

Synthesis and evaluation of N^4,N^9-fatty acid conjugates of N^1,N^{12}-diamidino-spermine as non-viral siRNA delivery vectors

Abdelkader A. Metwally and Ian S. Blagbrough
Department of Pharmacy and Pharmacology, University of Bath, Bath BA2 7AY, UK

INTRODUCTION

siRNA sequence specific gene silencing has many potential therapeutic applications [1]. Guanidine groups with their high pK_a = 12.5 are practically fully protonated at physiological pH [2]. Four N^1,N^{12}-diamidino-spermine N^4,N^9-fatty acid derivatives were designed, synthesized, purified, characterized, and evaluated as non-viral vectors for siRNA.

AIMS

To characterize and evaluate the four synthetic N^1,N^{12}-diamidino-spermine fatty acid conjugates as non-viral vectors for the delivery of siRNA and its sequence specific gene knock-down.

MATERIALS AND METHODS

The N^4,N^9-fatty acid spermine conjugates were prepared by DCC coupling of the corresponding fatty acids (erucic, lauric, linoleic, and oleic), after di-*N*-phthalimido protection of the primary amines. Deprotection of the primary amines, guanidinylation with 1,3-di-BOC-2-(trifluoromethylsulfonyl)guanidine triethyl amine followed by TFA deprotection yielded the di-TFA salts of the cationic lipids. Particle size was measured by DLS and zeta-potential by measuring electrophoretic mobility of the lipoplexes. All transfection studies were carried out in the presence of foetal calf serum (FCS) 10% in DMEM on HeLa cells stably expressing green fluorescent protein (GFP). siRNA concentration in 24-well plates was 15 pmol/well. FACS analysis was carried out 48 h post transfection to measure mean geometric fluorescence intensity of Alexa Fluor® 647 labelled-siRNA and GFP. The alamarBlue® assay [3] was used to evaluate cytotoxicity.

RESULTS AND DISCUSSION

The particle size of the prepared lipoplexes varied from 132-575 nm with zeta-potential in the range +28 to +50 mV. After FACS gating a healthy cell population, N^1,N^{12}-diamidino-N^4-linoleoyl-N^9-oleoylspermine showed the best siRNA delivery compared to the other vectors and also showed the best GFP knock-down (reduced GFP to 26% of control). N^1,N^{12}-Diamidino-N^4,N^9-dioleoylspermine was the next most efficient with GFP reduction to 43% of the control value. Although N^1,N^{12}-diamidino-N^4,N^9-dierucoylspermine showed comparable delivery to the dioleoyl conjugate over the different N/P ratios, the GFP fluorescence was reduced only to 85% at the highest N/P = 18. Guanidines interact efficiently with anionic cell membrane components [4]. The alamarBlue cell viability assay showed that HeLa cells 48 h post transfection had good viability (64%-83% compared to control), except the dilauroyl conjugate, which resulted in almost complete cell death at N/P = 26.

CONCLUSIONS

These results show that N^1,N^{12}-diamidino-spermine with N^4,N^9 unsaturated fatty acid conjugates of chain length C18 are potentially good non-viral vectors for siRNA mediated gene silencing.

ACKNOWLEDGMENTS

We thank the Egyptian Government for a fully-funded studentship to AAM. We also thank Dr Charareh Pourzand (University of Bath) and Dr Olivier Reelfs (KCL) for helpful discussions.

REFERENCES

[1] I.S. Blagbrough and C. Zara, "Animal models for target diseases in gene therapy - using DNA and siRNA delivery strategies" *Pharm. Res.*, **26** (2009) 1-18.

[2] I.S. Blagbrough, A.A. Metwally and A.J. Geall, "Measurement of polyamine pK_a values" in *Polyamines Methods and protocols*, A.E. Pegg and R.A. Casero, New York, USA, Humana Press, 2011, ch 32, pp. 493-503.

[3] R. Asasutjarit, *et al.*, "Effect of solid lipid nanoparticles formulation compositions on their size, zeta potential and potential for in vitro type pHIS-HIV-Hugag transfection" *Pharm. Res.*, **24** (2007) 1098-1107.

[4] P.A. Wender, W.C. Galliher, E.A. Goun, L.R. Jones, and T.H. Pillow. "The design of guanidinium-rich transporters and their internalization mechanisms" *Adv. Drug Del. Rev.*, **60** (2008) 452-472.

siRNA lipoplex stability with glycosaminoglycans (GAGs)

Nour Alhusein, Abdelkader A. Metwally, and Ian S. Blagbrough*
Department of Pharmacy and Pharmacology, University of Bath, Bath BA2 7AY, U.K.

INTRODUCTION

Glycosaminoglycans (GAGs) are important negatively charged components of the extracellular matrix [1]. They could affect the composition and stability of lipoplexes, e.g. gene carrying DNA nanoparticles [2]. Studying the formation of siRNA nanoparticles and their interactions with GAG components are important for the design and development of successful siRNA carriers.

AIMS

We have carried out a comparative study between four lipopolyamines in their efficiency both in siRNA condensation and in the stability of their lipoplexes against GAGs. Such a pre-formulation analytical study might be correlated with the transfection efficiency of these siRNA-lipopolyamine nanoparticles.

MATERIALS AND METHODS

Chemicals were purchased from Sigma-Aldrich, UK. N^4,N^9-Dierucoylspermine, N^4,N^9-dioleoylspermine, N^1,N^{12}-diamidino-N^4,N^9-dierucoylspermine, and N^1,N^{12}-diamidino-N^4,N^9-dioleoylspermine were synthesized, purified, and characterized. siRNA (21 b.p., Negative Control, Qiagen) (2.97 µg, 10 µl) was diluted in HEPES buffer (1.5 ml, pH = 7.3). Immediately prior to analysis, ethidium bromide (EthBr) solution (3.3 µl, 0.5 mg/ml) was added to the stirring solution and allowed to equilibrate for 1 min [3]. Separately, aliquots (according to the N/P ratio required) were added to the stirring solution and the fluorescence measured after 1 min equilibration using fluorimeter (λ_{excit} = 260 nm, λ_{emiss} = 595 nm). Aliquots of each GAG were then added according to the negative charge that the GAG carries/ammonium (at N/P = 5) and finally the fluorescence recovery was measured.

RESULTS AND DISCUSSION

N^4,N^9-Dioleoylspermine shows good condensing efficiency for siRNA as the normalised fluorescence is quenched by 90% at N/P = 2. N^4,N^9-Dierucoyl-spermine and N^1,N^{12}-diamidino-N^4,N^9-dioleoyl-spermine formed weaker complexes with siRNA as they quenched the fluorescence by about 60% at N/P = 2. N^1,N^{12}-Diamidino-N^4,N^9-dierucoyl-spermine caused the lowest reduction in fluorescence of only 20% at N/P = 2.

Whilst on reaction with dermatan sulfate, N^4,N^9-dioleoylspermine siRNA lipoplex fluorescence only recovered to 40% of the normalised value (i.e. by 30%), fluorescence recovered to about 60% with the other three lipopolyamines. Our recent transfection data show that N^4,N^9-dioleoylspermine gave the best knock down of GFP in HeLa cells which stably express GFP, with reduction to 19 %. N^4,N^9-Dierucoylsperm-ine and N^1,N^{12}-diamidino-N^4,N^9-dioleoylspermine both caused reduction of GFP to 43% whilst N^1,N^{12}-diamid-ino-N^4,N^9-dierucoylspermine only gave a reduction to 85%.

CONCLUSIONS

These assays yield important information about the interactions between siRNA and lipopolyamines, and their stability against GAGs. These data offer an early pre-formulation indicator of potential transfection efficiency.

ACKNOWLEDGMENTS

We thank Damascus University, Syria, for a fully-funded studentship to NA and the Egyptian Government for a fully-funded studentship to AAM.

REFERENCES

[1] J.M. Trowbridge and R.L. Gallo, "Dermatan sulfate: new functions from an old glycosaminoglycan." *Glycobiology*, **12** (2002) 117R-125R.

[2] M. Ruponen, S. Ylä-Herttuala, and A. Urtti, "Interactions of polymeric and liposomal gene delivery systems with extracellular glycosaminoglycans: physicochemical and transfection studies." *Biochim. Biophys. Acta*, **1415** (1999) 331-341.

[3] A.J. Geall and I.S. Blagbrough, "Rapid and sensitive ethidium bromide fluorescence quenching assay of polyamine conjugate-DNA interactions for the analysis of lipoplex formation in gene therapy." *J. Pharm. Biomed. Anal.*, **22** (2000) 849-859.

Synthesis and evaluation of N^4,N^9-di-fatty acid conjugates of N^1,N^{12}-diamidino-spermine as non-viral siRNA delivery vectors

Abdelkader A. Metwally and Ian S. Blagbrough
Department of Pharmacy and Pharmacology, University of Bath, Bath BA2 7AY, UK

PURPOSE

To evaluate four synthetic N^1,N^{12}-diamidino-spermine N^4,N^9-di-fatty acid conjugates as non-viral vectors for the delivery of siRNA and its sequence specific gene knock-down.

METHODS

N^4,N^9-Di-fatty acid spermine conjugates were prepared by DCC coupling of the corresponding fatty acids (erucic, lauric, linoleic, and oleic), after di-*N*-phthalimido protection of the primary amines. Deprotection of the primary amines, guanidinylation, followed by TFA deprotection yielded the di-TFA salts of the cationic lipids. Particle size was measured by DLS, zeta-potential by electrophoretic mobility of the lipoplexes, and all transfection studies were carried out in the presence of fetal calf serum (FCS) 10% in DMEM on HeLa cells stably expressing green fluorescent protein (GFP). siRNA concentration in 24-well plates was 15 pmol/well. FACS analysis was carried out 48 h post transfection to measure mean geometric fluorescence intensity of Alexa Fluor® 647 labeled-siRNA and GFP. The alamarBlue® assay was used to evaluate cytotoxicity.

RESULTS

Lipoplex particle sizes varied from 132-575 nm with zeta-potentials from +28 to +50 mV. After FACS gating a healthy cell population, N^1,N^{12}-diamidino-N^4-linoleoyl-N^9-oleoylspermine showed the best siRNA delivery compared to the other vectors and also showed the best GFP knock-down (reduced to 26% of control). N^1,N^{12}-Diamidino-N^4,N^9-dioleoylspermine reduced GFP to 43%. Although N^1,N^{12}-diamidino-N^4,N^9-dierucoylspermine showed comparable delivery to the dioleoyl conjugate over the different N/P ratios, the GFP fluorescence was reduced only to 85% at the highest N/P = 18. Guanidine groups, with their high pK_as = 12.5, interact efficiently with anionic cell membrane components. The alamarBlue cell viability assay showed that HeLa cells 48 h post transfection had good viability (64%-83% compared to control), except the dilauroyl conjugate, which resulted in almost complete cell death at N/P = 26.

CONCLUSIONS

These results show that N^1,N^{12}-diamidino-spermine N^4,N^9-di-fatty acid conjugates with C18 chain length are good non-viral vectors for siRNA mediated gene silencing.

We thank the Egyptian Government for a fully-funded studentship to AAM.

Poster abstract submission #895
2011 AAPS Annual meeting and Exposition, 23-27 October 2011, Washington, DC, USA

Efficient siRNA delivery and gene silencing by symmetrical fatty acid conjugates of spermine

Abdelkader A. Metwally, Charareh Pourzand, and Ian S. Blagbrough
Department of Pharmacy and Pharmacology, University of Bath, Bath BA2 7AY, UK

PURPOSE

To study the SAR of five synthetic spermine fatty acid conjugates and to evaluate these non-viral vectors for siRNA delivery and gene knock-down.

METHODS

Five N^4,N^9-di-fatty acid spermine conjugates were prepared using DCC coupling of the corresponding erucic, lauric, linoleic, oleic, and stearic carboxylic acids, after di-*N*-phthalimido protection of the primary amines. Particle size was measured by DLS, zeta-potential by electrophoretic mobility of the lipoplexes, and all transfection studies were carried out in the presence of fetal calf serum (FCS) 10% in DMEM on HeLa cells stably expressing GFP. siRNA concentration in each well of 24-well plates was 15 pmol/well. FACS analysis was carried out 48 h post transfection to measure mean geometric fluorescence intensity of Alexa Fluor® 647 labeled-siRNA and GFP. The alamarBlue® assay was used to evaluate cytotoxicity.

RESULTS

Lipoplex particle sizes were in the range 145-353 nm, with positive zeta-potentials. After FACS gating of healthy cells, siRNA delivery did not relate directly to gene silencing efficiency as N^4,N^9-dierucoyl spermine resulted in higher siRNA delivery (9-fold) compared to N^4,N^9-dioleoyl spermine. GFP silencing in HeLa cells showed that unsaturated fatty acid amides are more efficient than saturated fatty acid amides, with N^4,N^9-dioleoyl spermine resulting in the most efficient gene silencing (reduced GFP to 19%) followed by N^4,N^9-dilinoleoyl spermine (reduced GFP to 28%) in the presence of 10% FCS. The alamarBlue assay showed that spermine fatty acid amides have good viability (75%-85% compared to control), except N^4,N^9-dilauroyl spermine with its lower cell viability of 50% at N/P = 15.

CONCLUSIONS

These results show that our synthetic unsaturated C18 chain length fatty acid amides of spermine are efficient, non-toxic, non-viral vectors for siRNA mediated gene silencing in HeLa cells. The symmetrical lipopolyamines N^4,N^9-dioleoyl spermine and N^4,N^9-dilinoleoyl spermine are efficient siRNA delivery vectors producing effective gene silencing even in the presence of FCS.

We thank the Egyptian Government for a fully-funded studentship to AAM. We thank Dr Olivier Reelfs (KCL) for helpful discussions.

Poster abstract submission #896
2011 AAPS Annual meeting and Exposition, 23-27 October 2011, Washington, DC, USA